Regulation of glucose transport in cardiomyocytes

Peter Ronald Thomas Bowman

BSc (Hons) MRes

Submitted in fulfilment of the requirements for the Degree of PhD

November 2018

University of Glasgow

Institute of Molecular, Cell and Systems Biology

College of Medical, Veterinary and Life Sciences

Abstract

Major common complications of diabetes such as myocardial infarction arise from the onset of vascular disease. However, there is also evidence of a direct impairment of cardiac contractile function in diabetic individuals in the absence of atherosclerosis and hypertension, termed diabetic cardiomyopathy (DCM). This is characterised by early diastolic dysfunction that progresses to systolic dysfunction and heart failure through a pathological remodelling process. The earliest identified mechanism underlying this disease is the onset of metabolic perturbations such as cardiac insulin resistance. However, currently there are no specific treatments available, partly due to the lack of an appropriate experimental model with which translational research could be performed.

iPSC-CM are a recently developed technology, whereby human dermal fibroblasts can be reliably harvested, dedifferentiated into a pluripotent form, and then differentiated into cardiomyocytes. These cells have an established intracellular calcium handling system and contractile capacity, however are generally considered to be at a foetal stage of development. A key aim of this project was to characterise the metabolic phenotype of these cells, in order to assess their potential suitability as the basis of a novel cellular model of DCM. Specifically, it was investigated if these cells exhibited robust insulin stimulated glucose uptake through insulin sensitive intracellular trafficking of the glucose transporter GLUT4, as impairment of this response is a central feature of any diabetic model.

After adaptation of a [^{3}H]-2-deoxyglucose uptake assay to a 96-well plate format, and optimisation of experimental factors, it was determined that iPSC-CM could not display robust insulin (or IGF-1) stimulated glucose uptake. Inhibition of the spontaneous contractile capacity of these cells did not induce a response upon subsequent insulin stimulation. iPSC-CM were found to express and activate central insulin signalling molecules such as Akt and Erk1/2, and also possess elements of the GLUT4 trafficking machinery such as the SNARE proteins Syntaxin 4 and SNAP23. However, the critically limiting factor identified was an approximate 10-fold lower expression of GLUT4 in iPSC-CM compared to primary adult cardiomyocytes, accompanied by strong expression of GLUT1. This data was supported by the finding that inhibition of GLUT4 had no impact on glucose uptake in iPSC-CM, whereas inhibition of GLUT1 significantly reduced uptake by ~50%.

This phenotype suggests that iPSC-CM are also at a foetal-like stage of development with regards to their metabolic capacity, and are currently not suitable for modelling DCM.

Subsequently, initial interventions based upon the literature were implemented in order to try and increase iPSC-CM GLUT4 content. However, neither increasing metabolic reliance upon fatty acid (rather than glucose) nor exposure to triiodothyronine were successful. In contrast, Lipofectamine 2000 mediated transfection of a customised GLUT4 plasmid facilitated a reliable 3-5 fold increase in iPSC-CM GLUT4 content. This increased basal glucose uptake, however did not induce an insulin response. It was concluded that a further increase in expression levels may be required. Finally, it was demonstrated that iPSC-CM are highly amenable to lentiviral mediated infection, and initial steps were taken towards the generation of a virus targeting the overexpression of GLUT4.

Additionally, SNARE proteins are essential in facilitating insulin stimulated GLUT4 expression at the plasma membrane. Therefore they represent a possible mechanism by which cardiac insulin resistance could occur in disease states such as DCM. On account of this, the expression of a wide range of SNARE protein isoforms was assessed in cardiac lysates generated from 2 diabetic mouse models (*db*/*db* and high fat diet induced). The expression of SNAP29 and VAMP5 were found to differ in lysates from the high fat diet model, although the role of these proteins in GLUT4 trafficking is unclear. In contrast, in the more severe diabetic *db*/*db* model GLUT4 protein content was found to be significantly reduced, but SNARE protein content was unaffected.

Finally, there is also an established link between glycemic control and both the risk of developing and subsequent prognosis for myocardial infarction (MI). There is a line of evidence suggesting that cardiac insulin sensitivity may also be highly relevant in this disease context. Accordingly, it was demonstrated that cardiomyocytes isolated from a clinically relevant 8-12 weeks post-MI rabbit model exhibited impaired insulin stimulated glucose uptake. This strengthens the association between MI and cardiac metabolic parameters. However, insulin stimulated phosphorylation of Akt, GLUT4 levels, and SNARE protein expression were unaffected post-MI. Therefore future work must identify both the underlying mechanism and clinical relevance of this finding.

Table of Contents

List of Tables

List of Figures

Acknowledgements

First and foremost I would like to express my sincerest gratitude to the British Heart Foundation for their generous funding and support of this project. The 4-year PhD programme was a fantastic experience and learning opportunity that I will always value for the rest of my career. In particular I would like to thank the volunteers who selflessly give up their time in order to raise funds for the BHF, their commitment and passion to make a positive impact is inspiring.

I would also like to express my deepest thankfulness to Prof. Gwyn Gould. I could not have hoped for a more supportive, engaging, and knowledgeable supervisor. From the second I saw the Hokas on your office floor, I knew that we would be a great combination. I would also like to thank my second supervisor Prof. Godfrey Smith for his valued contribution whenever called upon.

I am also grateful to have completed my PhD studies in a uniquely warm and supportive research environment in Lab 241. Weekly meetings and close association with Dr. Ian Salt's group provided a constant stimulus for reflection upon my work and helped me to find solutions to research problems on several occasions. However, in particular I must express my thanks to Dr. Mohammed Nasser Rashid Al-Tobi and Omar Janha, who taught me so much about life both in and outside of the lab. Meeting you guys was the highlight of my PhD by far.

Additionally, I would like to say a massive thank you to all of my friends and family for their constant support throughout my PhD. Whenever battling the inevitable challenges of postgraduate research I was lucky to have several other interests to follow and keep everything in perspective.

Finally, I am so grateful to CC. I know that you probably will not read past this part of the thesis, however without your unwavering love and support I would not have been able to write the following pages with efficiency and a smile on my face.

Thank you all,

PeBo.

Author's Declaration

I declare that the work presented in this thesis is my own, unless otherwise cited or acknowledged. It is entirely of my own composition and has not, in whole or in part, been submitted for any other degree.

Peter Ronald Thomas Bowman

November 2018

Definitions/Abbreviations

α	Prefix alpha
ß	Prefix beta
θ	Prefix theta
k	Prefix kilo
m	Prefix milli
μ	Prefix micro
n	Prefix nano
p	Prefix pico
º	Degrees
2DG	2-deoxy-glucose
A	Amps
AMPK	Adenosine monophosphate activated protein kinase
APD	Action potential duration
ATP	Adenosine triphosphate
BCA	Bicinchoninic acid
BMI	Body mass index
BMP	Bone morphogenetic protein
BNP	Brain natriuretic peptide
BSA	Bovine serum albumin
CamKII	Calcium/calmodulin dependent protein kinase II
CB	Cytochalasin B
CDI	Cellular Dynamics International
Ci	Curie
CPM	Counts per minute
CPT	Carnitine palmitoyltransferase

DAG	Diacylglycerol
DCM	Diabetic cardiomyopathy
DNA	Deoxyribonucleic acid
E.Coli	Escherichia coli
eNOS	Endothelial nitric oxide synthase
ERK	Extracellular signal regulated kinase
FATP	Fatty acid transport protein
FBS	Foetal bovine serum
FFA	Free fatty acid
g	gram
GAP	GTPase activating protein
GAPDH	Glyceraldehyde 3 phosphate dehydrogenase
GFP	Green fluorescent protein
GST	Glutathione S transferase
GSV	GLUT4 storage vesicle
HEK cell	Human embryonic kidney cell
HFD	High fat diet
IGF-1	Insulin like growth factor 1
IgG	Immunoglobulin G
iPSC-CM	Induced pluripotent stem cell derived cardiomyocytes
IR	Insulin resistance
IRAP	Insulin regulated aminopeptidase
IRS-1	Insulin receptor substrate 1
kDa	kilo Daltons
L	Litre
LRP1	Low density lipoprotein receptor related protein 1

LSB	Laemmli sample buffer
LTCC	L-type calcium channel
MAPK	Mitogen activated protein kinase
MCP-1	Monocyte chemoattractant protein 1
MEF	Myocyte enhancer factor
m	Metre
M	Molar
MI	Myocardial infarction
Min	Minute
MM	Maturation medium
MOI	Multiplicity of infection
mRNA	Messenger ribonucleic acid
NCS	New born calf serum
NO	Nitric oxide
PCr	Phospho-creatine
PDK1	Phosphoinositide dependent kinase 1
PI3K	Phosphoinositide 3 kinase
PIP2	Phosphatidylinositol 4,5-Bisphosphate
PIP3	Phosphatidylinositol 3,4,5-trisphosphate
PKA	Protein kinase A
PKC	Protein kinase C
ROS	Reactive oxygen species
Rpm	Revolutions per minute
RyR	Ryanodine receptor
SERCA	Sarcoplasmic reticulum calcium ATPase
SGLT2	Sodium-Glucose linked transporter

SM	Sec1p/Munc18
SNARE	Soluble N-ethylmaleimide-sensitive factor activating protein receptor
SOC	Super optimal broth with catabolite repression
SR	Sarcoplasmic reticulum
T_3	Triiodothyronine
TDI	Tissue Doppler imaging
TGN	*Trans* Golgi network
TNF	Tumour necrosis factor
U	Units
V	Volts
v/v	volume per volume
VAMP	Vesicle associated membrane protein
VCAM-1	Vascular cell adhesion molecule 1
w/v	weight per volume
WHO	World Health Organisation

1 Introduction

1.1 Diabetes

1.1.1 Diabetes is a growing healthcare burden

Diabetes is primarily defined by a pathological sustained elevation in blood glucose concentration. WHO guidelines published in 2006 indicated that blood glucose cut off scores of >7 mmol/L (126 mg/dL) when fasting or >11.1 mmol/L (200 mg/dL) 2 hours after ingestion of 75 g glucose should be used to diagnose the presence of this condition. These guidelines were updated in 2011 to recommend that the detection of circulating glycated haemoglobin (HbA1c) above 6.5% is also an appropriate marker.

Recent analysis underlined the rising scale of the challenge diabetes is posing as a developing global issue. In 2015, there were an estimated 415 million individuals between the ages of 20 and 80 living with diabetes, at a worldwide healthcare cost of 673 billion dollars (Ogurtsova *et al.*, 2017). In order to further demonstrate the magnitude of this burden, this analysis also estimated that approximately 5 million deaths that year were primarily attributable to diabetes, which is almost equal to the entire population of Scotland. Statistical modelling produced predictions that by 2040 the number of individuals impacted by diabetes may rise to 642 million, just shy of 10% of the world's entire population. Therefore, diabetes is a growing healthcare problem that requires urgent intervention to both reduce its prevalence through preventative measures, and enhanced treatment options to reduce associated mortality rates.

1.1.2 Complications

The urgency for the development of novel strategies to improve diabetes care is strongly linked to the severity of complications of this condition. An acute rise in blood glucose concentration is not a critical issue, however prolonged elevation is highly toxic to blood vessels and has profound implications for the tissues they supply.

With regards to the effects of diabetes upon microvasculature – small vessels such as arterioles and capillary beds that are proximal to target organs and tissues - there are 3 main recognised complications. Diabetic retinopathy and nephropathy refer to loss of function of the vessels serving the eyes and kidneys respectively,

which can result in blindness and kidney failure (Cade, 2008). However, the complication perhaps most strongly associated with diabetes is related to neuropathy - dysfunction of the microvessels serving nerves - and referred to as diabetic foot. A combination of decreased afferent sensation, loss of autonomic functions such as sweating, and reduced vascular perfusion in peripheral anatomical regions such as the feet lead to not only a significant increase in the risk of developing ulcers and infections but also a reduced awareness and ability to detect these events, which often delays treatment and results in the only available option being amputation (Pendsey, 2010).

All of these conditions summarised are severely debilitating in advanced forms and possibly even life threatening. However, the greatest threat to diabetic individuals comes from complications within larger vessels such as arteries. There is a long appreciated association between diabetes and the risk of classic cardiovascular disease (Kannel and McGee, 1979), and indeed this is the leading cause of death in this patient population. Of particular concern is the elevated risk of developing atherosclerosis, which is an inflammatory driven remodelling process within the vascular wall that results in the formation of a characteristic lipid rich lesion/plaque that results in narrowing of the vessel lumen (Fowler, 2008). Combined with several other factors these changes greatly increase diabetic patients risk of sustained elevations in blood pressure i.e. hypertension (Sowers *et al.*, 2001), which is a strong independent risk factor for heart failure. Alternatively, if atherosclerotic lesions rupture then this can result in total occlusion of a vessel and therefore prevention of perfusion of the downstream tissue. Where this occurs in the coronary vasculature this is referred to as a myocardial infarction (MI), and is immediately life threatening. This condition is discussed further in section 1.5.1.

An important issue to consider is how sustained hyperglycemia can lead to the myriad of pathological events described. The physiological mechanisms underlying these associations are complex and multifaceted, however one particularly important factor is endothelial dysfunction. In healthy individuals, smooth muscle vascular tone is regulated by the release of nitric oxide (NO) from associated endothelial cells. This provides a mechanism by which blood flow can be directed to where it is needed by increasing or decreasing vessel diameter through

muscular relaxation or constriction respectively. Additionally, NO is considered vasoprotective on the basis of its actions to reduce aberrant smooth muscle cell proliferation, the permeability of the vascular wall and the oxidation of lipids (all key events in plaque formation), and also to decrease the expression of several proteins (e.g. MCP-1 and VCAM-1) that are key in recruiting the inflammatory cells that drive the atherosclerosis process (Li and Forstermann, 2000). Experimental models have indicated that hyperglycemia may increase mitochondrial superoxide production, which in turn increases the production of hexosamines that reduce the phosphorylation and therefore activity of eNOS – the enzyme responsible for NO production (Du *et al.*, 2001). Reduced NO availability will thereafter reduce vascular function and also increase susceptibility to injury.

1.1.3 Causes

Diabetes is generally split into 2 distinct categories. Whilst terminology can vary, each category has a distinct phenotype related to the action of insulin. Post-prandially, in response to an increased presence of glucose in the bloodstream at the end point of the digestive process, insulin is released from the pancreas in order to stimulate the uptake of glucose into peripheral insulin sensitive tissues (most notably muscle and fat). This action is necessary to maintain blood glucose concentration below approximately 5.5 mmol/L.

In type one diabetic individuals insufficient insulin is produced by the pancreas, therefore they are reliant upon regulated insulin injections in order to maintain glycemic control. This condition is an autoimmune disease whereby immune cells target and destroy the beta cells of the pancreas that produce insulin. It is largely attributed to genetic factors (Todd *et al.*, 2007), however there is an emerging belief that there may also be important environmental triggers, for example exposure to certain viruses (Knip *et al.*, 2005). In contrast, type two diabetes is the predominant form of this condition, whereby the sensitivity of peripheral tissues to insulin is significantly reduced. Where this occurs, this is referred to as insulin resistance (IR). It is this form of the condition that is of primary interest in this thesis. Whilst genetic factors have been cited as influencing an individual's risk of developing type 2 diabetes (Dupuis *et al.*, 2010), this condition is primarily associated with lifestyle factors leading to weight gain and the development of obesity (Resnick *et al.*, 2000).

1.1.4 Treatments

With regards to managing diabetes, regardless of whether it is type 1 or type 2, the key concept is to regularly monitor and maintain blood glucose values within an acceptable range. However, the means by which this may be achieved will vary between conditions and also between individuals. The primary area of treatment for type 1 diabetics is insulin injections, at appropriate times and of sufficient dosage to substitute for normal physiological functioning. Individuals with type 2 diabetes may also eventually require insulin therapy, however during the early stages of treatment insulin production is not a primary issue and therefore this is not typically required. There are a range of drugs typically prescribed for type 2 diabetics, each with a specific mechanism(s) of action. For example, metformin improves peripheral insulin sensitivity, sulphonylureas enhance insulin release from the pancreas, and SGLT2 inhibitors increase the excretion of glucose from the body via urine. A systematic review identified that when delivered as a monotherapy, metformin was determined to be the most effective and safest treatment option, relative to a range of other drugs (Maruthur *et al.*, 2016). This was based upon key outcomes, including cardiovascular mortality, HbA1c levels, and body weight. This finding supports current clinical practice whereby metformin is most commonly delivered as a first-line pharmaceutical therapy.

Asides from pharmacological strategies, the most important and widely prescribed therapeutic interventions for diabetic individuals are lifestyle based. A combination of improved diet and exercise regime can be used to target better management of blood glucose values and whole body composition, in particular aiming for sustained weight (fat) loss. A recent meta-analysis concluded that a weight loss of greater than 5% total body weight was required to elicit sustained significant metabolic improvements in diabetic patients, and the authors suggested that this was a challenging goal to meet for this patient population (Franz *et al.*, 2015). However, in scientific literature exercise is often treated as a single concept, ignoring the almost unlimited possible combinations of duration/frequency/intensity/modality that can be implemented, each providing a unique stimulus for adaptation. A 12-week high intensity cycling based interval programme significantly improved cardiac function and reduced liver fat content in type 2 diabetics, accompanied by small improvements in glycemic control

(Cassidy *et al.*, 2016). Therefore, further optimisation of these interventions is required, as it is highly likely improved outcomes can be achieved.

Finally, bariatric surgery is currently receiving widespread attention as a novel therapy for obesity by means of regulating food intake by physically reducing the size of the stomach. For example, gastric banding led to remission of 73% of diabetic patients 2 years after undergoing this procedure, reflected in a reduction in fasting blood glucose and Hb1Ac values below diagnostic cut off scores, largely attributed to drastic weight loss (20% of body weight) relative to patients undergoing a standard course of treatment (Dixon *et al.*, 2008). Similarly impressive results have been achieved with alternative forms of bariatric surgery (Mingrone *et al.*, 2012). This treatment option holds great promise for the treatment of diabetes in general, however longer term outcomes, safety, and sustainability as a widespread intervention (considering the prevalence of diabetes) require further assessment.

What can be concluded with confidence is that based upon current prevalence and mortality rates associated with diabetes, current treatments are not sufficient. In order to change this, research must be performed in order to further our understanding of the key physiological processes underlying diabetes. These are primarily related to the action of insulin in peripheral tissues. This will require innovation and the development of novel experimental models, in order to maximise the translational value of generated findings and provide platforms for assessing the impact of various derived interventions.

1.2 Insulin stimulated glucose uptake

1.2.1 GLUT4 trafficking overview

Insulin is a critical hormone in the regulation of whole body metabolic homeostasis, with multiple effects on several target tissues. For example, it suppresses the production and release of glucose within the liver (Puigserver *et al.*, 2003), in part contributing to its overall effect of reducing blood glucose concentration in order to return it to an optimal set point after transient deviations, typically after the digestion of food. This balance is required to ensure glucose is constantly available to provide vital metabolic fuel to tissues such as

the brain, but does not chronically accumulate to levels that risk the complications outlined in section 1.1.2. The primary mechanism through which insulin achieves this regulatory action is to stimulate the uptake of glucose into peripheral tissues, where it is either used to produce adenosine triphosphate (ATP) or is stored as glycogen or in lipid form. Predominantly this uptake refers to transport into skeletal muscle, with only approximately 10% of glucose entering the bloodstream ending up in adipose tissue. It is important to note that this does not undermine the importance of adipose tissue in whole body glucose homeostasis. A recently developed understanding of adipose tissue has led to its recharacterisation as an endocrine organ, rather than simply an energy storage depot, and hormones released by adipose such as adiponectin strongly influence systemic insulin sensitivity and therefore blood glucose values (Lihn *et al.*, 2005).

The mechanism by which insulin stimulates an increase in glucose uptake is dependent upon complex interactions between dozens of proteins that regulate the subcellular localisation of the glucose transporter type 4 (GLUT4) (Leto and Saltiel, 2012). This process is referred to as GLUT4 trafficking and is fundamental to metabolic control. Each of the most relevant components of GLUT4 trafficking will be detailed in subsequent sections, however Figure 1-1 details the fundamental concept to provide an initial basic overview. Under basal conditions, the majority of GLUT4 is contained intracellularly within specialised structures termed GLUT4 storage vesicles (GSVs). In response to insulin stimulation these GSVs are shuttled to the plasma membrane where they dock and fuse in order to promote integration of GLUT4, which facilitates the uptake of glucose. After cessation of insulin stimulation, GLUT4 is reinternalised into a general endosomal system, before being sorted back into GSVs at the *trans* Golgi network (TGN) (Huang and Czech, 2007).

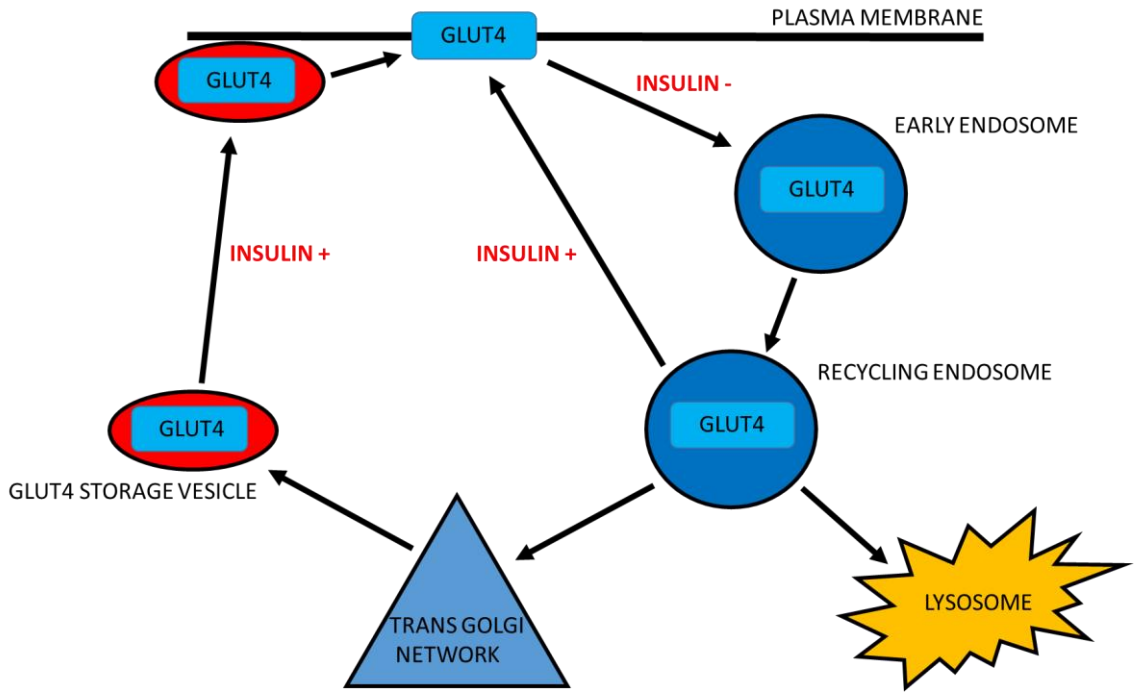

Figure 1-1 GLUT4 trafficking overview
GLUT4 must be expressed at the plasma membrane in order to facilitate cellular glucose uptake. After endocytosis it enters a general endosomal recycling pathway. From here it can either be cycled back to the plasma membrane, targeted for degradation in the lysosome, or sequestered into a specialised insulin sensitive storage pool of GSVs via the TGN. Upon subsequent insulin stimulation the primary response is translocation of GSVs to the plasma membrane, where they are subsequently tethered in place and ultimately fuse in order to promote GLUT4 expression at the cell surface. Insulin also acts to reduce rates of GLUT4 endocytosis and increase cycling from endosomes back to the plasma membrane.

1.2.2 GLUT transporters

Insulin stimulation is required in order to facilitate the uptake of glucose into target cells because it cannot simply diffuse across the plasma membrane. Rather, specialised glucose transporters are required to perform this function. The SLC2 genes encode for 14 isoforms of a family of hexose transporters collectively referred to as GLUTs, which are each composed of approximately 500 amino acids and predominantly vary in their substrate specificity and tissue distribution (Mueckler and Thorens, 2013). The structure of these proteins is defined by a characteristic series of α-helices that spans the plasma membrane 12 times, a central substrate binding site, and N-linked glycosylation on an exofacial domain (Mueckler and Thorens, 2013).

In the context of diabetes and this project, the GLUT isoform that facilitates the increase in glucose transport in muscle and adipose in response to insulin stimulation is of primary interest. As will be fully explained and evidenced in

section 4.1, this isoform is GLUT4. As reviewed by Minokoshi *et al.* (2003) a variety of GLUT4 knockout out rodent models have been generated, and the consistent finding regardless of the specific details (such as tissue knockout specificity) is the onset of severe systemic IR. The importance of GLUT4 to the regulation of glucose metabolism via insulin is also reflected in its near exclusive expression in the predominant insulin sensitive tissues of muscle and adipose (Huang and Czech, 2007).

The most important factor that regulates the action of GLUT4 is its subcellular localisation. Under basal conditions a very small fraction of cellular GLUT4 content is located at the plasma membrane, whereas in response to insulin stimulation a potent redistribution towards the plasma membrane occurs. Reinternalisation of any membrane bound molecule facilitates entry into the general endosomal recycling pathway, whereby after initial generation of early endosomes vesicular cargo can be targeted to lysosomes for degradation, to the TGN for repackaging, or returned to the plasma membrane (Grant and Donaldson, 2009). In rat skeletal muscle 2 separate pools of GLUT4 content were identified, one that exhibited a limited response to insulin and that colocalised with the transferrin receptor and annexin II, which are markers of this general endosomal system, and another that did not colocalise with these markers and was highly sensitive to insulin stimulation (Aledo *et al.*, 1997). Similarly, only approximately 40% of GLUT4 containing vesicles from 3T3-L1 adipocytes contained the transferrin receptor, and specific ablation of transferrin receptor positive vesicles only depleted around 40% of cellular GLUT4 content (Livingstone *et al.*, 1996). Combined these studies provide strong evidence of a specialised highly insulin sensitive storage pool of GLUT4, which we now know to be contained within GSVs.

Initial characterisation of GSVs has revealed that in addition to GLUT4 they also contain IRAP, sortillin, LRP1, and Vesicle associated membrane protein 2 (VAMP2), based upon analysis of their protein composition and cotranslocation to the plasma membrane in response to insulin (Bogan and Kandror, 2010). Specific knock down of IRAP (>90%) in 3T3-L1 adipocytes reveals a crucial role for facilitating sorting of GLUT4 into GSVs and therefore basal retention, as an increased content of GLUT4 was located in the endosomal system and was able to traffic back to the plasma membrane (Jordens *et al.*, 2010). Interestingly corresponding knock down

of GLUT4 has no discernible impact upon the trafficking of IRAP (Yeh *et al.*, 2007). Similarly, manipulation of sortillin expression in these cells reveals this protein to be critical in the biogenesis of GSVs, with a corresponding impact upon cellular insulin stimulated glucose uptake capacity (Shi and Kandror, 2005). A proteomic screen of GSVs isolated from primary rat adipocytes revealed identification of ~100 proteins, which underlines the complexity of these vesicles, however LRP1 was identified as a major component capable of interacting directly with both GLUT4 and insulin signalling molecules (Jedrychowski *et al.*, 2010). The exact function of LRP1 is still unclear, however its deletion also impacted the capacity of 3T3-L1 adipocytes to increase glucose uptake in response to insulin. Finally, ~90% of cellular VAMP2 content localises to the GSVs (Martin *et al.*, 1996), however the action of this protein will be discussed in detail in section 1.2.4.

The uptake of glucose into muscle and adipose tissue cannot be complete without acknowledgement of the role of GLUT1. The expression of this transporter is far more widespread in a range of tissues and it is mostly located permanently within the plasma membrane rather than under the regulation of any hormone or other signalling molecules. In rat muscle, where the expression of GLUT4 is strongly linked to the maximal insulin stimulated glucose uptake capacity of that tissue, acute changes in GLUT1 expression much more strongly correlate with basal metabolic glucose uptake (Kraegen *et al.*, 1993), and indeed this is its generally accepted role. Whilst reduced vastus lateralis GLUT1 protein content was associated with reduced basal glucose uptake in type 2 diabetic patients (Ciaraldi *et al.*, 2005), this transporter is not considered particularly relevant to the pathogenesis of IR and diabetes when compared to GLUT4.

1.2.3 Insulin signalling

As stated, insulin stimulation is the key factor that initiates rapid redistribution of GLUT4 from its specialised internal location to the plasma membrane, in order to increase cellular glucose uptake. It achieves this action primarily through the action of 2 intracellular signalling cascades, one which is dependent upon the activation of phosphoinositide-3-kinase (PI3K), and one which is dependent upon APS activation (adaptor protein with pleckstrin homology and Src homology 2 domains) (Leto and Saltiel, 2012). The key concept is that these pathways either directly, or indirectly through the activation of small GTPases (and associated

GTPase activating proteins (GAPs)), activate trafficking machinery capable of initiating GSV translocation, tethering, and fusion with the plasma membrane (Stenmark, 2009). These pathways are depicted in Figure 1-2.

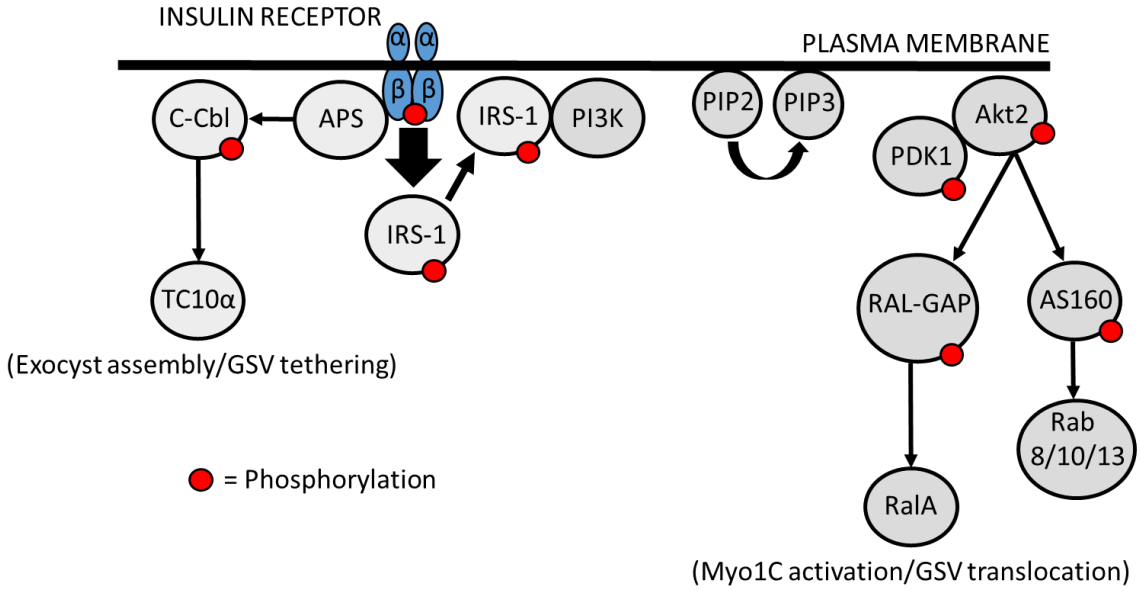

Figure 1-2 Insulin signalling cascades relevant to GLUT4 trafficking
Key signalling events in the process of insulin stimulated GLUT4 trafficking are depicted. Note that this list is not exhaustive, but highlights the best characterised and known interactions. A series of phosphorylation/activation events triggered by activation of the insulin receptor eventually results in the activation of small GTPases, which interact with effector proteins in order to initiate GSV translocation, tethering, and fusion with the plasma membrane. Where specific molecular interactions of GTPases (TC10α, RalA, Rab 8/10/13) that underpin trafficking events have been identified, these are indicated. For full details see main text.

Insulin initially binds to the 2 α-subunits of its corresponding membrane bound receptor, which induces autophosphorylation and activation of the tyrosine kinase activity in its internal facing ß-subunits (Lee and Pilch, 1994). This leads to tyrosine phosphorylation of the insulin receptor substrate (IRS-1), which in turn activates PI3K. Disruption of the function of either of these proteins leads to impaired insulin stimulated glucose uptake and GLUT4 plasma membrane expression in adipocytes (Clarke *et al.*, 1994; Quon *et al.*, 1994). PI3K catalyses the conversion of PIP2 to PIP3, which is necessary to recruit PDK1 and protein kinase B (Akt) to the cell membrane. Phosphorylation and therefore activation of Akt2 by PDK1 is a central step in this cascade. Accordingly, rapid pharmacological activation of Akt2 to a physiologically relevant degree was able to induce a level of GLUT4 translocation comparable to the action of insulin (Ng *et al.*, 2008).

It must be stated that at all points in this process there have been multiple additional signalling branches and interactions proposed, however Akt2 dependent activation of the RAL-GAP complex and the GAP AS160, each of which regulate the activation of distinct GTPases, are consistently cited as particularly important. AS160 is associated with GSVs under basal conditions and acts to maintain several Rab GTPases in their inactive form in order to sustain the basal retention of GLUT4, as exemplified by inhibition of AS160, which enhances plasma membrane GLUT4 expression (Larance *et al.*, 2005). One key target of AS160 in adipocytes is Rab 10, as not only is an increase or decrease in its expression mirrored in changes in GLUT4 plasma membrane expression, but in the AS160 knockdown model just described, subsequent additional knockdown of Rab 10 is sufficient to partially re-establish basal GLUT4 intracellular detention (Sano *et al.*, 2007). There is evidence that AS160 signalling through Rab 8 and Rab 13 may assume this role in skeletal muscle (Sun *et al.*, 2010), indicative of cell type specific mechanisms in the process of GLUT4 trafficking. Similarly, knock down of the RAL-GAP complex in adipocytes increased glucose uptake in association with increased activity of the downstream Rab RalA (Chen *et al.*, 2011). With regards to relating these experimental findings to the *in vivo* action of insulin, in both cases Akt mediated phosphorylation of the respective GAP proteins is thought to relieve their inhibitory effects upon their target downstream GTPases, which in turn activate different parts of the trafficking machinery.

The insulin dependent APS pathway is less well defined, however impairment of this pathway was also found to significantly blunt insulin stimulated GLUT4 translocation in 3T3-L1 adipocytes (Liu *et al.*, 2002). Although overexpression of APS was found to enhance and prolong insulin receptor autophosphorylation and activation of the PI3K pathway (Ahmed and Pillay, 2003), this is not the primary mechanism through which it impacts GLUT4 trafficking. In response to cellular insulin stimulation, tyrosine phosphorylation of APS increases as it binds directly to the insulin receptor, resulting in subsequent activation of the proto-oncogene c-Cbl. The downstream target of this pathway is ultimately the GTPase TC10α, which displays activation in response to insulin even in the presence of pharmacological inhibition of PI3K (Chang *et al.*, 2007). Furthermore, subsequent knockdown of TC10α reduced insulin stimulated GLUT4 translocation and glucose uptake, without impacting Akt activation (Chang *et al.*, 2007).

A key question arising from the described model and mechanisms so far is exactly how these PI3K dependent and independent signalling cascades translate activation of the insulin receptor into the regulated movement of GSVs. Whilst there is evidence that insulin may reduce the rate of reinternalisation of GLUT4 from the plasma membrane (Czech and Buxton, 1993) and increase the rate of exocytosis of GLUT4 from the general endosomal cycle (Muretta *et al.*, 2008), by far the major action of this hormone is to increase the rate of exocytosis of GLUT4 from GSVs. This requires initiation of translocation of GSVs to the plasma membrane, docking and tethering at this location, and then finally fusion of the membranes to permit integration of GLUT4 at the cell surface. This final fusion step is regulated by interactions of SNARE proteins, and will be discussed in section 1.2.4.

The integrity and remodelling capacity of microtubule and actin networks are essential for the translocation of GSVs to the cell membrane in response to insulin stimulation (Olson *et al.*, 2001; Tong *et al.*, 2001). Evidence suggests that insulin may stimulate an increase in phosphorylation and therefore activity of the myosin ATPase motor protein Myo1C, which in association with enhanced colocalisation with GSVs may power movement of this vesicle along developed actin tracks to the cell membrane (Bose *et al.*, 2002; Yip *et al.*, 2008). Once GSVs arrive at the plasma membrane, prior to fusion they are initially tethered in place via a multi-protein complex referred to as the exocyst. One of the key components Exo70 exhibits translocation to the membrane in response to insulin stimulation and its mutation reduces insulin stimulated glucose uptake without impairing GLUT4 trafficking (Inoue *et al.*, 2003). Similarly, two other components of the exocyst (Sec6 and Sec8) have also been shown to redistribute towards the plasma membrane in response to insulin, and their overexpression enhances insulin stimulated glucose uptake without impacting the rate of activity of other exocytosis pathways (Ewart *et al.*, 2005). These results suggest that the exocyst complex may be specifically involved in the regulation of GLUT4 exocytosis.

The interactions between GTPases at the end point of insulin signalling cascades and these effector proteins are at an early stage of characterisation, however already important links have been established. For example, activated TC10α interacts directly with Exo70 in order to initiate exocyst complex formation (Inoue

et al., 2006). Similarly, RalA has been demonstrated to associate with the GSV and interact with both Myo1C and elements of the exocyst complex, suggesting that it could initiate GSV translocation and targeted docking at appropriate locations at the plasma membrane (Chen *et al.*, 2007). Continued investigation of similar mechanisms will facilitate further understanding of the cross over between insulin signalling and GLUT4 translocation.

1.2.4 SNARE proteins

Soluble N-ethylmaleimide-sensitive factor attachment protein receptors (SNAREs) are evolutionary conserved proteins that are vital in the understanding of intracellular trafficking and exocytosis due to their primary action of facilitating the fusion of biological membranes. Classically, different SNAREs have been grouped according to their functional location. SNAREs located on a vesicular membrane that are mostly from the VAMP family were referred to as v-SNAREs, whereas SNAREs on the target membrane (to where the cargo is being delivered) that are typically from the Syntaxin and SNAP families were referred to as t-SNAREs. VAMP and Syntaxin proteins are anchored to the respective membrane via their C-terminus, and each contain one classic SNARE motif, which is a ~60 amino acid sequence that is critical to the action of these proteins (Hong, 2005). In contrast, SNAP proteins are anchored to the membrane via palmitoylation, and contain 2 SNARE motifs.

The formation of a functional SNARE complex refers to the generation of a highly stable 4 α-helix complex derived from 4 SNARE motifs, and therefore at minimum require the interaction of one VAMP, one Syntaxin, and one SNAP isoform. At the core of this 16 layered structure there is an interaction between one residue from each motif referred to as the "0 layer", and the presence of either a glycine or arginine residue from each respective motif has led to the proposed structural reclassification of Q or R SNAREs respectively. The SNARE hypothesis dictates that the formation of this complex in a "zippering" action from N-terminus to C-terminus brings the opposing membranes into intimate physical proximity and provides the necessary energy for their fusion (Fasshauer, 2003).

Intracellular trafficking requires a high degree of specificity so that molecules only end up at their intended and required destination. A central component of the

SNARE hypothesis is that only unique combinations of SNAREs will functionally interact *in vivo*, thus providing a mechanism of regulation (McNew *et al.*, 2000). SNARE proteins are critical to the process of insulin stimulated GLUT4 trafficking (Cheatham *et al.*, 1996), and identification of the specific isoforms in this process and understanding the regulation of their interactions in a state of both health and disease is of importance for the pathophysiological mechanisms underlying diabetes.

With regards to the fusion of GSVs and the plasma membrane, it is widely accepted that the t-SNAREs involved are Syntaxin 4 and SNAP23 (Olson *et al.*, 1997; Kawanishi *et al.*, 2000). However, on account of the promiscuity of SNAREs both *in vitro* and *in vivo* (particularly upon overexpression), the VAMP family isoform involved in this complex had been the source of greater debate (Bryant and Gould, 2011). Sadler *et al.*, (2015) underlined this issue by demonstrating that all 7 of the known VAMP isoforms were capable of forming the characteristic SDS-resistant SNARE complex with SNAP23 and Syntaxin 4. However, based primarily upon relative expression levels and subcellular distribution, it was concluded that VAMP2 was the v-SNARE involved in this reaction *in vivo*, at least in 3T3-L1 adipocytes, which are a widely used experimental model for insulin stimulated GLUT4 trafficking.

Based upon the described mechanism by which SNARE proteins promote membrane fusion, it can be appreciated that the primary factor determining their action is their intracellular localisation, which in the case of any GSV associated SNARE is tightly regulated by insulin, as described in section 1.2.3. However, the ability of Syntaxin proteins to participate in SNARE complex assembly is also believed to be regulated by proteins from the Sec1p/Munc18 (SM) family. Specifically, Munc18c regulates the action of Syntaxin 4 through a direct mechanism, however the exact nature of this regulation is unclear and may be partially dependent upon the conformation state of Syntaxin 4 upon binding (it can exist in an open or closed form) and the phosphorylation status of Munc18 (Laidlaw *et al.*, 2017). To underline this confliction, overexpression of Munc18c in 3T3-L1 adipocytes impaired insulin stimulated GLUT4 (and IRAP) expression at the plasma membrane, suggesting that this protein has an inhibitory action on Syntaxin4-VAMP2 interactions (Thurmond *et al.*, 1998). In contrast, heterozygous Munc18c

knockout mice exhibited impaired systemic insulin sensitivity and skeletal muscle GLUT4 plasma membrane translocation, suggesting that it is essential for SNARE complex assembly (Oh *et al.*, 2005).

When considering the involvement of SNAREs in insulin stimulated glucose uptake, it is common to only consider the action of Syntaxin 4, VAMP2, and SNAP23. However, the efficiency of the intracellular sorting process of GLUT4 after reinternalisation (or initial synthesis) back into GSVs in preparation for future insulin stimulation is equally critical for the continued efficacy of this response. Arguably, and perhaps related to the increased complexity of this process, this part of GLUT4 trafficking is less well characterised, however key players have been identified.

For example, in 3T3-L1 adipocytes, whilst Syntaxin 7, 8, and 12/13 were all found to colocalise with the GSV to a small degree, approximately 85% of cellular Syntaxin 6 was associated with the GSV and also exhibited insulin stimulated translocation to the plasma membrane (Perera *et al.*, 2003). Impairment of the action of Syntaxin 6 resulted in increased basal glucose uptake, attributed to impaired GLUT4 reinternalisation and sorting into GSVs after the cessation of insulin stimulation, which would therefore permit spontaneous recycling of GLUT4 back to the plasma membrane. Similarly, the reduction of Syntaxin 16 expression by >90% resulted in a ~30% reduction in cellular GLUT4 content and impaired insulin stimulated GLUT4 translocation (Proctor *et al.*, 2006). The cycling of the transferrin receptor was unchanged, indicative of no impact upon general endosomal trafficking, which strongly suggests that Syntaxin 16 is vital to the sequestration of GLUT4 away from general endosomal recycling into its specialised GSV pool. It has also been demonstrated that the integrity of a short amino acid in the C-terminus of GLUT4 is integral for its efficient sorting into GSVs (Shewan *et al.*, 2000), leading to the proposal of a model whereby this sequence enables the exit of GLUT4 from the general endosomal system, and Syntaxins 6 and 16 facilitate subsequent entry into the specialised insulin sensitive pool (Shewan *et al.*, 2003).

It must be acknowledged that the majority of knowledge regarding the action of SNARE proteins in insulin stimulated GLUT4 trafficking has been obtained from the

study of 3T3-L1 adipocytes. The specific isoforms and actions of these proteins in the heart will be discussed in section 5.1.2.

1.2.5 Theories of insulin resistance

Whilst the diagnostic criteria for diabetes refers to the levels of glucose (directly or indirectly) in the blood, this is largely a reflection of systemic insulin sensitivity. Accordingly, given that the vast majority of glucose is transported into skeletal muscle, the main phenotype of diabetes is strongly related to the development of IR in this tissue. As will become clear, this does not mean that alterations in metabolic regulation in other tissues is not of critical importance. However, the pathology underlying IR has been widely studied in skeletal muscle, and consideration of this literature provides an excellent platform for understanding this general concept.

1.2.5.1 Fatty acid overload?

Primarily, the development of IR in skeletal muscle has been linked to increased fatty acid availability, associated with chronic over feeding and the onset of obesity. This general association was demonstrated by study of first degree relatives of diabetics, who have an elevated risk of also developing this condition. These individuals exhibited elevated resting circulating FFA and insulin concentrations relative to control subjects, indicative of a prediabetic phenotype, and a significant inverse correlation between FFA levels and systemic insulin sensitivity as measured by euglycemic-hyperinsulinemic clamp (Perseghin *et al.*, 1997). The strength of this association was enhanced by a separate study of a similar subject group (predisposed to diabetes but currently within the healthy range) that identified that pharmacologically reducing circulating FFA concentration up to almost half over the course of 7 days resulted in (and correlated with) significantly improved insulin mediated systemic glucose disposal and suppression of hepatic glucose production (Bajaj *et al.*, 2004). During physiological testing insulin concentrations were unchanged, indicating the enhanced responses were due to improved sensitivity and not merely reflective of increased production of insulin by the pancreas. Finally, advanced imaging with proton nuclear magnetic resonance spectroscopy revealed a significant inverse

correlation between skeletal muscle lipid content and whole body insulin sensitivity in a group of healthy individuals (Krssak *et al.*, 1999).

The logical assumption from the described work thus far is that increased skeletal muscle lipid content must somehow impair the action of insulin to increase the trafficking of GLUT4 to the cell surface. One mechanism through which this could be achieved is through a reduction in GLUT4 content, however there is much stronger evidence that actually intracellular insulin signalling pathways may be impaired. For example, in healthy human subjects acute lipid infusion resulted in a significant reduction in skeletal muscle glucose-6-phosphate levels relative to controls, associated primarily with a near total loss of activation of IRS-1 and therefore prevention of cellular glucose uptake (Dresner *et al.*, 1999). This acute study is supported by a wealth of evidence demonstrating reduced activation of proximal insulin signalling (IRS-1, PI3K) in samples from type 2 diabetic patients (Björnholm *et al.*, 1997; Kim *et al.*, 1999; Bouzakri *et al.*, 2003). In contrast, whilst controversial, it has been demonstrated that the expression of GLUT4 is generally not altered in the skeletal muscle of diabetic individuals (Garvey *et al.*, 1992).

1.2.5.2 Impaired oxidative capacity?

Importantly, merely the presence of elevated intramyocellular lipid content is not sufficient to impair insulin sensitivity. This is demonstrated most clearly in endurance trained athletes, who exhibit similarly large skeletal muscle lipid depots compared with diabetic individuals, yet are highly insulin sensitive (Goodpaster *et al.*, 2001). This is largely linked to their enhanced mitochondrial oxidative capacity, thereby ensuring an even balance between lipid availability and the ability to metabolise it. In contrast, lipid overload in the absence of this trained phenotype can rapidly lead to the accumulation of toxic lipids such as diacylglycerol (DAG) and activation of corresponding protein kinase C (PKC) mediated signalling pathways (Itani *et al.*, 2002). Indeed, in a lipid overload induced insulin resistant rat model, a 4-fold increase in PKC-θ in its active form was detected in skeletal muscle (Griffin *et al.*, 1999). Direct experimental evidence further implicates the involvement of this protein kinase, as PKC-θ knockout mice were protected against the onset of lipid induced impairments in skeletal muscle IRS-1/PI3K insulin signalling and insulin stimulated glucose

transport (Kim *et al.*, 2004). Importantly, in this model activation of the insulin receptor was unchanged.

Increased abundance of other lipid derivatives such as ceramide has been associated with IR in human skeletal muscle through inhibition of the activation of Akt, however the presence of this mechanism is more controversial (Adams *et al.*, 2004; Skovbro *et al.*, 2008). Research in this area is ongoing, and more subtle factors are being identified. For example, there is evidence that the subcellular localisation of potentially toxic lipids – not just their total cellular accumulation – may be of importance with regards to subsequent physiological consequences (Perreault *et al.*, 2018). However, further investigation is required as experimental interventions have generated contradictory results. For example, enhancing skeletal muscle mitochondrial FA uptake in a HFD rat model of IR via overexpression of carnitine palmitoyltransferase (CPT) resulted in improved insulin sensitivity linked to reduced DAG accumulation and an associated reduction in PKC-θ activity (Bruce *et al.*, 2009). In contrast, a separate study identified that inhibition of CPT protected mice against the onset of IR induced by a HFD, and claimed that enhanced ß-oxidation in a state of over feeding could generate increased ROS or other metabolites that may impair insulin signalling (Koves *et al.*, 2008). Therefore the relationship between increased skeletal muscle lipid content and impairments in insulin signalling requires further clarification.

1.2.5.3 Altered adipokine profile?

As introduced earlier, adipose tissue is no longer considered to be an inert energy store, but rather has important metabolic and endocrine actions. In particular, it is proposed that sequestering lipid in adipose stores prevents its accumulation in skeletal muscle, and that the secretion of adipokines enhances peripheral insulin sensitivity (Guilherme *et al.*, 2008). In the context of obesity, an inflammatory response is induced in expanding adipose stores as evidenced by enhanced macrophage infiltration and TNF-α production, which can induce adipose specific IR (Xu *et al.*, 2003). The primary action of insulin on adipose tissue is to suppress lipolysis, and a progressive reduction of this action has been linked to rises in circulating fatty acid concentration that may induce skeletal muscle IR (Gastaldelli *et al.*, 2017).

Additionally, it has been proposed that the adipokine profile is altered in a state of adipose IR that may further enhance the development of IR in skeletal muscle. For example, adiponectin has been associated with enhanced peripheral insulin sensitivity, and in a group of healthy and diabetic subjects circulating levels of this hormone was significantly negatively associated with whole body adiposity, circulating lipid values, and systemic insulin sensitivity (Blüher *et al.*, 2006). The importance of this hormone was highlighted by the observation that adiponectin receptors exhibited a compensatory upregulation in skeletal muscle in diabetic individuals, and a training programme significantly increased circulating adiponectin values in association with improvements in body composition and metabolic parameters. Manipulation of adiponectin in diabetic mouse models confirms its role in skeletal muscle insulin sensitivity, which is proposed to be mediated through enhancing mitochondrial ß-oxidation and energy dissipation, functioning overall to reduce myocyte lipid content (Yamauchi *et al.*, 2001). Additionally, the presence of the cytokine TNF-α has been demonstrated to be elevated in the adipose tissue of obese humans (Hotamisligil *et al.*, 1995). In contrast to the action of adiponectin, infusion of TNF-α impaired proximal insulin signalling and associated glucose uptake in the skeletal muscle of healthy human subjects (Plomgaard *et al.*, 2005).

1.2.5.4 Hyperinsulinemia?

Whilst lipid mediated mechanisms appear to almost certainly primarily contribute to the onset of IR in skeletal muscle, other mechanisms may facilitate maintenance or progression of this phenotype towards a full diabetic state. For example, the induction of physiologically relevant hyperinsulinemia for at least 24 hours specifically inhibited the action of glycogen synthase (and therefore the synthesis of glycogen) in skeletal muscle (Iozzo *et al.*, 2001). After the initial onset of IR, often an elevation in circulating insulin concentration is observed, and presumed to be an attempt to regain metabolic control by compensating for the reduced potency per unit of insulin released by the pancreas. However, this may actually be counterproductive in the long term, and aid the progression from IR to diabetes. Therefore, overall it is apparent that the physiology underlying the development of IR is multifactorial and complex beyond the initial mechanisms introduced, with significant further research required to answer questions that will lead to the development of improved novel therapeutic interventions.

1.3 Diabetic cardiomyopathy

As introduced in section 1.1.2., the predominant pathological consequence of diabetes is vascular disease, with several notable consequences for the downstream tissue. With regards to the heart, this often manifests as either progression to heart failure on account of chronic pressure overload associated with hypertension, or MI on account of atherosclerosis. However, the characteristic changes reflected in blood chemistry in diabetic individuals may also exert a direct pathological effect upon the heart, further contributing to the cardiovascular burden of this condition. Where reduced cardiac function is observed in diabetic individuals with no accompanying vascular disease this is referred to as diabetic cardiomyopathy (DCM), and is a key area of study within this thesis.

1.3.1 Key features of DCM

In any given cardiac cycle, two factors are critical to ensuring an adequate volume of blood is pumped from the heart with each beat. These are the ability of the heart to rapidly relax and refill with blood (diastole), and its capacity to subsequently contract and eject the blood efficiently from the right and left ventricles (systole). Disruption of either of these actions can limit blood supply to vital tissues around the body, and is therefore of critical concern. In heart failure, where cardiac pump capacity can no longer meet the demands placed upon it (which could be initiated by one of several pathogenic stimuli), most typically systolic function is initially impaired, however a pathological (initially adaptive) remodelling process occurs that ultimately ends up debilitating global cardiac structure and function (Kemp and Conte, 2012). In contrast, an impairment of diastolic contractile function is most often the first detected sign of DCM, before ultimate progression to a heart failure phenotype if left untreated (Miki *et al.*, 2013).

Whilst there was initially some controversy even regarding the existence of DCM, it has now been thoroughly characterised and demonstrated to be present in several independent diabetic populations. One of the earliest associations between diabetes and cardiac failure came in the Framingham study (Kannel *et al.*, 1974). In an 18 year follow up of over 5,000 individuals, the authors noted

that the risk of developing heart failure was significantly greater in diabetic patients relative to controls, even when controlling for factors such as vascular disease, blood pressure, and body weight.

This work is complemented by more recent studies using advanced *in vivo* imaging techniques. For example, using tissue Doppler imaging (TDI - an improved derivative of echocardiography) in combination with older techniques, 75% of a diabetic population without pre-existing vascular disease were observed to have impaired diastolic function, as indicated by impairment of at least one index of diastolic function such as a decrease in the mitral annular E/A ratio (Boyer *et al.*, 2004). The E/A ratio compares early (E) to late (A) diastolic tissue velocity, with a decrease in relaxation capacity reducing the early response and therefore the overall ratio. The authors highlighted the importance of obtaining measurements such as this due to its independence from cardiac pre-load (Nagueh *et al.*, 1997). This essentially means that it can reflect alterations in contractility regardless of the left ventricular filling pressure, which is important as an increase in this variable could compensate for reduced intrinsic myocardial performance. This is on account of the fact that TDI records the velocity of movement of tissue, not blood, as with conventional techniques. To underline this point, the authors reported that TDI exhibited enhanced diagnostic sensitivity within their experimental population compared to previously widely implemented techniques, which in hindsight may have underestimated the prevalence of DCM in prior literature.

A second study confirmed the presence of diastolic dysfunction as indicated by an impaired E/A ratio via TDI in otherwise asymptomatic diabetic patients (Zahiti *et al.*, 2013). Separate work using slightly older parameters (E/A blood flow velocity ratio) identified the presence of diastolic dysfunction in 40% of a population of 305 diabetic individuals, yet only 9% displayed impaired systolic function as indicated by left ventricular ejection fraction (Poulsen *et al.*, 2010). Whilst this diastolic number may be an underrepresentation for reasons just introduced, it still highlights the predominant diastolic dysfunction observed in DCM patients. However in an additional study, utilisation of TDI allowing measurement of more sensitive indices of systolic function such as peak systolic tissue velocity identified significant impairment of function in type 2 diabetic individuals relative to control

subjects, even though ejection fraction (a common marker of systolic function) was within the normal range (Andersen *et al.*, 2003). This research suggests that systolic function may not be completely unaffected during the initial stages of DCM, as can be portrayed in the literature.

In combination, this work described indicates that diabetic individuals are at a high risk of impaired cardiac diastolic function, which often progresses to impaired systolic function and ultimately heart failure. In any cardiac disease where cardiac function is initially impaired, a range of adaptive processes may occur in order to compensate for this loss of functional capacity (Kemp and Conte, 2012). For example, increased release of hormones such as angiotensin and vasopressin act to induce vasoconstriction and enhance blood volume (Goldsmith, 2006). These adaptations function to maintain peripheral blood pressure and enhance pre-load in the ventricles respectively, the latter of which can enhance diastolic filling velocity and induce increased stretch on the myocardium to increase systolic contractility via the Frank-Starling mechanism (Kemp and Conte, 2012).

However, over time, the range of chemical, hormonal, and physical stimuli the failing diabetic heart is exposed to lead to structural adaptations (Walker *et al.*, 2016). For example, using cardiac magnetic resonance imaging, concentric left ventricular remodelling was observed in a DCM patient group, as determined by an increase in the ratio of left ventricular mass to chamber volume (Shang *et al.*, 2016). This is indicative of left ventricular hypertrophy, which is also observed after certain forms of exercise training (Pelliccia *et al.*, 1991). However, after exercise training this increase in size is largely reflective of a functional increase in myocyte contractile myofilament content driven by IGF-1-Akt signalling that contributes to enhanced cardiac performance. In contrast, in the context of pathological hypertrophy this increase in myocyte volume is also associated with increased deposits of collagen (fibrosis) and cell death driven by activation of MAPK and calcium sensitive signalling pathways, which together ultimately lead to a decrease in overall contractile capacity (Bernardo *et al.*, 2010). Accordingly, a diabetic rat model exhibited increased cardiomyocyte size and cardiac collagen content, associated with reduced diastolic contractile function (Huynh *et al.*, 2010). However, overexpression of the IGF-1 receptor exerted protection against this phenotype, underlining both the physiological importance of this hormone,

and the role fibrosis has in stiffening the myocardium and therefore contributing to reduced contractile function.

As DCM advances, global cardiac function progressively declines until it reaches a clinical heart failure phenotype whereby it can no longer sustain the cardiac output required to maintain the necessary delivery of oxygen and nutrients to other vital organs. However, it is important to note that an impairment in contractile function is observed prior to structural changes (Schannwell *et al.*, 2002). Therefore, whilst ventricular remodelling is important in the progression of this disease, it is limitations in contractility that initially drive DCM. Consequently, understanding how diabetes initially impacts cardiac contractility is of great experimental, theoretical, and most importantly clinical significance.

1.3.2 Excitation contraction coupling

In order to understand how cardiac function may become impaired in any given disease, it is imperative to first of all detail the physiological processes that determine cardiac contractility in a healthy baseline state. A key parameter often used to indicate cardiac function is cardiac output, which is essentially the volume of blood being ejected from the heart per minute. This is a product of heart rate and stroke volume (the amount of blood ejected per beat), of which the latter is far more important in the context of cardiac disease.

Stroke volume is influenced by a range of factors including the amount of blood entering the heart during diastole, the mechanical properties (stiffness) of the myocardial tissue, and the volume of contractile myofilaments available to generate active contractile force. However, primarily cardiac contractility is dependent upon the collective force generation capacity of individual heart muscle cells (cardiomyocytes), and it is here that deficits in overall cardiac performance primarily originate within the context of DCM. This capacity is directly determined by the process of excitation contraction coupling within each cardiomyocyte, which is summarised in Figure 1-3.

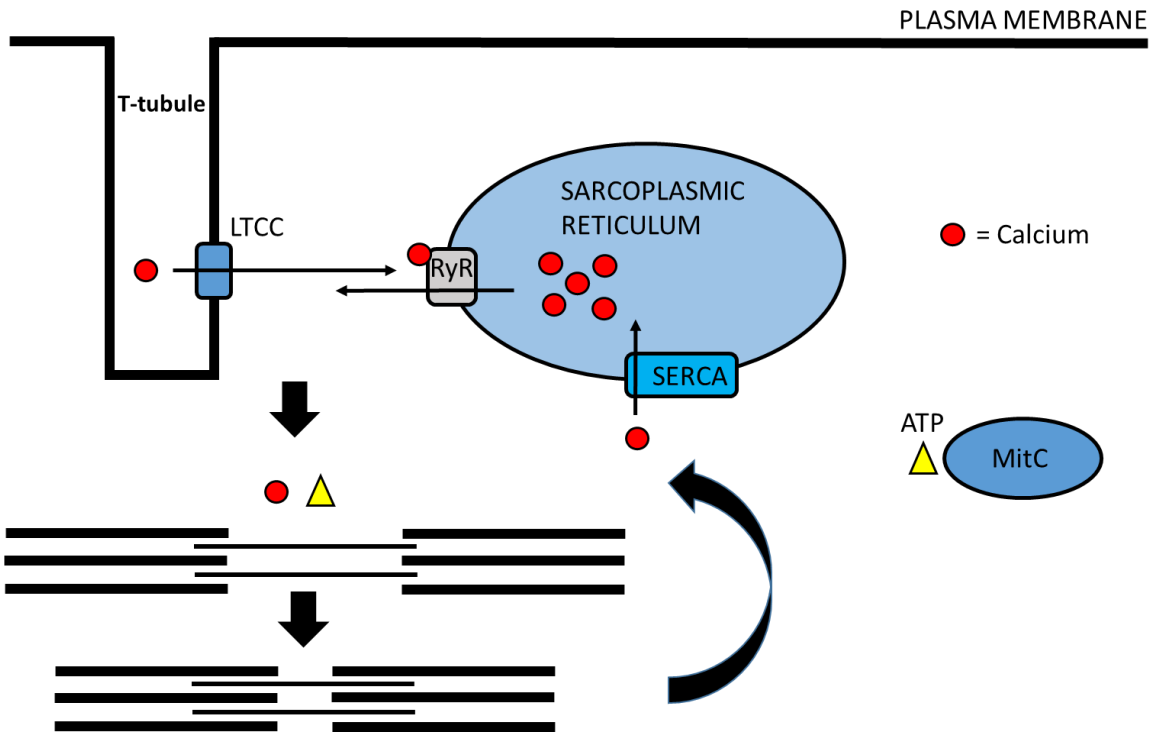

Figure 1-3 Cardiac excitation contraction coupling
Cardiomyocyte membrane excitation initiates the opening of L-type calcium channels (LTCC) located predominantly within t-tubules, and therefore also entry of a small amount of calcium. This binds to ryanodine receptors (RyR) on the sarcoplasmic reticulum and triggers a much larger release of calcium from this intracellular store. The availability of calcium and ATP (predominantly from mitochondrial β-oxidation) facilitates the active sliding of the thick (myosin) and thin (actin) myofilaments relative to one another, that within their striated structure functions to initiate cell shortening (contraction). Relaxation is predominantly initiated by the reuptake of calcium into the sarcoplasmic reticulum via the SERCA calcium ATPase transporter.

The first step of myocyte contraction, regardless of anatomical location, is electrical activation. In contrast to the specific activation of individual skeletal muscle fibres via designated motor neurons that facilitates the graded recruitment of individual muscles, activation of the heart is a more binary system. Pacemaker cells within the sinoatrial node in the right atrium initiate electrical excitation that spreads from cell to cell via gap junctions in a highly coordinated fashion, in order to initiate contraction within individual myocytes with the required order and timing to produce effective whole organ level transient structural changes during contraction and relaxation (Lo, 2000). Disruption of this process of activation is a common cause of arrhythmia, and can lead to fatal sudden cardiac death (Myerburg *et al.*, 1992).

At the cellular level, activation refers to the rapid exchange of ions (predominantly sodium and potassium) across the myocyte membrane that causes

a characteristic change in membrane potential referred to as an action potential. Invaginations of the myocyte membrane referred to as t-tubules ensure near simultaneous activation across the whole cell (Ibrahim *et al.*, 2011). During this activation, membrane bound voltage sensitive L-type calcium channels (LTCC) open and permit a small influx of calcium. This then binds to and opens ryanodine receptors (RyR) on the intracellular sarcoplasmic reticulum (SR), which triggers a much larger rise in cytoplasmic calcium concentration through a secondary release of calcium from this organelle in a process classically referred to as calcium induced calcium release (Fabiato, 1983). The liberated calcium then binds to the troponin-tropomyosin complex and initiates a conformational change that permits the interaction of the contractile myofilaments actin and myosin. Provided there is sufficient ATP availability, a cyclical attachment, sliding, and detachment process commonly referred to as a power stroke is initiated, whereby attachment and subsequent hydrolysis of ATP on the myosin heavy chain powers the active movement of actin and myosin relative to one another (Lombardi *et al.*, 1992). Due to the striated global structure of individual muscle cells, this contraction functions to shorten the overall muscle within its structural framework. Within the myocardium, this functions to compress the chambers of the heart to power the movement of blood into the next chamber, or blood vessel, as appropriate.

Relaxation of cardiomyocytes is not a passive process that facilitates the return of chamber dimensions to their baseline state on account of elastic recoil. Rather, it relies upon the active, heavily ATP dependent, removal of calcium from the cytoplasm. Whilst some calcium is transported back out of the cell altogether or can be taken up by mitochondria during diastole, the majority is returned to the SR via the sarcoplasmic reticulum calcium ATPase transporter (SERCA) (Periasamy and Kalyanasundaram, 2007). The function of SERCA is closely regulated by an endogenous inhibitor called phospholamban. The action of SERCA also strongly influences systolic function, because end diastolic SR calcium content is a powerful regulator of subsequent SR calcium release and therefore also contractile capacity (Bassani *et al.*, 1995). Pathological changes in the expression and activity of SERCA are strongly implicated in several cardiac disease phenotypes (Arai *et al.*, 1994). In general, the cyclical changes in calcium concentration associated with excitation contraction coupling are referred to as

a calcium transient, and the profile of this transient is a strong predictor of cardiomyocyte function.

Excitation contraction coupling is not a statically defined process, but rather it can be adapted depending upon acute and chronic demands. For example, during exercise the workload of the heart increases, in order to pump more oxygen and nutrients to the activated skeletal muscles. This has to occur within a cardiac cycle of reduced duration as heart rate will almost certainly also be increased. Therefore, the efficiency of intracellular calcium handling must be transiently enhanced in order to meet these demands. An experimental model employing Calcium/calmodulin dependent protein kinase II (CamKII) inhibition revealed that activation of this kinase during increased workloads (higher frequency stimulation) was essential to enhance SERCA activity and therefore also diastolic SR calcium reuptake in mouse cardiomyocytes, which could largely account for enhanced contractile performance under acute stress (Picht *et al.*, 2007). This finding is supported by evidence that a period of exercise training enhanced cardiac SERCA protein expression and associated calcium handling in rat cardiomyocytes (Wisløff *et al.*, 2001). Interestingly, peak systolic calcium concentration did not increase despite enhanced myocyte contractile shortening, indicating myofilament calcium sensitivity was improved. A separate study largely replicated these functional findings after exercise training in mice, but also identified that the phosphorylation of CamKII and phospholamban were chronically elevated (Kemi *et al.*, 2007). This would function to alleviate the inhibitory action of phospholamban on SERCA, further enhancing its action. Inhibition of CamKII ablated training induced improvements in cardiomyocyte contractility, but did not fully abolish enhancements in myofilament calcium sensitivity, indicating additional mechanisms are responsible for the adaptive response to exercise.

The plasticity of excitation contraction coupling is also displayed in a more permanent manner when comparing skeletal and cardiac muscle. This process is responsible for the contraction of both category of myocytes. However, whilst they rely on the same principles, they are finely tuned to optimally perform the workload required for each cell type. For example, the abundance of mitochondria in cardiac muscle is at least 2 fold greater than that of skeletal muscle, in order to ensure a constant supply of ATP to power contraction (Park *et al.*, 2014). In

contrast, skeletal muscle is adapted for more powerful contractions in order to power demanding actions such as locomotion or the lifting of objects. This sort of output leads to fatigue and the need for rest and recovery, something that cannot be afforded to the heart. This adaptation is reflected in the isoforms of varying proteins that are expressed, which vary in maximal activity and efficiency, in particular that of the myosin heavy chain and SERCA (Weiss and Leinwand, 1996; Periasamy and Kalyanasundaram, 2007).

1.3.3 Alterations in calcium handling are important in DCM

When outlining the general progression of DCM in section 1.3.1, reference was made to several factors that are associated with the pathophysiological events underlying this disease state. It is important to acknowledge that a myriad of additional factors related to the general diabetic phenotype have been associated with reduced cardiac contractile function and structural remodelling in DCM, including increased oxidative stress, activation of the renin angiotensin system, inflammation, and many more (Bugger and Abel, 2014). However, whilst the full physiological explanation of DCM will undoubtedly be complex and multifactorial, there is strong evidence that one of the most critical and early factors is an impairment of the excitation contraction coupling process outlined in section 1.3.2.

A major limitation in previous studies within this area is the dependence upon animal models. However, to some extent this has been unavoidable, and the *db/db* mouse model, which has a mutation in the leptin receptor gene leading to over feeding and obesity, recapitulates key features of DCM (Kobayashi *et al.*, 2000). Crucially, this model reproducibly displays impaired cardiac function attributable to impaired intracellular calcium handling. Specifically, collective work has demonstrated reduced whole heart contractility from these mice, indicated by reduced fractional shortening, stroke volume, and developed pressure as measured by echocardiography or Langendorf perfusion (Belke *et al.*, 2004; Stølen *et al.*, 2009). In all cases, this was attributed to reduced systolic and diastolic peak intracellular calcium concentrations, reduced calcium transient amplitude, and most importantly slower SR calcium reuptake on account of reduced overall SERCA activity. This in turn was attributed to reduced SERCA protein expression and increased inhibition by phospholamban. These changes

can, at least in theory, fully account for the reduced function of the hearts from these mice.

It is important to state that these findings have been closely replicated in a very different diabetic model (insulin resistant Wistar rats induced by a high sucrose diet), thereby increasing confidence in their translational relevance (Dutta *et al.*, 2001). However, one issue with this collective data is the consistent finding that systolic contractile function (whole heart or isolated myocyte) is also reduced in these models, which does not accurately reflect the human early clinical setting where diastolic dysfunction predominates, as described in section 1.3.1. This could be related to the observation that in addition to impaired SERCA activity, increased SR calcium leak was also observed (Belke *et al.*, 2004; Stølen *et al.*, 2009). This would further compound the reduction in SR calcium content caused by delayed diastolic refilling, and could perhaps account for the discrepancy in phenotype between species.

In summary, available literature suggests that deficits in the reuptake of calcium into the SR via SERCA within cardiomyocytes appear to largely account for reduced diastolic cardiac contractility in the context of DCM. Interestingly, changes in intracellular calcium regulation may also partly explain the onset of structural remodelling that drives the progression of this condition. The calcium sensitive kinase CamKII has been shown to be activated in heart failure models, and manipulation of its expression/activity has been demonstrated to alter the progression of structural remodelling in accordance with it being a central mediator of this process (Anderson *et al.*, 2011). This is initially surprising given its beneficial role in enhancing excitation contraction coupling in response to exercise, as described. However, its action and molecular targets may vary greatly depending on the mechanism and source of activation, and which specific isoform of this protein is being studied.

1.3.4 The role of metabolism in DCM

Metabolism is the general process by which cells generate ATP in order to power any physiological process requiring active work. There are several factors determining the efficiency and productivity of this process, including the primary substrate being metabolised. Whereas a single molecule of fatty acid will provide

several fold more ATP in comparison to a glucose molecule, the oxidation of glucose is more rapid and comes with a lower oxygen cost. In the heart, the primary metabolic substrate is fat, with a lesser contribution from glucose (An and Rodrigues, 2006). Therefore it is not immediately clear why IR (a key facet of the diabetic phenotype) and reduced glucose uptake would significantly impact cardiac function. However, there is a strong line of evidence that this initial perturbation of metabolic regulation in cardiac tissue is the critical factor initiating the onset of cardiomyopathy.

In skeletal muscle, the impact of ectopic lipid storage upon insulin sensitivity has been well defined in experimental models. Similarly, the diabetic heart is defined by an increased uptake and utilisation of fatty acids, linked to impaired insulin sensitivity. For example, a diabetic rat model exhibited a significant reduction in the cardiac accumulation of [^{3}H]-2DG (2-deoxyglucose) in response to insulin stimulation, which was linked to a corresponding reduction in the expression and activation of GLUT4 and IRS-1 protein (Desrois *et al.*, 2004). Additionally, in hearts from both *ob*/*ob* and *db*/*db* mice, decreased insulin stimulated glucose uptake and increased FA utilisation were recorded prior to the onset of systemic hyperglycemia (Buchanan *et al.*, 2005).

Importantly, there is a noted association between these metabolic changes in the heart, and impairment of its contractile function. For example, in a sample population of obese women, there was a significant association between BMI (average of this group was 38 kg/m^2) and myocardial oxygen consumption, indicating reduced cardiac efficiency (and therefore performance) (Peterson *et al.*, 2004). This coincided with IR, which was independently associated with increased myocardial fatty acid uptake and utilisation. Similarly, in a diet induced rat model of diabetes, decreased cardiac insulin stimulated GLUT4 localisation at the plasma membrane and enhanced fatty acid transporter (FATP1) expression correlated with reduced stroke volume and ejection fraction (Deng *et al.*, 2007). Finally, and perhaps most convincingly, increased myocardial lipid accumulation was a direct independent predictor of diastolic cardiac dysfunction in a population of asymptomatic type 2 diabetic patients (Rijzewijk *et al.*, 2008).

The first evidence that these metabolic changes do not merely coincide with but actually contribute towards the onset of contractile impairments comes from

studying the temporal pattern of development of these physiological events underlying DCM. Study of multiple tissues in a high fat diet (HFD) induced mouse model of diabetes revealed impaired cardiac insulin sensitivity – as indicated by impaired activation of Akt and reduced GLUT4 protein content – and a corresponding reduction in glucose uptake occurred prior to systemic markers of IR, and also well in advance of impaired cardiac contractility (Park *et al.*, 2005). Increases in blood glucose concentration have been cited as capable of directly pathologically activating CamKII and therefore contributing towards cardiac dysfunction in DCM (Erickson *et al.*, 2013), however this evidence suggests that cardiac IR and associated metabolic changes may be an earlier important pathogenic factor.

The nature of the relationship between cardiac IR, increased fatty acid oxidation, and the onset of cardiac dysfunction requires further study. There is an accumulated body of work describing the impact of lipotoxicity (largely from lipid metabolites such as DAG and ceramide) upon insulin signalling and cardiomyocyte survival (and therefore cardiac function) (Drosatos and Schulze, 2013). This suggests that the only link between IR and reduced cardiac function in DCM is that they share a common causal mechanism. However, there is compelling evidence that IR *per se* may directly impair cardiac function.

In *db*/*db* mice, overexpression of cardiac GLUT4 normalised both the perturbed metabolic profile described above, and the induced impairment of cardiac function observed in this model (Belke *et al.*, 2000). These findings were replicated in an independent study, which identified no difference between *db*/*db* mice overexpressing GLUT4 and appropriate controls in measures of diastolic E/A ratio and systolic fractional shortening (Semeniuk *et al.*, 2002). Combined, this work strongly implicates the availability of GLUT4 transporters and the ability to rapidly increase glucose uptake as being critical to normal cardiac function, and that IR is not merely an irrelevant by product of increased fatty acid utilisation. In contrast, it suggests that cardiac IR could even be the central mechanism underlying cardiac dysfunction in the context of DCM. This evidence is particularly valuable as a large body of work in this area is associative, without studying the effect of direct manipulation of potentially important variables upon cardiac function.

A key question arising from this line of investigation is why insulin stimulated glucose uptake is so critical to cardiac function, when in a baseline healthy condition the heart predominantly metabolises fatty acids. There are 2 leading theories, both of which require further study. First of all, the cardiac PCr:ATP ratio was found to be significantly reduced in the myocardium of diabetic patients, indicative of impaired energy production (Scheuermann-Freestone *et al.*, 2003). This is an important observation as this ratio has been shown to be a key predictor of cardiovascular mortality in patients suffering from dilated cardiomyopathy (Neubauer *et al.*, 1997). Additionally, this suggests that the ability to increase glucose uptake and therefore minimise the oxygen cost of ATP production in the diabetic heart is essential to sustain ATP output at the required rate. Perhaps this is particularly important under times of stress, such as when subclinical alterations in vascular and/or cardiac function are increasing demands on the surviving healthy myocardium. The activity of SERCA is critically dependent upon sufficient ATP availability, therefore this may explain why diastolic dysfunction is the first clinical sign of DCM. Whilst the cycling of the contractile myofilaments required for systolic contraction is also ATP dependent, compensatory mechanisms such as enhanced filling pressures may be able to maintain this action at the required level during the initial stages of this condition.

Secondly, there is experimental evidence that suggests that impairments in the activation of myocardial insulin signalling pathways may directly influence mitochondrial ATP production, and therefore also cardiac contractile function. In a cardiac specific insulin receptor knock out mouse model mitochondrial bioenergetics were impaired, linked to increased reactive oxygen species (ROS) production and increased uncoupling when fatty acid was the primary metabolic substrate (Boudina *et al.*, 2009). This suggests that IR could contribute to impaired metabolism of the increased cardiac lipid content, which would only increase the accumulation of toxic metabolites that may promote further cardiomyocyte dysfunction and death.

Overall prior literature has built up an overview of the pathophysiological events underlying contractile dysfunction in DCM, as summarised in Figure 1-4. However, there are still several important unanswered questions. For example, both the causal direction of the relationship between increased myocardial fatty acid

utilisation and IR, and the primary mechanism linking alterations in metabolism and contraction via calcium handling, are unclear. These questions require answering in order to develop specific treatments for DCM, which are currently lacking yet are urgently needed. Research in this area would benefit from improved experimental models, ideally of a human origin, and indeed development of such a model is the key aim of this thesis.

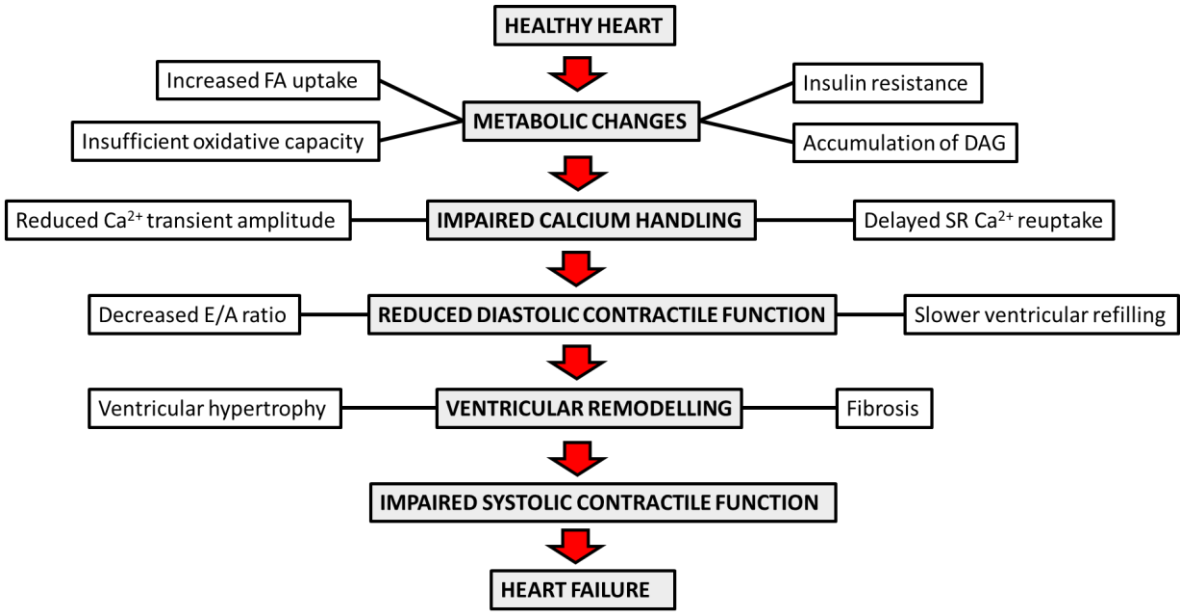

Figure 1-4 Proposed model of DCM development
Key events in the pathogenesis of DCM are highlighted, in addition to contributing factors and relevant aspects of the phenotype at each stage.

1.4 iPSC-CM

1.4.1 Initial development

The field of stem cell research is well established, and has thoroughly detailed the possible advantages of this technology. Thus far, embryonic stem cells have been most widely studied and demonstrated to have the capacity to differentiate into almost any cell type, provided they are exposed to the appropriate stimuli, which has potential far reaching consequences for the study of tissue specific embryonic development (Rippon and Bishop, 2004). Additionally, with the capacity to subsequently differentiate these cells into functional specialised cells such as cardiomyocytes (Boheler *et al.*, 2002) or neurons (Ban *et al.*, 2006) there is also the potential for disease modelling or even therapeutic tissue regeneration, however this has been limited by both safety concerns and ethical issues.

Induced pluripotent stem cell derived cardiomyocytes (iPSC-CM) are a relatively more recent adaptation of this technology that could in theory overcome the limitations associated with embryonic cells. The big breakthrough in this field occurred in 2006, when it was reported that embryonic or adult mouse fibroblasts could be reprogrammed into a phenotype closely resembling that of embryonic stem cells through retroviral mediated expression of only 4 transcription factors associated with embryonic pluripotency (Oct3/4, Sox2, c-Myc, Klf4), as indicated by both cellular morphology and gene expression markers (Takahashi and Yamanaka, 2006). This group then extended these findings by successfully using this protocol (with minor adaptation) to induce dedifferentiation of human derived dermal fibroblasts into a pluripotent stem cell-like form (Takahashi *et al.*, 2007). As with their foundational work, generated cells expressed genetic markers indicative of undifferentiated cells, were highly proliferative, and demonstrated the capacity to spontaneously differentiate into a range of cell types both *in vitro* and *in vivo* (in mice). Critically, they also successfully directed the iPS cells to specifically differentiate into contractile cardiomyocytes.

These findings were ground breaking and opened up the possibility of harvesting easily obtainable cells from an adult human and subsequently deriving specific cells of interest (with that individuals unique genetic background) for research or therapeutic purposes. As reviewed by Batalov and Feinberg (2015), in response to recognition of their potential, several protocols targeting the reproducible and efficient reprogramming of iPS cells into cardiomyocytes (iPSC-CM) were devised, with varying degrees of success. The most effective thus far have employed simple 2D cell culture whilst exposing cells to physiologically relevant growth factors in order to activate relevant developmental signalling pathways, such as BMP4 and Wnt, and direct cells down the cardiac lineage. The development of these protocols is ongoing, where the central aim is to achieve maximal efficiency and reliability of cardiac differentiation. Great progress has been made in a relatively short time frame, and the already significant commercial interest in these cells is likely to see this rapid pace of development continue.

1.4.2 iPSC-CM are a potentially valuable research tool

Our knowledge of the physiology and possible application of iPSC-CM is constantly expanding due to the interest and attention they are receiving in the current

scientific field. They have been shown to have indirect cardiac benefits with regards to predicting cardiotoxic effects of drugs, but perhaps more importantly there are 2 main themes through which they could directly transform the treatment approach to a range of cardiac conditions.

Firstly, there is a growing body of evidence that iPSC-CM could partially regenerate the heart post-MI. Current treatment options primarily target reducing the burden on the surviving myocardium, for example through reducing blood pressure. However, substantial evidence generated in a variety of animal MI models – from rodents through to monkeys – indicates that direct injection of human stem cell derived cardiomyocytes (from an embryonic or somatic origin) may be able to ameliorate to some degree the characteristic structural and functional changes observed post-MI described in section 1.5.1. (Laflamme *et al.*, 2007; Chong *et al.*, 2014; Shiba *et al.*, 2016). There is evidence of the inserted cardiomyocytes maturing *in vivo*, and crucially they are able to form a contractile graft that functionally couples with the host myocardium in order to make a meaningful difference to global cardiac function (Shiba *et al.*, 2012). Indeed research is now focussed more upon optimising this process, for example addressing how to promote optimal survival and integration of the injected cells with interventions such as co-injection of a "pro-survival cocktail" of hormones and drugs (Ogasawara *et al.*, 2017). Importantly, this approach could also overcome risks associated with the potential immune rejection of embryonic stem cell derived tissue.

In addition to potentially being a treatment option themselves, iPSC-CM should also in theory be able to act for the purpose of disease modelling. Indeed, iPSC-CM generated from patients suffering from cardiac conditions with a defined genetic origin such as LEOPARD syndrome and long QT syndrome were able to recapitulate key structural and functional features of the disease phenotype, for example a prolongation of the action potential (Carvajal-Vergara *et al.*, 2010; Itzhaki *et al.*, 2011). This provides the opportunity to study not only disease specific pathology but perhaps also patient specific mechanisms, thereby facilitating superior identification of the most appropriate treatment option.

Clearly not all pathophysiological conditions are caused solely by genetic factors. Rather, there is a significant contribution of lifestyle factors to the growing burden

of cardiometabolic disease that is currently reaching epidemic levels. Therefore, there is also an opportunity to induce disease phenotypes and create tissue specific cellular models, for example a DCM model in iPSC-CM, through exposing these cells to relevant external stimuli. Again this would facilitate the identification of underlying pathophysiological mechanisms and provide a safe translatable human model upon which novel compounds could be tested. This would also reduce the need for animal testing, which is in line with the governments' principles of refinement, replacement and reduction outlined in the Animals Scientific Procedures Act 1986.

Finally, from a practical experimental viewpoint iPSC-CM provide the benefit of being able to generate a theoretically unlimited number of cardiomyocytes with which experiments could be performed. This is in stark contrast to the current study of cardiomyocytes that relies upon the isolation of non-proliferative primary cells, which typically do not retain their functional phenotype in vitro for more than a few days.

1.4.3 Characterisation of iPSC-CM phenotype

In order to achieve the aims discussed in section 1.4.2., it is essential that the phenotype of iPSC-CM closely matches that of mature adult cardiomyocytes. Of greatest importance is that the process of excitation contraction coupling (outlined in section 1.3.2.) is functionally active and responds to relevant stimuli in an appropriate manner, which will be underpinned by the expression of relevant genes and proteins.

The first part of excitation contraction coupling is electrical excitation of the myocyte membrane. Genetic profiling revealed that generated iPSC-CM expressed all 14 of the major membrane bound ion channels that regulate cardiomyocyte excitation (sodium and potassium channels) and calcium entry (LTCC) (Liang *et al.*, 2013). Just as in primary cardiomyocytes, these channels work together to produce an action potential, which in turn initiates contraction. It has been claimed, based upon clear differences in specific parameters such as action potential duration (APD) and frequency and rate of initial depolarisation, that when generating a population of iPSC-CM, subsets of atrial, ventricular, and pacemaker like cells will emerge. This assumption has been challenged, and it is

claimed that variations in experimental conditions such as plating density may strongly impact recorded values, and that action potential characteristics are actually normally distributed across one population of iPSC-CM (Du *et al.*, 2015). This complicates general comparisons between iPSC-CM and primary cells.

Prior characterisation of individual channel activity and the overall action potential was undertaken by Ma *et al.*, (2011). It is highly challenging to directly compare the action potential characteristics of different cells when measurements are obtained within different experimental set ups, due to the extreme sensitivity of these values to experimental variables. Despite this limitation, the authors reported a high degree of correspondence between iPSC-CM and previously reported values for primary cells with regards to both whole cell based measurements such as APD and also the activity of individual channels. The biggest issue identified is that iPSC-CM are spontaneously contractile, on account of the expression and strong activity of a pacemaker channel.

Similarly detailed characterisation of the calcium handling capacity of iPSC-CM was undertaken by Itzhaki *et al.*, (2011). Once again, the genes encoding for the proteins central to this process were expressed, including SERCA, RyR, and LTCC. In accordance with the spontaneous activation of iPSC-CM, in the presence of external physiological levels of calcium (1.8 mM), spontaneous calcium transients were recorded using a fluorescent calcium dye. Critically, in the absence of external calcium, or in the presence of a calcium channel blocker (nifedipine), no calcium transients were recorded. This suggests that iPSC-CM contractile activity is dependent upon voltage gated calcium influx, which is a key feature of adult cardiomyocytes. Using a similar experimental approach, inhibition of RyR and SERCA demonstrated that the actions of these proteins was as expected in the generation of the intracellular calcium transient. Caffeine is a potent stimulus for opening of the RyR, and was implemented to demonstrate the presence and vital role of SR calcium loading. Overall, it was clear that the basic mechanisms of cardiac calcium handling were present and correct in iPSC-CM.

In contrast, further quantification and characterisation of iPSC-CM calcium handling in an independent study revealed that the calcium transient in these cells was of smaller amplitude than that of more mature cardiomyocytes, with a slower rate of rise and decay, attributable to poor expression of RyR and SERCA (Lee *et*

al., 2011). Critically there was also a lack of synchronicity with regards to calcium release across the width of the cell, which is related to associated structural immaturity. More recent research indicated that calcium handling was actually highly comparable between iPSC-CM and primary isolated adult rabbit cardiomyocytes, perhaps due to improvements in iPSC-CM differentiation protocols (Hwang *et al.*, 2015). However, this paper still concluded that the rate of decay of intracellular calcium via SERCA was still of a slower, immature phenotype. This finding is particularly challenging when considering any potential model of DCM with these cells, considering impaired diastolic SR calcium reuptake is a key feature of this condition.

The most apparent limitation of iPSC-CM with regards to comparison with mature cardiac cells, alongside being spontaneously contractile, is their small circular phenotype indicative of a disordered array of myofilaments. This is in clear contrast to the larger striated rectangular phenotype of primary adult cardiomyocytes. As will be discussed, this may be a product of the unique physical and chemical environment cardiomyocytes are exposed to during development *in vivo*. To underline the difference in cell size, cell volumes of iPSC-CM and adult mouse ventricular cardiomyocytes have been recorded at 3.96 and 29 pL, respectively (Hwang *et al.*, 2015). However, arguably a bigger limitation is that stem cell derived cardiomyocytes in general do not exhibit robust expression of T-tubules, which prevents synchronous excitation of the cell (and therefore also synchronous release of SR calcium), and can create a wave like contractile profile (Lieu *et al.*, 2009). Indeed, a loss of T-tubule density is a characteristic change in myocytes from individuals with heart failure (Lyon *et al.*, 2009).

Collective consideration of the factors that determine primary cardiomyocyte contractility indicate that the fundamental proteins and processes are present and functional in iPSC-CM, however they are generally considered to be of an immature foetal like phenotype. This generalisation may also extend to the metabolic phenotype of these cells, however in comparison to the other aspects of iPSC-CM physiology introduced, there is a significant lack of experimental evidence in this area. This is surprising given the vital importance of metabolic processes to general cellular physiology, not just myocyte contractile capacity. This concept will be discussed further in section 4.1.3., and indeed a large section

of this thesis is devoted to expanding our knowledge of the iPSC-CM metabolic profile. However, a key concept is that iPSC-CM predominantly rely upon glycolysis in order to generate ATP, particularly under typical cell culture conditions whereby medium is rich in glucose. This is another key marker of foetal physiology, and was demonstrated most clearly by essentially unchanged levels of total cellular ATP production in the presence of inhibitors of mitochondrial ATP production, and was also supported by relatively weak protein expression of the mitochondrial oxidative metabolic complexes (Rana *et al.*, 2012).

The primary function of cardiomyocytes is to contract in order to support the overall pump capacity of the heart. However, on account of the limitations in excitation contraction coupling described, it is technically challenging to directly compare the contractile profile of iPSC-CM with adult cardiomyocytes. In isolated adult cells, contraction of the rod shaped myocytes induces a uniaxial shortening. The extent and rate of this shortening is most commonly used to indicate contractile capacity. However, in iPSC-CM the disordered myofilament content prevents direct comparisons with these measurements. Despite this, innovative measurements of the contractile function of iPSC-CM have estimated their force generation capacity to be 2-6 fold less powerful than that of primary cells, and once again more similar in phenotype to foetal cardiomyocytes (Pioner *et al.*, 2016; Kolanowski *et al.*, 2017).

1.5 Myocardial infarction

1.5.1 Overview of MI physiology

A complete, detailed review of the pathophysiological events underlying MI requires intricate explanation of several areas of physiology out with the scope of this thesis. As will be discussed and explored in chapter 5, there is a complex yet clinically important link between IR/diabetes and the prevalence/outcomes related to MI. Therefore, only a brief overview of key aspects of the MI phenotype is provided here, before more detailed consideration of these specific issues in section 5.1.

The fundamental event characteristic of an MI is blockage of a coronary vessel, usually on account of the rupture of an atherosclerotic lesion, which leaves the

downstream myocardium starved of vital oxygen and nutrients. The cellular signalling response to ischemia involves a complex combination of multiple pathways, but if prolonged enough often results in a significant degree of both necrotic and programmed apoptotic cell death (McCully *et al.*, 2004). The ability for self-renewal of cardiomyocytes is almost non-existent, which creates a significant problem in trying to maintain the overall pump function of the heart at the required levels if a considerable number of cells are lost. Rather than being able to generate new contractile myocytes, collagen is deposited in order to form scar tissue that maintains the structural integrity of the affected chamber wall. However, this places a significant burden upon the surviving myocardium in order to compensate for the loss of contractile machinery. As alluded to earlier, where this occurs in any cardiac disease a range of compensatory mechanisms are activated in order to help to maintain cardiac output, however often these eventually contribute to ventricular remodelling and the progression to heart failure.

An additional common complication for post-MI patients is the development of arrhythmias. As explained earlier, the activation of cardiomyocytes is dependent upon cell to cell communication and the tightly coordinated spread of electrical excitation. Significant scar tissue development can interrupt this intercellular communication and promote aberrant contractile coordination between different regions of myocardium, ultimately leading to reduced cardiac output (Stuart *et al.*, 2016). Furthermore, the initial clearance of dead cells and initiation of fibrotic remodelling is an inflammatory driven process (Frangogiannis, 2014) that if excessive in duration and intensity can lead to the deposition of excessive collagen (fibrosis) and therefore stiffening of the myocardium (Stuart *et al.*, 2016), further increasing the burden on the contractile capacity of the heart.

It must be clearly stated that not all individuals survive the initial myocardial ischemic insult associated with MI. Logically, both the chances of surviving and long term prognosis are strongly associated with the extent of tissue infarcted, and therefore also the duration of the initial blockage/ischemia. Therefore, there is an urgency in acute treatment associated with restoring blood flow. Often this is achieved with anti-clotting agents and surgical interventions to remove/bypass the embolism. However, there is also a well described phenomenon whereby upon

reperfusion a second and potentially severe injury may be induced in response to revascularisation. This is referred to as ischemia-reperfusion injury, and is thought to be mediated primarily through increased cellular ROS in response to ATP depletion, overload of intracellular calcium concentration, and reactivation of the oxidative metabolic machinery (Dorweiler *et al.*, 2007). This therefore complicates the implementation of treatment strategies that must balance swift restoration of blood flow without inducing an excessive secondary loss of tissue, and then sensitively manage the subsequent remodelling process to delay or even prevent the progression to heart failure.

1.5.2 Demand for novel treatment options

Similar to the case described for diabetes, the prevalence and mortality rate associated with MI – largely linked to rising rates of obesity - creates the urgent demand for novel effective therapeutic options. In order to meet this clinical demand further comprehension of the infarction process is required, both in terms of the underlying physiological processes involved but also the distinct timing and order in which they occur.

Research is still making significant progress in this area, and identifying potential novel therapeutic targets. For example, the expression of the transcription factor RUNX1 has been observed to be upregulated in surviving cardiomyocytes post-MI, functioning to enhance cardiomyocyte calcium handling and therefore limit the progression of pathological remodelling (McCarroll *et al.*, 2018). As will be discussed in section 5.1, another area requiring further investigation is our understanding of the relationship between myocardial insulin sensitivity/glucose uptake and cardiac function post-MI.

1.6 General aims of thesis

The primary aim of this thesis is to assess the potential of iPSC-CM to act as the basis of a novel cellular model of DCM. The most important criteria in order to achieve this is to demonstrate that these cells are capable of displaying a robust and reproducible insulin stimulated glucose uptake response, of a similar magnitude to adult primary cardiomyocytes. Many aspects of iPSC-CM physiology have been determined to be at a foetal stage of development, which if extended

to their metabolic phenotype would mean exhibiting this response would be unlikely. In this event, strategies to mature iPSC-CM will be investigated. Additionally, the expression of SNARE proteins in a range of cardiac disease models will be assessed, in order to both fully characterise the expression of these proteins in primary cardiac tissue for the first time, and assess if changes in their expression may contribute to impairments in cardiac glucose transport in either DCM or post-MI.

2 Materials and methods

2.1 Materials

2.1.1 Commercially derived cells

Identity	Origin
3T3-L1 Fibroblasts	American Tissue Culture Collection, Manassas, Virginia, USA
HEK 293FT	American Tissue Culture Collection, Manassas, Virginia, USA
HeLa	American Tissue Culture Collection, Manassas, Virginia, USA
iPSC-CM (Cor.4U) P/N: Ax-B-HC02-1M	NCardia (Axiogenesis), Cologne, Germany
iPSC-CM (iCell Cardiomyocytes^2) P/N: CMC-100-012-000.5	Cellular Dynamics International (CDI), Wisconsin, USA
XL-1 Blue *E.Coli*	Agilent Technologies, Santa Clara, California, USA
5-alpha Competent *E.coli* P/N: C2987I	New England Biolabs, Ipswich, Massachusetts, USA

Table 2-1 List of commercially obtained cells

2.1.2 Primary cardiac cells and/or tissue

Identity	Details	Origin
Db/db and db/m mice	Male, 13-15 weeks old, homo/heterozygous for mutation in leptin receptor gene.	Gifted by Dr Augusto Montezano
High Fat Diet (HFD) and control CHOW fed mice	Male, 20 weeks old. Both groups were fed normal CHOW diet for 8 weeks after birth, then HFD mice were switched to a diet whereby 60% of total calories were obtained from fat for the next 12 weeks.	Gifted by Dr Anna White
Wistar Rats	Male, approximately 250 g, approximately 20 weeks old. Animals were maintained as normal for 8 weeks prior to MI procedure (or non-operated control group), and then maintained for a further 12 weeks.	Gifted by Aline Gurgel
New Zealand White Rabbits	Male, approximately 3 kg, approximately 20 weeks old. Animals were maintained as normal for 8 weeks prior to MI procedure (or sham operated / non-operated control groups), and then maintained for a further 12 weeks.	Gifted by Aileen Rankin
Human myocardial segment from single donor	Sample obtained from 56 year old white European male undergoing transplantation procedure. Previous MI and hypertrophic cardiomyopathy.	Gifted by Dr Cherry Alexander

Table 2-2 List and description of primary cardiac material used
All tissues were obtained from the indicated colleagues at the University of Glasgow.

2.1.3 Plasmids

IDENTITY	DESCRIPTION	SOURCE
PCDH-CMV-MCS-EF1-HA-GLUT4-GFP	Lentiviral plasmid containing gene sequence for GLUT4 tagged with green fluorescent protein reporter	Generated by Silke Machauer
PCDNA3.1(+)-GLUT4	pcDNA3.1(+) mammalian expression plasmid containing untagged functional GLUT4 gene sequence	Generated by GenScript, Piscataway, New Jersey, USA
PCDH-CMV-MCS-EF1-SX4(Y115/251E), 2P	Lentiviral plasmid containing gene sequence for Syntaxin 4, with mutations mimicking phosphorylation on 2 residues	Generated by Dr. Mohammed Nasser Rashid Al-Tobi
PCDH-CMV-MCS-EF1-GLUT4	Lentiviral plasmid containing untagged functional GLUT4 gene sequence	Generated within this project, as reported in section 2.5.4

Table 2-3 List and description of plasmids

2.1.4 General materials and reagents

Listed are key materials used in this project and the corresponding suppliers, with the product number (P/N) also detailed where possible.

AbCam, Cambridge, UK

Blebbistatin (P/N: ab120425)

Axiogenesis, Cologne, Germany

Cor.4U maintenance medium (contains FBS) for Axiogenesis iPSC-CM (P/N: Ax-M-HC250)

Cor.4U BMCC serum free medium (does not contain FBS) for Axiogenesis iPSC-CM (P/N: Ax-M-BMCC250)

Bio-Rad Laboratories Ltd., Hertforshire, UK

Precision Plus Protein All Blue Prestained Protein Standards (P/N: 1610373)

Cambridge Bioscience, Cambridge, UK

Ionomycin (P/N: CAY10004974)

Cellular Dynamics International, Wisconsin, USA

iCell Cardiomyocytes^2 Maintenance Medium (P/N: CMM-100-120-001)

iCell Cardiomyocytes^2 Plating Medium (P/N: CMM-100-110-001)

Corning Incorporated, Maine, USA

100mm x 20mm Polystyrene Cell Culture Dish (P/N: 430167)

12 well polystyrene TC-treated cell culture plate (P/N: 3513)

24 well TC-treated cell culture plate (P/N: 3524)

75cm^2 Polystyrene Cell Culture Flask (P/N: 430641U)

96 well clear flat bottom polystyrene TC-treated microplates (P/N: 3596)

Expedeon, Cambridge, UK

Instant Blue Coomassie (P/N: ISB1L)

Fisher Scientific, ThermoFisher Scientific, Leicestershire, UK

Ammonium Persulfate (P/N: A/6160/60)

Bovine Serum Albumin (P/N: BP9702-100)

D-Glucose anhydrous (P/N: G/0500/53)

Glycerol (P/N: G/0650/17)

Potassium Dihydrogen Orthophosphate (KH_2PO_4) (P/N: P/4800/53)
Tris Base (P/N: BP152-1)

Formedium, Norfolk, UK

Agar (P/N: AGA02)
Tryptone (P/N: TRP02)
Yeast Extract Powder (P/N: YEA02)

Gibco by Life Technologies, ThermoFisher Scientific, Paisley, UK

Dulbecco's Modified Eagle Medium (1x) 0 g/L D-Glucose (P/N: 11966025)
Dulbecco's Modified Eagle Medium (1x) 1 g/L D-Glucose (P/N: 11885084)
Dulbecco's Modified Eagle Medium (1x) 4.5 g/L D-Glucose (P/N: 41965039)
Dulbecco's Phosphate Buffered Saline (1x) (P/N: 14190094)
Fetal Bovine Serum (FBS) (P/N: 10500064)
L-Glutamine 200mM (100x) (P/N: 25030024)
MEM Non-Essential Amino Acids Solution (100X) (P/N: 11140-050)
Newborn Calf Serum (P/N: 16010159)
OPTI-MEM (1X) Reduced Serum Medium (P/N: 31985062)
Penicillin-Streptomycin (Pen-Strep) (10,000U/mL) (P/N: 15140122)
0.05% Trypsin-EDTA (P/N: 25300054)

MatTek Corporation, Massachusetts, USA

Glass-bottomed 96-well plates

Melford Laboratories Ltd., Suffolk, UK

Dithiothreitol (DTT) (P/N: MB1015)

Merck, Darmstadt, Germany

Sodium dihydrogen phosphate (NaH_2PO_4) (P/N: 106342)
Akt inhibitor VIII (isozyme-selective Akti1/2) (P/N: 124018)

Mirus Bio, Wisconsin, USA

*Trans*IT-TKO Transfection Reagent (P/N: MIR2155)

New England Biolabs, Massachusetts, USA

SOC Outgrowth Medium (P/N: B9020S)
T4 DNA Ligase (P/N: M0202S)
10X T4 DNA Ligase Reaction Buffer (P/N: B0202S)

Pall Life Sciences, New York, USA

BioTrace NT Nitrocellulose Transfer Membrane 0.2µm pore thickness (P/N: 66485)

Perkin Elmer, Massachusetts, USA

Deoxy-D-glucose, 2-[1,2-^{3}H (N)] (P/N: NET328A001MC)

Ultima Gold Liquid Scintillation Counting Cocktail (P/N: 6013326)

Promega, Wisconsin, USA

Blue/Orange DNA Loading Dye, 6X (P/N: G1881)

Buffer H restriction enzyme buffer (P/N: R008A)

EcoR1 restriction enzyme (P/N: R601A)

FuGENE HD Transfection Reagent (P/N: E2311)

1kb DNA ladder (P/N: G5711)

Not1 restriction enzyme (P/N: R643A)

Wizard Plus SV Minipreps DNA Purification Systems (P/N: A1330)

Qiagen, Hilden, Germany

Nuclease-Free water (P/N: 129115)

QIAfilter Plasmid Midi and Maxi Kits

Sartorius, Gottingen, Germany

Minisart 0.2 um pore size syringe filter (P/N: 16534K)

Severn Biotech Ltd., Worcestershire, UK

Acrylamide Bis-Acrylamide Stock Solution, 30% Acrylamide (w/v) Ratio 37.5:1 (P/N: 20-2100-10)

Sigma-Aldrich, Dorset, UK

Ampicillin Sodium Salt (P/N: A0166)

Bromophenol Blue (P/N: B0126)

(±)-Carnitine hydrochloride (P/N: C9500)

Creatine (P/N: C0780)

Cytochalasin B from *Drechslera dematioidea* (P/N: C6762)

2-Deoxy-D-glucose (P/N: D8375)

Dexamethasone (P/N: D4902)

Dulbecco's Phosphate Buffered Saline (DPBS) with $MgCl_2$ and $CaCl_2$ (P/N: D8662)

Ethidium Bromide Solution (P/N: E1510)

Fibronectin from bovine plasma (P/N: F1141)

HEPES (P/N: H3375)

Insulin from porcine pancreas (P/N: I5523)

Insulin-like Growth Factor-1 human (P/N: I3769)

Insulin-transferrin-sodium selenite media supplement (P/N: I1884)

3-isobutylmethylxanthine (IMBX)

Laminin from Engelbreth-Holm-Swarm murine sarcoma basement membrane (P/N: L2020)

Linoleic Acid-Oleic Acid-Albumin media supplement (100x) (P/N: L9655)

Magnesium sulfate ($MgSO_4$) (P/N: M3409)

Medium 199 (P/N: M7528)

Nifedipine

N,N,N',N'-Tetramethylethylenediamine (TEMED) (P/N: T9281)

Palmitic acid (P/N: P0500)

Ponceau S (P/N: P3504)

Sodium deoxycholate (P/N: D6750)

Taurine (P/N: 86329)

3,3',5-Triiodo-L-thyronine sodium salt (P/N: T6397)

Triton X-100 (P/N: T9284)

Trypan Blue Solution (0.4%) (P/N: T8154)

TWEEN 20 (P/N: P7949)

Wortmannin

STARLAB, Milton Keynes, UK

StarTub Reagent Reservoir 55ml (P/N: E2310-1010)

ThermoFisher Scientific, Illinois, USA

Lipofectamine 2000 Transfection Reagent (P/N: 52887)

Pierce BCA Protein Assay Reagent A (P/N: 23228)

Pierce BCA Protein Assay, Reagent B (P/N: 23224)

Pierce Protease Inhibitor Mini Tablets, EDTA Free (P/N: 88666)

PureLink Quick Gel Extraction Kit (P/N: K210012)

UltraPure Agarose (P/N: 16500500)

Tocris Bioscience, Abingdon, UK

Troglitazone (P/N: 3114)

Toronto Research Chemicals, Ontario, Canada

5-Aminoimidazole-4-carboxamide-1-ß-D-ribofuranoside (AICAR)

VWR Chemicals, Leicestershire, UK

Calcium chloride ($CaCl_2$) (P/N: 190464K)

di-Sodium hydrogen phosphate anhydrous (Na_2HPO_4) (P/N: 102494C)

Ethanol absolute (P/N: 20821.330)

Magnesium chloride hexahydrate (P/N: 25108.260)

Potassium chloride (KCl) (P/N: 26764.260)

Sodium chloride (NaCl) (P/N: 27810.295)

Sodium dodecyl sulphate (SDS) (P/N: 442444H)

2.1.5 Specialised equipment

Beckman Coulter, High Wycombe, UK

LS6500 Liquid Scintillation Counter

Bio-Rad Laboratories Ltd., Hertforshire, UK

All immunoblotting apparatus - power supplies, gel casting apparatus, electrophoresis chamber etc. – was obtained from the Bio-Rad Mini-PROTEAN range

BMG Labtech, Ortenberg, Germany

FLUOstar OPTIMA Microplate Reader

Clyde Biosciences, Motherwell, UK

CellOPTIQ imaging system

LI-COR Biosciences, Lincoln, Nebraska, USA

LI-COR Odyssey Sa Infrared Imaging System

2.1.6 Recipes for solutions

All ingredients diluted in distilled water unless otherwise stated.

Basic Krebs Buffer (Cardiac Isolation)

130 mM NaCl

5 mM Hepes

4.5 mM KCl

0.4 mM NaH_2PO_4

3.5 mM $MgCl_2$

10 mM Glucose

140 µM $CaCl_2$

(pH adjusted to 7.25 prior to use)

Krebs-Ringer-Phosphate (KRP) Buffer for [^{3}H]-2DG Uptake Assay

128 mM NaCl

4.7 mM KCl

5 mM NaH_2PO_4

1.25 mM $MgSO_4$

1.25 mM $CaCl_2$

(pH adjusted to 7.4 prior to use)

2x Laemmli Sample Buffer (LSB)

100 mM Tris pH 6.8

4% SDS (w/v)

20% Glycerol (v/v)

0.2% bromophenol blue (w/v)

100 mM DTT

LB Broth

1% (w/v) Tryptone

0.5% (w/v) Yeast Extract

1% (w/v) NaCl

(Autoclaved prior to use)

Phosphate Buffered Saline (PBS)

137 mM NaCl

2.7 mM KCl

1.8 mM KH_2PO_4

10 mM Na_2HPO_4

(pH adjusted to 7.4 prior to use)

Phosphate Buffered Saline with TWEEN 20 (PBS-T)

PBS containing 0.1% TWEEN 20 (v/v)

Ponceau S

0.1 % Ponceau (w/v)

5% acetic acid (v/v)

RIPA Buffer

50 mM Tris pH 8

150 mM NaCl

1% Triton X-100 (v/v)

0.5% Na deoxycholate (w/v)

0.1% SDS (w/v)

5 mM DTT

1x Protease Inhibitor Cocktail Tablet

TAE Buffer

40 mM Tris

1 mM EDTA

(pH adjusted to 7.2-7.4 prior to use)

Tris Buffered Saline (TBS)

20 mM Tris pH 7.5

137 mM NaCl

(pH adjusted to 7.4 prior to use)

Tris Buffered Saline with TWEEN 20 (TBS-T)

TBS with 0.1% TWEEN 20 (v/v)

2YT

1.5% (w/v) Tryptone

1% (w/v) Yeast Extract

0.5% (w/v) NaCl

(Autoclaved prior to use)

2.1.7 List of primary antibodies

Antigen	Details	Working Dilution	Source
VAMP 1	Rabbit polyclonal	1:1000 in 1% milk in PBS-T	Synaptic Systems (P/N: 104002)
VAMP 2	Rabbit polyclonal	1:1000 in 1% milk in PBS-T	Synaptic Systems (P/N: 104202)
VAMP 3	Rabbit polyclonal	1:1000 in 1% milk in PBS-T	Synaptic Systems (P/N: 43080)
VAMP 4	Rabbit polyclonal	1:1000 in 1% milk in PBS-T	Synaptic Systems (P/N: 136002)
VAMP 5	Rabbit polyclonal	1:1000 in 1% milk in PBS-T	Synaptic Systems (P/N: 176003)
VAMP 7	Rabbit polyclonal	1:1000 in 1% milk in PBS-T	Synaptic Systems (P/N: 232003)
VAMP 8	Rabbit polyclonal	1:1000 in 1% milk in PBS-T	Synaptic Systems (P/N: 104302)
SNAP 23	Rabbit polyclonal	1:1000 in 1% milk in PBS-T	Synaptic Systems (P/N: 111202)
SNAP 29	Rabbit polyclonal	1:1000 in 1% milk in PBS-T	Synaptic Systems (P/N: 111303)
SNAP 47	Rabbit polyclonal	1:1000 in 1% milk in PBS-T	Synaptic Systems (P/N: 111403)
Syntaxin 2	Rabbit polyclonal	1:1000 in 1% milk in PBS-T	Synaptic Systems (P/N: 110022)
Syntaxin 3	Rabbit polyclonal	1:1000 in 1% milk in PBS-T	Synaptic Systems (P/N: 110032)
Syntaxin 4	Rabbit polyclonal	1:1000 in 1% milk in PBS-T	Synaptic Systems (P/N: 110042)
Syntaxin 5	Rabbit polyclonal	1:1000 in 1% milk in PBS-T	Synaptic Systems (P/N: 110053)
Syntaxin 6	Mouse	1:1000 in 1% milk in PBS-T	BD Biosciences (P/N: 610635)
Syntaxin 7	Rabbit polyclonal	1:1000 in 1% milk in PBS-T	Synaptic Systems (P/N: 110072)
Syntaxin 8	Rabbit polyclonal	1:1000 in 1% milk in PBS-T	Synaptic Systems (P/N: 110083)
Syntaxin 16	Rabbit polyclonal	1:1000 in 1% milk in PBS-T	Synaptic Systems (P/N: 110162)
Pan Akt	Mouse monoclonal	1:2000 in 3% BSA in TBS-T	Cell Signalling Technology (P/N: 2920)
Phospho-Akt	Rabbit monoclonal,	1:1000 in 3% BSA in TBS-T	Cell Signalling Technology (P/N: 4058)

	targeting residues of Serine 473		
P44/42 MAPK (total Erk1/2)	Rabbit polyclonal	1:2000 in 3% BSA in TBS-T	Cell Signalling Technology (P/N: 9102)
Phospho-p44/42 MAPK (Phospho-Erk1/2)	Mouse monoclonal, targeting residues of Threonine 202 and Tyrosine 204	1:1000 in 3% BSA in TBS-T	Cell Signalling Technology (P/N: 9106)
GAPDH	Mouse monoclonal	1:80,000 in 1% milk in PBS-T	Ambion (P/N: 4300)
GLUT 1	Rabbit polyclonal	1:1000 in 1% milk in PBS-T	AbCam (P/N: 652)
GLUT 4	Rabbit polyclonal	1:2000 in 5% milk in PBS-T	AbCam (P/N: 654)
GLUT 8	Rabbit polyclonal	1:1000 in 1% milk in PBS-T	AbCam (P/N: 191269)
GLUT 10	Rabbit polyclonal	1:1000 in 1% milk in PBS-T	ThermoFisher Scientific (P/N: PA1-46137)
GLUT 12	Rabbit polyclonal	1:1000 in 1% milk in PBS-T	AbCam (P/N: 191298)
CD36	Mouse monoclonal	1:1000 in 1% milk in PBS-T	AbCam (P/N: 23680)
Total OXPHOS Human WB Antibody Cocktail	Commercially prepared cocktail of 5 mouse monoclonal antibodies	1:1000 in 3% BSA in PBS-T	AbCam (P/N: 110411)
GFP	Rabbit polyclonal	1:1000 in 1% milk in PBS-T	AbCam (P/N: 290)
SERCA 2a	Mouse monoclonal	1:1000 in 1% milk in PBS-T	AbCam (P/N: 2861)

Table 2-4 List and description of primary antibodies

2.1.8 List of secondary antibodies

Antigen	Details	Working Dilution	Source
Rabbit IgG	IRDye 800CW Donkey anti Rabbit IgG	1:5000-10,000, in 1% milk in PBS-T	LI-COR Biosciences (P/N: 926-32213)
Mouse IgG	IRDye 680LT Donkey anti Mouse IgG	1:5000-10,000, in 1% milk in PBS-T	LI-COR Biosciences (P/N: 926-68022)

Table 2-5 List and description of secondary antibodies

2.2 Cell culture methods

2.2.1 Growth and maintenance of HEK 293 and HeLa cells

Both HEK 293 and HeLa cells were grown and maintained in T75 flasks located within a sterile humidified incubator. Conditions were kept constant at 37°C and 5% CO_2. Cells were maintained in DMEM (4.5 g/L glucose) supplemented with 10% (v/v) FBS, 1% (v/v) L-glutamine, and 1% (v/v) pen-strep. This media was replaced every 2-3 days until cells were subjectively judged to be at >80% confluence via visual inspection. At this point the cells were either split (passaged) into a new set of flasks to facilitate continued growth, or seeded into the relevant multi-well plate for use in either a [^{3}H]-2DG uptake assay or in preparation for transfection.

2.2.2 Passaging and plating of HEK 293 and HeLa cells

To passage HEK 293 and HeLa cells, first of all the media was aspirated and cells were washed once with pre-warmed sterile PBS (pH 7.4, 37°C). Subsequently, cells were incubated for approximately 5 min with 2 mL 0.05% trypsin-EDTA in order to liberate them from the growth surface. After ensuring the majority of cells were detached, this cellular suspension was diluted in fresh pre-warmed medium and transferred into as many new flasks as was desired. The volume of medium added was determined by how densely populated the new flasks were required to be, with approximately 10 mL medium per flask.

Similarly, when cells were required for use in a [^{3}H]-2DG uptake assay they were first washed and trypsinised as described above, and then resuspended in 5 mL fresh medium. Then a manual cell count was performed with a hemocytometer to

provide an estimate of the total number of cells in the suspension. The volume of medium was further adjusted to give the desired number of cells per 200 µL, which was then pipetted to each well of a 96 well plate. Final plating density is denoted on relevant figures. Assays were performed as soon as was practically possibly post plating (typically the next day) in order to limit the difference between the number of cells plated into each well, and the number of cells actually present at the time of the assay, as these cells replicate rapidly.

HeLa cells were also used in transfection experiments. Cells were passaged as described above, however rather than performing a cell count the approximate dilution required to plate cells at a density of 50% growth surface coverage was performed. This was achieved through a simple calculation based upon the knowledge of the different growth surface areas of the appropriate culture vessels. Transfection was performed on both a 12 and 96 well scale, therefore volumes were adjusted accordingly. Cells were maintained until they reached a confluence suitable for transfection, which according to manufacturer's recommendations was 70-90% confluency.

2.2.3 Growth and maintenance of 3T3-L1 adipocytes

In their immature fibroblast-like form 3T3-L1 pre-adipocytes were grown and maintained in T75 flasks located within a sterile humidified incubator with conditions maintained at 37°C and 10% CO_2. The medium contained 10% (v/v) NCS and 1% (v/v) pen-strep in DMEM (4.5 g/L glucose) and was replaced every 2 days until cells were judged to be at >80% confluence. At this point the cells were either split into a new set of flasks, or seeded into a multi-well plate either for use in a [^{3}H]-2DG uptake assay or for the purpose of generating lysates.

2.2.4 Passaging and plating of 3T3-L1 adipocytes

3T3-L1 fibroblast-like pre-adipocytes were passaged and plated in a highly similar manner to HEK 293 and HeLa cells, as detailed above. The 2 key differences were the composition of medium used, and also that when plating into a 96-well plate in preparation for performing a [^{3}H]-2DG uptake assay, cells were not plated at a specific density. Rather they were plated at a subconfluent density and grown to confluence, in preparation for differentiation.

2.2.5 Differentiation of 3T3-L1 adipocytes

Prior to use for either measurement of insulin stimulated glucose uptake or protein expression, 3T3-L1 adipocytes were required to be differentiated in to their mature adult form. Cells were maintained in NCS medium until 100% confluence was achieved. 2-3 days later differentiation was initiated by replacing this medium with 10% (v/v) FCS, 1% (v/v) pen-strep, 0.5 mM IBMX, 172 nM insulin, 0.25 µM dexamethasone, and 5 µM troglitazone in DMEM (4.5 g/L glucose). 3 days later this medium was exchanged for 10% (v/v) FCS, 1% (v/v) pen-strep, 172 nM insulin, and 5 µM troglitazone in DMEM (4.5 g/L glucose). Finally, a further 3 days later this medium was exchanged for 10% (v/v) FCS and 1% (v/v) pen-strep in DMEM (4.5 g/L glucose). This medium was then exchanged every 2 days up until the day of use, which was typically 9-12 days post differentiation.

2.2.6 Plating of Axiogenesis iPSC-CM

Cor.4U iPSC-CM were purchased from Axiogenesis (Cologne, Germany) and immediately transferred into liquid nitrogen for long term storage upon receipt. [During the latter stages of this project Axiogenesis merged with a separate company called Pluriomics to form a new company called NCardia. However, the Cor.4U product was unaffected.]

Approximately 3 hours prior to plating, 96-well plates were coated with 70 µL fibronectin from bovine plasma diluted 1:100 in PBS (supplemented with $MgCl_2$ and $CaCl_2$) to give a final concentration of approximately 2 µg/cm^2. Cells were retrieved from liquid nitrogen and defrosted in a 37°C water bath for approx. 1-2 min, until only a small volume of solution remained frozen. Then 500 µL pre-warmed Cor.4U maintenance medium was added to the vial to give a total volume of 1 mL. This suspension was then slowly pipetted dropwise into a 50 mL falcon tube containing an additional 3 mL of pre-warmed Cor.4U media to minimise the risk of heat shock to the cells, and with constant gentle manual agitation in order to reduce the risk of cells clumping. The empty vial was rinsed with a further 1 mL of media in order to harvest any remaining cells and this was also added to the suspension. As instructed by manufacturers' guidelines, great care was taken regarding timings and pipetting, as these cells are sensitive to rapid temperature changes and shear stress.

Once a 5 mL cellular suspension was attained, a live cell count was performed. To achieve this, the suspension was gently mixed and a 10 µL sample was withdrawn and combined with 10 µL 0.4% trypan blue. This dye penetrates and bypasses the plasma membrane of severely damaged and dead cells and stains them blue, therefore observation of the internal colour of cells down a light microscope permits determination of cell viability. Through manual counting with a hemocytometer, an estimation of total number of living cells per mL suspension was obtained. Typically >80% of cells were deemed viable. The suspension was then diluted as required to give the desired number of cells per mL. Finally the PBS was aspirated from each well and 100-200 µL suspension was added as required, to each specific well of the 96-well plate(s). Plating density ranged from 25,000 – 50,000 living cells per well, and is reported on all relevant figures. On the few occasions where iPSC-CM were plated into a larger multi-well plate, volumes were scaled appropriately based upon relative growth surface areas.

2.2.7 Plating of iCell CDI iPSC-CM

iCell iPSC-CM were purchased from CDI and immediately transferred into liquid nitrogen for long term storage upon receipt. 3 hours prior to plating, 96-well plates were coated with fibronectin as described above. At the appropriate time cells were retrieved and the vial was placed in a 37°C water bath for approximately 3 min. Subsequently, the contents of the vial were transferred directly into a sterile, empty 50 mL falcon centrifuge tube. The vial was then rinsed with 1 mL of room temperature CDI plating medium, which was added dropwise to the cellular suspension. An additional 3 mL plating medium was carefully added to give a final volume of 5 mL. From this, a 10 µL sample was withdrawn and a live cell count was performed as described above (section 2.2.6) in order to confirm cell count and viability as reported in the certificate of testing. The suspension was diluted as required and then immediately after aspiration of the PBS 100 µL was pipetted into each well. In all cases CDI iPSC-CM were used at the manufacturers recommended plating density of 50,000 viable cells per well of a 96-well plate. Finally, medium was replaced with pre-warmed (37°C) CDI maintenance medium approximately 4 hours post-plating.

2.2.8 Maintenance of Axiogenesis and iCell CDI iPSC-CM

Both Axiogenesis and iCell CDI iPSC-CM were kept in a sterile humidified incubator with conditions maintained at 37°C and 5% CO_2. Cor.4U (Axiogenesis) and CDI maintenance media were replaced approximately 24 hours post plating and every 1-2 days thereafter up until the day of use, which was typically 7 (+/- 1) days post plating regardless of whether the intended use was for a functional assay or to make protein lysates. Where this was not the case, it is detailed within all relevant figure legends. Media was generally replaced by manual pipetting rather than use of an aspirator, in order to cause minimal disturbance to cells.

In many experiments, interventions were implemented prior to the day of the specified assay in an attempt to alter iPSC-CM phenotype. Primarily, cells were cultured in the presence of palmitate (conjugated to BSA), triiodothyronine (T_3), or maturation medium (MM). Where the data generated from these experiments is presented, the conditions are clearly stated with regards to the concentrations implemented and the duration of the interventions. In all cases the interventions started a minimum of 3 days post-plating, in order to allow recovery of the cells after liquid nitrogen storage and adoption of a stable contractile phenotype. Conditions were then maintained, with media changes every 1-2 days as required, up until the day of use. Interventions involving the introduction of exogenous plasmid DNA are detailed separately in section 2.5.

2.2.9 Plating and maintenance of primary rabbit cardiomyocytes

Approximately 30 min post-isolation (this protocol is detailed below in section 2.3.1), septal primary rabbit cardiomyocytes were put through several cycles of settling and resuspension in Krebs buffer containing increasing concentrations of calcium chloride (0.1, 0.2, 0.5, 1, 1.8 mM). This was performed in order to increase the physiological relevance of subsequent experiments and maintain optimal functioning of the cells as calcium is critical to several intracellular processes (Bers, 2002). Attaining the final concentration via a stepwise progression minimised the risk of the well described calcium paradox whereby rapid overload of isolated cardiomyocytes with physiological levels of calcium induces hypercontraction and cell death. Subsequently, cells were transferred into Medium 199 (M199) supplemented with 1 mM L-Glutamine, 5 mM creatine, 5

mM taurine, and 5 mM carnitine. A manual cell count was performed to estimate the total number of elongated “rod” shaped cardiomyocytes in the cellular suspension. Cardiomyocytes that adopt a rounded “ball” phenotype are considered likely to be dedifferentiated, dead, or hypercontracted, therefore determination of rod number does not provide an estimate of total number of living cells, but rather those that are considered likely to still be viable and functional (Mitcheson *et al.*, 1998). Cells were plated on 96-well plates at an estimated density of 15,000 rods per well in a minimum of 100 µL medium M199. Wells had been pre-coated with laminin (1-2 µg/cm^2) for a minimum of 2 hours and washed 3 times with PBS prior to plating. After initial experimentation with different time points (data not shown) it was determined that optimal timing for functional assays was approximately 3 hours post plating.

2.3 Protein methods

2.3.1 Isolation of primary cardiac samples

Isolated primary cardiac myocytes/tissue was obtained from a number of sources throughout this project. In the case of primary mouse (multiple sources), human, and rat tissue, this was received as a stored snap frozen whole organ or large sections of intact myocardium. Protein lysates were made directly from these samples, without isolation, as described below. In contrast, rabbit samples were received as freshly isolated cardiomyocytes, in order to allow measurement of glucose uptake and insulin dependent activation of Akt. Lysates used for immunoblotting were generated both directly from these isolated myocytes in suspension, and also after plating, depending upon the context of the experiment.

Isolation of primary rabbit cardiomyocytes was performed by Mrs Aileen Rankin and Mr Mike Dunne (University of Glasgow). Briefly, rabbits were euthanized by injection of 100 mg/kg pentobarbital into the marginal ear vein in accordance with the Animal (Scientific Procedures) Act 1986. Subsequently, the heart was excised and reverse perfused with Krebs buffer (37°C, pH 7.25) supplemented with heparin (5000 U/mL) on a Langendorff rig, in order to prevent clotting and clear the vasculature of residual blood. Then Krebs buffer supplemented with protease and collagenase was passed through the heart for approximately 15 min, until the heart was subjectively judged to be ready for manual processing.

Thereafter, the heart was removed from the rig, dissected into distinct anatomical regions (e.g. left ventricle/ atria/ septum), and diced with a sterile surgical scalpel blade in Krebs buffer supplemented with 1% BSA (w/v). These much smaller cardiac segments were then agitated for approximately 10 min. The solution was then filtered using a gauze strip into a 15 mL centrifuge tube, in order to remove large segments of undigested/unprocessed tissue, and harvest a more pure solution of isolated myocytes. Thereafter cells underwent the plating procedure described above, or the lysate generation procedure described below. In this thesis, isolated cells were provided using this procedure.

2.3.2 Induction and confirmation of disease phenotypes

As mentioned above, throughout this project cardiac samples were obtained from multiple sources and species. In all cases tissue was obtained from male animals in order to minimise the effect of variables such as female hormonal cycles, however it is recognised that sex specific differences in physiology and disease outcomes may be of great importance in this area of research and must be accounted for within future work. Within the present study different models of cardiac disease and relevant controls were also provided. In all cases these were from well characterised and published models of either diabetes (*db*/*db* and HFD) or MI, as described in Table 2-2. Appropriate corresponding literature or data from the providers of the samples was supplied in order to ensure that the desired phenotype was successfully induced. In the case of rabbit and rat models of MI, this phenotype was induced by technicians at the University of Glasgow. Briefly, animals were anaesthetised prior to thoracotomy and permanent ligation of the left anterior descending coronary artery. With regards to the rabbit model, data was provided to indicate a reduction of left ventricular fractional shortening below 50%, indicative of impaired systolic contractile capacity (data not shown).

2.3.3 Generation of lysates

2.3.3.1 Primary cardiac tissue

Snap frozen whole hearts or segments of myocardium were placed in a 10 cm dish on ice in 0.5-2 mL RIPA buffer, dependent upon the size of the sample. Samples were then manually diced as much as possible with a sterile scalpel blade. The solution, now containing many much smaller segments of tissue, was transferred

into a specialised 1.5 mL maximum capacity glass tube, and a Dounce style manual tissue grinder was used to further mechanically lyse the cells via exposure to shear stress, with 5-10 compressions of the apparatus. The samples were then left on ice for approximately 20 min, before another 5-10 compressions of the manual homogenisation apparatus to ensure maximal lysis. On one occasion an alternative homogenisation protocol was employed. This methodology is described within the text preceding Figure 5-3, within section 5.2.1. The sample was then transferred to a 1.5 mL capacity eppendorf and spun at 14,000 rpm for 15 min at 4°C. The supernatant was then aliquoted and stored at -20°C until required for use, and the pellet was discarded.

2.3.3.2 Isolated rodent primary cardiomyocytes

When lysed without initial plating, isolated rabbit cardiomyocytes were first of all allowed to settle in Krebs solution in a 15 mL centrifuge tube. Subsequently, this was aspirated and replaced with 0.5-2 mL RIPA buffer, determined by the size of the pellet. This suspension was then transferred into the glass homogenisation tube as described above and compressed 5-10 times twice with 20 min break on ice in between. Finally, the solution was again centrifuged at 14,000 rpm for 15 min at 4°C and the supernatant was aliquoted and stored at -20°C.

2.3.3.3 iPSC-CM

Regardless of whether iPSC-CM were from Axiogenesis or CDI, lysates were generated from a 96-well plate using the same protocol. Initial attempts to harvest the cells in RIPA buffer via a method suitable for measuring protein concentration from the samples was deemed unsuitable, due to the low protein concentrations of the samples that were generated. In contrast, the application of 30 µL 2x LSB directly to wells for 20 min whilst the plate was sitting on ice, before scraping and harvesting the contents of each well with a P20 pipette tip, was found to give a much more concentrated and effective yield of protein (Bowman, unpublished results). Finally, samples were heated to 65ºC for 10 min and then stored until required for use. Using this technique renders it impossible to estimate protein concentration using conventional techniques, therefore this increased the importance of using loading controls such as GAPDH expression and Ponceau S staining when interpreting the results of any immunoblot containing

these samples. However, particularly when comparing between iPSC-CM that have undergone different interventions, as long as a similar number of cells are present across different wells, and the method of lysate generation remains the same, then total protein loaded should be expected to be approximately equal.

Similar to when describing the plating of iPSC-CM, on occasion lysates were generated from cells on a larger scale (e.g. 12 or 24 well plate). In this case the general principle of the lysate generation protocol remained the same, but the initial volume of 2x LSB applied to each well was scaled appropriately. The aim was to add the minimally required volume to cover the surface area, in order to generate the most concentrated lysate possible.

2.3.3.4 HeLa cells, 3T3-L1 adipocytes, and plated primary cardiomyocytes

The method of generating protein lysates from HeLa cells, 3T3-L1 adipocytes, and primary (rabbit) cardiomyocytes that had been plated on a 96-well plate format was identical to that as described above for iPSC-CM.

2.3.4 Phospho-Akt/Erk1/2 assay

In certain experiments it was assessed if insulin stimulation altered the phosphorylation of the central insulin signaling intermediates Akt and Erk1/2 in isolated primary rabbit cardiomyocytes and/or iPSC-CM. In all cases this experiment was performed on a 96-well plate format. When performing this assay with iPSC-CM, cells were incubated in serum free DMEM (4.5 g/L glucose) for a minimum of 2 hours prior to insulin stimulation. After this initial serum starvation, insulin was added directly to the medium at a final concentration of 860 nM for 30 min. When performing this assay with primary rabbit cardiomyocytes, serum starvation was not performed. Instead approximately 3 hours post plating medium was simply replaced with fresh M199 and insulin was directly added, again at a final concentration of 860 nM. For both cell types, insulin stimulation was terminated by aspiration of the medium and immediate generation of cell lysates as described above. In order to assess the primary outcomes, samples were then prepared for and run through SDS-PAGE and immunoblotted for phospho Akt (ser473) and pan Akt (iPSC-CM and primary rabbit cardiomyocytes), and phospho and total Erk 1/2 (iPSC-CM only).

2.3.5 Micro BCA assay

When appropriate, a micro BCA assay was employed to measure protein concentrations. 10 µL of each unknown protein sample and a range of BSA protein standards (0-10 mg/mL) in duplicate were combined with the manufacturer's micro BCA assay mix, and incubated at 37°C for 30 min. Further duplicates of each sample with 50% protein concentration (diluted 1:1 with distilled water) were also performed in order to increase confidence in generated estimates and also increase the chances of at least one set of duplicates falling within the range of the BSA standards. The absorbance at 562 nm was recorded using a microplate reader.

2.3.6 SDS-PAGE

A polyacrylamide resolving gel was cast using the Biorad mini-Protean III equipment. The final percentage of acrylamide was determined by the size of the protein of interest, but typically ranged from 10-15%. Other components were 375 mM Tris (pH 8.8), 0.1% SDS (w/v), 0.1% APS (w/v), and 200 nM TEMED, diluted in distilled water. Typical gel thickness was 1.5 mm. The stacking gel was cast on top of the resolving gel once it had set. The reagents required to make this gel were the same as the resolving gel, but at a final concentration of 5% acrylamide, 125 mM Tris (pH 6.8), 0.1% SDS (v/v), 0.1% APS(v/v), and 200 nM TEMED. Samples were usually electrophoresed at 100V for approximately 2 hours.

2.3.7 Immunoblotting

After SDS-PAGE, if the intention was then to immunoblot using antibodies to detect specific proteins then samples were transferred onto a nitrocellulose membrane. To achieve this, the gel was placed in direct contact with a membrane within a tight sandwich of transfer sponges and 3 mm Whatman chromatography paper in a transfer cassette. This in turn was placed within a transfer tank that was filled with transfer buffer (25 mM tris, 192 mM glycine, 20% ethanol absolute (v/v) in distilled water). To initiate transfer, a 200 mA current was applied for 2 hours. Where required, transfer was also occasionally performed at 30 mA for 15 hours (overnight), or at 100V for 1 hour (with an ice pack to prevent overheating). In general, transfer efficiency was not found to vary between protocols.

After transferring was complete, nitrocellulose membranes were incubated with the reversible protein stain Ponceau S in order to assess transfer efficiency. This was then washed off with PBS-T, and a blocking solution was applied for 30-60 min in order to reduce non-specific binding of the primary antibody. This solution was typically 5% milk powder (w/v) in PBS-T, apart from when subsequently assessing the expression of phospho antibodies such as Akt or Erk1/2, in which case 3% BSA in TBS-T was required. After completion of blocking, membranes were then incubated with the desired primary antibody on an oscillating roller at 4°C for 16 hours (overnight) in a 50 mL centrifuge tube, in order to facilitate optimal and even antibody binding. Details regarding the preparation of all primary antibodies used are found in Table 2-4. Occasionally, particularly if an overnight transfer was performed, primary antibody incubation would be performed at room temperature for 1-2 hours.

After incubation with the relevant primary antibody, membranes were washed 3 times for 5-10 min with PBS-T (or TBS-T as appropriate). Then the fluorescent secondary antibody specific to the species in which the primary antibody was raised in was applied for 1-2 hours. The details of all secondary antibodies used are found in Table 2-4. At this point, and for the remainder of the protocol, the 50 mL centrifuge tubes containing the membranes were wrapped in tin foil in order to prevent exposure to excessive light, as the secondary antibodies are light sensitive. After this second incubation, membranes were again washed 3 times for 5-10 min in P(T)BS-T, before visualisation with the Odyssey infra-red LICOR imaging system. Images were only obtained within the linear range of fluorescent signal measurement.

2.3.7.1 Densitometry

Scanning of nitrocellulose membranes that had undergone the described process of immunoblotting was performed at 100 μm resolution and generated a high quality composite image of 2 channels of excitation/emission. From this a subjective assessment of protein expression from each sample could be gained, most notably whether or not the target protein was expressed and/or if any intervention had an impact on the level of expression. Where a difference was visibly detectable, quantification was performed for further objective assessment. This was achieved by importing the image in to Image Studio Lite (Version 5.2),

the most up to date software designed by LICOR and recommended for use with these images. The analysis feature was used to place a box around each band of interest, with settings to record the mean pixel intensity (arbitrary units), which is automatically background corrected by this programme. The precise method of determining background intensity was altered slightly depending on factors such as interference of nonspecific bands, however was kept consistent between bands within the same blot.

2.3.8 Coomassie staining

Instant Blue Coomassie staining was used to visualise proteins for certain applications. Gels were incubated with sufficient Instant Blue solution to completely cover them on a shaking platform for a minimum of 1 hour. Thereafter, the gel was washed briefly with water to reduce the background signal, before being scanned.

2.4 Cellular methods

2.4.1 [^{3}H]-2DG uptake assay

2.4.1.1 General protocol

[^{3}H]-2DG uptake assays were performed as a surrogate assay of glucose uptake. A range of optimisation steps are reported in the results chapters, with a clear description of the protocol employed for each experiment for each cell type. Therefore only a general overview of the methodology for iPSC-CM is reported.

First of all, iPSC-CM were incubated in serum free medium for 2 hours. The exact medium used varied and is discussed in the appropriate results section. Subsequently, plate(s) were transferred to a hot plate (37°C) and washed once in prewarmed KRP buffer (37°C, pH 7.4), and incubated for 30 min with all combinations of 100 µL KRP +/- 40 µM cytochalasin B (CB) +/- 860 nM porcine insulin. Each condition was performed in a minimum of triplicate wells. Following this, 100 µL ^{3}H 'assay mix' was added for a further 30 min. This contained 2-deoxyglucose and [^{3}H]-2-deoxyglucose at a final concentration of 50 µM and 0.4 µCi respectively. The assay was terminated by manually pipetting off the solution and washing cells once in ice cold PBS. Subsequently, plates were air-dried before

150 µL 1% Triton X-100 was added to each well for a minimum of 1 hour in order to promote lysis. Thereafter the solution from each well was individually collected and radioactivity levels measured using scintillation counting.

2.4.1.2 Analysis of [^{3}H]-2DG results

At minimum, within a typical individual [^{3}H]-2DG uptake experiment, 3 replicate samples were obtained within 4 distinct conditions. This raw data was plotted and visually inspected to gain an initial impression of the data and assess if there may be any outliers or anomalies. The primary (and rare) reason that may be accepted to justify exclusion of a data point would be if it were lower than the corresponding CB value, as this indicates measurement error. Thereafter, the mean CB value for each condition (e.g. +/- insulin) was calculated. Then these values were subtracted from each data point from the corresponding condition in the absence of CB. This data was thereafter referred to as background corrected, and is what is reported in most figures, apart from where the signal to background noise ratio was of interest. At this point statistical comparisons could now be made between conditions and final graphs were plotted, both using GraphPad Prism.

2.4.2 Contractility

As reported in chapter 3.2.3, during one set of experiments within this project contractility was recorded from iPSC-CM using the Cell OPTIQ imaging system. First of all, cells were plated at 25,000 or 50,000 cells per well and maintained as normal until 6 days post plating. At this point, the iPSC-CM were transferred into a microscope stage incubator, which maintained constant conditions of 37°C and 5% CO_2. Within this technical set up, the image obtained through the 40x objective lens of the microscope could be rapidly redirected from the normal eye piece output to a high speed capture camera system, which obtains high resolution images at a rate of 100 frames per second from within the field of view.

Spontaneous contraction of the iPSC-CM within this field of view was video recorded for 5 seconds from 3 distinct areas of each well, and in total 8 wells were assayed per condition (each specified plating density). The average contraction rate of iPSC-CM is approximately 1 Hz, therefore in general 5 contractions (and subsequent relaxations) were captured. The location of each recording was

subjectively determined, but in general were as far apart as possible. The only strict requirement was that the field of view contained a group of cells that were contracting in unison, as two distinct contractile profiles within the same trace was unusable for the purposes of analysis. The movement of the microscope stage was controlled via an external joystick, which facilitated rapid movement of the field of view between areas of the same well, or indeed between different wells. Therefore the overall time taken to record all measurements was limited, which decreased the risk of order effects occurring. This was important because despite efforts being made to maintain optimal environmental conditions, any progressive change in a relevant variable that may strongly influence myocyte contraction (e.g. pH, temperature) could influence the values recorded from each well to a different extent, dependent upon the time of measurement after initial removal from the incubator.

After all recordings had been obtained the data was imported into Image J. Thereafter, custom designed software written by Dr. Francis Burton (a software developer and member of staff at both the University of Glasgow and Clyde Biosciences) was used to analyse each video individually and produce the contractile output trace displayed in Figure 3-11. From this trace, a range of parameters were quantified, most notably the amplitude and frequency of contraction, and the speed of contraction and relaxation. These variables are explained and discussed further in chapter 3.2.3. However, it is important to note that the data for each variable was processed by first of all taking the average value for each parameter from every trace (each distinct location within a well). Then the mean value of every set of 3 technical repeats was calculated and a single value was produced for each well. It is this value that is reported in the final output, providing 8 replicate samples for each condition. Finally, all of the parameters apart from amplitude of contraction are independent of the number of cells from which contraction is recorded. However, amplitude takes in to account the total extent of disordered contraction detected. Therefore the final output of this parameter had to have a correction factor applied that adjusted the data for the number of cells plated per well.

2.5 Molecular methods

2.5.1 Purified protein production

Within this project, samples of various purified recombinant SNARE proteins were required. Some of these were generated as part of this project, however the majority of those used and from which results are reported were kindly donated by Dr. Jessica Sadler. Therefore, a brief summary of the generation of these samples is described below.

Appropriate DNA plasmids were expressed in BL-21 *E.coli* and these cells were then amplified via serial cultures of increasing volume in appropriate medium supplemented with 100 µg/mL ampicillin until a 1 L culture with an optical density reading at 600 nm of 0.6 (indicative of optimal growth phase) was obtained. At this point the expression of the intended gene and therefore production of associated protein was induced by incubating the cells with 0.5 mM Isopropyl B-D-1-thiogalactopyranoside (IPTG) overnight at 22ºC. The following day cells were centrifuged and then resuspended in lysis buffer, which was PBS supplemented with a protease inhibitor tablet and lysozyme at a final concentration of 1 mg/mL, for 20 min at 4 degrees on a rotating platform. Subsequently, cells were sonicated for 4 x 30 sec, centrifuged, and the pellet was discarded. At this point a cell lysate was obtained, therefore a method capable of extracting the recombinant protein of interest was required. This was achieved by incubating lysates with glutathione sepharose beads for 2 hours, as the recombinant proteins were tagged with glutathione S-transferase (GST), which binds the protein to the beads. Subsequently, the beads were washed with PBS in order to remove unbound protein and elution buffer was used to harvest the protein from the beads.

Once purified recombinant fusion protein samples were obtained, quantification of protein concentration was performed against known volumes of BSA through SDS-PAGE and coomassie staining. These were then subsequently used as standards for the quantification of each target SNARE protein in samples of primary cardiomyocyte lysate via SDS-PAGE and immunoblotting. Both of these quantification procedures are more fully explained in chapter 5.

2.5.2 Amplification of GLUT4 Plasmid DNA

Within this project a pcDNA3.1(+)-GLUT4 plasmid was purchased from Genscript. An important immediate aim was to amplify this DNA stock in order to obtain volumes suitable for subsequent aims. It should be noted that all relevant steps described in this protocol were performed at a flame in order to work under sterile conditions. First of all the plasmid was transformed into XL-1 Blue *E.coli*. This was achieved by incubating 1 µL of the stock plasmid with 50 µL competent cells in a 1.5 mL capacity eppendorf for 30 min on ice. This solution was then heated at 42ºC for 45 seconds, and then maintained on ice for a further 2 min. Thereafter, 900 µL of 2YT medium was added and the solution was shaken vigorously at 37 ºC for 45 min. Cells were then briefly centrifuged and resuspended in approximately 150 µL 2YT. This suspension was then plated out on to antibiotic selection plates (all of the plasmids used within this study exhibit ampicillin resistance) and incubated overnight at 37ºC. Additionally, one plate contained untransformed cells in order to provide a negative control.

Successful transformation was indicated by growth on intended plates only. Thereafter, single colonies were scraped with a P20 pipette tip and grown via vigorous shaking at 37ºC in serial cultures of 2YT + 100 µg/mL of increasing volume until a confluent 100 mL solution was obtained. A commercially obtained Maxi-prep kit was then used to extract plasmid DNA. The concentration of this preparation was measured via a NanoDrop spectrophotemer. A highly similar process was undertaken previously in the lab with the two other home-produced plasmids referenced in this thesis, PCDH-CMV-MCS-EF1-HA-GLUT4-GFP (by Silke MacHauer) and PCDH-CMV-MCS-EF1-SX4(Y115/251E), 2P (by Dr. Mohammed Al-Tobi). Where these plasmids are referenced in the following protocols, any procedures were performed on these concentrated Maxi-prep DNA stocks unless otherwise mentioned.

2.5.3 Transfection of mammalian cells

2.5.3.1 Transfection of HeLa cells via Lipofectamine 2000

HeLa cells were plated onto a 6-well plate and maintained as described previously until they reached 70-90% confluence, at which point they were deemed suitable for transfection. Lipofectamine 2000 was used with the intention of increasing

transfection efficiency. In preparation, 6-15 µL Lipofectamine 2000 was diluted in 150 µL Opti-MEM medium. Then 14 µg of pcDNA3.1(+)-GLUT4 plasmid DNA was diluted in 700 µL Opti-MEM medium. Lipofectamine 2000 and plasmid DNA were then combined at a ratio of 1:1 (150 µL of each) and incubated for approximately 5 min at room temperature. Finally, 250 µL of this solution was added to 2 mL fresh maintenance medium in each target well. This resulted in the final addition of 2500 ng plasmid DNA and 5-12.5 µL Lipofectamine 2000 per well. 2 wells received fresh DMEM only and therefore acted as negative controls. Cells were incubated at 37°C and 5% CO_2 for ~3 days prior to the generation of cell lysates as described previously. The expression of GLUT4 in lysates was then assessed by SDS-PAGE and immunoblotting (see section 2.3.6.).

This technique was also performed with HeLa cells on a 12-well plate format when transfecting the newly developed pCDH-CMV-MCS-EF1-GLUT4 plasmid. Similar principles applied, however the volumes of all components were scaled appropriately to give a final volume of 2.5-6.25 µL Lipofectamine 2000 and 1250 ng plasmid DNA per well. In this experiment an equal number of wells containing the stated range of volumes of Lipofectamine 2000 only were also performed.

2.5.3.2 Transfection of iPSC-CM via Lipofectamine 2000

A key experimental aim within this project was to develop a protocol that facilitated the overexpression of GLUT4 in iPSC-CM via transfection of the pcDNA3.1(+)-GLUT4 plasmid. The initial protocol attempted simply followed manufacturer's recommendations, and is described below. Thereafter several adaptations to this protocol were made, and these are fully described and discussed in chapter 4.

iPSC-CM were plated and maintained for 3 days on a 96-well plate format. Thereafter, 1-2.5 µL Lipofectamine 2000 was diluted in 25 µL Opti-MEM medium. Then 2.5 µg of pcDNA3.1(+)-GLUT4 plasmid DNA was diluted in 125 µL Opti-MEM medium. Lipofectamine 2000 and plasmid DNA were then combined at a ratio of 1:1 (25 µL of each) and incubated for approximately 5 min at room temperature. Finally, 10 µL of this solution was added to fresh Cor.4U maintenance medium in each target well. This resulted in the final addition of 100 ng plasmid DNA and 0.2-0.5 µL Lipofectamine 2000 per well. Where appropriate, specified wells

received equivalent volumes of Lipofectamine 2000 only. Cells were then maintained for a further 3 days as normal prior to the generation of cell lysates as described previously. Once again the expression of GLUT4 in lysates was then assessed by SDS-PAGE and immunoblotting.

Similar to HeLa cells, this transfection protocol was also performed on a larger 12-well plate format. However, in this case a final volume of 6 µL Lipofectamine 2000 +/- 1250 ng plasmid DNA was added to target wells.

2.5.3.3 Transfection of iPSC-CM and HeLa cells via FuGENE HD and *Trans*IT-TKO

Within this project 2 additional transfection reagents were assessed for their capacity to efficiently transfect HeLa cells or iPSC-CM. In all cases the standard protocol recommended by the manufacturer was employed, and therefore no extensive optimisation process occurred as in the case of Lipofectamine 2000 mediated transfection. As before, in all cases transfection occurred 3-4 days post-plating for iPSC-CM or at an appropriate density for HeLa cells.

Briefly, when transfecting iPSC-CM on a 96-well plate format with *Trans*IT-TKO, an initial preparation of 100 µL Opti-MEM + 5 µL *Trans*IT-TKO +/- 3 µg plasmid DNA was incubated for 10-15 min. Subsequently, 10 µL of this solution was added to each target well, achieving final volumes of 0.5 µL *Trans*IT-TKO +/- 300 ng plasmid DNA. Similarly, when transfecting iPSC-CM on a 96-well plate format with FuGENE HD, an initial preparation of 100 µL Opti-MEM + 6 µL FuGENE HD +/- 3 µg plasmid DNA was incubated for 10-15 min. Once again, 10 µL of this solution was added to each target well, achieving final volumes of 0.6 µL FuGENE HD +/- 300 ng plasmid DNA. When transfecting HeLa cells on a 12-well plate format with FuGENE HD, this initial preparation was simply directly added to the specified well(s) in its entirety.

2.5.4 Generation of GLUT4 lentiviral plasmid

In order to generate a plasmid suitable for subsequent lentivirus development, it was required to sub-clone the GLUT4 gene sequence from the pcDNA3.1(+)-GLUT4 plasmid into the pCDH backbone of the pCDH-CMV-MCS-EF1-HA-GLUT4-GFP plasmid. In order to achieve this, first of all plasmids underwent double restriction

digest with the enzymes Not1 and EcoR1. This was performed with 7.5-9 units of each enzyme, 2 µL of manufacturers 10x reaction buffer, and 2 µL of plasmid DNA (2-3 µg per plasmid, in separate reactions), made up to 20 µL total with nuclease free water. This reaction was incubated for approximately 2 hours at 37ºC. A control reaction was also performed for each plasmid without enzymes present.

Digests were analysed on agarose gels and the relevant bands excised using a scalpel. Fragments were purified using a commercial kit. A small aliquot of these fragments were then run through a new 1% agarose gel in order to ensure not only that the intended fragment was successfully isolated, but also that no detectable contamination from other unwanted DNA fragments had occurred.

Once purified fragments of the pCDH backbone and GLUT4 insert were obtained, ligation reactions were performed in 20 µL total volume. Ligations were incubated at 16ºC (in a cooling block) overnight, for a maximum of 24 hours. Appropriate control conditions were also performed, most notably individual DNA fragments only, with and without ligase. Ligation reactions were transformed into 5-alpha competent *E.coli*. In order to confirm successful ligation, individual colonies were selected and grown in 5 mL cultures containing 100 µg/mL ampicillin overnight on a shaking platform at 37 ºC. These samples were then mini-prepped and digested via the same original restriction enzymes in order to confirm that the backbone (pCDH) and insert (GLUT4) were of the correct molecular size. Once this was confirmed to be the case, this novel plasmid PCDH-CMV-MCS-EF1-GLUT4 was once again transformed into 5-alpha *E.coli* and amplified in order to provide enough DNA to transfect HeLa cells and confirm that it could induce mammalian cells to produce robust amounts of GLUT4 protein.

2.5.5 Infection of iPSC-CM

Within this project, iPSC-CM were infected with 2 separate lentivirus on a 96-well scale. First of all, Dr. Mohammed Al-Tobi generated a lentivirus with the pCDH-CMV-MCS-EF1-Sx4(Y115/251E), 2P plasmid using reagents and a relevant protocol from Clontech (California, USA). Although the concentration of this lentivirus was not calculated (in either transducing units/mL (TU) or plaque forming units/mL (pfu)), a protocol had been developed by Dr. Al-Tobi that resulted in the successful overexpression of Syntaxin 4 in HEK293 cells and 3T3-L1 adipocytes (in both their

pre-adipocyte and differentiated form). Based upon this, approximately 48 hours post plating iPSC-CM were incubated for 4 or 24 hours, in the presence or absence of 8 µg/mL polybrene (a reagent designed to improve infection efficiency), with fully concentrated or 1:10 diluted lentivirus. Medium was then exchanged and lysates were generated approximately 72 hours later. Thereafter, samples were probed for Syntaxin 4 expression via SDS-PAGE and immunoblotting.

Secondly, iPSC-CM were plated on a 96-well plate scale as normal, however this time the plates were glass-bottomed as opposed to plastic. Approximately 72 hours post-plating cells were incubated with a lentivirus based upon the previously mentioned pCDH-CMV-MCS-EF1-HA-GLUT4-GFP lentiviral plasmid that was commercially generated by Systems Biosciences Inc. Cells were exposed to 0/2/4/6 µL of this virus in 50 µL medium for approximately 24 hours, which based upon the manufacturer's reported transducing units value reported for the virus and the approximate plating density of iPSC-CM resulted in an estimated multiplicity of infection (MOI) of 0/35/70/105. Cells were maintained in normal maintenance medium for a further 72 hours, prior to imaging of GLUT4-GFP via confocal microscopy. As this protein is already modified to be tagged with an excitable fluorescent reporter, no extensive protocol requiring labelling with secondary antibodies was necessary. Each well containing iPSC-CM was simply imaged directly via a Zeiss LSM Pascal Exciter laser scanning confocal microscope using a 63x objective lens and the appropriate Zeiss LSM software. Images were then exported to Image J and processed for presentation purposes. Finally, after being imaged, cells were lysed and probed for GLUT4 and GFP expression via SDS-PAGE and immunoblotting.

2.6 Statistical analysis

In all cases throughout this thesis, the appropriate statistical analysis was performed with GraphPad Prism (version 7). In general this was deemed to be an unpaired t-test or ANOVA (1- or 2-way) and the level of significance was set at P=0.05. Full details are contained within the figure legend of all relevant figures.

3 Insulin stimulated glucose uptake in iPSC-CM

3.1 Introduction

The precise matching of ATP synthesis and breakdown is required to maintain optimal function of all cells in the body. This matching is particularly important in highly energetic organs such as the heart, where maintenance of pump capacity is required to transport nutrient and oxygen rich blood around the body, the first rate limiting step of ATP generation for most tissues. A mismatch between cardiac energy demand and supply could rapidly lead to potentially fatal limitations in contractile performance (cardiomyopathy). In diabetic hearts, cardiomyopathy is often observed independently of commonly occurring vascular disease (DCM) (Boudina and Abel, 2010). This is primarily attributed to reduced efficiency of intracellular calcium handling on the level of individual cardiomyocytes coupled with organ level structural changes such as fibrosis (Belke and Dillmann, 2004; Miki *et al.*, 2013). However, there is a credible line of evidence that indicates that the original underlying cause preceding limitations in cardiac contractility is metabolic adaptation to chronic energy overload, namely IR (Belke *et al.*, 2000; Semeniuk *et al.*, 2002; Park *et al.*, 2005).

IR in general is a central facet of the overall diabetic phenotype. The current leading theory is that cardiac IR occurs due to ectopic fat storage resulting in the accumulation of toxic metabolic intermediates/ metabolites such as DAG (Zhang *et al.*, 2011). It is proposed that these may inhibit intracellular insulin signalling cascades, possibly via PKC mediated inactivation of IRS-1, thereby preventing delivery of GLUT4 to the cell membrane in the presence of insulin stimulation (Erion and Shulman, 2010). However, ultimately no matter how logical this theory may be or how promising initial evidence is, the quality of currently available models strongly hinders the confidence in - and ability of - these results to translate into clinical outcomes for human diabetic patients. Ideally what is required is a controlled environment in which we can study the in depth functional and molecular phenotype of human hearts or human cardiomyocytes in the presence and absence of diabetes, identify mechanisms underlying pathological metabolic and contractile adaptations, and then test interventions. Currently this is not possible, however iPSC-CM provide an opportunity to achieve these aims, albeit on a cellular level.

3.1.1 Could iPSC-CM act as a novel cellular model of DCM?

Prior to any attempt to induce a DCM like phenotype in iPSC-CM, the standard 'healthy' phenotype with regards to relevant parameters must be established. As discussed in the introduction, this has been largely achieved with regards to electrophysiological, contractile, and structural parameters (Ma *et al.*, 2011; Karakikes *et al.*, 2015). Whilst these are not perfect matches in all cases, the difference between baseline and the ultimate model (human adult cardiomyocytes) is known. Therefore attempts to bridge this gap through maturation protocols can be made, or more simply these can be taken into account when analysing the effect of interventions. This scenario does not exist for metabolic parameters. There is currently no literature detailing basal or insulin stimulated glucose uptake in iPSC-CM, let alone the activation or even just expression of key proteins involved in GLUT4 trafficking. Indeed it is not even known if these cells express GLUT4.

There has been one notable prior attempt to induce a DCM phenotype in iPSC-CM (Drawnel *et al.*, 2014). To begin with, the authors cultured cells in a medium designed to mature the cells. This will be discussed in more detail in chapter 4, however the key idea was that the medium contained no glucose, and instead cells were forced to rely on fatty acids as the primary metabolic substrate. This was designed to mimic more closely the *in vivo* metabolic environment of developing cardiac cells. Primary outcomes were structural parameters and action potential dynamics. Excitation of myocyte cell membranes is a prerequisite for contraction. This is regulated by the movement of ions across the membrane. Measurement of changes in voltage produces a characteristic trace, referred to as the action potential. Cells have a resting negative membrane potential, which then rapidly increases upon excitation, before being restored to baseline before the next contraction. Key parameters, specifically rate of upstroke (rate of increase in membrane potential) and duration were found to be increased towards a more mature phenotype. Crucially, cells were then cultured in 10 mM glucose because this exceeds the fasting blood glucose values determined to indicate diabetes (~7mM), in addition to endothelin-1 and cortisol in an attempt to mimic a pre-diabetic milieu. This was determined to have induced a DCM like phenotype due to changes in cellular gene expression and structure consistent with hypertrophy,

reduced strength and coordination of contraction, and increased brain natriuretic peptide (BNP) release (Drawnel *et al.*, 2014).

In humans, circulating BNP levels have been inversely correlated with insulin sensitivity (Kim *et al.*, 2017) and risk of diabetes (Lazo *et al.*, 2013). Therefore if this correlation were extended to the cellular level and applied to these results, in isolation it would indicate an improvement in iPSC-CM insulin sensitivity, not the onset of diabetes. However, the authors intended purpose of showing this data was in reference to the more appreciated positive correlation between BNP levels and cardiac hypertrophy, a key marker of cardiomyopathy (Nishigaki *et al.*, 1996). Therefore, although this previous study provides many interesting insights and is a very useful starting point, it is not credible to claim that a model of DCM had been created, primarily because no parameter closely related to insulin stimulated glucose uptake or GLUT4 trafficking was studied. Additionally, it is surprising that only 10 mM glucose was enough to induce a DCM phenotype, given that the cells (along with most cell lines) are normally maintained in 4.5 g/L glucose which is equivalent to approximately 25 mM.

Based upon the accumulated literature described, it appears that iPSC-CM could be a useful tool to help fill an unmet clinical need. However, the first step towards achieving this end goal is characterisation of key metabolic features, in particular basal and insulin stimulated glucose transport, and the expression and activation of key GLUT4 trafficking proteins, including GLUT4 itself. In order to assess results, these must be compared to a gold standard criteria, which in this case is the adult cardiac metabolic phenotype. However, the exact details are much harder to specifically define than may be assumed, on account of the range of techniques and models reported in the literature.

3.1.2 Insulin stimulated glucose uptake in isolated cardiomyocytes

When considering the abundance of data generated from isolated adult rodent cardiomyocytes, the results and interpretation are clear. In both primary rat and mouse cardiomyocytes insulin robustly and consistently activates important intracellular targets such as the insulin receptor and Akt, initiates the translocation of GLUT4 to the plasma membrane, and most importantly stimulates

a several fold increase in 2-deoxyglucose uptake (Fischer *et al.*, 1996, 1997; Mazumder *et al.*, 2004; Graveleau *et al.*, 2005; Mora *et al.*, 2005). It is of interest to note that two of these studies demonstrated that GLUT1 also translocated to the plasma membrane in response to insulin, albeit with a much lower overall fold response (Fischer *et al.*, 1996, 1997). In practice, given the much lower overall expression of GLUT1 in primary cardiomyocytes the functional contribution of this will likely be low. On account of the range of fold responses in glucose uptake recorded in response to insulin, most likely linked to variations in protocols for myocyte isolation and glucose uptake, it is hard to state with confidence the exact response that should be expected from iPSC-CM. However, as a minimum, expectations should be for at least a 2-3 fold response.

A common criticism of data generated from isolated cardiomyocytes – not restricted to measurements of glucose transport - is that the digestion protocol may alter the physiology of the cells. The quality of this procedure is absolutely critical in obtaining a large number of viable, reliable cells (Louch *et al.*, 2011). Primarily, membrane damage could occur due to over digestion, preventing normal activation of membrane bound receptors such as the insulin receptor. From the data discussed above reporting strong responses, this does not seem to be a common problem. However, a second and perhaps more difficult to account for potential problem is that cardiomyocyte isolation is a technically challenging procedure during which a moderate to high percentage of isolated cells die (Graham *et al.*, 2013). Through personal experience, many other cells die soon after subsequent stimulation, particularly when artificially initiating contraction. Therefore there is always a selection process, which could lead to data being representative of only a subset of cells from the whole heart. In theory iPSC-CM are cultured as a large group of individual cells that are immune from this process. Another one of their attractions is that when maintained at confluence they become electrically coupled, in a similar phenomenon to what is observed *in vivo*. Additionally, unlike isolated primary cells these cells are spontaneously contractile, which is a potent stimulus for glucose uptake. Therefore it is also essential to consider the effect of insulin stimulation on glucose uptake in an intact, contracting heart *in vivo*, when setting expectations for the response anticipated from iPSC-CM.

3.1.3 Insulin stimulated glucose uptake in intact hearts

In vivo human cardiac glucose uptake studies rely largely upon the euglycemic hyperinsulinemic clamp procedure. The key concept is that blood insulin levels are externally measured and maintained at an elevated concentration, whilst glucose is infused at the rate required to maintain a specified blood glucose concentration. The required rate of glucose infusion is directly related to the rate of clearance from the blood stream, and is taken as an index of whole body insulin sensitivity. Using a similar protocol fluorodeoxyglucose may also be infused, a form of 2-deoxyglucose that is tagged suitably for detection via positron emission tomography, therefore allowing detection of tissue specific uptake.

There is a significant - although not universally accepted (Utriainen *et al.*, 1998) - body of literature that collectively demonstrate whole body (presumably mostly skeletal muscle and adipose) IR in type 2 diabetics due to the lower rate of glucose infusion required during the clamp procedure, with a corresponding lower accumulation of fluorodeoxyglucose in the myocardium also indicating cardiac IR (Voipio-Pulkki *et al.*, 1993; Ohtake *et al.*, 1995; Iozzo *et al.*, 2002; Dutka *et al.*, 2006; Rijzewijk *et al.*, 2009). Typically a reduction in myocardial transport of ~30% is reported, which is relatively small provided conditions are optimised for maximal insulin sensitivity (subjects are at rest, fasted, and experience a prolonged high exposure to insulin with sustained normal blood glucose values). Additionally, it is challenging to separate the contribution of a reduction in basal glucose uptake from any impairment in the insulin response when considering the global reduction in myocardial glucose uptake recorded using this technique, and in no case was an attempt made to measure a fold change in glucose uptake in response to insulin stimulation. Therefore apart from working backwards to infer that insulin most likely increases myocardial glucose uptake in the intact human heart *in vivo* on account of reduced uptake in presumed insulin resistant diabetics, it is difficult to compare this data to that of isolated rodent cardiomyocytes or make recommendations regarding the required response to be recorded from iPSC-CM.

Fortunately, there is a group of data that acts as an intermediary between single cell and whole heart data that completes the required background information before working with iPSC-CM. Perhaps the most compelling evidence

demonstrating clear GLUT4 dependent insulin stimulated glucose uptake in the intact contracting heart was generated by performing the euglycemic hyperinsulinemic clamp in conscious rats (Kraegen *et al.*, 1993). Animals were then euthanised and [^{3}H]-2DG accumulation in the heart and several skeletal muscles was determined. Critically they also measured tissue specific uptake under basal conditions, where insulin would have been present at low levels, but certainly not at the supra-physiological values used during the clamp procedure. This revealed a clear (30-40%) increase in cardiac glucose uptake upon maximum insulin stimulation. The fold increase in skeletal muscle was much higher, largely due to the much smaller basal uptake values recorded. Crucially, there was a very strong (r^2 = 0.97) correlation between insulin sensitivity and GLUT4 content across the range of muscles studied. This data is supported by demonstration of a clear increase in 2DG uptake in isolated mouse hearts in response to insulin stimulation (Abel *et al.*, 1999). However, this response was totally abolished in hearts from cardiac specific GLUT4 knockout mice. Interestingly, in these mice basal glucose uptake increased in a similar manner to GLUT1 protein expression. Finally, studies using HFD feeding in C57BL/6 mice have shown the progressive onset of cardiac (and whole body) IR using the *in vivo* measurement technique described, in part linked to inhibition in Akt signalling and a reduction in GLUT4 protein content (Park *et al.*, 2005; Kowalski *et al.*, 2015). This supports the suggestion that the data collected from humans does indeed primarily indicate reduced insulin stimulated glucose uptake, rather than decreased basal transport, under conditions of diabetes/IR.

3.1.4 Requirements for iPSC-CM

Collectively, the aforementioned data determines that a minimum requirement of iPSC-CM, in order to be considered to have potential to act as a novel cellular model of DCM, is that they must exhibit a clear GLUT4 dependent increase in 2DG uptake in response to insulin stimulation, mediated through intracellular activation of key insulin signalling molecules such as Akt. Whilst contraction mediated uptake may interfere with this, a minimum 2-3 fold response should be reliably recorded. As a requisite to meet these biological demands, an appropriate assay must be identified and customised that is technically capable of detecting both a clear basal glucose uptake signal above background noise, yet does not saturate and can therefore also reproducibly record a robust insulin response.

3.1.5 Aims of chapter

The main aim of this chapter of work is to characterise key aspects of the metabolic profile of iPSC-CM in order to assess their suitability as a potential novel cellular model of DCM. This will be achieved by addressing the following aims;

- Customisation of an appropriate assay to determine glucose uptake
- Characterisation of basal and insulin stimulated glucose uptake in iPSC-CM
- Assessment of importance of contraction mediated glucose uptake in iPSC-CM
- Assessment of expression (and where appropriate activation) of essential proteins involved in insulin stimulated GLUT4 trafficking
- Assessment of response of iPSC-CM glucose uptake to maturation medium conditioning

3.2 Results

3.2.1 Adaptation of [^{3}H]-2DG uptake assay

Commercially derived iPSC-CM are expensive and terminally differentiated, thereby making it necessary to perform assays as efficiently and on as small a scale as is practically possible, without damaging the validity or quality of research. When assaying cells that have easily detectable rates of basal glucose uptake and a clear reliable insulin response, such as 3T3-L1 adipocytes, typically a 12 or 24 well plate format may be used. However, this is simply not a sustainable approach for iPSC-CM, and it is also realistic to assume the insulin response of these cells (if present) would be much smaller than what is recorded in 3T3-L1s. Therefore, prior to assessing the baseline glucose uptake kinetics of iPSC-CM, it was first of all assessed if this assay could be adapted to a 96-well plate format. Key experimental variables were systematically varied in order to identify conditions that facilitated detection of a basal glucose uptake signal above background noise in two relatively inexpensive and abundant cell types.

HEK293 and HeLa cells were plated at a range of densities and [^{3}H]-2DG uptake assays performed with a varying number of initial washes in KRP. In all cases the uptake shown is background corrected by subtracting values obtained from identical conditions in the presence of the GLUT inhibitor CB (Bloch, 1973). The average background noise signal was approximately 500 CPM for all conditions. There was a highly significant effect of plating density upon measured uptake signal ($P<0.0001$) in HEK293 cells (Figure 3-1). Subjectively, an increased number of washes appeared to increase the variability of recorded uptake signals, however the effect of this factor was not statistically significant ($P>0.05$). There was no interaction detected between these factors. The trends appear similar for identical experiments performed with HeLa cells (Figure 3-2) and indeed there was found to be a significant effect of plating density upon [^{3}H]-2DG uptake ($P<0.01$) but no statistically significant effect of number of washes ($P>0.05$).

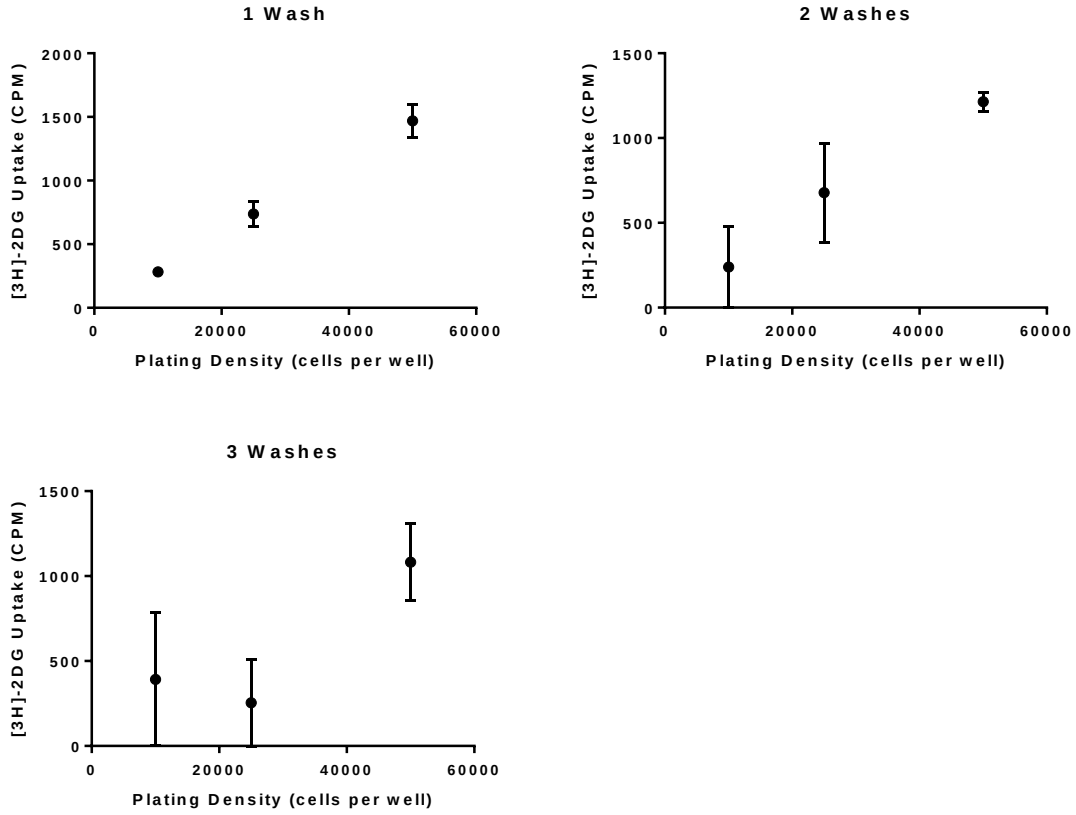

Figure 3-1 Adaptation of [^{3}H]-2DG uptake assay to 96 well plate format with HEK293 cells
Background corrected [^{3}H]-2DG uptake was assayed using HEK293 cells plated at 10,000, 25,000, or 50,000 cells per well. Cells were washed 1, 2, or 3 times in KRP prior to a 30 min incubation with [^{3}H]-2DG. Data shown is mean of 3 replicates from one experiment +/- S.D. Statistical analysis was performed with a 2 way ANOVA, where the identified experimental factors were number of washes and plating density. The level of significance was set at P=0.05.

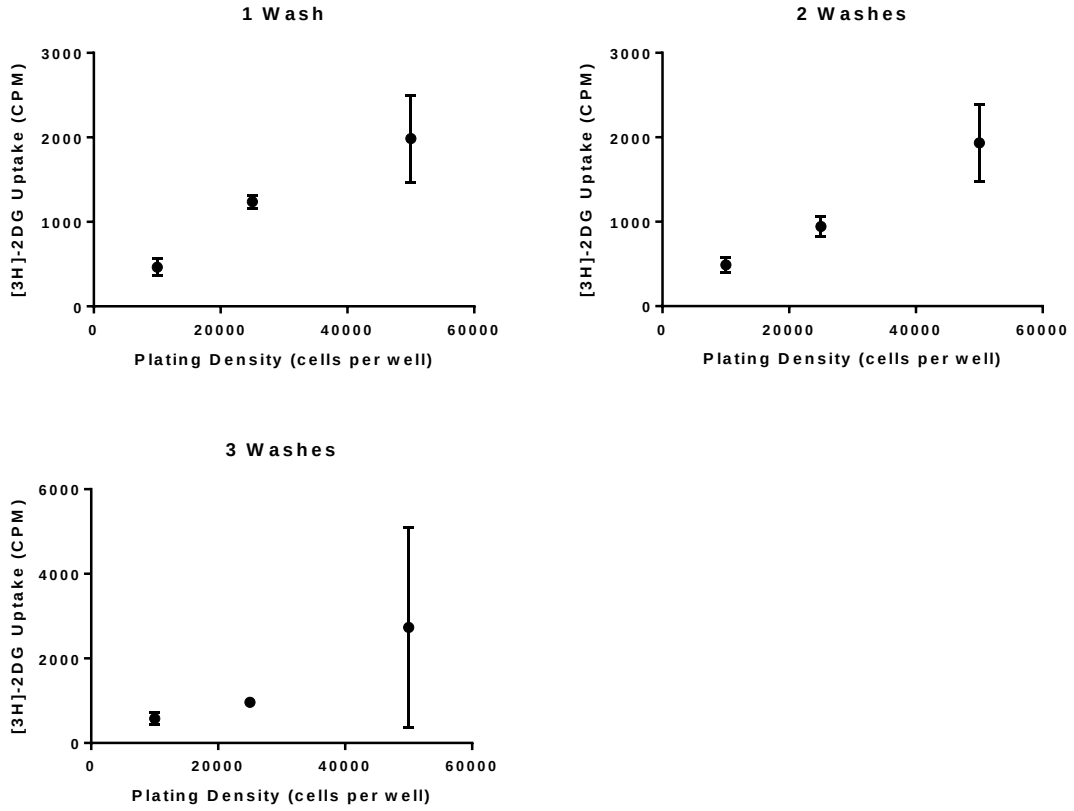

Figure 3-2 Adaptation of [^{3}H]-2DG uptake assay to 96 well plate format with HeLa cells
Background corrected [^{3}H]-2DG uptake was assayed using HeLa cells plated at 10,000, 25,000, or 50,000 cells per well. Cells were washed 1, 2, or 3 times in KRP prior to a 30 min incubation with [^{3}H]-2DG. Data shown is mean of 3 replicates from one experiment +/- S.D. Statistical analysis was performed with a 2 way ANOVA, where the identified experimental factors were number of washes and plating density. The level of significance was set at P=0.05.

Initial results demonstrated that it was possible to detect a clear cellular basal glucose uptake signal using a 96-well plate format, and also provided a starting point regarding setting desirable experimental conditions. However, on this scale a relatively low number of cells are used which creates a more narrow absolute range of detectable values. Therefore the assay was performed with 3T3-L1 adipocytes, a cell type known to have a robust insulin stimulated glucose uptake response (Kohn *et al.*, 1996; Takahashi *et al.*, 2008), in order to assess if both a clear basal signal and a clear insulin response could be detected. Additionally, data generated with isolated cardiomyocytes from a male adult rabbit are presented, which are less insulin sensitive than 3T3-L1s, but more relevant to iPSC-CM.

Insulin stimulation significantly ($P<0.0001$) increased [^{3}H]-2DG uptake in 3T3-L1 adipocytes by around 5000 CPM (Figure 3-3; Basal vs Insulin; Means +/- S.E.M: 1134

+/- 214 CPM vs 6048 +/- 732 CPM) and by around 5.3-fold. Background noise was approximately 300 CPM. Similarly, although to a lesser extent, insulin stimulation significantly (P<0.001) increased [^{3}H]-2DG uptake in isolated cardiomyocytes by ~700 CPM and 1.8-fold (Figure 3-4; Basal vs Insulin; Means +/- S.E.M: 821 +/- 83 CPM vs 1483 +/- 135 CPM). Background noise was approximately 450 CPM. These fold increases in both cell types equate well to published values from a range of other groups (Kohn *et al.*, 1996; Graveleau *et al.*, 2005).

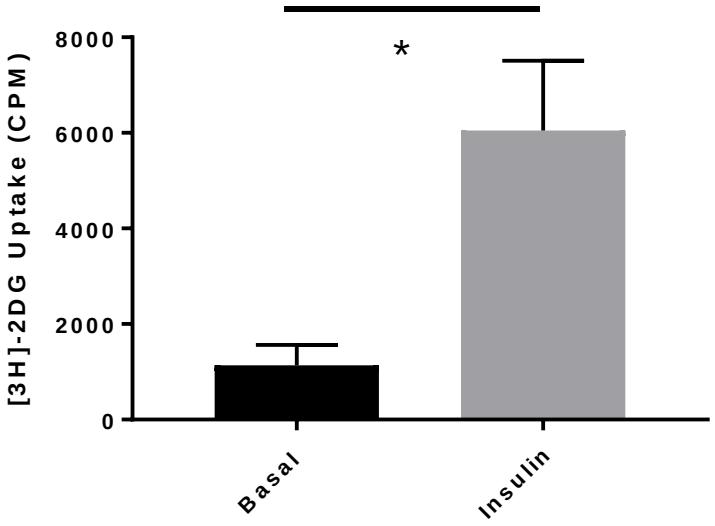

Figure 3-3 Insulin stimulated glucose uptake response in 3T3-L1 adipocytes
Background corrected basal and insulin stimulated glucose uptake in CPM was assayed using fully differentiated 3T3-L1 adipocytes. Cells were serum starved (serum free DMEM) for 4 hours prior to 30 min stimulation with 860 nM insulin. Cells were incubated with [^{3}H]-2DG for 10 min. Data shown is mean of 4 replicates from one experiment +/- S.D. Statistical analysis was performed with an unpaired t-test, and the level of significance was set at P=0.05. * indicates P<0.0001.

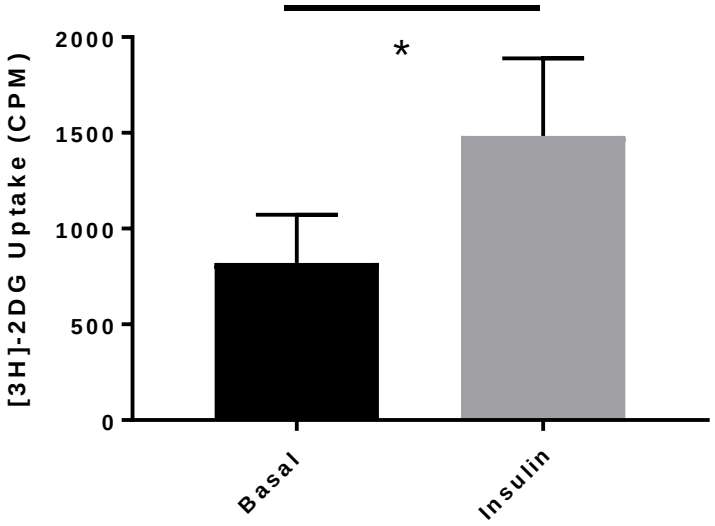

Figure 3-4 Insulin stimulated glucose uptake response in primary rabbit cardiomyocytes Background corrected basal and insulin stimulated glucose uptake in CPM was assayed in primary rabbit cardiomyocytes approximately 3 hours post isolation. Cells were stimulated with 860 nM insulin for 30 min prior to 20 min incubation with [^{3}H]-2DG. Data shown is mean of 9 replicate samples obtained from one animal +/- S.D. Statistical analysis was performed with an unpaired t-test, and the level of significance was set at P=0.05. * indicates P<0.001.

3.2.2 Characterisation of iPSC-CM insulin stimulated glucose uptake

After determination of an appropriate technique, initial characterisation of the insulin stimulated glucose uptake response of iPSC-CM was performed. Figure 3-5 displays insulin stimulated glucose uptake in the presence and absence of inhibitors targeting the key intracellular insulin signalling molecules Akt (Akti) and PI3K (wortmannin). Overall, in the Akti experiments, insulin significantly increased glucose uptake ($P<0.0001$). This signal was significantly ($P<0.001$) reduced in the presence of Akti, although not fully back down to basal levels as there was still a significant difference ($P<0.01$) between basal glucose uptake and uptake in the presence of insulin and Akti. Similarly, wortmannin significantly ($P<0.001$) reduced glucose uptake in the presence of insulin relative to when insulin alone was present. In both cases there was a highly significant ($P<0.0001$) effect of experimental day on the recorded CPM for each condition.

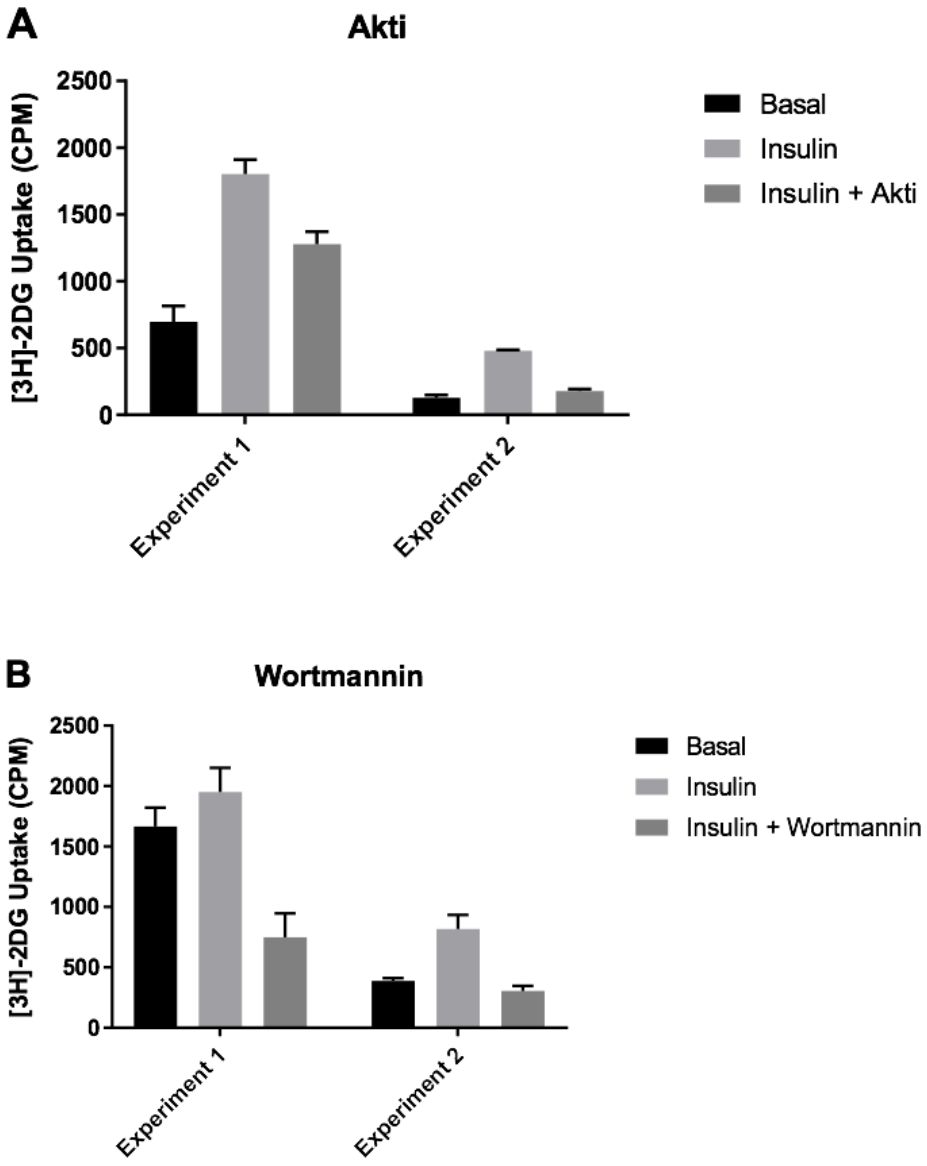

Figure 3-5 iPSC-CM can exhibit a PI3K and Akt dependent insulin response
Background corrected basal and insulin stimulated [^{3}H]-2DG uptake was measured in iPSC-CM. Prior to uptake cells were incubated for 30 min with 100 nM insulin, 100 nM insulin and 1 µM Akti (A), 100 nM insulin and 100 nM wortmannin (B), or no additional compounds (basal). Data shown is mean of 3 replicate samples +/- S.E.M, from 2 independent experiments. Statistical analysis was performed with a 2 way ANOVA, where the identified factors were drug treatment and experimental day. The level of significance was set at P=0.05.

This data suggested that iPSC-CM may be capable of exhibiting an insulin stimulated glucose uptake response. However, out with the data presented in Figure 3-5 the response of these cells appeared subjectively weak and unreliable between batches despite only minor adaptations in protocol. To quantitatively assess this observation, data from 6 independent experiments was pooled and analysed. In this dataset background noise values (CB +/- insulin) are also presented in order to display the signal to noise relationship for each assay. Conditions were not completely identical between experiments performed on

different days, with subtle alterations in variables such as insulin concentration or length of incubation with [^{3}H]-2DG. However analysing the data with a 2-way ANOVA, where drug treatment and day effects are considered, takes these minor differences in to account. The data is displayed in 2 ways. First of all a summary of each individual experiment is presented (Figure 3-6A) in order to facilitate comparison across different experiments. Secondly, an overall summary of the effects of CB and insulin is presented (Figure 3-6B), with key statistical summaries in Table 3-1.

Overall, basal [^{3}H]-2DG uptake was statistically significantly higher by an average of 154 CPM compared to uptake measured in the presence of CB (Table 3-1; Basal vs Basal + CB; Means +/- S.E.M: 682 +/- 105 CPM vs 528 +/- 79 CPM; P<0.0001; 95% CI of difference between means: 82-226 CPM). Similarly, [^{3}H]-2DG uptake in the presence of insulin alone was also statistically significantly higher by an average of 304 CPM than when both insulin and CB were present (Table 3-1; Insulin vs Insulin + CB; Means +/- S.E.M: 840 +/- 135 vs 537 +/- 98 CPM; P<0.0001; 95% CI of difference between means: 232-376 CPM). Finally, insulin statistically significantly elevated glucose uptake by an average of 158 CPM above basal only values (Table 3-1; Basal vs Insulin; Means +/- S.E.M: 682 +/- 105 vs 840 +/- 135 CPM; P<0.0001; 95% CI of difference between means: 86-230 CPM).

The 95% confidence intervals presented suggest that whilst significant effects of insulin and CB were recorded, the estimated true magnitude of these effects in a wider population of iPSC-CM is uncertain. In support of this, there were highly significant (P<0.0001) day and interaction effects.

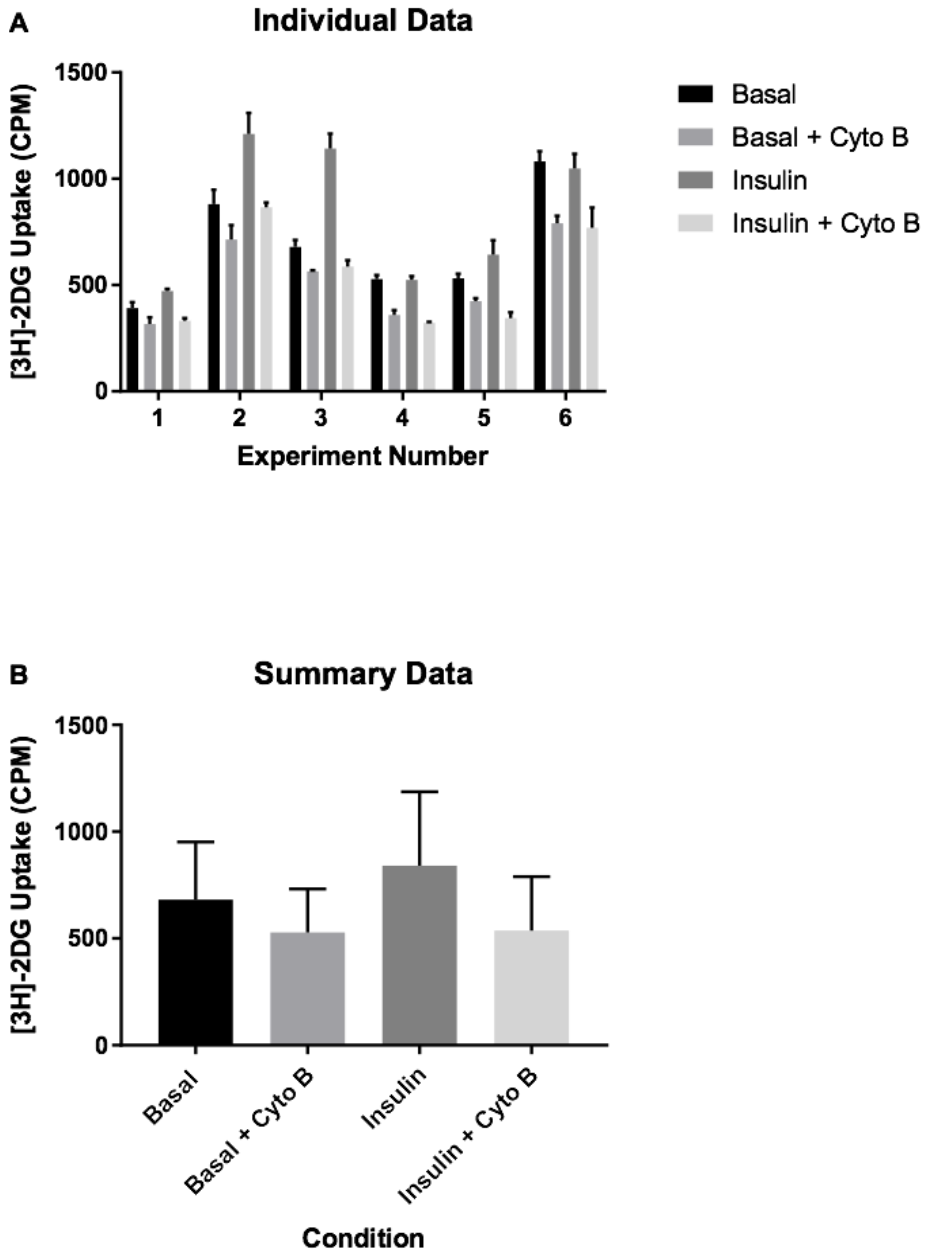

Figure 3-6 Summary of initial insight into insulin stimulated glucose uptake in iPSC-CM Individual experiments (A) and an overall summary (B) of [^{3}H]-2DG uptake in iPSC-CM under basal conditions +/- 860 nM insulin +/- 40 µM CB in 6 independent experiments are presented. Data presented is mean of 3 replicate samples +/- S.E.M. from each experimental day (A) or mean of the 6 independent experiments +/- 95% confidence intervals (B). Statistical analysis was performed with a 2-way ANOVA, taking experimental day and drug incubation as experimental factors. The level of significance was set at P=0.05.

Condition 1	Condition 2	Mean Condition 1	Mean Condition 2	Mean Diff.	95% CI of Diff.	P value
Basal	Basal + Cyto B	682.2	528.4	153.8	81.84 to 225.7	<0.0001
Basal	Insulin	682.2	840.3	-158	-230 to -86.12	<0.0001
Basal + Cyto B	Insulin + Cyto B	528.4	536.7	-8.224	-80.15 to 63.71	0.9901
Insulin	Insulin + Cyto B	840.3	536.7	303.6	231.7 to 375.5	<0.0001

Table 3-1 Key statistical comparisons of initial iPSC-CM transport data

As shown in Figure 3-6, there was a large amount of variation with regards to both the absolute counts recorded for each condition and the magnitude of relative insulin response between different experimental days. Logically, it is likely that this variation is primarily attributable to either technical aspects of the assay, or is inherent to the iPSC-CM. This was tested by comparing replicate assays with 3T3-L1 adipocytes across several independent experimental days. Assessing the variation in absolute counts and fold response from these cells, and also variation in [^{3}H]-2DG assay mix standards, will provide insight into the reliability of this technique.

Across 3 independent experiments, insulin overall significantly ($P<0.0001$) increased [^{3}H]-2DG uptake (Figure 3-7A). Whilst there was also a significant ($P<0.0001$) effect of experimental day on the recorded values, post-test multiple comparisons revealed that the only individual significant difference between basal values or between insulin values on different experimental days was between insulin values on experimental days 2 and 3 ($P<0.0001$). This indicates a higher reliability of this assay when performed with 3T3-L1 adipocytes compared to iPSC-CM.

Additionally, 4 different volumes of [^{3}H]-2DG assay mix, normalised as CPM per µL, were highly similar both within and between experimental days (Figure 3-7B). As a reminder, 100 µL of this assay mix is added per well of a 96-well plate during the assay, regardless of cell type. This indicates a high reliability of the scintillation counting measurement system and preparation of the assay mix.

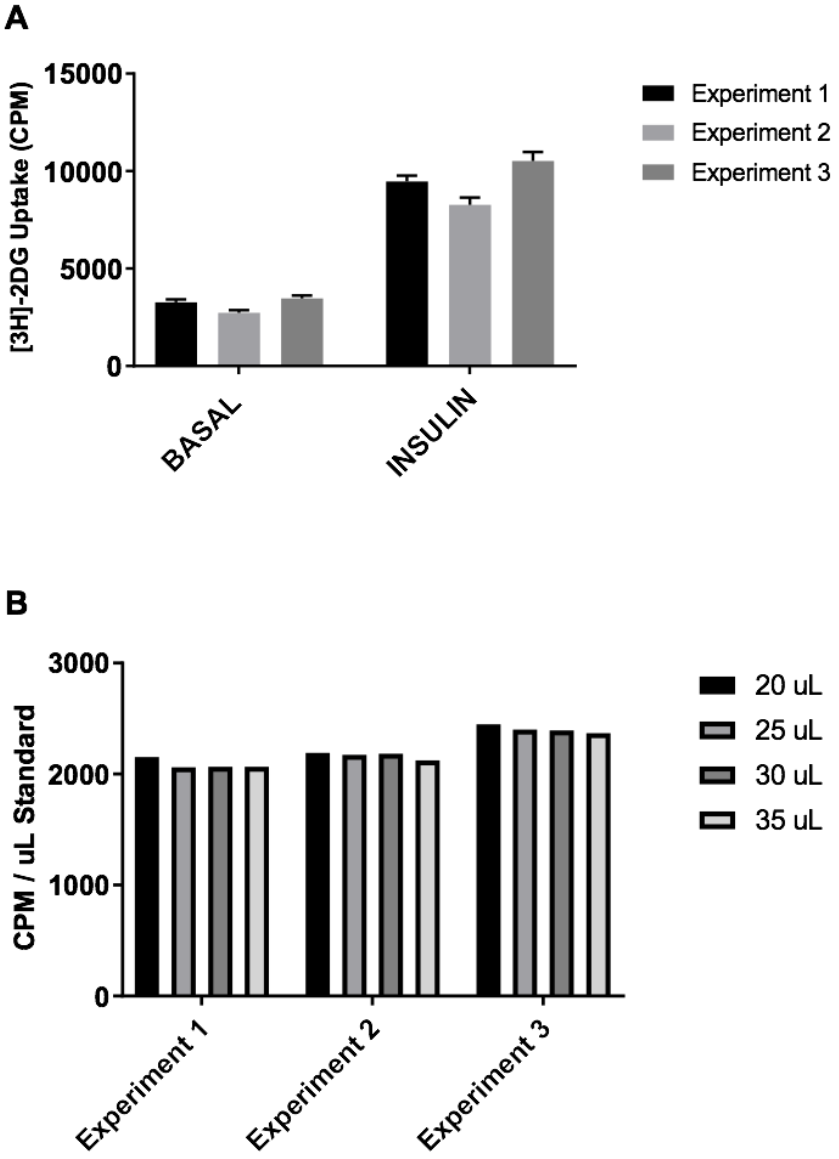

Figure 3-7 Assessment of reliability of [^{3}H]-2DG uptake assay with 3T3-L1 adipocytes
A: Background corrected basal and insulin stimulated [^{3}H]-2DG uptake was measured from 3T3-L1 adipocytes. Prior to uptake cells were serum starved for 3 hours prior to stimulation with 860 nM insulin for 20 min and subsequent incubation with [^{3}H]-2DG for 10 min. Data shown is mean of 12 replicate samples for each experimental day +/- S.E.M, from 3 independent experiments. Statistical analysis was performed with a 2 way ANOVA, where the identified factors were insulin stimulation and experimental day. The level of significance was set at P=0.05. B: Comparison of [^{3}H]-2DG assay mix standards, normalised per µL, within and between different experimental days.

As a final preliminary insight into iPSC-CM, the impact of short term palmitate conditioning upon glucose transport was studied. This was designed to mimic the effect of a HFD and obesity on the heart. As demonstrated in Figure 3-6, at this point of the project the cells were producing weak glucose uptake signals and an unreliable insulin response. Although after reoptimisation (explained below) in this set of experiments a strong set of basal signals were detected, no insulin response was observed. Therefore, Figure 3-8 depicts basal glucose uptake only in

iPSC-CM maintained in manufacturer's media supplemented with palmitate and BSA or BSA only (control), across 3 independent experiments. Overall, palmitate significantly reduced basal glucose transport ($P<0.05$). However, post-test multiple comparisons revealed that this effect was primarily attributable to the effect observed in experiment 3. The lack of a recorded insulin response was not due to the presence of BSA (data not shown).

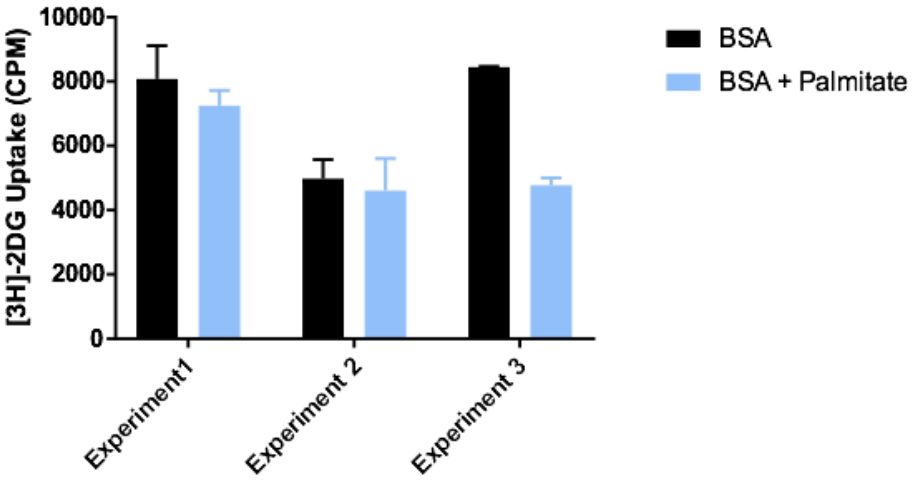

Figure 3-8 The effect of palmitate conditioning upon basal glucose transport in iPSC-CM
Background corrected basal [^{3}H]-2DG uptake was assayed in iPSC-CM maintained in either manufacturers media supplemented with BSA alone, or BSA and palmitate, in 3 independent experiments. Data presented is mean of 3 replicate samples for each experimental day +/- S.E.M. Palmitate/BSA incubation lasted approximately 4 days and was commenced 3 days post plating. Palmitate and BSA concentration varied from 440 to 1000 µM and 2-4.5 mg/mL respectively. Background noise was approximately 2000 CPM. Statistical analysis was performed with a 2 way ANOVA, where the identified factors were experimental day and palmitate conditioning. The level of significance was set at P=0.05.

3.2.3 Manipulation of experimental conditions

After initial characterisation of iPSC-CM, it was deemed necessary to further adapt the assay more specifically to the unique physiology of these cells. The aim was to identify conditions that facilitated a reliable, strong basal signal (e.g. >30% above background noise, >300 CPM) and, if possible, also an insulin response. Therefore experimental variables predicted to influence glucose uptake rate and the recorded signal were identified and systematically manipulated.

Most prominently, the effects of altering the duration for which iPSC-CM were incubated with the [^{3}H]-2DG assay mix, and the plating density of cells per well, were studied. In this first instance, the primary focus was upon identifying

conditions that stimulated a desirable basal signal. In some of the experiments presented insulin stimulation was also performed, however no reliable response was recorded. Given that stimulation was not performed in all experiments, this data is not shown in the following figures.

Figure 3-9A depicts basal [^{3}H]-2DG uptake in iPSC-CM from 3 independent experiments, where cells were incubated with [^{3}H]-2DG for either 15 or 60 min. [^{3}H]-2DG uptake is presented as CPM, and background CB signals are also presented in order to evaluate the signal to noise ratio. Figure 3-9B depicts background corrected basal [^{3}H]-2DG uptake from the same 3 independent experiments. Finally, Figure 3-9C shows the same data but now converted to absolute uptake in estimated picomoles of 2-deoxyglucose taken up per minute per million cells. It is anticipated that cellular [^{3}H]-2DG uptake should increase with longer incubation durations. However, high uptake rates could deplete intracellular ATP levels because of the ATP-dependent action of hexokinase in phosphorylating 2DG immediately upon entry into the cell. ATP synthesis would be limited as 2DG does not undergo metabolism. This would prevent further uptake, and the amount of [^{3}H]-2DG internalised per cell per unit time would decrease. It is essential that measurements are taken within the linear range - prior to ATP depletion – otherwise differences in uptake between conditions may not be detected.

Statistical analysis revealed that overall, incubation duration significantly increased adjusted absolute [^{3}H]-2DG uptake ($P<0.05$). However, this effect was weak, as post-test multiple comparisons revealed no significant difference in uptake between 15 and 60 min in any individual experiment. There was also a highly significant ($P<0.001$) effect of experimental day upon the recorded values. This suggests saturation of uptake did not occur over the measured range of incubation durations.

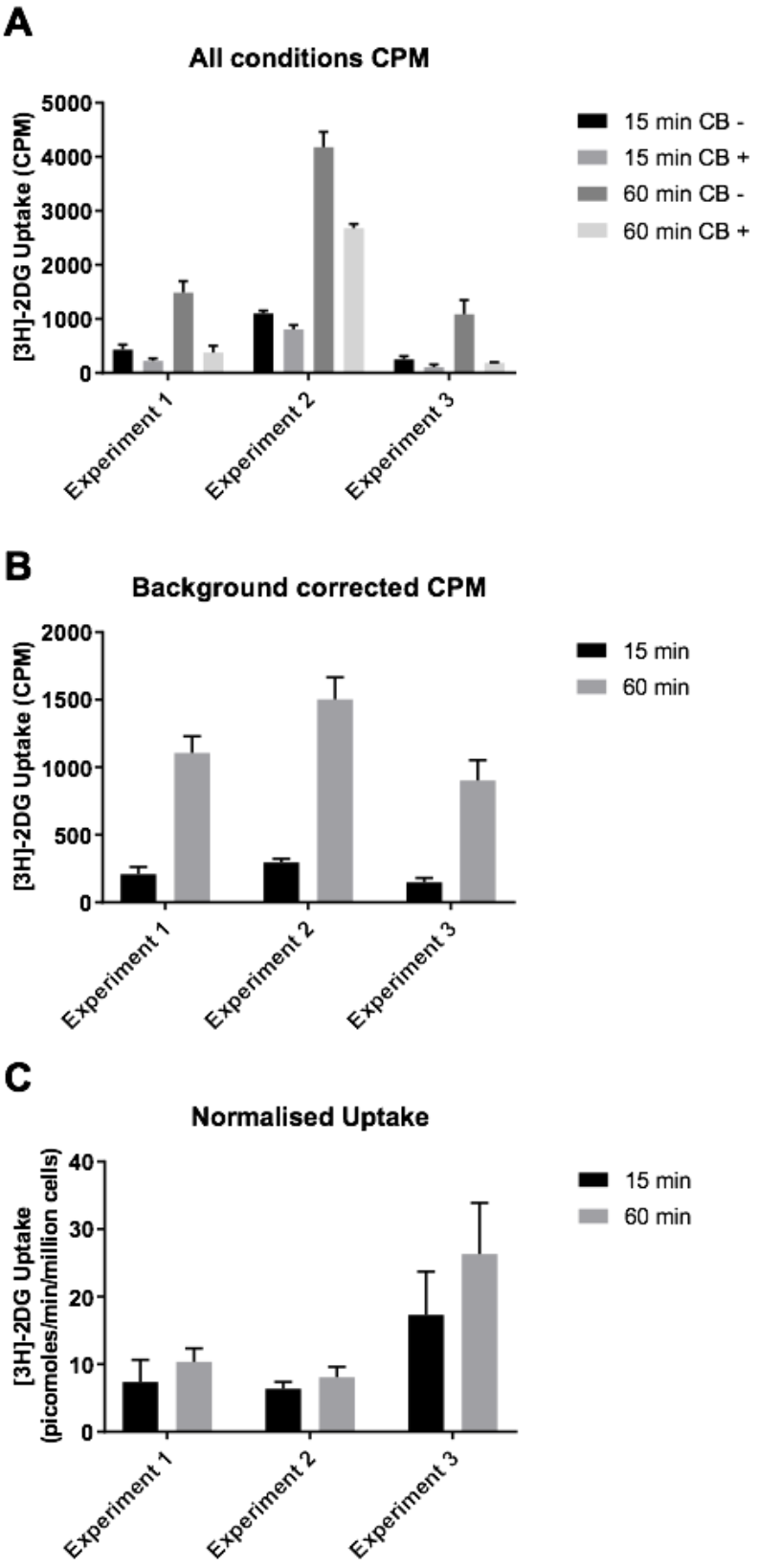

Figure 3-9 The effect of incubation duration upon [^{3}H]-2DG uptake in iPSC-CM
Basal uptake was recorded from iPSC-CM incubated with [^{3}H]-2DG for 15 or 60 min +/- 40 µM CB. Data is shown as raw uncorrected data (A), background corrected (B), or adjusted in picomoles per minute per million cells (C). In all cases data shown is mean (+ S.E.M.) of 3 replicate samples for each experimental day, from 3 independent experiments. Statistical analysis was performed with a 2 way ANOVA on the final adjusted data (C), where the identified factors were experimental day and incubation duration. The level of significance was set at P=0.05.

Whilst performing the initial experiments described so far, in general cells were plated at approximately the density recommended by the manufacturers (~30,000 cells per well). However, this was not adhered to rigidly. Subjectively it appeared as though cell density was influencing the recorded [^{3}H]-2DG uptake with more power than would be expected from a linear increase in signal relative to the number of cells that were present in the well. Therefore, Figure 3-10A and Figure 3-10B depict basal [^{3}H]-2DG uptake from cells plated at either a low density (in experiment 1 this is 37,500 cells per well, in experiments 2 and 3 this is 25,000 cell per well) or a high density (in all cases 50,000 cells per well), with and without background correction. In Figure 3-10C this background corrected data is then normalised per cell and displayed as a relative percentage of the mean low density value obtained in each experiment. Ideally this final figure would have been presented as absolute uptake (picomoles per minute per million cells) but technical error prevented this from being possible. Statistical analysis revealed a highly ($P<0.001$) significant effect of plating density upon the background corrected and adjusted recorded uptake signal.

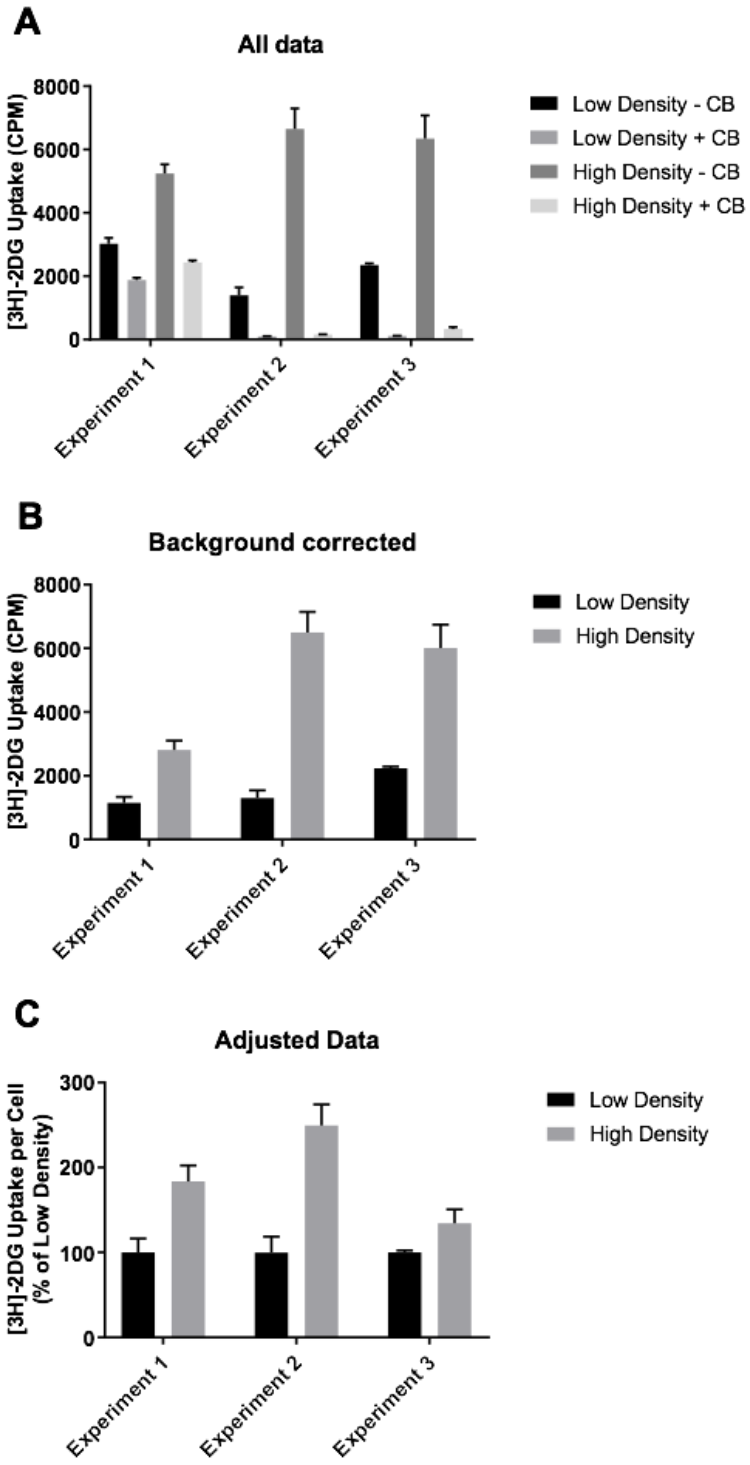

Figure 3-10 The effect of plating density upon [^{3}H]-2DG uptake in iPSC-CM
Basal [^{3}H]-2DG uptake in iPSC-CM plated at 25,000/37,500 cells per well (low density) or 50,000 cells per well (high density) expressed as full uncorrected data +/- 40 μM CB in CPM (A), background corrected in CPM (B), or as a percentage of the mean value obtained in the low density condition (C). In experiments 1 and 3 data shown is mean (+ S.E.M.) of 3 replicate samples, whereas in experiment 2 data shown is mean (+ S.E.M.) of 6 replicate samples. Statistical analysis was performed with a 2 way ANOVA, where identified factors were experimental day and plating density, and was performed upon normalised background corrected data prior to expression as a relative percentage of the low density data. The level of significance was set at P=0.05.

Based upon the data collected in Figure 3-10 it was considered possible that an increase in glucose uptake per cell at higher plating densities may be at least partly linked to changes in contractile activity. Contraction is heavily ATP dependent, and in turn the capacity to increase ATP synthesis (to match contraction induced breakdown) is directly linked to substrate availability. Therefore it follows that increases in contractile demand could increase the uptake of the main metabolic substrate in iPSC-CM – glucose. This increased contractility in theory could occur due to increased electrical coupling between cells at higher densities.

To test this, iPSC-CM were plated at 25,000 or 50,000 cells per well, and key parameters of contraction were measured via CellOPTIQ from 8 separate wells for each condition, as described in methods sections 2.4.2. A typical field of view of the CellOPTIQ microscope is displayed in Figure 3-11. Figure 3-12 shows an example output trace from the associated analysis software, whereby 5 contractions of an identically sized area of a well (not an individual cell) have been recorded over a 5 second period. Key quantified parameters include amplitude of contraction, which refers to the total extent of contraction. To be explicit, this is analogous to but not interchangeable with fractional shortening, which is typically reported when referring to the contractility of individual myocytes and refers to relative shortening of the cell on account of well-defined and structured myofilaments. Rather, this is an index of the total extent of the disordered contraction of all iPSC-CM in the field of view, with upwards of 10 cells present. From this, other important measurements are the time from 10-90% contraction (Up90), time from 10-90% relaxation (Down90), time from 50% contraction to 50% relaxation (CD50), and time between contractions (Interval). Combined, these measurements inform us regarding the frequency, overall amount, and velocity of contraction.

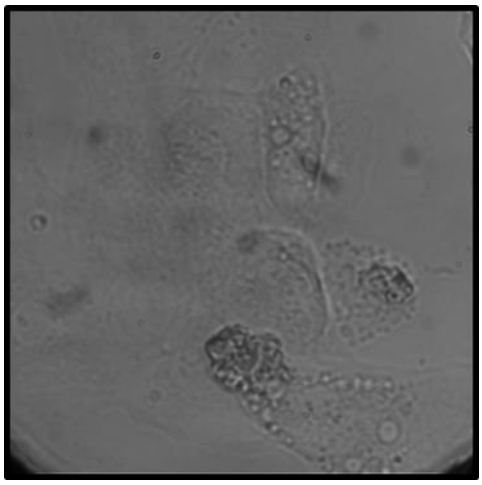

Figure 3-11 Representative field of view of CellOPTIQ imaging system
Cells were plated at 25,000 cells per well, and maintained until 6 days post-plating.

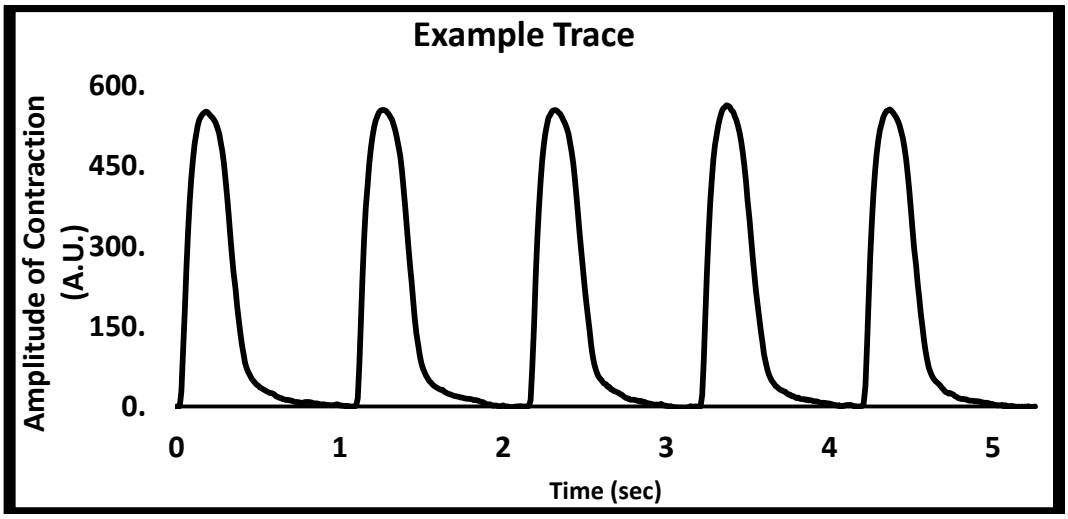

Figure 3-12 Example CellOPTIQ iPSC-CM contraction output trace
5 spontaneous contractions from iPSC-CM within the field of view at the expected rate of approximately 1 Hz were captured and analysed via CellOptiq software over a 5 second period. The trace is collated from the activity of several cells, which is possible due to the electrical coupling between cells and therefore synchronicity of contraction.

No statistically significant difference was detected between conditions when assessing the measurements of contractile activity likely to most strongly influence metabolic demand; beat to beat interval (Figure 3-13A; 25,000 vs 50,000; Means +/- S.E.M.: 939 +/- 37 ms vs 1002 +/- 23 ms; $P>0.05$) and total amplitude of contraction (Figure 3-13B; 25,000 vs 50,000; Means +/- S.E.M.: 679 +/- 71 A.U. vs 658 +/- 48 A.U.; $P>0.05$).

In contrast, more subtle measurements of contractile dynamics revealed conflicting results. Markedly, there was a highly significant difference in CD50 between conditions (Figure 3-14A; 25,000 vs 50,000; Means +/- S.E.M.: 287 +/- 4 ms vs 320 +/- 7 ms; $P<0.01$) despite no significant difference in either Up90 (Figure

3-14B; 25,000 vs 50,000; Means +/- S.E.M.: 70 +/- 2 ms vs 74 +/- 5 ms; P>0.05) or Down90 (Figure 3-14C; 25,000 vs 50,000; Means +/- S.E.M.: 242 +/- 15 ms vs 223 +/- 5 ms; P<0.01).

This conflict was investigated further by analysing the raw data presented in Table 3-2 where the time to reach different percentages of total contraction or relaxation is reported, expressed in ms after initiation of contraction. This permits assessment of the difference between conditions in a more in-depth and specific manner. It reveals a significantly slower progression from 90% contraction to 10% relaxation in cells plated at 50,000 cells per well, which is then sustained until approximately 50% relaxation, at which point an acceleration in relaxation occurs in order to return values to an equal setting by 75% relaxation. This suggests a longer time under near maximal tension for cells plated at a higher density.

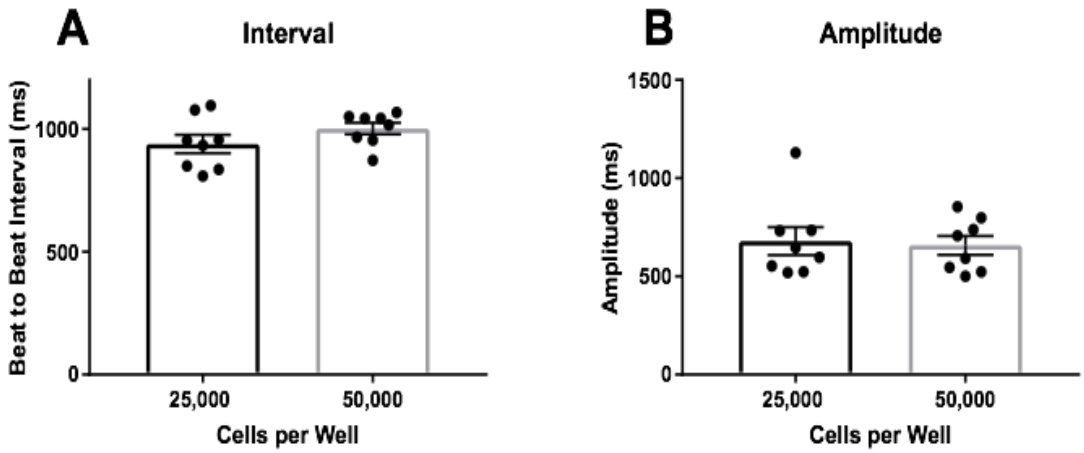

Figure 3-13 Frequency and extent of contraction in iPSC-CM plated at a high or low density
iPSC-CM were plated at either 25,000 or 50,000 cells per well and then maintained for approximately 1 week. Thereafter contractility was measured via CellOptiq video based analysis software in order to produce quantification of beat to beat interval (A) and contraction amplitude (B). Values are reported as 8 replicate samples corresponding to the average of 3 recordings from geographically distinct locations in 8 separate wells. Individual data points are shown in addition to mean +/- S.E.M. Statistical testing was performed using an unpaired t-test, where the level of significance was set at P=0.05.

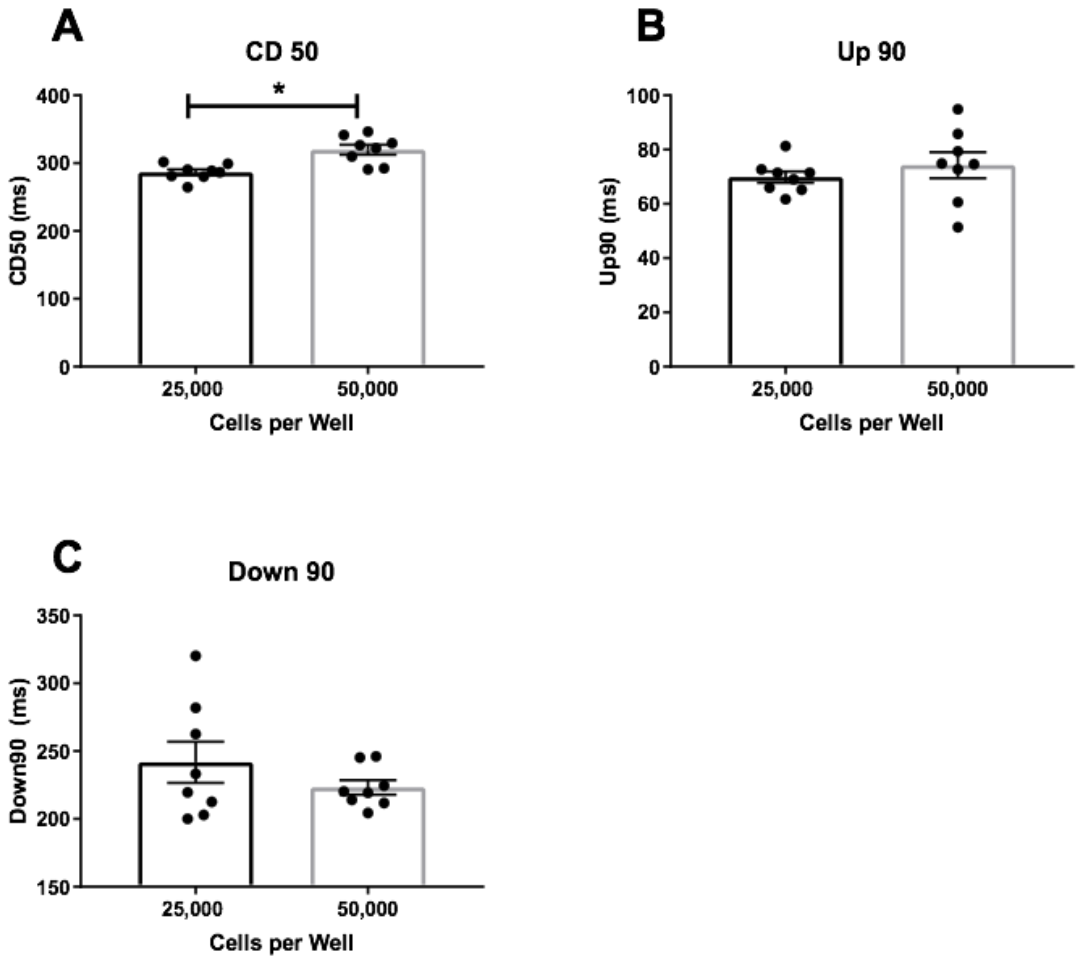

Figure 3-14 Speed of contraction and relaxation in iPSC-CM plated at a high or low density
iPSC-CM were plated at either 25,000 or 50,000 cells per well and then maintained for approximately 1 week. Thereafter contractility was measured via CellOptiq video based analysis software in order to produce quantification of CD50 (13A), Up90 (B), and Down90 (C). Values are reported as 8 replicate samples corresponding to the average of 3 recordings from geographically distinct locations in 8 separate wells. Individual data points are shown in addition to mean +/- S.E.M. Statistical testing was performed using an unpaired t-test, where the level of significance was set at P=0.05. * indicates P<0.05

	% Contraction											
Cells per well	10	20	25	30	40	50	60	70	75	80	90	100
25,000	40.2 (0.6)	46.3 (0.6)	48.9 (0.6)	51.6 (0.6)	57.0 (0.5)	62.9 (0.6)	69.8 (0.7)	78.7 (1)	84.2 (1.2)	90.8 (1.5)	110.1 (2.5)	175.0 (5.9)
50,000	39.7 (0.6)	45.3 (0.7)	47.7 (0.8)	50.2 (0.8)	55.4 (1.0)	61.2 (1.3)	68.3 (1.8)	77.8 (2.7)	83.7 (3.2)	90.8 (3.7)	114.0 (5.2)	203.6 (9.9)
Mean diff.	0.5	1.1	1.2	1.4	1.6	1.8	1.5	0.9	0.6	0.0	3.9	28.6
P<0.05 ?	No	No	No	No	No	No	No	No	No	No	No	Yes
	% Relaxation											
Cells per well	10	20	25	30	40	50	60	70	75	80	90	
25,000	252.5 (8.1)	284.1 (7.0)	296.8 (6.6)	307.2 (6.3)	329.9 (4.5)	349.5 (4.2)	370.5 (5.3)	394.2 (6.5)	408.9 (7.4)	428.6 (9.2)	494.1 (16.2)	
50,000	290.0 (6.9)	319.4 (6.8)	332.9 (6.9)	344.0 (7.1)	362.9 (7.2)	381.1 (7.0)	398.5 (6.9)	417.9 (6.7)	429.6 (6.5)	444.6 (6.4)	513.2 (5.5)	
Mean diff.	37.6	35.2	36.0	36.8	33.0	31.6	28.1	23.7	20.7	16.1	19.1	
P<0.05 ?	Yes	Yes	Yes	Yes	Yes	Yes	Yes	Yes	No	No	No	

Table 3-2 Speed of contraction and relaxation in iPSC-CM plated at a high or low density
All values are expressed as time (ms) after initiation of contraction and are mean (S.E.M.) of the 8 replicate samples described in the preceding figures. Statistical testing was performed between the 2 groups at each point using an unpaired t-test, where the level of significance was set at P=0.05.

After optimisation of plating density and incubation duration, a range of conditions had been identified that facilitated the reliable detection of suitable basal [^{3}H]-2DG uptake, significantly above background noise but not at risk of saturating cellular uptake capacity. Thereafter, the focus was to manipulate key experimental variables that may be able to elicit an insulin response. Firstly, the effect of stimulating cells with insulin like growth factor 1 (IGF-1) in comparison to insulin was assessed. IGF-1 can activate the insulin receptor directly, in addition to its own separate receptor, both of which activate intracellular Akt related signalling cascades (Stitt *et al.*, 2004). The relative effect of insulin and IGF-1 on a given cell type is related to the relative expression of the receptors, which in turn may be governed by maturation status (Boucher *et al.*, 2010). However, neither IGF-1 nor insulin was found to significantly increase [^{3}H]-2DG uptake in iPSC-CM across 2 independent experiments (Figure 3-15).

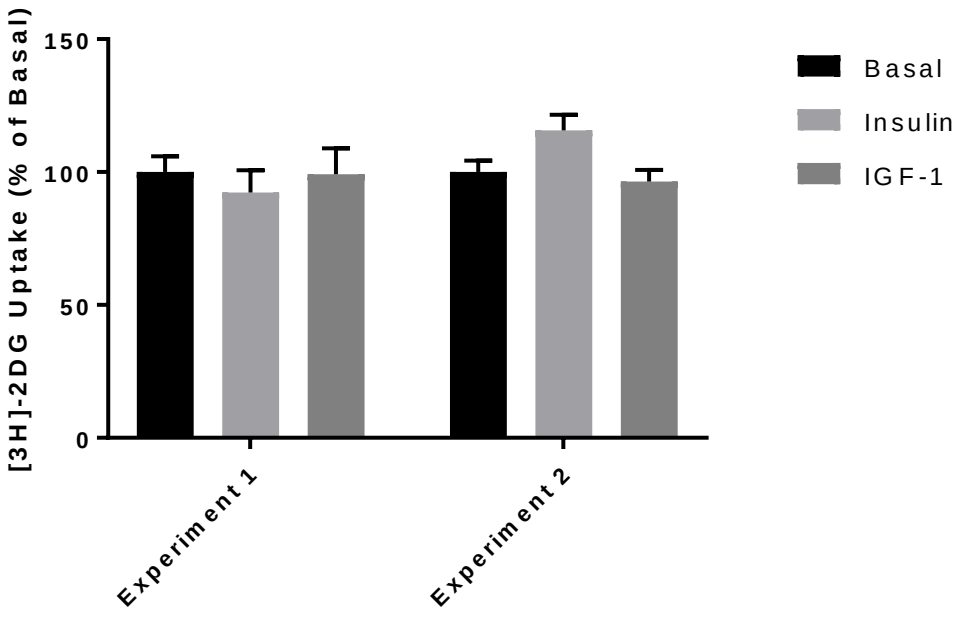

Figure 3-15 IGF-1 vs insulin stimulated glucose uptake in iPSC-CM
[^{3}H]-2DG uptake was assayed in iPSC-CM stimulated for 30 min with either 860 nM porcine insulin or 25 ng/mL IGF-1, relative to basal only values, across 2 independent experiments. [^{3}H]-2DG incubation was performed for 20 min. Values are expressed as a percentage of the mean basal uptake value recorded on each experimental day (+S.E.M.). Statistical analysis was performed on raw data with a 2-way ANOVA, where the identified factors were experimental day and drug stimulation. The level of significance was set at P=0.05.

A second experimental factor thought to influence the insulin sensitivity of iPSC-CM was the presence or absence of serum in the medium prior to performing the [^{3}H]-2DG uptake assay. Serum starvation is a tool widely used to enhance reproducibility of measurements but also more importantly it is used to enhance

physiological responses, as many growth factors and hormones are present in serum that activate intracellular signalling pathways and physiological processes. Serum starvation was performed for 2-3 hours in some of the earlier experiments, but not consistently. In some cases serum free medium provided by the company Axiogenesis (BMCC) was used, and in other cases serum free DMEM (4.5 g/L) was used. The presence of other interventions or conditions makes this collated data difficult to fairly compare, therefore an independent experiment was performed.

The data presented in Figure 3-16 is a representation of a typical insulin response recorded from iPSC-CM after experimental optimisation. A tight and clear basal uptake signal was recorded significantly ($P<0.0001$) above background noise over 20 minutes incubation duration, which we know from Figure 3-9 will not have saturated the uptake capacity of the cells. However, 15 mins 860 nM insulin stimulation, after 3 hours serum free DMEM incubation, failed to significantly increase the recorded [^{3}H]-2DG uptake signal after background correction (Figure 3-16; Basal vs Insulin; Means +/- S.E.M.: 2277 +/- 33 CPM vs 2447 +/- 54 CPM; $P>0.05$).

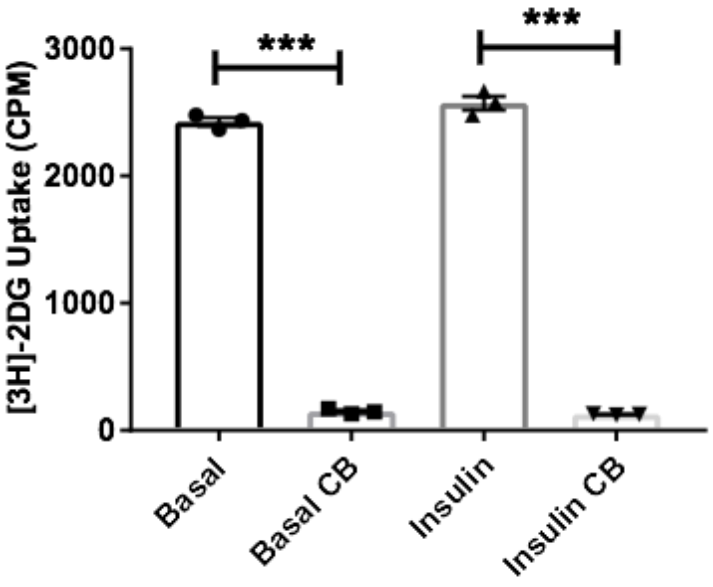

Figure 3-16 Insulin stimulation in serum starved iPSC-CM
[^{3}H]-2DG uptake was measured in iPSC-CM maintained in serum free DMEM (4.5 g/L) for 3 hours prior to 20 min stimulation with 860 nM porcine insulin or unstimulated basal control. Individual data points for each replicate sample are shown, in addition to mean +/- S.E.M. for each condition. Statistical analysis was performed with a 1-way ANOVA. Background corrected basal and insulin stimulated uptake (data not shown) was then compared with an unpaired t-test. In all cases the level of significance was set at P=0.05. * denotes P<0.0001.**

It can be inferred from the results displayed thus far that, regardless of experimental conditions, iPSC-CM very rarely exhibit a robust insulin response on top of a robust basal signal. To quantify this observation, all experiments recording basal and insulin stimulated [^{3}H]-2DG uptake only, performed with untreated (e.g. without drug stimulation or altered media conditions) iPSC-CM, were pooled and analysed (Table 3-3). Out of 38 total experiments, 25 basal signals >300 CPM were recorded, which was determined to be the minimally acceptable threshold. In total, 12 experiments had a fold insulin response >50%, which was also determined to be the minimally acceptable response. However, only 3 experiments met both of these criteria. Despite a large range of conditions and therefore basal uptake signals, the average insulin response (regardless of fold change) was remarkably consistent at 303.5 CPM. This demonstrates why the majority of acceptable fold insulin responses were recorded only when the basal signal was lower than 300 CPM (9/12 experiments).

Total	Basal>300 CPM	Insulin Response > 50%	Combined	Ave. Insulin Response (CPM)
38	25	12	3	303.5 (54.2)

Table 3-3 Overview of basal and insulin stimulated [^{3}H]-2DG transport experiments

3.2.4 Insulin stimulated [^{3}H]-2DG uptake in quiescent iPSC-CM

In addition to insulin, contraction is a potent stimulus for glucose uptake in muscle (Kramer *et al.*, 2006). As discussed in the introduction, in intact contracting myocardium it is still possible to detect an increase in glucose uptake in response to insulin stimulation. However, it could be that the spontaneous contractile activity of iPSC-CM could mask a smaller – but still robust – response in this cell type. Therefore basal and insulin stimulated glucose uptake was measured in non-contracting iPSC-CM.

To achieve this quiescent state, cells were treated with the drug blebbistatin, which selectively inhibits contractile myofilament interactions by targeting the myosin ATPase, but avoids interfering with other aspects of excitation contraction coupling such as intracellular calcium handling (Farman *et al.*, 2008). For optimal insight, blebbistatin was serially diluted to its working concentration and applied for the duration of the serum starvation prior to the main [^{3}H]-2DG uptake assay. This drug is fast acting, however it was deemed necessary to expose the iPSC-CM

for a prolonged period in advance of measuring glucose uptake to give time for any metabolic changes to occur and reach a new steady state. Cessation of contractile activity was confirmed through visual inspection via a standard light microscope. As described, the first step of the assay involves washing cells, to remove residual media. This would also remove the blebbistatin and rapidly reverse its action. Therefore it was reapplied at the same time insulin stimulation was initiated, preventing reinitiation of contraction until termination of the assay.

Blebbistatin incubation for 3 hours prior to, and during the assay, significantly reduced [^{3}H]-2DG uptake in the presence ($P<0.001$) and absence ($P<0.001$) of insulin stimulation (Figure 3-17). However, there was no significant effect of insulin upon transport rates either in the presence ($P>0.05$) or absence ($P>0.05$) of blebbistatin. Nifedipine, a calcium channel blocker that also inhibits myocyte contraction, was found to have a similar effect (n=1, data not shown).

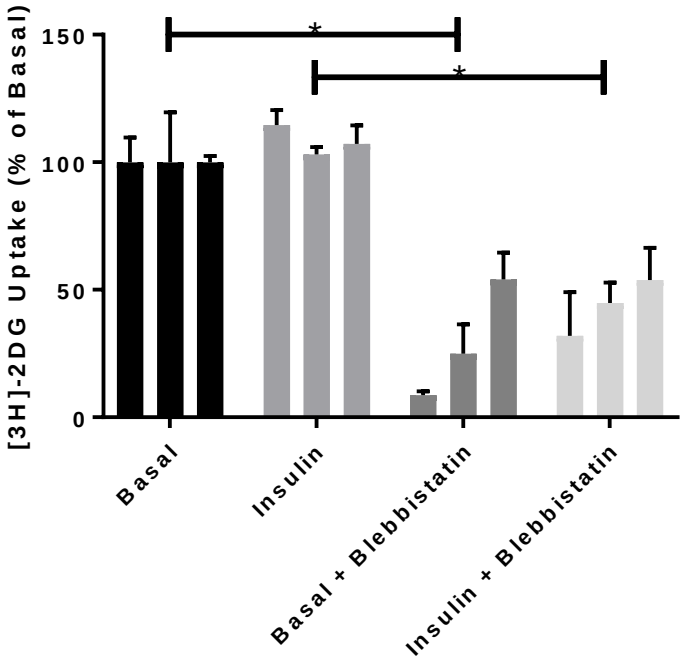

Figure 3-17 The effect of blebbistatin on [^{3}H]-2DG uptake in iPSC-CM
Cells were incubated with 3-10 μM blebbistatin for 3 hours prior to and also throughout the assay. Cells were stimulated for 20-30 min with 860 nM insulin and incubated with [^{3}H]-2DG for 15-20 min. Data shown is mean (+S.E.M.) of 3 replicate samples for each experimental day, across 3 independent experiments. Statistical analysis was performed on raw data with a 2-way ANOVA, where the identified factors were drug incubation and experimental day. The level of significance was set at P=0.05.

3.2.5 The expression of GLUT4 trafficking proteins in iPSC-CM

After extensive experimental optimisation and manipulation of contraction it became clear that iPSC-CM were not capable of producing the required response. Therefore, investigation into identifying why this was the case began. First of all, it was assessed if iPSC-CM express the necessary proteins to facilitate the cellular process of GLUT4 trafficking. This demands the expression and capacity to activate intracellular insulin signalling cascades, the expression of key SNARE proteins, and most fundamentally the expression of GLUT4.

Relative to primary rodent cardiomyocytes, iPSC-CM were found to express low levels of GLUT4, and high levels of GLUT1 (Figure 3-18). The data shown are from one biological sample, however the same trend was observed in 5 independent replicates (data not shown). The precise amount of iPSC-CM lysate loaded could not be accurately estimated due to the method of lysate generation preventing the opportunity to perform a micro BCA assay or equivalent. However, from the GAPDH and ponceau signals, an approximately equal amount of total protein appears to be present. Even if no loading control were available, an identical volume of the same samples were loaded for each immunoblot, therefore the relative difference in signals between blots still supports the conclusion reached. Issues such as the validity of GAPDH as a loading control between samples from different species and quantification of GLUT1/4 levels in iPSC-CM relative to adult cells are addressed in chapter 4. At this stage the key conclusion was that iPSC-CM appear to be foetal like with regards to their GLUT isoform expression. For all of the following blots, borders between sections of the same blot indicate that images have been cropped for presentation purposes, however the images are taken from the same blot, with no alteration to brightness or contrast settings between segments.

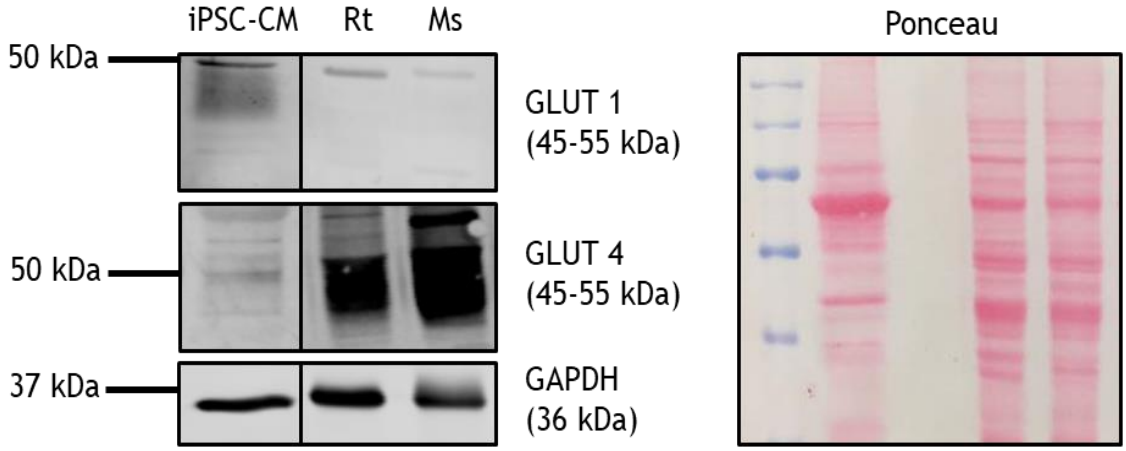

Figure 3-18 GLUT1 and GLUT4 protein expression in iPSC-CM
Representative immunoblot depicting 30 µL iPSC-CM lysate and approximately 25 µg of lysates generated from primary adult rat (Rt) and mouse (Ms) cardiomyocytes that were subjected to SDS-PAGE and immunoblotting, probing for the expression of GLUT1 and GLUT4. GAPDH, in combination with Ponceau S staining, acted as relative loading controls. Data from a typical experiment is shown, with 5 independent experiments performed in total. The approximate position of molecular weight markers is indicated.

Syntaxin 4 and SNAP23 are integral membrane bound t-SNAREs critical for the fusion of GSVs and the plasma membrane (see chapter 1) (Kioumourtzoglou *et al.*, 2014). Immunoblotting of 3 independent samples indicated that iPSC-CM express both of these proteins (Figure 3-19). The expression of Syntaxin 4 was variable, whereas the expression of SNAP23 was more consistent. On account of the consistent signal obtained from 3T3-L1 adipocyte lysate, it is likely that this reflects the actual protein expression, rather than just variable antibody binding.

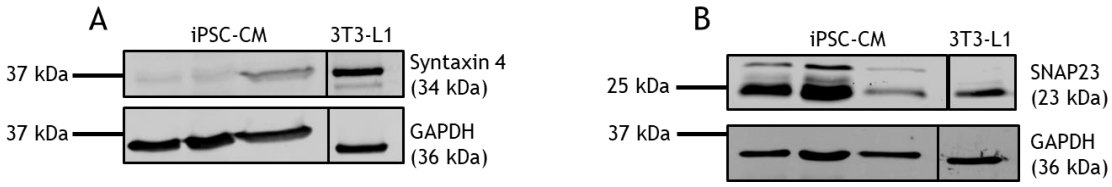

Figure 3-19 The expression of key SNARE proteins in iPSC-CM
Representative immunoblots depicting 20/30 µL of 3 biologically independent iPSC-CM lysates that were subjected to SDS-PAGE and immunoblotting, probing for the expression of SNAP23 or Syntaxin 4 respectively. 5 µL 3T3-L1 adipocyte lysate was also loaded in order to act as a positive control, and GAPDH acted as an indicator of relative loading.

Activation of intracellular signalling cascades provides the link between stimulation of the plasma membrane bound insulin receptor and the movement of GLUT4 to the cell surface in order to increase glucose uptake. There are dozens of intermediates involved in these pathways, including Akt. ERK1/2 have also been implicated in insulin sensitivity in human skeletal muscle (Rajkhowa *et al.*, 2009). Figure 3-20 reveals that not only do iPSC-CM express these proteins, but they are

also phosphorylated and activated in response to insulin. In total, activation was assessed and/or detected in 3 biologically independent samples for Erk 1/2 and 7 biologically independent samples for Akt. The reason so many more repeats were performed for Akt is that a large amount of variability was detected in the response, which appeared to be primarily linked to the relatively strong basal phosphorylation of Akt. Subjectively this appeared most strongly related to whether or not cells were serum starved prior to the assay. To properly address this issue, iPSC-CM were insulin stimulated either after serum starvation or normal incubation in Cor4U medium, and the activation of Akt was quantitatively assessed (Figure 3-21). The presented graph allows assessment of the reliability of phosphorylation measurements in all conditions, and how it changed in response to serum starvation or insulin stimulation. Serum starvation clearly reduced basal phosphorylation, however a similar fold response to insulin (approx. 1.5 fold) was observed between conditions.

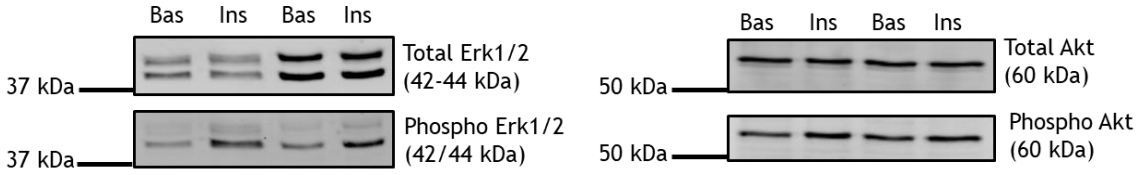

Figure 3-20 Expression and activation of Erk 1/2 and Akt in iPSC-CM
Representative immunoblots depicting the expression of total and phosphorylated Erk 1/2 and Akt in lysates from iPSC-CM that had been stimulated for 30 min with 0 (basal control) or 860 nM insulin and then subjected to SDS-PAGE and immunoblotting. The Erk 1/2 images depict basal and insulin stimulated lysates from 2 biologically independent replicates, whereas the Akt image depicts 2 technical replicates of basal and insulin stimulated lysates from 1 biological sample. Data from a typical set of experiments is shown, and in total 3 biological replicates were performed for Erk 1/2, and 7 biological replicates were performed for Akt.

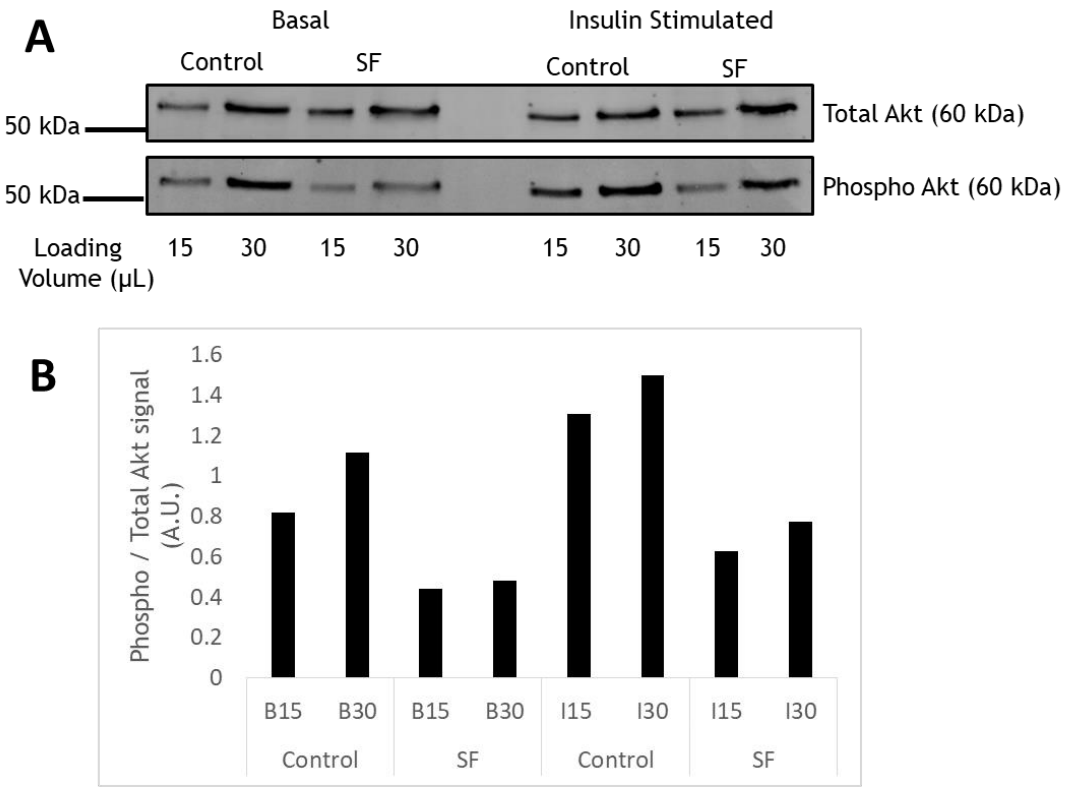

Figure 3-21 The effect of serum starvation upon basal and insulin stimulated phosphorylation of Akt in iPSC-CM
A: Representative immunoblot depicting the expression of total and phosphorylated Akt in lysates generated from iPSC-CM that had been stimulated for 0 (basal control) or 30 min with 860 nM insulin, +/- 2.5 hours serum starvation in DMEM (4.5 g/L glucose), and then subjected to SDS-PAGE and immunoblotting. B: Quantification of the immunoblot displayed in panel A was performed via densitometry, expressed as the ratio of phosphorylated to total Akt in each lysate.

3.2.6 The effect of maturation medium on iPSC-CM glucose transport

The relative expression of GLUT1 and GLUT4 in iPSC-CM indicate the possibility of metabolic immaturity in this cell type. Therefore, MM conditioning as described by (Drawnel *et al.*, 2014) was implemented, whereby cells were forced to rely on fatty acid metabolism rather than glucose to support ATP generation with the aim of promoting maturation, and the impact on glucose transport was assessed. This intervention was performed on 4 separate occasions, and was found to be toxic to cells. This increased the variation observed in results. Therefore, findings from only one of these experiments are reported, where an increased number of technical replicates were performed in order to gain a more robust and valid insight. However, the general findings can be applied to all independent assays performed (data not shown).

MM conditioning significantly reduced [^{3}H]-2DG transport into iPSC-CM in the presence or absence of insulin ($P<0.01$) (Figure 3-22). As alluded to, rather than indicating a reduction in glucose uptake per cell, this is almost certainly primarily attributable to a reduced total cell number at the time of assay in conditioned cells. Insulin stimulation did not significantly increase [^{3}H]-2DG uptake in either control or conditioned cells ($P>0.05$).

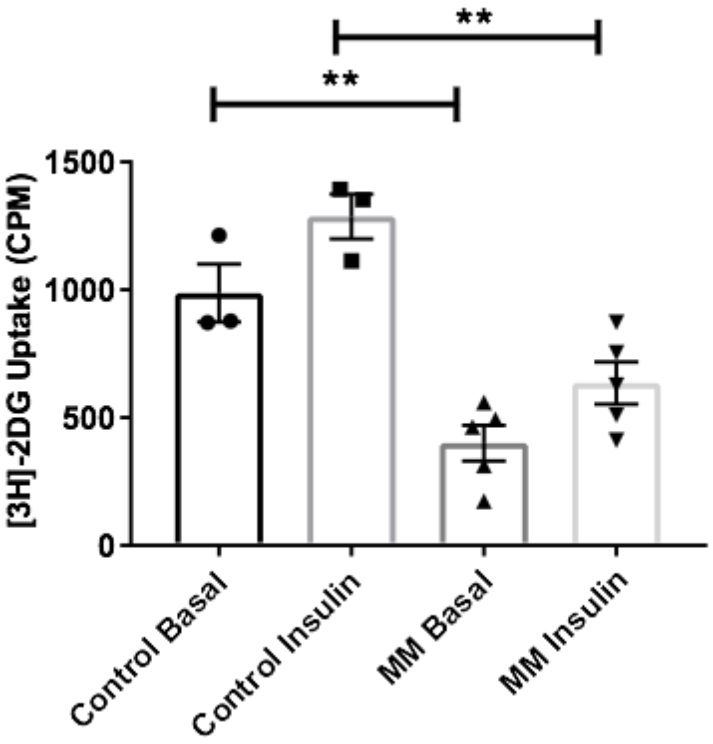

Figure 3-22 The effect of maturation medium upon glucose transport in iPSC-CM
iPSC-CM were plated and maintained in normal Cor.4U medium for 3 days. Subsequently, cells were either kept in Cor.4U medium (control) or maturation medium (MM) as described by Drawnel *et al*. for 4 days. Basal and insulin stimulated [^{3}H]-2DG uptake was then measured. Cells were incubated for 30 min with 860 nM insulin, prior to a 20 min incubation with [^{3}H]-2DG. Data is mean of 3 (control) or 5 (MM) replicate samples (+S.E.M.). Statistical analysis was performed with a 1-way ANOVA, where the level of significance was P=0.05.

3.2.7 Insulin sensitivity and GLUT expression in CDI iPSC-CM

All of the data displayed and discussed thus far was generated with iPSC-CM purchased from Axiogenesis. It was considered possible that cells from a different company, who may employ alternative differentiation protocols or selection procedures, could be at a more advanced stage of maturation. Therefore, key assays were repeated with iPSC-CM purchased from Cellular Dynamics International (CDI).

Basal [^{3}H]-2DG uptake was readily detectable in CDI cells, however there was no significant (P>0.05) increase in this signal in response to insulin stimulation (Figure 3-23). Additionally, relative to primary cardiomyocyte lysate, CDI iPSC-CM expressed much higher levels of GLUT1 protein and much lower levels of GLUT4 protein (Figure 3-24). However, a clear increase in phosphorylation of Akt in response to insulin stimulation was detected in lysates generated from these cells (Figure 3-25). In all cases these measurements were performed in 3 biologically independent samples.

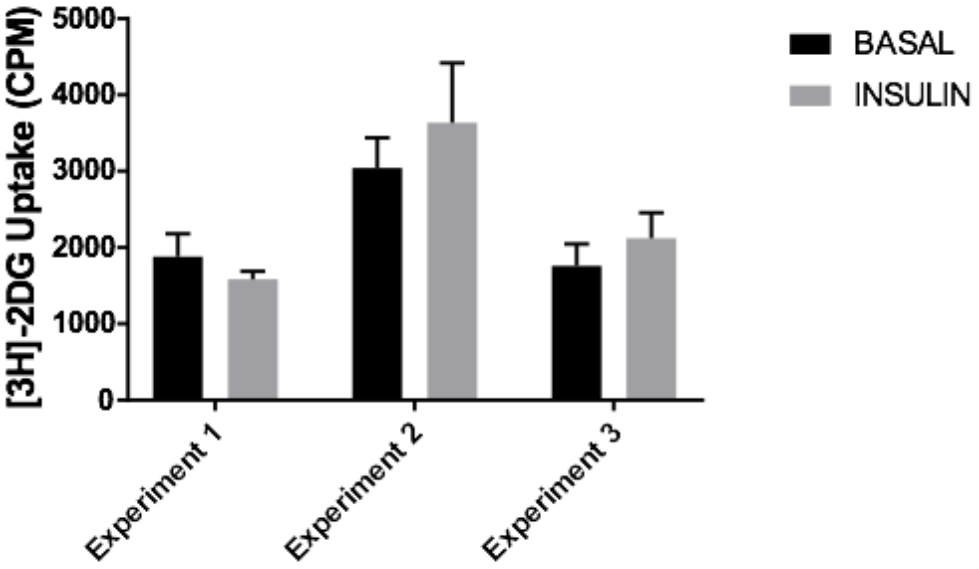

Figure 3-23 Insulin stimulated glucose uptake in CDI iPSC-CM
[^{3}H]-2DG uptake was assayed using CDI iPSC-CM plated at 50,000 cells per well. Cells were incubated with 860 nM insulin for 20 min prior to a 10 min incubation with [^{3}H]-2DG. Cells were serum starved for 4 hours prior to the assay. Data shown is mean (+S.E.M.) of 6 replicate samples for each experimental day, across 3 independent experiments. Statistical analysis was performed with a 2-way ANOVA, where the identified factors were experimental day and insulin. The level of significance was set at P=0.05.

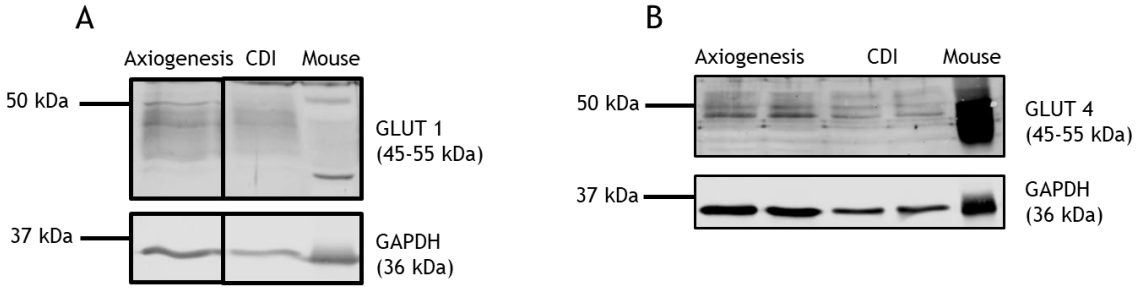

Figure 3-24 GLUT1 and GLUT4 expression in CDI iPSC-CM
Representative immunoblots (of 3 independent biological replicates) probing for total GLUT1 and GLUT4 protein expression in 1 or 2 samples of cell lysate generated from CDI and Axiogenesis iPSC-CM, and primary mouse cardiomyocytes. An equal amount of samples was loaded between immunoblots (20 µL iPSC-CM, 5 µg total protein mouse), and GAPDH expression is also shown to indicate relative loading. Note that 20 µL iPSC-CM corresponds to lysate generated from approximately 20,000 cells.

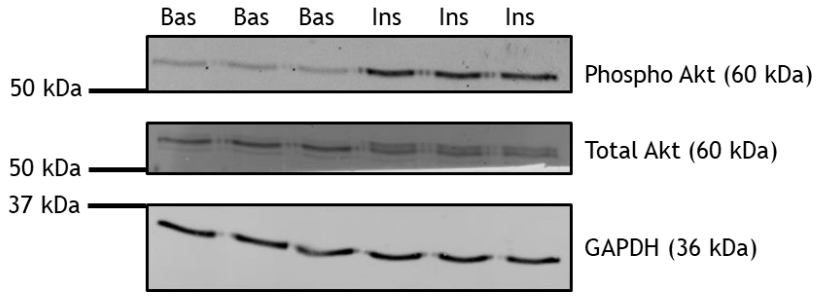

Figure 3-25 Insulin stimulated phosphorylation of Akt in CDI iPSC-CM
Representative images depicting total and phosphorylated Akt expression in lysates generated from CDI iPSC-CM that were stimulated with 0 (basal control) or 860 nM insulin for 30 min, and then subjected to SDS-PAGE and immunoblotting. Cells were serum starved for 3 hours prior to the assay, and 20 µL lysate was loaded for each sample. GAPDH expression was also probed in order to indicate relative loading. This is a representative immunoblot showing 3 replicate samples for each condition within one experimental day, and in total 3 independent experiments were performed.

3.3 Discussion

3.3.1 Insulin stimulated [^{3}H]-2DG uptake can be measured on a 96-well plate format

In order to maximise the progress and viability of this project the measurement of glucose uptake had to be adapted to a 96-well plate format. Real-time assay of glucose uptake via 2-(N-(7-Nitronez-2-oxa-1,3-diazol-4-yl)Amino)-2-Deoxyglucose (2-NBDG) was attempted. However, this was unsuccessful as the rapid photobleaching of this fluorescent glucose derivative prevented reliable detection of uptake. Hence, we turned to a radioactive based assay widely used in the field. Results from Figure 3-1 and Figure 3-2 indicate that this assay was successful in a 96-well plate format as a clear basal glucose uptake signal was detected above background noise in both HEK293 and HeLa cells. There are no universally accepted guidelines for determination of what is or is not an acceptable signal to noise ratio using this technique, however experience of this assay and common practice dictate that a basal signal should certainly be at least 25% above background noise. In addition to a relative margin, a difference of at least 300 CPM should be expected. These were set as standard criteria in the determination of whether glucose uptake had actually been detected. It is easily possible to detect a signal statistically significantly greater than background but still within the noise of the assay in real terms. For example, if a signal was significantly greater by 50 CPM over a background of 1000 CPM it is not credible to claim uptake has been sufficiently detected and then make any subsequent conclusions about a fold insulin response.

In both experiments with HEK293 and HeLa cells there was a significant effect of plating density upon recorded [^{3}H]-2DG uptake. This is to be expected, as a greater number of cells per well should lead to a greater absolute amount of [^{3}H]-2DG uptake/well, and therefore in turn a greater detected signal. The relationship between cell number per well and detected uptake signal appeared linear across the range of plating densities tested (10-50,000 cells per well). Additionally, a background corrected signal of 500-1000 CPM was recorded at 25,000 cells per well. Combined, these observations were valuable gauges for working with iPSC-CM, as they suggest that a strong basal uptake signal should be detectable at the recommended plating density for iPSC-CM (25-30,000 cells per well), without risk

of saturating cellular uptake capacity. It was thought possible that the number of washes prior to [^{3}H]-2DG uptake would also impact the signal recorded. If glucose contained in maintenance media is not adequately washed away prior to the assay then this could inhibit [^{3}H]-2DG uptake, thereby leading to a lower detected signal. However, excessive washing could lead to the detachment of cells and a lower and noisier signal, particularly for the somewhat more fragile iPSC-CM. Whilst there was no statistically significant effect of the number of washes, subjectively it does appear as though the relationship between plating density and uptake was indeed noisier when 3 washes were performed prior to the assay, compared to when only 1 was performed.

Critically, basal and insulin stimulated [^{3}H]-2DG uptake values for 3T3L1 adipocytes and primary rabbit cardiomyocytes (Figure 3-3 and Figure 3-4) recorded on the same 96-well plate format clearly indicated that this assay can detect a robust, statistically significant insulin response, if the cells are capable of producing it. For both cell types, the responses recorded were within the typically reported range of responses in the literature, albeit perhaps towards the lower end of the spectrum for the isolated rabbit cardiomyocytes. This could be largely attributable to a high volume of dead cells that are more difficult to wash away when trapped in the wells of a 96-well plate. These cells could not be filtered out of the sample in any way prior to plating, and could increase the likelihood of trapping [^{3}H]-2DG uptake in the extracellular space, thereby increasing the noise of the results. The key point is that based on this collective data it can be concluded that if no insulin response is recorded in iPSC-CM then it is unlikely to be due to an inherent inability to detect it using this experimental technique.

3.3.2 iPSC-CM exhibit poor insulin stimulated glucose uptake

The most important and consistent feature of any diabetic model is an impairment of insulin stimulated glucose uptake, therefore to have any potential to act as a novel model of DCM, iPSC-CM must exhibit a robust baseline insulin response. Data from Figure 3-5 provided an initially favourable evaluation. Insulin significantly increased the rate of glucose uptake approximately 2-fold above basal values in the first set of experiments, and trended towards significance in the second set of experiments. The basal uptake values in experiment 1 of Figure 3-5B seem

erroneously elevated, however no justifiable reason could be provided for exclusion. Regardless, Akti and wortmannin significantly reduced glucose uptake in the presence of insulin. This is logical as Akt and PI3K are known to be central intracellular insulin signalling pathway molecules important in the insulin-stimulated delivery of GLUT4 to the plasma membrane (Kohn *et al.*, 1996).

As described in the introduction, myocardial glucose uptake is impaired in human diabetic patients in the presence of insulin, relative to healthy control subjects. This reduction in glucose transport likely reflects a combination of the onset of IR and a reduction in basal transport, although the exact relative contribution of each is unclear. In the dataset presented in Figure 3-8 no insulin response was recorded in control cells, therefore any development of IR could not be assessed. Presented results suggest that acute (3-4 days) incubation with palmitate may decrease basal glucose uptake in iPSC-CM. However, this effect was small and the underlying mechanism was not tested, therefore caution must be drawn when stating the wider importance of this individual dataset.

Despite several favourable observations of this initial data drawing comparison between iPSC-CM and the relevant published literature, Figure 3-6 reveals a couple of crucial issues. Whether looking at summaries of individual experiments or at the 95% confidence intervals of conditions in the overall dataset, the variation in both the absolute counts recorded and the relative effect of insulin appears to be considerable. This observation is supported by the finding that values differed significantly between experimental days. One possible explanation is to attribute this primarily to inherent variation of the assay, perhaps in the process of scintillation counting or dilution of the [^{3}H]-2DG stock. However, there was a significant interaction effect between experimental day and insulin, suggesting that the response of the cells to the [^{3}H]-2DG and particularly the insulin was indeed more pronounced on certain days and the primary cause of variation within the assay. This conclusion is strongly supported by the recording of highly similar basal and insulin stimulated counts across 3 independent experimental days with 3T3-L1 adipocytes (Figure 3-7A). Additionally the extremely tight experimental standard readings indicate that both the preparation of the assay mix and the output of the scintillation counter are consistent (Figure 3-7B).

In isolation, variation in results is not disastrous. However, an equally important observation from Figure 3-6 is the poor signal to noise ratio between conditions +/- CB. The central problem when background corrected CPM values are so small is that the 'insulin response' essentially represents the detection of some glucose uptake against no detection of glucose uptake, rather than a robust increase from one rate to another. This is an issue because we are interested in establishing a model whereby we can measure a reliable >2 fold response over and above a strong and stable basal signal. If the basal value is very low or even negligible, then this leaves open the possibility of small variations in absolute counts creating a disproportionate and misleading large range of fold responses. There is more of a buffer against this if basal counts are more substantial.

Table 3-1 reveals that the mean basal glucose uptake signal was around 22% higher than background, and hence fell below the required threshold of 25%. 95% confidence intervals also indicate the difference may be as little as 81 CPM in a wider population of cells under similar conditions. If following normal protocol then the mean background subtracted insulin stimulated increase in glucose uptake values represents essentially a 2-fold response, bringing it in line with data from primary rodent cardiomyocytes (Figure 3-4). However, given the variation and low basal CPM this would be an unjustifiable conclusion.

As stated, the true magnitude and biological relevance of the apparent insulin response recorded in Figure 3-6 is hard to interpret. This causes problems when progressing to the ultimate aim in the development of any biological model whereby attempts are made to manipulate the observed response and assess the effect of different interventions. All that could practically be achieved in this case is an inhibition/increase in the insulin response, or not. These concerns are heightened by the observation that no insulin response was recorded in control cells during the palmitate conditioning experiments. These experiments were performed with modified conditions that facilitated a much larger and more reliable basal glucose uptake signal, and are discussed in detail below. It is possible that the true insulin response of these cells is very small and only apparent when compared to a similarly weak basal signal. This underlines the importance of assessing both the absolute and relative effect of insulin on glucose uptake values, not just the fold response alone.

3.3.3 Manipulation of experimental conditions strongly impacts the recorded uptake signal from iPSC-CM, but not their insulin sensitivity

Initial characterisation of iPSC-CM was performed under a range of experimental conditions based upon the pilot data in HEK293 and HeLa cells. Despite recording a statistically significant insulin stimulated glucose uptake response that may be regulated by similar pathways as in mature cells, it was clearly necessary to re-optimise experimental conditions in order to assess if the same fold insulin response could be recorded in the presence of a more robust basal signal. As alluded to in the results section, this was a 2 step process. First of all variables thought to influence basal glucose uptake in iPSC-CM were systematically examined in order to reliably obtain the desired signal. This was successfully achieved, however this resulted in no insulin response being observed. Therefore further variables were examined to ascertain whether this was a reflection of an inherent lack of an insulin response, or due to confounding experimental conditions relating to iPSC-CM.

The first experimental variable identified was the duration for which iPSC-CM were incubated with the [^{3}H]-2DG assay mix. Intuitively, longer incubations should allow more time for [^{3}H]-2DG uptake and therefore a larger recorded signal; however at longer time points, ATP may be rate limiting and 'uptake' rates may then not reflect uptake but rather metabolism of 2DG. With a longer incubation duration we would also anticipate the signal to noise ratio to improve. The results from Figure 3-9 clearly indicate that across a range of 15-60 min, both the [^{3}H]-2DG uptake signal and the signal to noise ratio increased with time as expected. Critically, the rates normalised against cell number and time do not differ greatly between conditions, indicating a linear relationship between incubation duration and [^{3}H]-2DG uptake over the range tested. These data show that saturation of 2DG uptake was not a problem under the conditions employed. All glucose uptake measurements are presented as average rates across the duration for which cells were incubated with the [^{3}H]-2DG. Real-time assays of glucose uptake may have been useful and more insightful, but as noted above live glucose uptake using 2-NBDG was unsuccessful as the rapid photobleaching of this fluorescent glucose derivative prevented reliable detection of uptake.

In contrast to incubation duration, manipulation of cell density had a more powerful influence over the recorded uptake signal (Figure 3-10). The amount of recorded glucose uptake per cell increased by an average of almost 100% between conditions. This means that even minor variations in cell density can strongly increase or decrease the recorded basal signal, therefore making regulation of this factor critical. Interestingly it also suggests that saturation of the uptake signal did not occur even in cells plated at 50,000 cells per well, confirming further that a lack of insulin response is most likely due to a limitation within the cells and not the assay.

Consideration of why uptake may vary so strongly with plating density leads to several theories. The most intriguing is related to possible changes in contractile activity. iPSC-CM do not function as individual cells, sitting in isolation. Rather, they interact with their environment, particularly neighbouring cells. Just as occurs *in vivo*, functionally coupled networks of cardiomyocytes that beat in unison are formed. In contrast to mature cells, iPSC-CM do not need extrinsic excitation, and instead maintain a spontaneous contractile rate of around 1 hertz. It is credible to suggest that an increased degree of coupling between cells in a plate may alter the rate and/or strength of contraction, thereby having a direct impact on ATP requirements in each cell. The data presented in Figure 3-13, Figure 3-14, and Table 1-2 suggest this could be the case. Rather than altering the rate or strength of contraction it appears that the length of time that the cells were generating maximal tension (90-100% contraction) significantly increased. Additionally, to maintain the total duration of contraction, an acceleration of relaxation occurred. Both of these changes would increase ATP demand significantly, and therefore increase the demand for uptake of the primary metabolic substrate glucose. It is particularly feasible to suggest changes in coupling and contraction may occur between the densities that were chosen, because iPSC-CM only form a fully coupled monolayer at approximately 30-35,000 cells per well.

However, there are alternative theories that could account for changes in glucose uptake recorded per cell with alterations in cell density. Primarily, the stated densities are approximate plating densities, not a definitive measure of the number of cells that are still present at the time of the assay. It could be that

these cells are more healthy (or exhibit reduced stress responses) in confluent monolayers and therefore there is a reduction in the inevitable loss of some cells at higher densities over the course of a 1 week culture. Additionally, these cells are differentiated from a fibroblast like phenotype, and although a puromycin selection step is undertaken due to resistance to this antibiotic being artificially genetically linked to the insertion of cardiac specific genes as a marker of successful manipulation, it is probable that some fibroblasts survive and may proliferate. The extent to which this impacts overall cell number will depend upon how many cells are plated. Therefore combined these issues could lead to an even bigger difference in cell number at the time of assay than is assumed, and therefore normalisation against plating density could result in misleading differences in uptake arising. From visual inspection of the cells this is unlikely, but it cannot be discounted without consideration. For the practical purposes of the assay, explanation of the relationship between density and recorded uptake signal is not vital, as long as it is practically understood and managed.

Based upon this work, it was determined that a plating density of approximately 35,000 cells per well and an incubation duration of 20 min would facilitate the reproducible detection of the desired basal glucose uptake signal. Therefore, attempts were made to alter other experimental variables in the hope of revealing an insulin response. However, unfortunately neither stimulation of cells with IGF-1 nor serum starvation prior to the uptake assay had any effect of note on the insulin response (Figure 3-15 and Figure 3-16). Whilst it was always unlikely that these fairly simple interventions would induce a 2-fold insulin response or more, the absence of any effect suggested that these cells were perhaps entirely incapable of producing this, and that no particular detail of the protocol was a critically limiting factor.

3.3.4 Contraction is a potent stimulus for glucose uptake in iPSC-CM

The coupling of contractile activity and glucose uptake in muscle tissue is a logical mechanism to ensure that the highly energetic demands of excitation contraction coupling are met. The contrast in glucose uptake between resting and maximally contracting conditions will likely be far greater in skeletal muscle because of the ability of this tissue to completely rest, unlike the heart. Indeed, less than a 50%

increase in myocardial glucose uptake is typically reported *in vivo* in response to maximal insulin stimulation. When relating these findings to iPSC-CM, it is highly unlikely that this assumed contraction mediated elevation in basal glucose uptake (relative to a non-contracting state) would be sufficient to mask the required 2-3 fold insulin response. Indeed, Figure 3-17 confirms this to be the case. Blebbistatin mediated inhibition of contraction reduced detected glucose uptake by >50%, yet subsequent insulin stimulation did not significantly increase this signal. This strongly suggests, as would be expected, that contraction plays a vital role in regulating metabolic demand in these cells, however insulin does not.

Additionally, a concept introduced previously is supported by this dataset. In all of the independent experiments, the recorded basal glucose uptake signal was well in excess of 500 CPM, and insulin increased this signal by less than 10%. However, if this basal signal had been much lower and in the range of values typically recorded prior to experimental optimisation, then a robust fold response would have been recorded. This demonstrates fairly conclusively that any insulin response recorded in these cells is indeed minor, and not significantly inhibited by contraction mediated uptake.

3.3.5 iPSC-CM are metabolically immature

The fundamental limitation of iPSC-CM with regards to developing a novel cellular model of DCM is that they cannot produce a reliable and/or robust insulin stimulated glucose uptake response. The primary reason for this appears to be very low levels of expression of GLUT4 protein, the predominant insulin sensitive glucose transporter in mature muscle tissue (Figure 3-18). This observation, coupled with high levels of GLUT1 protein expression, are strongly indicative of metabolic immaturity in this cell type. This is consistent with limitations cited in other aspects of iPSC-CM physiology, for example their elevated resting membrane potential that contributes towards their spontaneous contractile activity, or poorly developed t-tubule network (del Álamo *et al.*, 2016). The difference observed in Figure 3-18 is subjective, yet conclusive. Whilst the relationship between GAPDH and total protein has not been confirmed to be identical between the different species/cell types implemented here, comparison with Ponceau S staining provides confidence that the GLUT signals are from similar amounts of

protein. However, even accounting for slight discrepancy, the difference in GLUT4 expression appears large.

These findings relate favourably to the [^{3}H]-2DG transport data displayed. GLUT4 is the predominant insulin sensitive transporter in muscle, therefore its low expression in iPSC-CM probably accounts for the very poor insulin response recorded. The occasional small and unsignificant absolute increase in glucose uptake in response to insulin stimulation could be partly accounted for by the GLUT4 that is present. Alternatively, it could also be due to the high levels of GLUT1, which also exhibits insulin-stimulated translocation to the plasma membrane in many cell types (e.g. Fischer *et al.*, 1996, 1997). Perhaps of more interest is the observation that contraction is clearly an important regulator of glucose uptake in iPSC-CM, yet there is very little GLUT4 present, which we would typically expect to mediate this response in adult cells. This strongly suggests that GLUT1 may be predominantly responsible for contraction mediated glucose uptake in iPSC-CM. In turn, this suggests that after progressing through development to a final fully mature state, GLUT4 expression not only gives cells the ability to mediate glucose uptake more selectively via insulin, but that it also takes over other responsibilities of GLUT1. Together these suggest that GLUT4 is used to more tightly couple metabolic demand and uptake, whereas GLUT1 is used to generally increase glucose uptake during the highly energetic initial stages of development.

It is possible that low GLUT4 expression is not the only factor limiting iPSC-CM increasing glucose uptake in response to insulin stimulation. The process of insulin stimulated GLUT4 trafficking requires the presence and sufficient activation and interaction of multiple signalling and effector proteins. It would be challenging to characterise and assess every single necessary relevant interaction. However, iPSC-CM do express, and can phosphorylate (and therefore activate) in response to insulin, the central signalling intermediate Akt (Figure 3-20). Additionally, they can also activate Erk 1/2, which has been proposed to mediate insulin sensitivity in human muscle populations (Rajkhowa *et al.*, 2009). The extent to which Akt was activated varied across a range of independent assays, primarily due to variations in basal Akt phosphorylation levels. Serum starvation prior to the assay was found to reduce this basal signalling (Figure 3-21), which increases the

chances of detecting a more robust insulin response. SNARE proteins are of particular importance in insulin-stimulated GLUT4 translocation to the plasma membrane. Syntaxin 4 and SNAP 23 are widely accepted to be the target t-SNAREs located on the plasma membrane (Kioumourtzoglou *et al.*, 2014). It appears that iPSC-CM express both of these proteins, albeit to an unclear extent (Figure 3-19). Together, this data confirms that intracellular signalling networks are activated to at least some degree by insulin, and that integral parts of the fusion machinery are present, suggesting the central limiting factor may indeed be limited GLUT4 availability.

3.3.6 'Maturation Medium' conditioning did not improve iPSC-CM insulin sensitivity

Whilst it would be an overstatement to conclude that absolutely no insulin response had been recorded from iPSC-CM, it was clearly far short of what was required. Therefore, a protocol recommended specifically for this cell type in order to stimulate maturation was employed. Essentially, by supplying iPSC-CM in culture with fatty acids rather than glucose, rapid maturation of a range of parameters has been reported (Drawnel *et al.*, 2014). However, as exemplified in Figure 3-22, when this approach was mimicked in this project with Axiogenesis iPSC-CM, the only clear effect was a reduction in detected basal [^{3}H]-2DG uptake. This was attributed to acute toxicity of the applied medium, and it certainly did not induce any insulin response. It is possible that iPSC-CM do not possess the necessary machinery to effectively metabolise fatty acids, and that the palmitate therefore accumulated intracellularly and essentially acted as a metabolic poison. Whilst this initial intervention had unexpected outcomes, the principle of this approach remained valid and was therefore explored in much greater detail in chapter 4.

3.3.7 The characterised phenotype may be ubiquitous to iPSC-CM

All of the data presented in chapter 3 from iPSC-CM up until Figure 3-23 was generated with cells purchased from Axiogenesis. This company was selected primarily on the basis of extensive work (mostly studying electrophysiological and structural parameters) in the lab of Prof Smith, which has determined this source to be the best available option in terms of reliability of phenotype and

representation of adult physiology. However, it is important to note that these cells are always produced from a single donor line and hence may be limited by the physiological status of the donor or affected by epigenetic factors which we cannot control. Replication of key assays performed with cells from an alternative commercial source returned broadly similar results arguing against this being of major concern. There were subtle differences in the data generated from Axiogenesis and CDI iPSC-CM, although the overall conclusions were the same. For example, basal glucose uptake was possibly slightly greater in CDI iPSC-CM, and was certainly more reliably detectable (Figure 3-23). Furthermore, the phosphorylation of Akt in response to insulin was far more pronounced in these cells, in part due to much lower basal phosphorylation (Figure 3-24). However, overall it was concluded that these cells are similarly metabolically immature, which was exemplified by the equally poor expression of GLUT4 protein (Figure 3-25). The decision was made to primarily keep working with Axiogenesis iPSC-CM on the basis that it is likely their limitations apply to iPSC-CM generally and also due to the more extensive characterisation of these cells, both within this project and the lab as a whole.

3.3.8 Methodological considerations

There were several limitations associated with the work described. First of all, primarily due to the expense of iPSC-CM and their inability to proliferate, the opportunity to perform extensive replicate experiments whilst still making significant overall progress is limited. The general approach taken to ensure a balance of reliability and confidence in generated data and forward progression was to perform independent experiments to address each identified question at least 3 times, with sufficient replicates (minimum of 3) within each experiment. This was adapted depending upon the noise of the relevant assay or clarity in the response recorded. Secondly, the decision to record the majority of results 6-8 days post-plating could in theory have led to recordings being made outside of an optimal window. However, based upon manufacturers recommendations and prior work in the lab it was found that iPSC-CM reach a stable reproducible global phenotype 48-72 hours post plating, and maintain this for 12-14 days thereafter (personal communication with Prof Smith). Therefore approximately 7 days post plating was identified as an ideal time point for experimental use. Finally, when measuring [^{3}H]-2DG uptake, recorded values could at best only be normalised

against plating density, rather than the number of cells present at the time of assay. It is possible, or perhaps even likely, that less than 100% of cells will survive one week in culture. This could generate misleading data, hence why unless explicitly required, data is present in raw CPM or as a percentage of control.

3.3.9 Conclusion and outline of further work required

In conclusion, a [^{3}H]-2-deoxyglucose uptake assay was adapted to a 96-well plate format and used to characterise the insulin sensitivity of iPSC-CM. Despite optimisation of experimental variables and inhibition of spontaneous contractile activity (and associated glucose uptake) no robust or reliable increase in glucose uptake was detected after insulin stimulation. Analysis of glucose transporter isoform expression indicates that this may primarily be due to iPSC-CM being metabolically immature. This conclusion is consistent with previously published data assessing the expression of a wide range of genes and proteins in this cell type that is suggestive of iPSC-CM displaying a general phenotype that corresponds to a foetal stage of cardiac development, as discussed in chapter 1.4.3. Consequently, in their current form these cells are not suitable to use as the basis for a novel cellular model of a complex metabolic condition such as DCM. Encouragingly, these cells do possess some of the core insulin sensitive machinery required to produce the desired response that is a key feature of adult cardiomyocyte physiology. Preliminary attempts to invoke maturation were unsuccessful, therefore this must be the primary focus of future work. Specifically, it is of importance to study the consequence of increasing GLUT4 expression in iPSC-CM, with regards to fundamental functional parameters and the underlying expression of relevant proteins.

4 Increasing GLUT4 protein expression in iPSC-CM

4.1 Introduction

Diabetes is a leading global healthcare challenge with pronounced direct pathological consequences for the heart. This project is concerned with evaluating the potential of iPSC-CM to act as a novel cellular model of DCM. As introduced in chapter 3 this has been attempted once previously, whereby Drawnel and colleagues (Drawnel *et al.*, 2014) detected structural and functional changes corresponding to cardiomyopathy after culturing cells in a 'pro-diabetic milieu'. However, their model made no reference to the detection of IR, which is a vital and requisite feature of any phenotype related to diabetes. This is a significant problem given that after initial characterisation and assessment of iPSC-CM physiology in this project (reported in chapter 3) it became clear that this cell type cannot produce an insulin stimulated glucose uptake response in the baseline condition, therefore at present they cannot be used to credibly model IR or by extension DCM.

4.1.1 GLUT4 is integral to insulin stimulated glucose uptake

As outlined in chapter 1, the increase in glucose uptake in (insulin sensitive) cells in response to insulin involves a highly complex network of interactions between dozens of proteins. Accordingly, manipulation of proximal insulin signalling has a knock on effect upon insulin stimulated glucose uptake. For example, preventing the inhibitory effect of the inositol pyrophosphate IP7 on Akt in a mouse model resulted in *in vivo* insulin hypersensitivity, improved glycemic control, and most importantly reduced weight gain and prevention of the onset of IR seen in control mice in response to a HFD (Chakraborty *et al.*, 2010). More directly, and in compliment of this work, disruption of the Akt gene in mice resulted in systemic IR (Cho *et al.*, 2001). Similarly, mutations of the insulin receptor and IRS genes in mice have been shown to result in severe IR in peripheral tissues and pancreatic beta cell hypertrophy, both key features of the diabetic phenotype (Tamemoto *et al.*, 1994; Kido *et al.*, 2000).

However, at the most fundamental level, the theory underlying insulin stimulated glucose uptake is that the glucose transporter GLUT4 is trafficked from an intracellular retention site to the cell surface. Based upon this it would therefore be predicted that the degree of expression of GLUT4 also has a critical influence

upon the effectiveness of this response, and indeed a range of insight from the literature supports this concept. For example, GLUT4 expression was found to be reduced in the adipose tissue of human type 2 diabetic patients, relative to controls (Hussey *et al.*, 2011). This association between GLUT4 expression and insulin sensitivity was strengthened by the observation that 4 weeks exercise training significantly increased GLUT4 protein expression, and coincided with improvements in a range of clinically relevant metabolic parameters (Hussey *et al.*, 2011). In further support of this work, both generic, muscle specific, and adipose specific downregulation of the GLUT4 gene in mice has been reported to induce systemic metabolic alterations consistent with diabetes, including hyperglycemia, hyperinsulinemia, and IR (Stenbit *et al.*, 1997; Minokoshi, *et al.*, 2003). Interestingly, in a heterozygous muscle specific GLUT4 knockout model proximal insulin signalling (IRS-1, Akt) was found to be significantly impaired (Kim *et al.*, 2005), suggesting that it is challenging to completely separate the roles of insulin signalling and GLUT4 expression when studying an integrated physiological action such as insulin stimulated glucose uptake. To add a further degree of complexity, adipose or muscle specific GLUT4 knockout mouse models resulted in IR in both tissues, suggesting that there is a degree of cross communication (Minokoshi, *et al.*, 2003)

Overall, based upon the current literature it can be concluded that both fully functional signalling networks and appropriate GLUT4 protein content are required to elicit insulin stimulated glucose uptake into the cells of target tissues. When this response is impaired in diabetic individuals both of these factors are certainly implicated although there is conflicting evidence with regards to their relative importance in different tissues (Garvey *et al.*, 1992; Kampmann *et al.*, 2011), perhaps related to at what stage of progression the diabetic phenotype is at time of measurement and the relative roles of the wide variety of possible pathological stimuli. Similarly, the specific molecular mechanisms impairing the complex insulin signalling networks may be specific to certain experimental models/the original pro-diabetic stimulus (Boucher, *et al.*, 2014).

In the context of the lack of response recorded from iPSC-CM, preliminary evidence presented in chapter 3 indicated that low levels of GLUT4 protein expression could be the primary issue. To strengthen this conclusion and provide

a more accurate description of the iPSC-CM metabolic phenotype, quantification of the difference in glucose transporter isoform expression between iPSC-CM and mature primary cardiomyocytes would be highly informative. Additionally, this would also enable identification of the specific modifications required to mature iPSC-CM into an adult-like phenotype. For example, it is possible that a 2-fold increase in iPSC-CM GLUT4 expression would represent a significant increase, but still fall well short of the expression recorded in primary cardiomyocytes.

Initial insight reported in chapter 3 also identified that GLUT1 protein expression is readily detectable in iPSC-CM and therefore appears different from measurements of primary adult cardiomyocytes. Consequently, it could be argued that addressing the imbalance in expression of GLUT1 between iPSC-CM and the cells they are meant to model could be of equal importance to intervening with regards to GLUT4. However, as just outlined, GLUT4 is essential in eliciting insulin stimulated glucose uptake, whereas GLUT1 is not. Similarly, GLUT4 expression can strongly influence cardiac contractility (Belke *et al.*, 2000). DCM is primarily defined by IR and impaired contractility of the heart, therefore it is logical and appropriate to first of all target GLUT4 in iPSC-CM.

4.1.2 Regulation of GLUT4 expression

In order to design appropriate and effective interventions to increase GLUT4 expression, the normal physiological regulation of this transporter must be elucidated. There are a range of transcription factors and stimuli that have been cited as having a possible role in the transcriptional regulation of GLUT4 (Zorzano, *et al.*, 2005). However, evidence indicates that there may be 3 key binding sites within the promoter region that have a critical influence over GLUT4 expression in muscle. Specifically, manipulation of the expression of the transcription factors MyoD, MEF2, and the thyroid hormone receptor (TRα1) and their target binding sites was shown to powerfully impact the activation of the GLUT4 gene in several myocyte cell culture models (Santalucía *et al.*, 2001).

This data is supported by a range of evidence that is more translatable and/or activates signalling networks further up the respective pathways, in order to identify multiple molecular targets. For example with regards to the role of MEF2, GLUT4 gene expression significantly increased in L6 and C2C12 myoblasts upon

overexpression of the coactivator PGC-1, which was found to be dependent upon the integrity of the MEF2 sequence in the GLUT4 promoter region (Michael *et al.*, 2001). In a separate cell culture model, exposure of isolated adult rat cardiomyocytes to IGF-1 resulted in the restoration of GLUT4 gene and protein expression, which spontaneously decreases in culture (Montessuit *et al.*, 2004). This effect was found to be mediated through the activation of p38 MAPK, and ultimately MEF2. Finally, an *in vivo* mouse model identified that changes in MEF2 protein expression and associated binding of the MEF2 DNA sequence was strongly linked to both an experimental diabetes induced reduction - and then subsequent insulin treatment induced increase - in skeletal and cardiac muscle GLUT4 gene expression (Thai *et al.*, 1998).

Similarly, there is a body of *in vivo* evidence that the thyroid hormone T_3 has a powerful role in GLUT4 expression. It is a key and characteristic feature of foetal to early post-natal development that the relatively high/low cardiac expression of GLUT1 and GLUT4 are reversed. The experimental induction of early hypothyroidism prevented this switch in rats, yet had no impact on GLUT4 protein expression when animals were fully mature (Castelló *et al.*, 1994). Furthermore, injection of T_3 at various stages of early development rapidly induced strong overexpression of GLUT4 mRNA and subsequently protein, with a corresponding repressive effect upon GLUT1, although this was less striking (Castelló *et al.*, 1994). As alluded to, this suggests direct transcriptional regulation of cardiac GLUT isoform expression by T_3. Similarly, short term (3 days) injection of high doses of T_3 have been found to enhance skeletal (fast and slow twitch) muscle GLUT4 protein content, which was associated with improved insulin stimulated glucose uptake in healthy rats, and significantly reduced circulating insulin levels in the obese zucker rat model of diabetes (Weinstein *et al.*, 1994; Torrance *et al.*, 1997).

Finally, perhaps the best known stimulus for increasing myocyte GLUT4 expression (and general metabolic health) is exercise. For example, a single swimming endurance training session was enough to significantly increase GLUT4 protein expression in the skeletal muscle of rats, and repetition of this workout the following day raised expression further to double baseline values (Rens *et al.*, 1994). Similarly, in humans a single acute exercise bout was enough to induce a

rapid (3 hours) and robust (100%) increase in GLUT4 mRNA and protein, regardless of exercise intensity (40 vs 80% VO_2 peak) (Kraniou *et al.*, 2006). Furthermore, a week long exercise training regime enhanced skeletal muscle GLUT4 expression and whole body insulin stimulated glucose disposal in type 2 diabetic patients (O'Gorman *et al.*, 2006). This link between muscular contractile activity and GLUT4 protein expression is strengthened further by denervation based studies. For example, 3 days post sciatotomy, GLUT1/4 expression was approximately doubled/halved respectively, in the extensor digitorum longus and soleus from Sprague-dawley rats (Coderre *et al.*, 1992).

The mechanism by which exercise exerts this effect is likely also partly through activation of MEF2. For example, 60 min cycling at a moderate intensity was found to increase MEF2 DNA binding 2-fold in the vastus lateralis of human subjects (McGee *et al.*, 2006). Using the same protocol, a separate study identified that increased association of MEF2 with PGC-1 and (phosphorylated) p38 MAPK coupled with reduced association and nuclear localisation of an inhibitory histone deacetylase was primarily attributable to enhanced MEF2 activity post-exercise (McGee and Hargreaves, 2004). The upstream signalling pathways require further examination, but AMPK was suggested to have an important role. Additionally, a wheel running exercise programme in mice was found to restore skeletal muscle GLUT4 protein content that had been originally decreased in association with the onset of obesity (Gurley *et al.*, 2016). However, this occurred independently of any change in GLUT4 mRNA, suggesting that exercise may also act via post-transcriptional mechanisms to regulate GLUT4 protein expression. One possible factor could be micro-RNAs, which are known to regulate the translation of mRNA, and have been receiving attention in the context of diabetes research recently (Esteves *et al.*, 2017).

4.1.3 Previously attempted strategies to mature iPSC-CM

The observation that iPSC-CM express low levels of GLUT4 and high levels of GLUT1 is clear evidence that they significantly differ from adult cardiomyocytes and could even be viewed as foetal-like. However this is not the only example of divergence between iPSC-CM and adult cardiomyocyte phenotypes. Most notably, the variable size and shape of iPSC-CM with poorly defined and disorganised sarcomeres and an unstable electrophysiological phenotype that leads to

spontaneous contraction contrasts starkly with the large rectangular appearance of isolated adult cardiomyocytes that have clear striations and t-tubules and only contract rhythmically upon external stimulation. These features, combined with a poorly developed calcium handling system, mean that the contractility of iPSC-CM is significantly less powerful compared to mature primary cardiomyocytes (Kolanowski *et al.*, 2017). On account of these differences and more, several previous attempts have been made to mature iPSC-CM, which may guide the approach implemented in the present project.

The first approach centres upon the metabolic environment that cells are cultured in. Typically, iPSC-CM are maintained in an unphysiologically high glucose concentration (4.5 g/L or 25 mM) despite the fact that cardiomyocytes depend primarily upon the oxidation of fatty acids *in vivo*. This may contribute to the observation that iPSC-CM rely primarily upon glycolytic metabolism, rather than the more powerful oxidative metabolism of primary cardiomyocytes (Rana *et al.*, 2012). In consideration of this, culturing iPSC-CM in medium containing fatty acids and insulin but no glucose for 3 days resulted in changes associated with maturation such as elongation of sarcomeres and enhanced action potential upstroke and duration, compared with cells maintained in manufacturers maintenance medium (Drawnel *et al.*, 2014). Similarly, in a separate study 20 days in medium containing no glucose and supplemented with fatty acid resulted in reduced iPSC-CM lactate production and increased oxygen consumption, indicative of a shift from glycolytic to oxidative metabolism, underlined by an increase in mitochondrial content (Correia *et al.*, 2017). As before this coincided with the onset of a host of adaptations that were interpreted as markers of maturation, including enhanced myofilament alignment, a decrease in expression of foetal genes, and improved excitation contraction coupling. Interestingly, some degree of lipotoxicity was observed, and was reduced by including galactose in the medium.

As introduced earlier the thyroid hormone T_3 may also have an important role in cardiac maturation *in vivo*, and is a strong regulator of metabolism. Accordingly, a week long supplementation of iPSC-CM with T_3 invoked structural and contractility changes consistent with maturation (Yang *et al.*, 2014). This was accompanied by improved calcium handling and enhanced mitochondrial activity

(but not content). Together the work discussed thus far suggests that the hormonal and metabolic environment of iPSC-CM has a very powerful influence over the maturation status of the cells, and that manipulation of one factor can induce significant widespread changes across several aspects of the iPSC-CM phenotype. Either the initial stimuli have several targets, or the identified metabolic effects act as a powerful stimulus/mechanism for maturation. An intervention utilising glucose depleted medium supplemented with both T_3 and fatty acids unsurprisingly resulted in a range of electrophysiological, structural, and genetic adaptations indicative of maturity (Lin *et al.*, 2017). However, no relevant baseline data for mature cardiomyocytes was provided to assess how much more maturation was still required.

In addition to the metabolic and hormonal environment, the spatial organisation and mechanical loading of the heart are important stimuli in promoting cardiac maturation *in vivo* (Yang, *et al.*, 2014). In response to this, a range of research has demonstrated the pro-maturation effect of culturing iPSC-CM in a way that better represents the *in vivo* environment than simple culture on a 2D plastic culture surface. Specifically, in isolation and/or in combination, culturing iPSC-CM with substrates designed to mimic the extracellular matrix, in a 3D format, co-culture with other relevant cell types (e.g. endothelial cells), and mechanical loading, have all been reported to enhance the iPSC-CM phenotype towards that of adult cardiomyocytes with regards to a range of physiological parameters (Tulloch *et al.*, 2011; Chun *et al.*, 2015; Fong *et al.*, 2016).

Finally, perhaps the most logical and simple stimulus that has been shown to enhance iPSC-CM physiology is time. Normal manufacturer's recommendations for use of commercially derived iPSC-CM are typically to perform assays up until 2 weeks post plating, however research has indicated that longer term culture of cells up to and above 6 months duration can promote maturation (Kamakura *et al.*, 2013; Guo *et al.*, 2017). This is an important finding that could help to combat the criticism of iPSC-CM (and all cultured cells) with regards to disease modelling, whereby attempts to replicate complex diseases that develop over years *in vivo* are made over the course of only a week or two in culture.

4.1.4 Aims of chapter

Low levels of GLUT4 protein expression appear to underly the lack of insulin-stimulated glucose uptake response in iPSC-CM. The critical transcriptional elements regulating GLUT4 protein expression in muscle have been identified, and might further be supported *in vivo* by post-transcriptional mechanisms such as the action of microRNAs or altered rate of degradation of GLUT4 protein. Several interventions have been implemented previously that induced metabolic adaptations and more general maturation in iPSC-CM, although the effect on GLUT4 expression was never assessed. So far, the most promising interventions that directly target metabolic pathways are T_3 and MM conditioning. Exercise training is also a potent stimulus for adaptation, however this is highly challenging to mimic in culture conditions with isolated cells. Similarly, bioengineering approaches hold promise for maturation of iPSC-CM, but are out with the scope of this project.

Therefore, the overall aim of this chapter is to identify a protocol (or protocols) that can facilitate an increase in expression of GLUT4 in iPSC-CM to the levels recorded in mature cardiomyocytes, with an ultimate view to assessing the subsequent impact on key physiological outcomes. More specifically, the following aims shall be addressed;

- Quantification of GLUT1/4 expression and functional importance in iPSC-CM and mature insulin sensitive cells

- Assessment of the impact of maturation medium upon GLUT1 and GLUT4 expression in iPSC-CM

- Assessment of the impact of T_3 upon GLUT4 expression in iPSC-CM

- Development of a Lipofectamine 2000 mediated transfection protocol to increase GLUT4 expression in iPSC-CM and subsequent assessment of impact on cellular glucose uptake

- Initial development of lentivirus mediated infection protocol to increase GLUT4 expression in iPSC-CM

4.2 Results

4.2.1 Expression and function of GLUT1 and GLUT4 in iPSC-CM

A key limitation of previous work reporting the effect of various interventions in maturing iPSC-CM is that too often the magnitude of adaptations that are desired are not explicitly stated. For example, significant increases in APD duration or mitochondrial content are reported, but the corresponding reference values of adult cardiomyocytes are not. Therefore, prior to attempting to increase GLUT4 expression in iPSC-CM, the relative and absolute difference in protein expression and functional relevance of GLUT1 and GLUT4 between iPSC-CM and mature cardiomyocytes was assessed.

In order to attempt quantification of transporter expression, a reference point of a known amount of GLUT1/4 protein was needed. In fully differentiated 3T3-L1 adipocytes it has previously been published that there are approximately 215 ng of GLUT1 protein and 45 ng of GLUT4 protein per 1.5 mg of total protein (Calderhead *et al.*, 1990). This corresponds to an estimated 950,000/280,000 copies of each transporter per cell, however due to variations in size across different cell types this number is less useful in this context. Therefore, the protein expression of GLUT1 and GLUT4 was assessed in iPSC-CM and primary mouse cardiomyocytes relative to 3T3-L1 adipocytes, where a similar amount of total protein was loaded as adjudged by GAPDH expression.

Figure 4-1A and 4-1B provide a clear visual depiction of the stark difference in GLUT1 expression between iPSC-CM and adult primary cardiomyocytes when assessed against a similar total amount of protein from 3T3-L1 adipocyte lysate. The expression of GLUT1 in iPSC-CM is abundant and easy to detect, in contrast to the faint (yet still detectable) expression in the primary cardiomyocyte lysates. Visually the difference between GLUT4 expression in the 2 sources of cardiomyocytes appears equally striking, but in an opposite manner to GLUT1 (Figure 4-2A and 4-2B). In all blots a range of 3T3-L1 lysates were also loaded to provide confidence in this reference signal.

In order to quantify the relative difference in transporter expression between sources of cardiomyocytes densitometry was performed and the signal from technical replicates (different loading volumes) for each lysate on each blot was normalised to GAPDH and then averaged. Then the average fold difference in expression for the relevant transporter in either iPSC-CM or primary mouse cardiomyocytes relative to 3T3-L1 adipocytes was calculated across the 3 biological replicates shown on each immunoblot. This experiment was performed in replicate for each transporter, for each cell type. Quantification depicting the relative difference in expression of GLUT1 and GLUT4 is shown in Figures 4-1C and 4-2C, and key outputs shown in Table 4-1. Because expression was conveyed relative to 3T3-L1 adipocytes, the data for iPSC-CM and primary cardiomyocytes is shown on the same graph for each transporter, despite being obtained from different blots. This analysis revealed that iPSC-CM express approximately 30-fold more GLUT1 than primary adult cardiomyocytes, and approximately 10-fold less GLUT4. The values obtained between replicate immunoblots was fairly consistent in all cases, which provides confidence in this technique.

iPSC-CM obtained from CDI were also probed for GLUT1 and GLUT4 expression relative to 3T3-L1 adipocytes in order to provide information from a second commercial source. However, whilst the same general concept was observed (high GLUT1/ low GLUT4), the poor GAPDH signal obtained from these cells was not representative of total protein loaded and therefore no quantification was performed (data not shown). Additionally, a segment of human myocardium was kindly donated by Dr. Cherry Alexander. Similar to CDI iPSC-CM, the GAPDH signal obtained from lysate of this sample did not suitably represent the total protein loaded (Appendix 7.1), however what can be observed is that in primary cardiomyocytes from a human origin there is an abundance of GLUT4 protein (Figure 4-3).

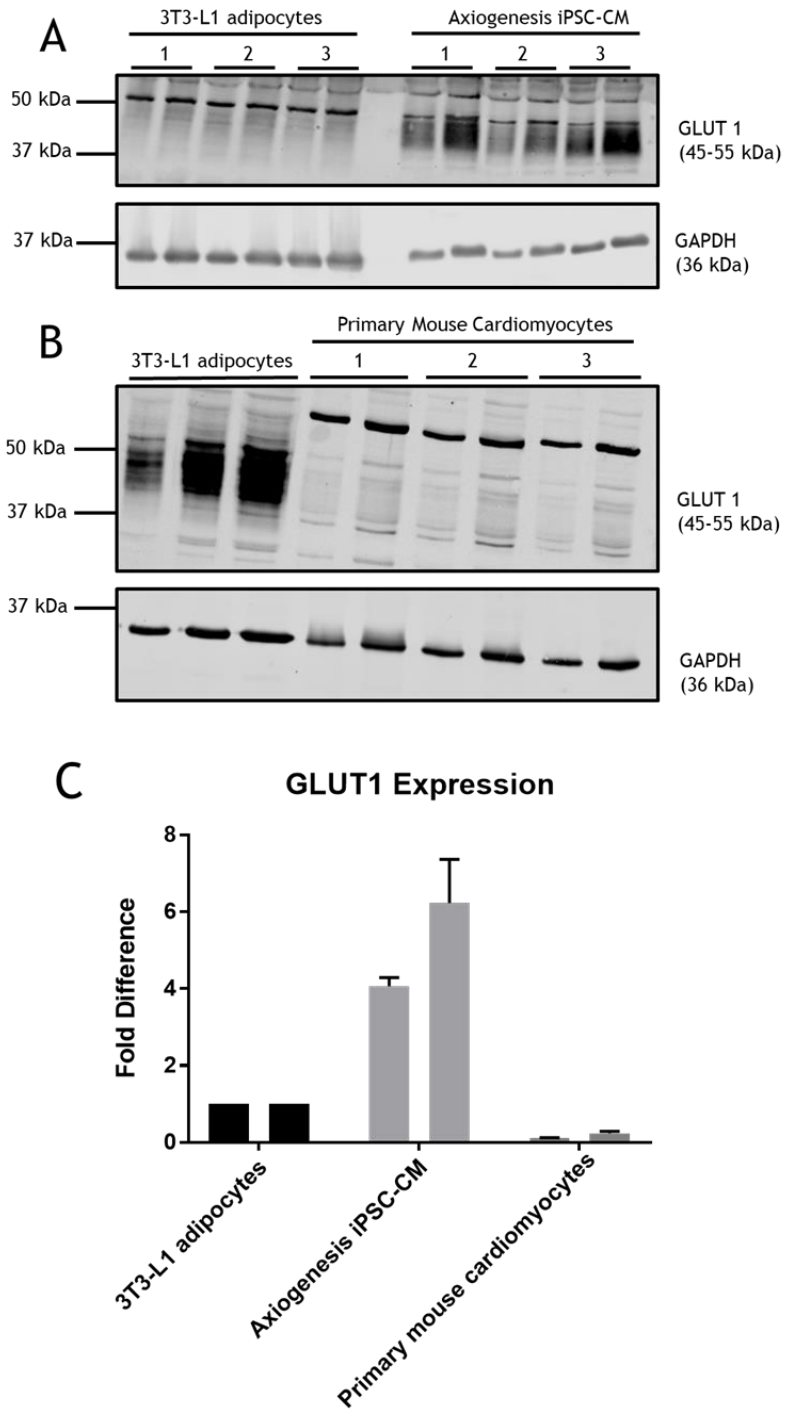

Figure 4-1 GLUT1 expression in iPSC-CM and primary mouse cardiomyocytes
Protein lysates generated from 3T3-L1 adipocytes, iPSC-CM, and primary mouse cardiomyocytes were subjected to SDS-PAGE and immunoblotting probing for the expression of GLUT1 and GAPDH (loading control). 3T3-L1 adipocytes acted as a reference signal, with either 2 different amounts of 3 technical replicate samples (A) or 3 different amounts of 1 sample (B) loaded. For both cardiomyocyte lysates 2 different amounts of 3 biologically independent samples were loaded. Quantification of relative GLUT1 expression is shown in panel C, expressed as the mean (+S.D.) fold difference between cardiomyocyte samples (n=3) and 3T3-L1 adipocytes (n=1). Each bar represents data from 1 immunoblot, and each immunoblot was performed in replicate.

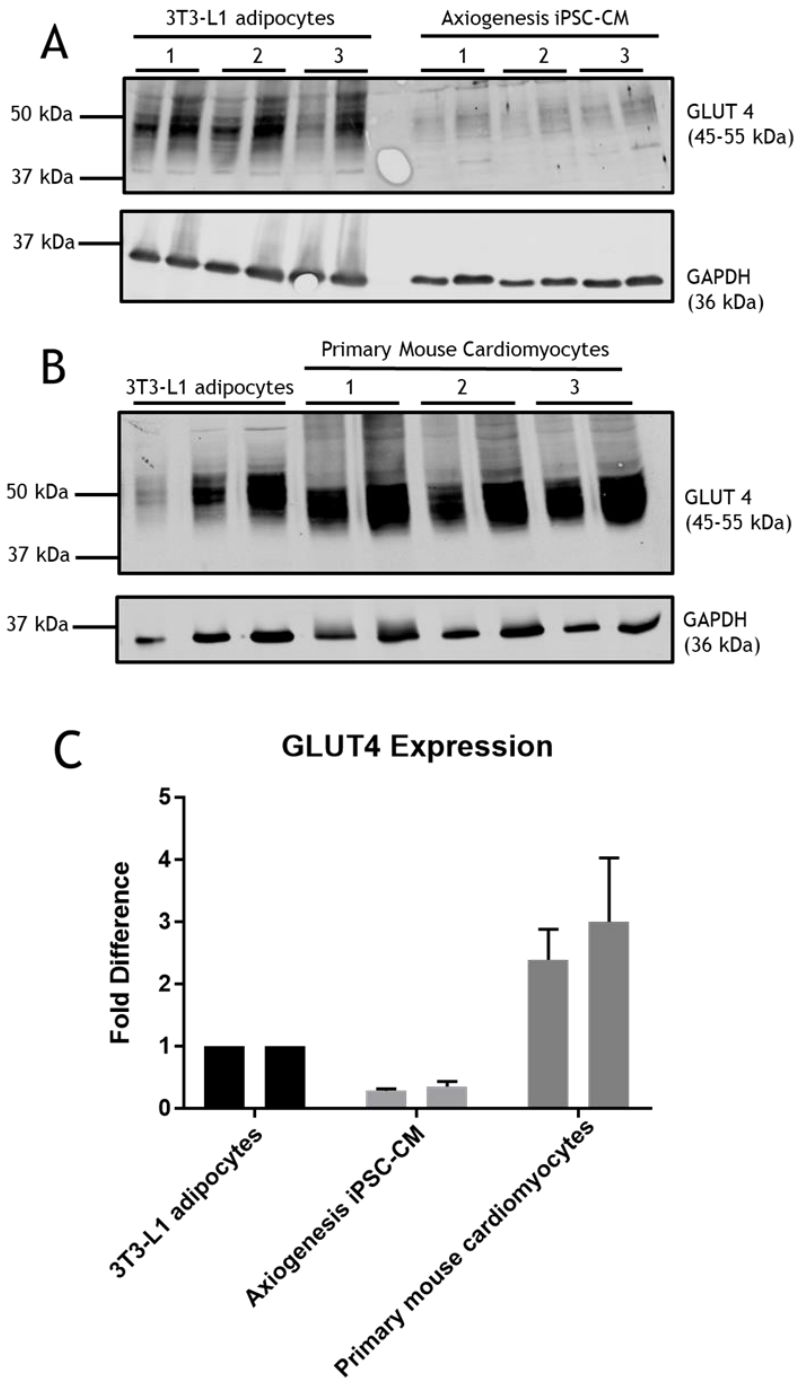

Figure 4-2 GLUT4 expression in iPSC-CM and primary mouse cardiomyocytes
Protein lysates generated from 3T3-L1 adipocytes, iPSC-CM, and primary mouse cardiomyocytes were subjected to SDS-PAGE and immunoblotting probing for the expression of GLUT4 and GAPDH (loading control). 3T3-L1 adipocytes acted as a reference signal, with either 2 different amounts of 3 technical replicate samples (A) or 3 different amounts of 1 sample (B) loaded. For both cardiomyocyte lysates 2 different amounts of 3 biologically independent samples were loaded. Quantification of relative GLUT4 expression is shown in panel C, expressed as the mean (+S.D.) fold difference between cardiomyocyte samples (n=3) and 3T3-L1 adipocytes (n=1). Each bar represents data from 1 immunoblot, and each immunoblot was performed in replicate.

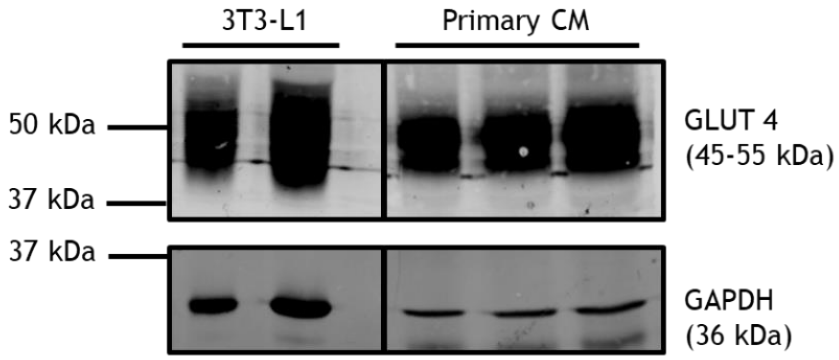

Figure 4-3 GLUT4 expression in primary human myocardial lysate
Protein lysates were generated from a human myocardial segment and subjected to SDS-PAGE and immunoblotting, probing for the expression of GLUT4 and GAPDH. 3T3-L1 adipocyte lysates were also probed to act as a reference and positive control. Several amounts of lysate were loaded for each sample (2.5-5 µL 3T3-L1 lysate; 5-10 µL primary human cardiac lysate). The immunoblots have been cropped for presentation purposes but no raw data has been altered.

Cell Type	*Ave. Fold Difference GLUT1*	*Estimated Amount GLUT1 (ng/1.5 mg total protein)*	*Ave. Fold Difference GLUT4*	*Estimated Amount GLUT4 (ng/1.5 mg total protein)*
3T3-L1 Adipocytes	1	215	1	45
iPSC-CM	5.1 fold higher	1106	3.1 fold lower	14.6
Primary Mouse CM	5.7 fold lower	37.5	2.7 fold higher	121.4

Table 4-1 Quantification of estimated absolute and relative fold difference in GLUT1 and GLUT4 between iPSC-CM, primary mouse cardiomyocytes, and 3T3-L1 adipocytes

Initial findings provided a clear insight and quantification of the difference in expression of GLUT1 and GLUT4, between iPSC-CM and the mature cardiomyocytes they are designed to represent. However, simply determining the level of expression of each transporter in the 2 cell types is not necessarily completely explanatory with regards to their functional relevance. From the literature, it has been extensively demonstrated that GLUT4 is the predominant transporter in mature cardiomyocytes, and that GLUT1 has a limited functional role. However, the activity of different transporters can vary based on a number of factors, including cellular localisation and substrate specificity. Therefore in order to gain further insight into iPSC-CM physiology, basal and insulin stimulated glucose

uptake was measured in the presence of GLUT1 inhibition and also a combination of GLUT1 and GLUT4 inhibition. The same measurements were also recorded from 3T3-L1 adipocytes - a mature highly insulin sensitive (GLUT4 dependent) culture line – for comparison.

In order to investigate the stated aim, the novel drug [N4-[1-(4-cyanobenzyl)-5-methyl-3-(trifluoromethyl)-1H-pyrazol-4-yl]-7-fluoroquinoline-2,4-dicarboxamide] (BAY-876) was used. This has been characterised to inhibit different hexose transporters at different concentrations. Specifically, its IC_{50} for GLUT1 is 2 nM, and IC_{50} for GLUT4 is 290 nM (Siebeneicher *et al.*, 2016). Therefore, concentrations of 20 nM and 2 μM were selected for use in this set of experiments.

As depicted in Figure 4-4, the response of 3T3-L1 adipocytes to the different concentrations of BAY-876 are consistent with what would be predicted from mature insulin sensitive cells. Key statistical outcomes are listed in detail in Appendix 7.2. More briefly, across 3 independent experiments, a robust and reproducible statistically significant ($P<0.0001$) insulin response was observed (Figure 4A). When GLUT1 only was inhibited by 20 nM BAY-876 both basal and insulin stimulated glucose uptake values decreased significantly ($P<0.01$) by approximately 25% (Figure 4-4B). However when both GLUT1 and GLUT4 were inhibited by 2 μM BAY-876, both basal and insulin stimulated uptake were highly significantly reduced further ($P<0.0001$) to almost no detectable signal (Figure 4-4B). Most importantly, the cells failed to respond to insulin only when GLUT4 was inhibited (Appendix 7.2). This suggests that GLUT4 is the predominant transporter in these cells. The stock of BAY-876 was originally prepared in DMSO and then serial dilutions were prepared prior to the assay. Therefore to ensure that the results obtained were not a product of different DMSO concentrations, basal and insulin stimulated glucose uptake was recorded in cells incubated with or without DMSO, at a final concentration equal to that of cells exposed to 2 μM BAY-876 i.e. the highest concentration used. As can be seen in Figure 4-4C, statistical analysis revealed that whilst there was a highly significant effect of insulin upon glucose transport ($P<0.0001$), there was no significant difference between basal or insulin stimulated [^{3}H]-2DG uptake in the presence and absence of DMSO ($P>0.05$).

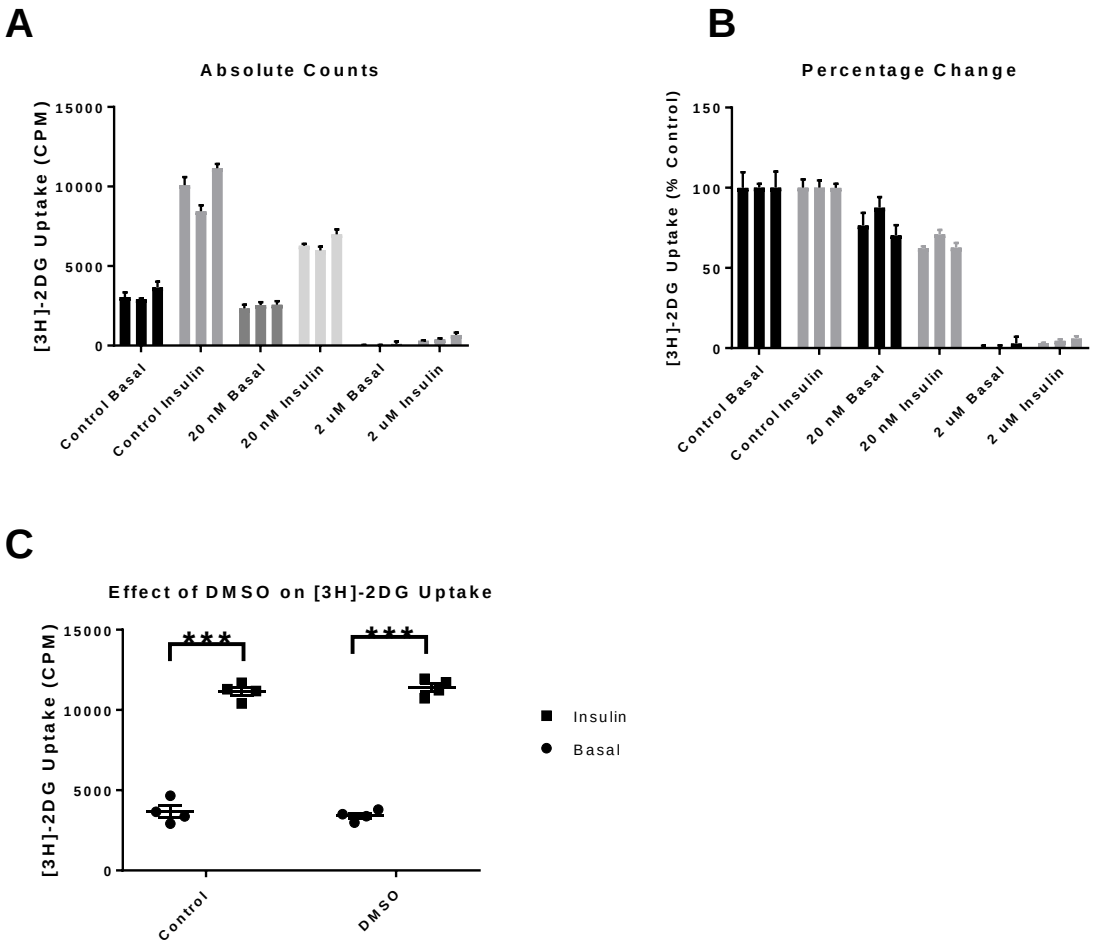

Figure 4-4 The effect of GLUT1 and GLUT4 inhibition on [^{3}H]-2DG uptake in 3T3-L1 adipocytes
A: Background corrected basal and insulin stimulated glucose uptake in CPM was assayed in fully differentiated 3T3-L1 adipocytes. Cells were serum starved (serum free DMEM) for 4 hours prior to 20 min stimulation with 860 nM insulin +/- 20 nM or 2 μM BAY-876. Cells were incubated with [^{3}H]-2DG for 10 min. Each bar represents the mean (+S.E.M.) of 4 replicate samples from one experimental day, with 3 independent experiments performed in total. Statistical analysis was performed with a 2-way ANOVA where the identified factors were drug treatment and experimental day. The level of significance was set at P=0.05. B: The same data from panel A is presented, but this time depicted relative to the average of control basal or control insulin, as appropriate. C: Background corrected basal and insulin stimulated glucose uptake in CPM was assayed in fully differentiated 3T3-L1 adipocytes. Cells were serum starved (serum free DMEM) for 4 hours prior to 20 min stimulation with 860 nM insulin +/- 0.02% DMSO. Cells were incubated with [^{3}H]-2DG for 10 min. Data shown is 4 replicate samples for each condition and mean +/- S.E.M. Statistical analysis was performed with a 2-way ANOVA where the identified factors were DMSO treatment and insulin stimulation. The level of significance was set at P=0.05. * indicates P<0.0001.**

As depicted in Figure 4-5, the response of iPSC-CM to BAY-876 was notably different. As has been well established, and is exemplified in Figure 4-5B, iPSC-CM do not robustly or reproducibly respond to insulin with regards to [^{3}H]-2DG uptake. Therefore the effect of 20 nM and 2 μM BAY-876 on basal [^{3}H]-2DG uptake only is shown across 3 independent experiments (Figure 4-5A). Statistical analysis

revealed that 20 nM BAY-876 significantly (P<0.0001) reduced uptake compared to control, however increasing the concentration to 2 μM had no additional effect (P>0.05). There was a significant (P<0.0001) interaction effect between experimental day and BAY-876 incubation, suggesting that the extent of the inhibition of each drug concentration was prone to variation. As before, the drug was prepared in DMSO, which has the potential to influence cellular physiology. However, in an independent experiment neither insulin nor DMSO (0.02% final concentration) significantly (P>0.05) altered [^{3}H]-2DG uptake in iPSC-CM (Figure 4-5B).

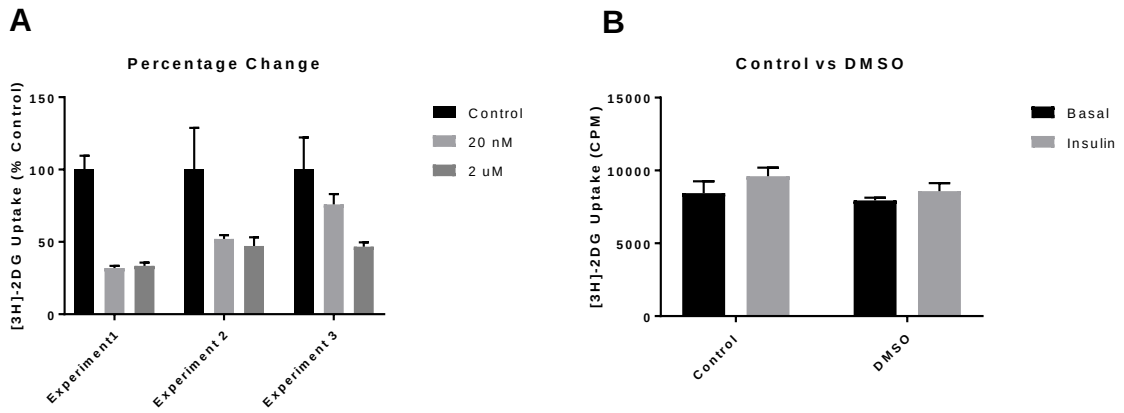

Figure 4-5 The effect of GLUT1 and GLUT4 inhibition on [^{3}H]-2DG uptake in iPSC-CM
A: Background corrected basal [^{3}H]-2DG uptake in CPM was assayed in iPSC-CM incubated with 0 / 20 nM / 2 μM BAY-876 for 20 min prior to incubation with the [^{3}H]-2DG for 15 min. Each bar represents the mean (+S.E.M) of 3 replicate samples expressed as a percentage of control data (0 nM BAY-876) from one experimental day, with 3 independent experiments performed in total. Statistical analysis was performed on raw data with a 2-way ANOVA where the identified factors were drug treatment and experimental day. The level of significance was set at P=0.05. B: Background corrected basal and insulin stimulated [^{3}H]-2DG uptake was assayed in iPSC-CM. Cells were incubated with 0 or 860 nM insulin +/- 0.02% DMSO for 20 min prior to incubation with [^{3}H]-2DG for 15 min. Data shown is mean of 3 replicate samples (+S.E.M.) for each condition. Statistical analysis was performed with a 2-way ANOVA where the identified factors were DMSO treatment and insulin stimulation. The level of significance was set at P=0.05.

4.2.2 The effect of maturation medium upon GLUT1 and GLUT4 protein expression in iPSC-CM

After initial characterisation of the role of GLUT1 and GLUT4 in iPSC-CM, interventions were designed in an attempt to mature the cells. The first approach was based upon the MM conditioning approach that was originally devised by Drawnel *et al.*, (2014) and was explained in section 4.1.4. The fundamental

principle is that forcing iPSC-CM to rely upon the same metabolic fuel (fatty acids) that primary cardiomyocytes utilise *in vivo* could stimulate maturation. Initial attempts to enhance insulin stimulated glucose uptake using this protocol (as reported in chapter 3) were unsuccessful and indicated that it was toxic to the cells. Therefore a range of 8 MM conditions were implemented, as outlined in Table 4-2. The overarching principle remained the same, however in addition to fatty acids cells were cultured in medium containing a combination of a range of insulin concentrations and either 0 or 1 g/L glucose. 1 g/L glucose is equivalent to approximately 5.5 mM, which is within the healthy circulating range for humans. However, for most cultured cells glucose concentration in medium is usually 4.5 g/L, so in this context it is considered 'low' glucose. Note that condition 1 (MM1) is an exact replication of the originally suggested formula. Cells were cultured in their respective conditions for either 4 or 11 days. Interventions were not initiated prior to 48-72 hours after collection from liquid nitrogen storage in order to allow sufficient recovery time, therefore cell lysates were generated 1 or 2 weeks post-plating, as indicated.

Condition	**Glucose Concentration**	**Serum content**	**Insulin concentration**	**Additional components**
MM1	0 mM	1x ITS supplement	860 nM	10 mM HEPES, 2 mM Carnitine, 5 mM Creatine, 5 mM Taurine, 1x NEAA, 1x linoleic-oleic acid
MM2	5.5 mM	1x ITS supplement	860 nM	Same as MM1
MM3	0 mM	10% (v/v) FBS	172 nM	Same as MM1
MM4	5.5 mM	10% (v/v) FBS	172 nM	Same as MM1
MM5	0 mM	10% (v/v) FBS	17.2 nM	Same as MM1
MM6	5.5 mM	10% (v/v) FBS	17.2 nM	Same as MM1
MM7	0 mM	10% (v/v) FBS	0 nM	Same as MM1
MM8	5.5 mM	10% (v/v) FBS	0 nM	Same as MM1

Table 4-2 Details of maturation medium conditions

As depicted in Figure 4-6A, the response of iPSC-CM to the different MM conditions over 4 days was varied. Quantification across 3 independent experiments revealed that there was a statistically significant near 2-fold increase ($P<0.05$) in GLUT4 expression (normalised to GAPDH) relative to control in response to MM conditions 3 and 5, and in general there was a larger response to conditions where no glucose was present (conditions with odd numbers). After 11 days of MM conditioning (14 days post-plating) there was a notable loss of cells in multiple conditions, as reflected by differences in GAPDH expression - which was used to indicate total protein - despite an equal total loading volume across conditions (Figure 4-6C). At this time point it again appeared as though in general conditions with no glucose resulted in greater GLUT4 expression than those with low glucose, however no fold difference was found to be statistically significant compared to control for any condition ($P>0.05$).

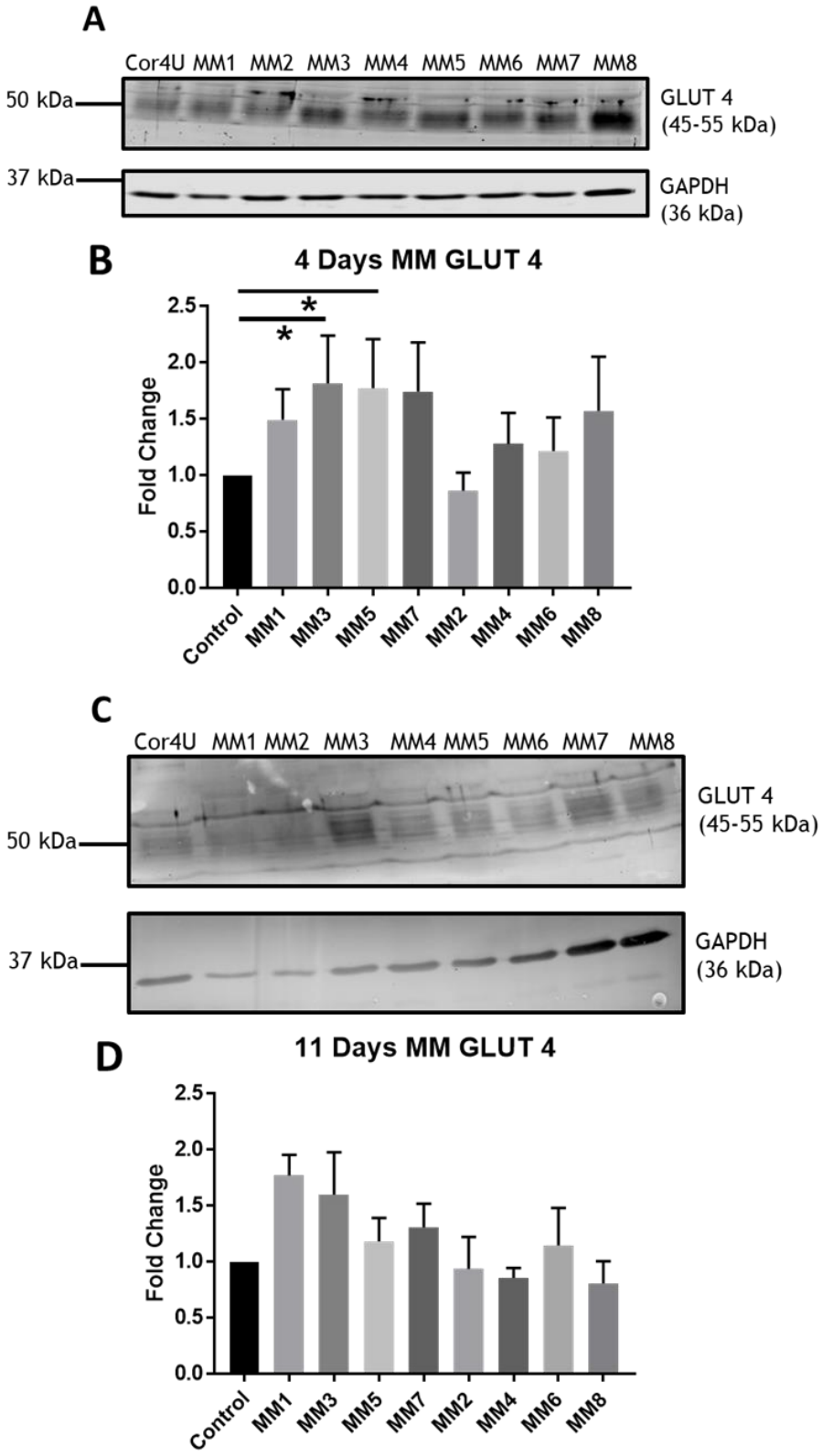

Figure 4-6 The effect of maturation medium conditioning upon iPSC-CM GLUT4 expression
Representative immunoblots depicting GLUT4 and GAPDH expression in iPSC-CM maintained for 4 (6A) or 11 (6C) days in a range of 'maturation medium' conditions. Densitometry was performed and quantification is shown as mean fold difference in GLUT4 expression normalised to GAPDH (+S.E.M) relative to control cells, across 3 independent experiments for each time point (6B and 6D). Statistical analysis was performed with a 2-way ANOVA, where the identified factors were experimental day and maturation medium conditioning. The level of significance was set at P=0.05. * denotes P<0.05.

In contrast to GLUT4, GLUT1 expression responded very clearly to MM conditioning regardless of whether cells were incubated for 4 or 11 days (Figure 4-7A and 4-7C). Across 3 independent experiments statistical analysis confirmed that conditions 3 and 5 significantly ($P<0.05$) increased GLUT1 expression above control cells at both time points, whereas condition 7 significantly ($P<0.05$) increased expression after 4 days only. No condition containing 1 g/L glucose significantly ($P>0.05$) increased expression above control levels at any point.

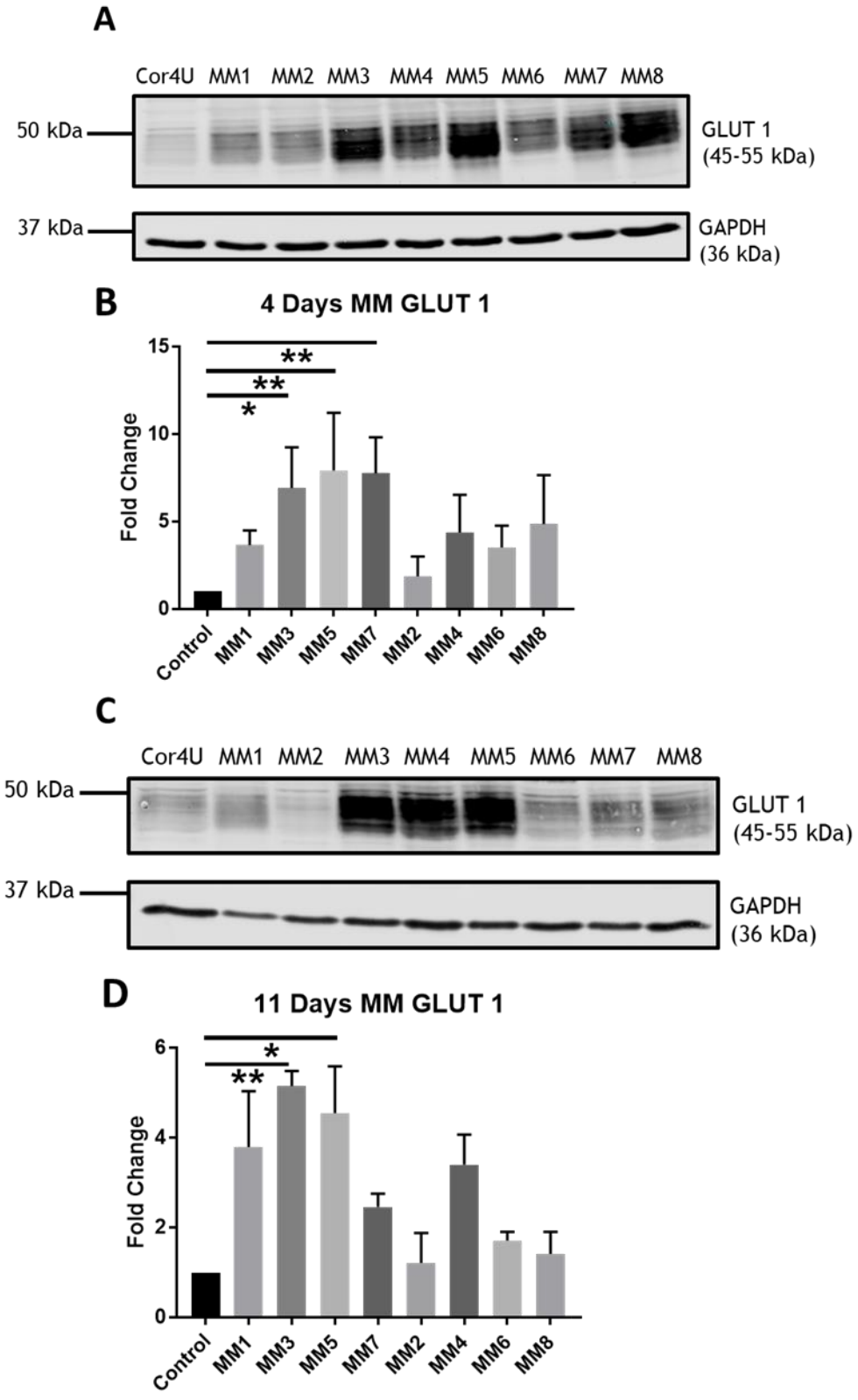

Figure 4-7 The effect of maturation medium conditioning upon iPSC-CM GLUT1 expression
Representative immunoblots depicting GLUT1 and GAPDH expression in iPSC-CM maintained for 4 (6A) or 11 (6C) days in a range of 'maturation medium' conditions. Densitometry was performed and quantification is shown as mean fold difference in GLUT1 expression normalised to GAPDH (+S.E.M) relative to control cells, across 3 independent experiments for each time point (6B and 6D). Statistical analysis was performed with a 2-way ANOVA, where the identified factors were experimental day and maturation medium conditioning. The level of significance was set at P=0.05. * denotes P<0.05. ** denotes P<0.01.

Based upon the response of iPSC-CM (Axiogenesis) to MM conditioning, it was concluded that these cells did not tolerate exposure to fatty acids and/or a lack of glucose particularly well. Prior MM interventions in the literature had utilised iPSC-CM from a different company (CDI). Therefore these measurements were repeated with CDI iPSC-CM to assess if these cells from an alternative source would respond differently. It was not possible to perform numerous replicates suitable for quantification and statistical analysis, however the images displayed in Figure 4-8 indicate a similar response to the MM conditions as was observed from Axiogenesis iPSC-CM. In particular, GLUT1 expression was increased notably in conditions where no glucose was present in the medium (conditions 1/3/5/7).

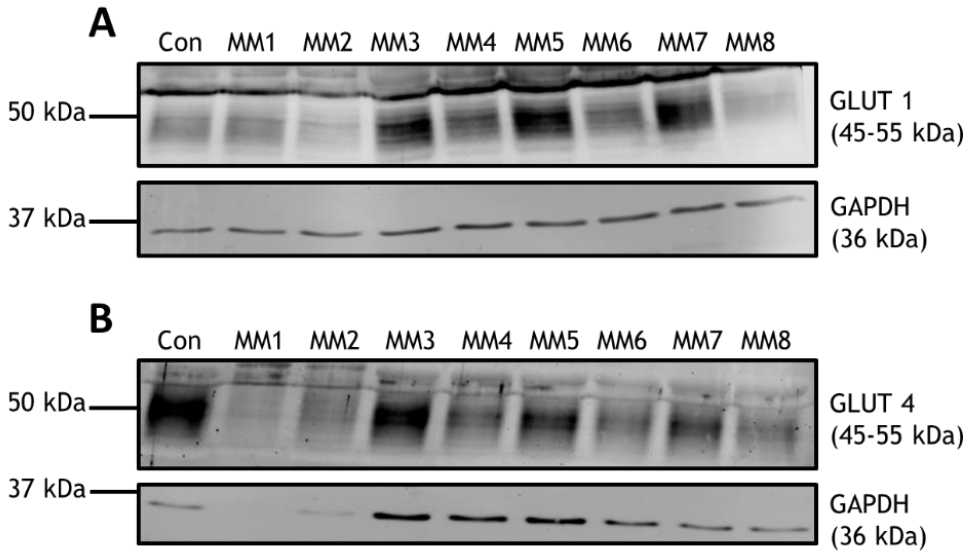

Figure 4-8 The effect of maturation medium conditioning upon CDI iPSC-CM
Representative immunoblots depicting GLUT1 and GAPDH expression (A) or GLUT4 and GAPDH expression (B) in iPSC-CM maintained for 4 (A) or 11 (B) days in a range of 'maturation medium' conditions.

Data from 2 separate commercial sources of iPSC-CM indicated that switching their primary metabolic fuel from glucose to fatty acids was not sufficient to induce metabolic maturation, and indeed it was accompanied by a degree of toxicity with longer incubation periods. It was considered possible that iPSC-CM do not possess the basic metabolic machinery required to transport and metabolise fatty acids. Therefore the expression of the fatty acid transporter CD36 and the mitochondrial electron transport chain complexes was assessed in iPSC-CM. Whilst not the only proteins with a rate limiting action in fatty acid metabolism, they are essential components. When compared with 3T3-L1 adipocytes and HEK 293 cells, it is clear

that iPSC-CM express at least 4 out of the 5 mitochondrial complexes required to complete the last step of oxidative metabolism (Figure 4-9B). The expression of complex I could not be assessed due to its low molecular weight. The expression of complex III appeared very weak in comparison to the other complexes, but this was also true for the other lysates assessed. In contrast, the expression of CD36 was undetectable in iPSC-CM lysate, whereas it is abundantly expressed in lysates from primary adult cardiomyocytes of murine or human origin (Figure 4-9A).

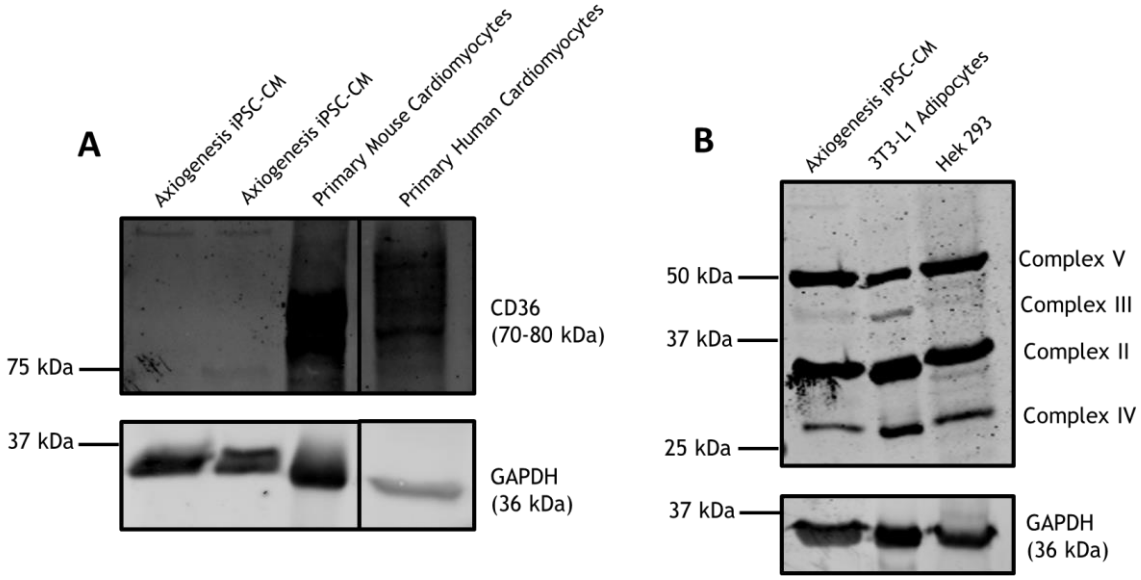

Figure 4-9 CD36 and OXPHOS expression in iPSC-CM
Protein lysates were generated from iPSC-CM, primary mouse cardiomyocytes, primary human cardiomyocytes, 3T3-L1 adipocytes, and HEK 293 cells. A volume of lysate adjudged to give an equal amount of protein between samples (approximately 20 µg) was loaded for each sample as necessary into a polyacrylamide gel and subjected to SDS-PAGE and immunoblotting, assessing the expression of CD36 (A) or the mitochondrial electron transport complexes (OXPHOS) (B). GAPDH was also assessed to act as an indicator of relative loading. Lines indicate that the blot has been cropped for presentation purposes, but no raw data was altered between segments.

As introduced, it has previously been reported that both the age of iPSC-CM and the physical characteristics of their culture conditions can have a strong influence over maturation. Therefore, to conclude this section of work, the expression of GLUT1 and GLUT4 was compared between iPSC-CM (from Axiogenesis) that had been maintained in normal manufacturer's maintenance medium for either 1 or 2 weeks post-plating. Additionally, cells were plated and maintained for 1 week on either a 12 or 24 well plate format.

As reflected in differences in GAPDH signal in Figures 4-10A and 4-10B, the method of lysate generation between conditions meant that different volumes of protein were loaded. However, across 2 independent experiments, quantification of GLUT1 and GLUT4 expression normalised to GAPDH provided no evidence of maturation. If anything, GLUT1 expression in iPSC-CM may slightly increase when culture conditions out with the manufacturers recommendations are implemented (96-well plate for 1 week), which could be indicative of a stress response. Furthermore, no conditions were even close to approaching the levels of GLUT4 expression recorded from primary adult mouse cardiomyocytes (Figures 4-10C and 4-10D).

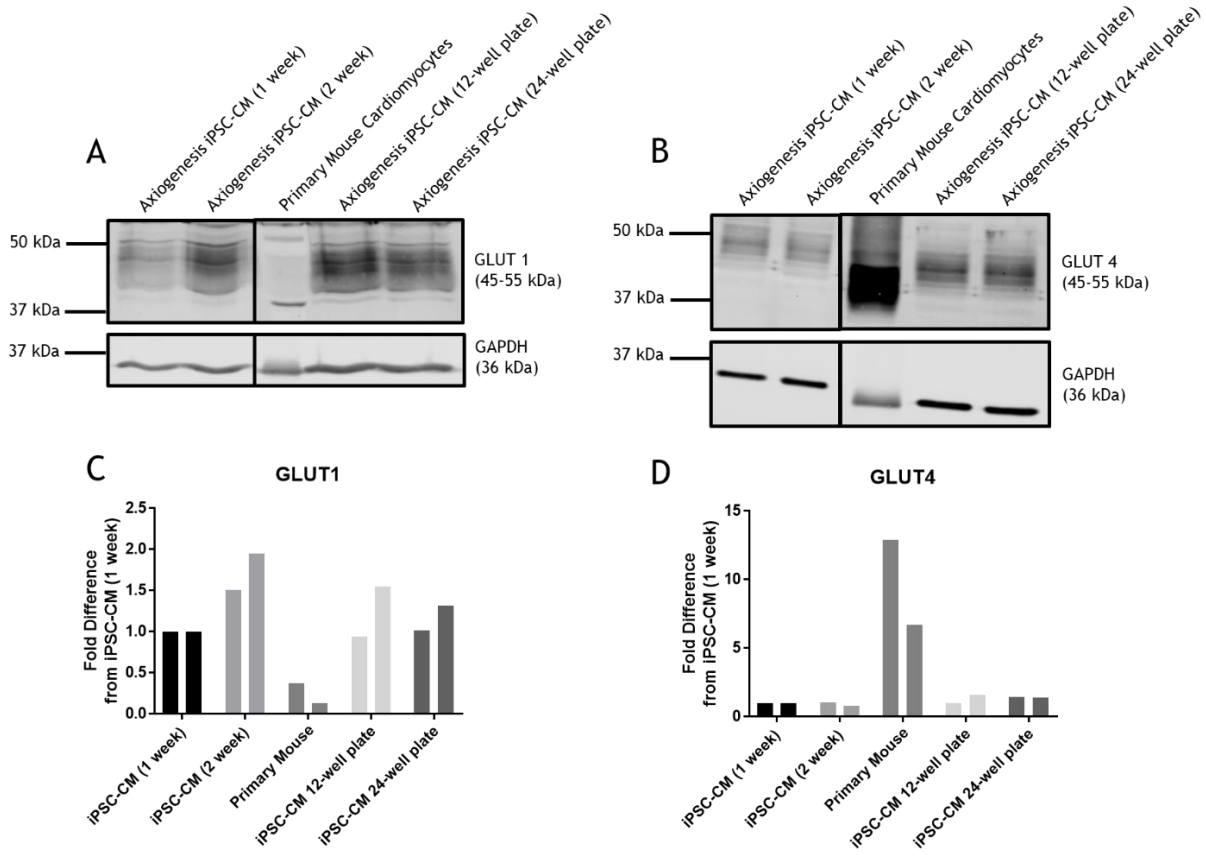

Figure 4-10 GLUT1 and GLUT4 expression in iPSC-CM maintained for different lengths of time and on different multi-well plates

Protein lysates were generated from iPSC-CM that were maintained in Cor4U medium for 1 week in either a 12, 24, or 96-well plate, or for 2 weeks on a 96-well plate. 20 µL lysate was loaded for each sample into a polyacrylamide gel and subjected to SDS-PAGE and immunoblotting, probing for the expression of GLUT4 or GLUT1 and GAPDH (loading control). Representative images are shown in panels A and B. 2 biologically independent experiments were performed and quantification is shown in panels C and D, where values are shown relative to the signal in lysates from cells cultured on a 96-well plate for 1 week. Each bar represents the value obtained from one immunoblot. Approximately 20 µg primary mouse cardiomyocyte lysate was also loaded and quantified for comparison.

4.2.3 The effect of triiodothyronine conditioning upon GLUT4 protein expression in iPSC-CM

Evidence has been outlined that implicates the thyroid hormone T_3 as having a vital role in inducing GLUT4 expression during cardiac development *in vivo*. Therefore the effect of incubating iPSC-CM with T_3 for 4 days after an initial minimum 3 day recovery period post-plating was assessed. It was determined that 4 concentrations would be used, which covered a range of both physiologically relevant values and recommendations based upon relevant literature. Figure 4-11A shows a representative immunoblot probing for GLUT4 expression in lysates from iPSC-CM that have been maintained in normal Cor4U medium supplemented with T_3. This experiment was performed in triplicate, and quantification revealed that there was no significant ($P<0.05$) difference in GLUT4 expression (normalised to GAPDH to control for protein loading) between any experimental group and control cells, which were maintained in normal Cor4U medium only.

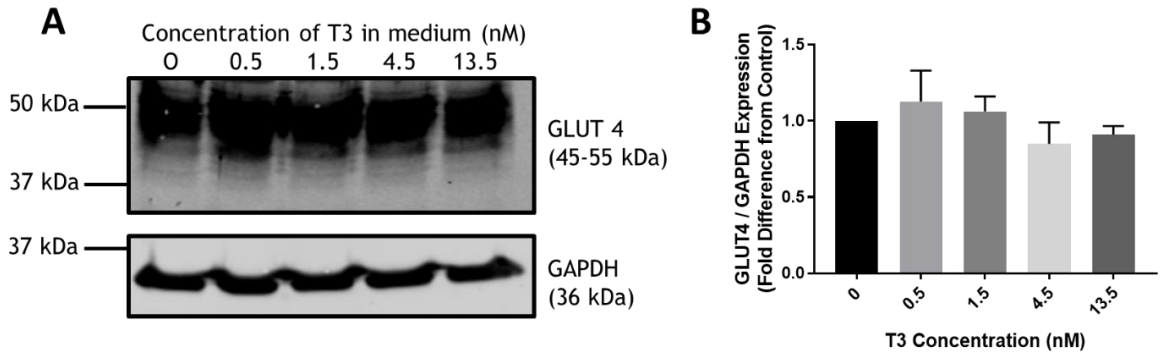

Figure 4-11 The effect of T_3 upon iPSC-CM GLUT4 expression
A: Axiogenesis iPSC-CM were plated and maintained for 3 days before subsequent addition of T_3 (0-13.5 nM) to the medium for a further 4 days. Lysates were then generated and subjected to SDS-PAGE and immunoblotting in order to assess the expression of GLUT4 and GAPDH. Depicted is one representative immunoblot. This experiment was performed with 3 biologically independent repeats. B: Quantification of fold difference in GLUT4 expression (normalised to GAPDH) relative to control cells (0 nM T_3). Values displayed are mean (+S.E.M.) across 3 independent experiments. Statistical analysis was performed with a 1 way ANOVA, where the level of significance was set at P=0.05.

4.2.4 Transfection of iPSC-CM

After initial attempts to increase iPSC-CM GLUT4 protein expression had limited success, more direct methods were developed. In order to facilitate this a commercially produced pcDNA3.1(+)-GLUT4 DNA plasmid containing the GLUT4 gene sequence was purchased from GenScript. The ultimate aim was to optimise

a protocol that facilitated overexpression of GLUT4 protein in iPSC-CM via Lipofectamine 2000 mediated transfection. First of all, in order to assess that the plasmid was indeed capable of producing GLUT4 protein, it was transfected into HeLa cells.

Figure 4-12A depicts GLUT4 expression in lysates generated from HeLa cells that were incubated with a range of volumes of Lipofectamine 2000 and 2.5 µg of pcDNA3.1(+)-GLUT4 plasmid DNA per well of a 6-well plate, in addition to lysates from untransfected HeLas and also 3T3-L1 adipocytes to act as a positive control. GLUT4 protein was detected at 45-55 kDa as anticipated, in addition to a range of smaller molecular weight precursor molecules ranging from approximately 30-45 kDa. HeLa cell lysates were generated via an identical protocol and 30 µL of each sample was loaded into the gel. The diminishing GAPDH signal indicates that higher volumes of Lipofectamine 2000 may have been toxic.

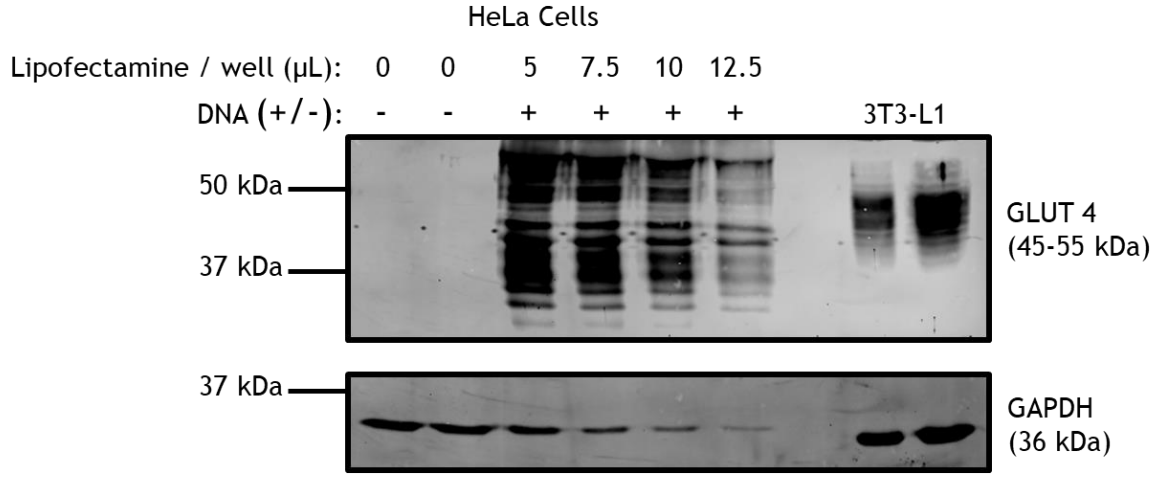

Figure 4-12 Transfection of HeLa cells with pcDNA3.1(+)-GLUT4 plasmid
HeLa cells were plated into wells of a 6-well plate and maintained until 90% confluence. Cells were then transfected according to the manufacturer's protocol, as described in methods section 2.5.3. Lysates were generated and 30 µL of each sample was subjected to SDS-PAGE and immunoblotting in order to assess the expression of GLUT4 and GAPDH (loading control). 2 different amounts of 3T3-L1 adipocyte lysate were also loaded in order to act as a positive control.

After initial insight from HeLa cells, it was decided to proceed into iPSC-CM based experiments. To begin with, the manufacturer's protocol was applied without modification. Therefore, similar to as just described with the HeLa cells, iPSC-CM were maintained for 3 days in normal maintenance medium plus a suggested range of volumes of Lipofectamine 2000 and 100 ng of plasmid DNA per well of a 96-well plate. Cells were initially incubated for 3 days after plating in normal medium to

allow recovery from liquid nitrogen storage. As depicted in Figure 4-13, this produced an approximate 2-fold overexpression of GLUT4 protein in iPSC-CM exposed to the higher volumes of Lipofectamine 2000, relative to control cells. This immunoblot was replicated, with highly similar findings (data not shown).

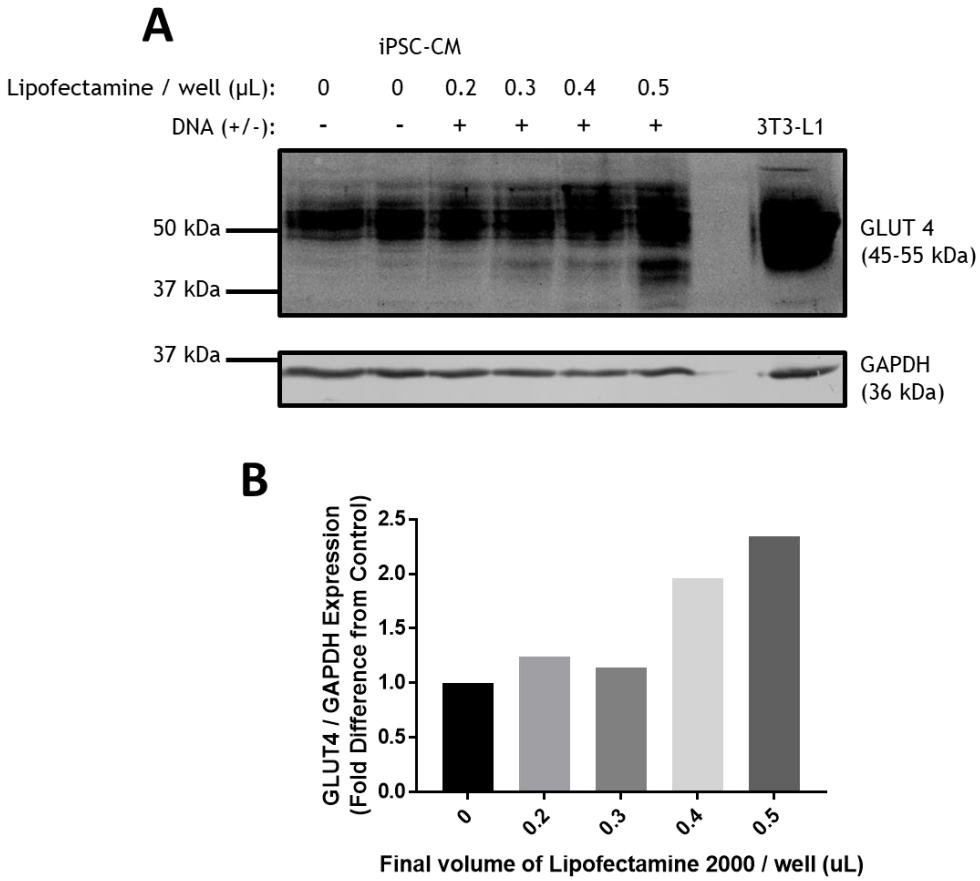

Figure 4-13 Transfection of iPSC-CM with pcDNA3.1(+)-GLUT4 plasmid
iPSC-CM were plated at 35,000 cells per well of a 96-well plate and maintained in standard Cor.4U medium for 3 days. Thereafter cells were transfected according to the manufacturer's protocol, as described in methods section 2.5.3. The final volume of Lipofectamine 2000 added to each well is indicated on the immunoblot, and in all cases the final amount of DNA per well was 100 ng. 3 days later lysates were generated and 20 µL of each sample was subjected to SDS-PAGE and immunoblotting in order to assess the expression of GLUT4 and GAPDH (loading control) (A). Quantification of the immunoblot was performed via densitometry and shown as the fold difference in GLUT4 expression normalised to GAPDH, relative to the average of control values (B).

The first attempt at increasing iPSC-CM GLUT4 protein expression provided confidence that this technique had the potential to realistically enhance GLUT4 content at least 3-fold to approximate levels recorded in 3T3-L1 adipocytes (Table 4-1). However, this would require further optimisation of the transfection protocol to meet the specific requirements of iPSC-CM. Several variables were altered individually over consecutive experiments, most notably the final volume of

Lipofectamine 2000 and plasmid DNA added per well, how long cells were incubated with the DNA post transfection, and at what point the initial media change post transfection occurred. The aim was to identify a protocol that maximally increased cellular GLUT4 content, but minimised any loss of cells by limiting the inevitable degree of toxicity associated with Lipofectamine and the overexpression of exogenous DNA. As depicted in Figures 4-14A and 4-14B, increasing the duration post-transfection for which cells were maintained until being harvested for lysates by a further 24 hours (96 hours total) appeared to enhance the increase in iPSC-CM GLUT4 expression to approximately 4 fold. Furthermore, subsequently also performing a media change after approximately 7 (rather than minimum 24) hours after initial transfection (and therefore reducing total exposure to Lipofectamine 2000) appeared to enhance cell survival as indicated by GAPDH expression, but still maintained an approximate 3-fold overexpression of GLUT4 protein (Figures 4-14 C and 4-14D). In these experiments a final volume of 0.4 or 0.5 µL Lipofectamine 2000 and 100 ng DNA per well as originally recommended was still utilised because it was found that increasing Lipofectamine volume further was ineffective, and increasing the volume of DNA did produce further increases in GLUT4 content when normalised to GAPDH, but also induced an unacceptable increase in the toxicity of the intervention (data not shown).

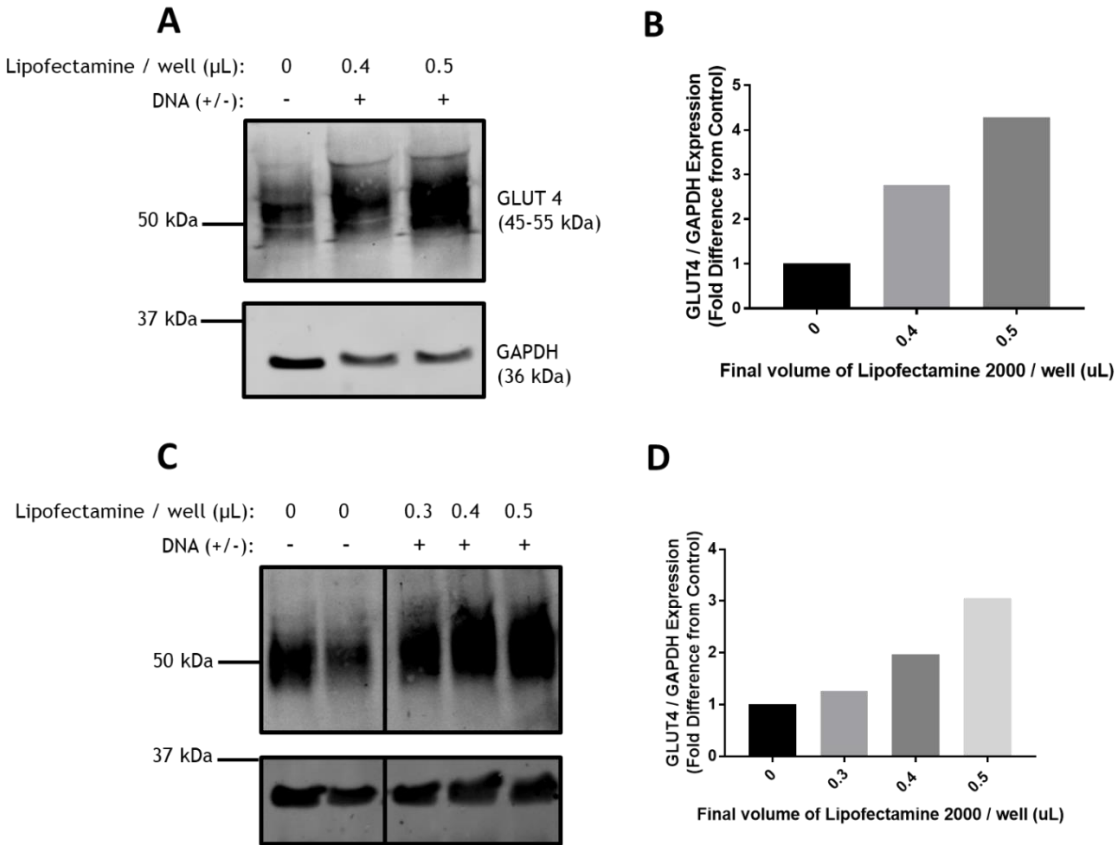

Figure 4-14 Optimisation of iPSC-CM transfection protocol
A&C: Immunoblots depicting GLUT4 and GAPDH expression in transfected and control iPSC-CM. Manufacturer's recommended protocol as described in methods sections 2.5.3. was adapted by increasing the time between transfection and generation of lysates from 72 hours to 96 hours (A) and then by also decreasing the time between transfection and the initial medium change from minimum 24 hours to 7 hours (C). B&D: Quantification of the immunoblots depicted in panel A and C was performed via densitometry and is displayed as GLUT4 expression normalised to GAPDH, relative to control.

After this initial optimisation period a protocol was established that elicited a 3-4 fold increase in GLUT4 content in iPSC-CM. This was still well short of the levels recorded from mature primary cardiomyocytes, however was deemed sufficient to warrant investigation into any subsequent impact on glucose transport. Therefore 3 independent experiments were performed, assessing [^{3}H]-2DG transport in transfected and control iPSC-CM. In each case, a sample of cells was also harvested for lysate and probed for GLUT4 expression in order to ensure that the transfection was successful. A representative image (Figure 4-15A) and quantification (Figure 4-15B) of one of these immunoblots shows that – in conjunction with Figures 4-14 and 4-15 – that final volumes of 0.5 µL Lipofectamine 2000 and 100 ng plasmid DNA was most effective at increasing iPSC-CM GLUT4 expression. Therefore this condition was taken forwards and performed for all transport experiments and is what is referred to when 'transfected' cells are discussed. Treatment with Lipofectamine 2000 only did increase GLUT4

expression slightly, but was still well short of the values obtained in fully transfected cells. Later experiments with a final volume of 0.5 µL Lipofectamine 2000 per well only confirmed the increase in GLUT4 expression is predominantly due to the presence of plasmid DNA (Figure 4-17). Regardless, GLUT4 expression was confirmed to be increased in all samples accompanying [^{3}H]-2DG uptake assays.

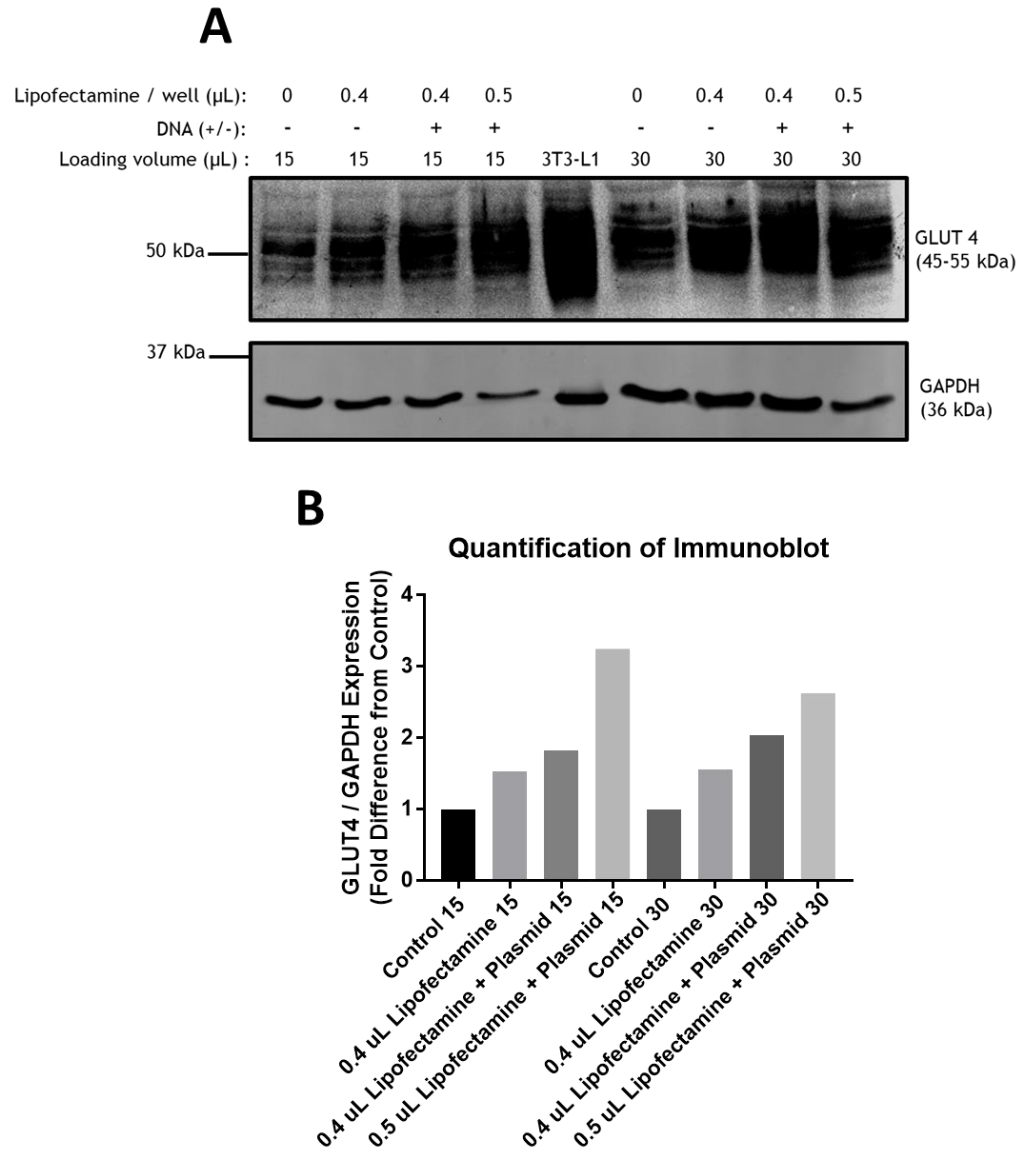

Figure 4-15 The effect of Lipofectamine 2000 and plasmid DNA upon iPSC-CM GLUT4 expression

A: Representative immunoblot displaying GLUT4 and GAPDH expression in lysates generated from transfected and control iPSC-CM. Cells were plated at 35,000 cells per well of a 96-well plate and maintained in standard Cor4U medium for 3 days. Thereafter identified cells were transfected with a final volume of Lipofectamine 2000 of 0.4 µL per well +/- 100 ng GLUT4 plasmid DNA or 0.5 µL + 100 ng GLUT4 plasmid DNA. Lysates were generated 96 hours after initial transfection and 15 or 30 µL of each sample was assessed. 3T3-L1 adipocyte lysate was also loaded to act as positive control. B: Quantification of immunoblot. Values are expressed as fold change in GLUT4 normalised to GAPDH, relative to the appropriate control (cells that were not exposed to Lipofectamine or DNA).

Figures 4-16A and 4-16B depict basal [^{3}H]-2DG uptake in control and transfected iPSC-CM. In one experiment control cells were incubated with Lipofectamine only, and in the other two control cells were exposed to neither Lipofectamine nor GLUT4 plasmid DNA. It is important to note that a correction factor was applied to raw data from transfected cells in order to account for the loss of cells observed with the intervention. This was generated by quantifying the fold change in GAPDH for the same volume of total lysate via immunoblotting. Across the 3 independent experiments there was a clear approximate 2-fold increase in basal uptake in transfected cells, and indeed statistical analysis confirmed a highly significant effect of transfection upon [^{3}H]-2DG uptake ($P<0.0001$).

In the first instance only basal transport is displayed in order to provide a clear picture of the effect of GLUT4 transfection, because no insulin response was recorded from either basal or transfected iPSC-CM during these experiments (data not shown). In one of the experiments, it was assessed if any of a range of drugs that are cited in the literature as being capable of increasing cellular glucose transport could stimulate an increase in iPSC-CM glucose uptake. However, as depicted in Figure 4-16 C, no significant ($P<0.05$) increase in [^{3}H]-2DG uptake was recorded in either control or transfected iPSC-CM in response to AICAR, Ionomycin, or indeed insulin. In fact, as can be inferred, [^{3}H]-2DG uptake was actually significantly ($P<0.05$) decreased in several conditions.

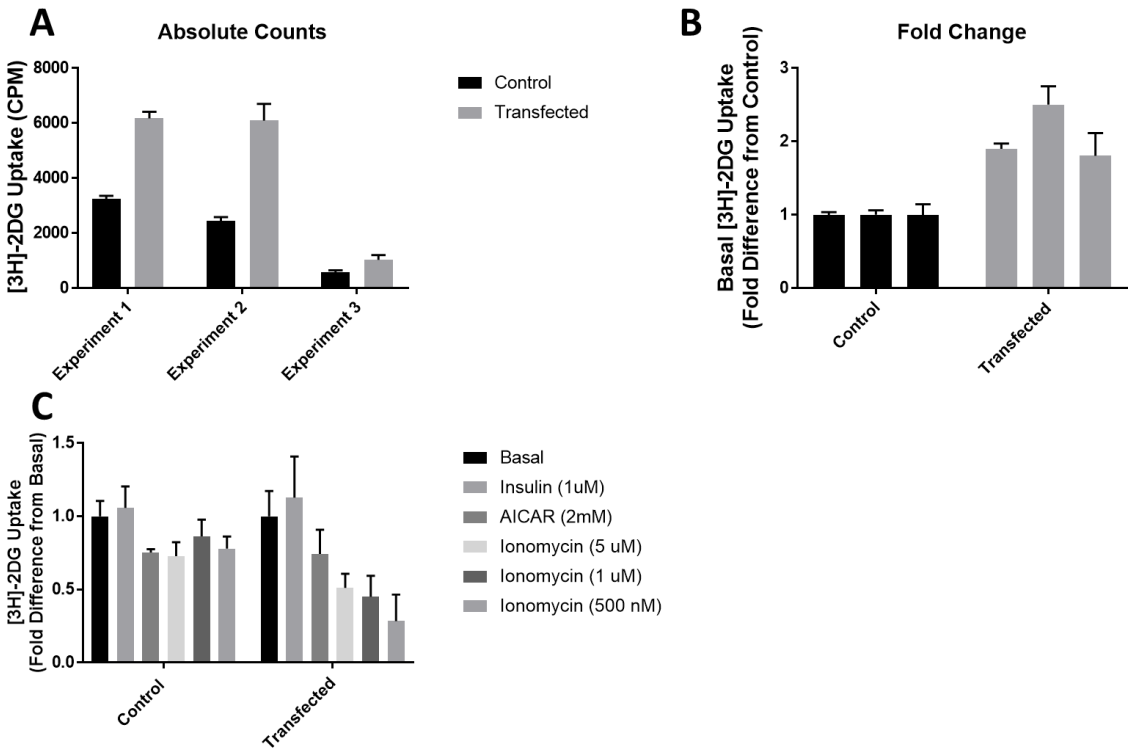

Figure 4-16 [^{3}H]-2DG uptake in control and transfected iPSC-CM
A: Background corrected basal [^{3}H]-2DG uptake in CPM was assayed in control and transfected iPSC-CM incubated with [^{3}H]-2DG for 15 min. Each bar represents the mean (+S.E.M) of 3 replicate samples from one experimental day, with 3 independent experiments performed in total. Statistical analysis was performed with a 2-way ANOVA where the identified factors were transfection and experimental day. The level of significance was set at P=0.05. B: The data presented in panel A was converted to the fold difference in [^{3}H]-2DG uptake in transfected iPSC-CM from values obtained in control cells. C: [^{3}H]-2DG uptake was recorded in control and transfected iPSC-CM +/- stimulation with 860 nM insulin (45 min), 2 mM AICAR (45 min), or 0.5-5 µM Ionomycin (15 min) prior to incubation with [^{3}H]-2DG for 15 min. Data is presented as fold difference in uptake relative to basal values, and depicts mean of 3 replicate samples (+S.E.M.) for each condition. Statistical analysis was performed with a 2-way ANOVA where the identified factors were drug treatment and transfection. The level of significance was set at P=0.05. In all cases, 'transfected' cells refers to iPSC-CM 4 days after initial incubation with 0.5 µL lipofectamine and 100 ng GLUT4 plasmid DNA per well of a 96-well plate, whereas control cells were incubated with 0 or 0.4 µL lipofectamine only.

Despite achieving a reliable 3-4 fold increase in iPSC-CM GLUT4 expression, this transfection based intervention only increased basal glucose uptake, and did not impact the lack of capacity of these cells to exhibit an insulin stimulated glucose uptake response. It was considered possible that GLUT4 expression had simply not been increased enough to achieve this intended goal. Therefore, before investigating alternative techniques, some final adaptations were made to this protocol.

First of all it was assessed if transfection reagents other than Lipofectamine 2000 were capable of supporting a more robust overexpression of GLUT4. As depicted

in Figure 4-17A, lysates from iPSC-CM cultured in Cor.4U maintenance medium only, Cor.4U supplemented with one of Lipofectamine 2000, FuGENE HD, or Transit TKO transfection reagents, or Cor.4U supplemented with one of the transfection reagents in addition to pcDNA3.1(+)-GLUT4 plasmid DNA, were probed for GLUT4 and GAPDH expression. As displayed in Figure 4-17B, quantification suggests that exposure to any of the transfection reagents alone did not alter GLUT4 expression. However, Transit TKO was able to facilitate over expression of the GLUT4 DNA plasmid to achieve an increase in GLUT4 protein of approximately 2.5 fold, which was similar in margin to that achieved with Lipofectamine 2000. FuGENE HD was less effective. A technical replicate of this immunoblot was performed with similar outcome, suggesting that Lipofectamine 2000 was indeed a suitable choice of transfection reagent. This data was supported by performing a similar experiment in HeLa cells. As can be seen in Figure 4-18, the overexpression of GLUT4 was much weaker when transfected with FuGENE HD in comparison to Lipofectamine 2000.

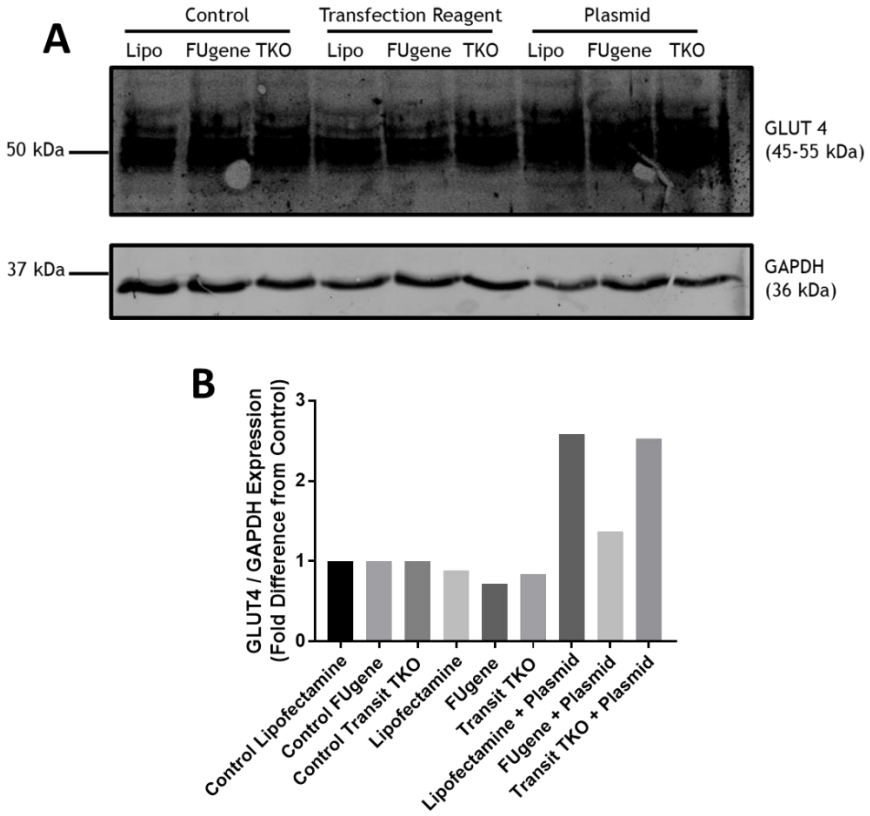

Figure 4-17 iPSC-CM transfection efficiency with different transfection reagents
A: Representative immunoblot of GLUT4 and GAPDH expression in lysates from iPSC-CM cultured in Cor.4U maintenance medium supplemented with one of 3 transfection reagents +/- GLUT4 plasmid DNA, or controls. For full transfection protocol details see methods section 2.5.3. Lysates were generated 72 hours post transfection, and 35 µL was loaded for each sample. B: Quantification of immunoblot. Values are expressed as fold change in GLUT4 normalised to GAPDH, relative to the appropriate control.

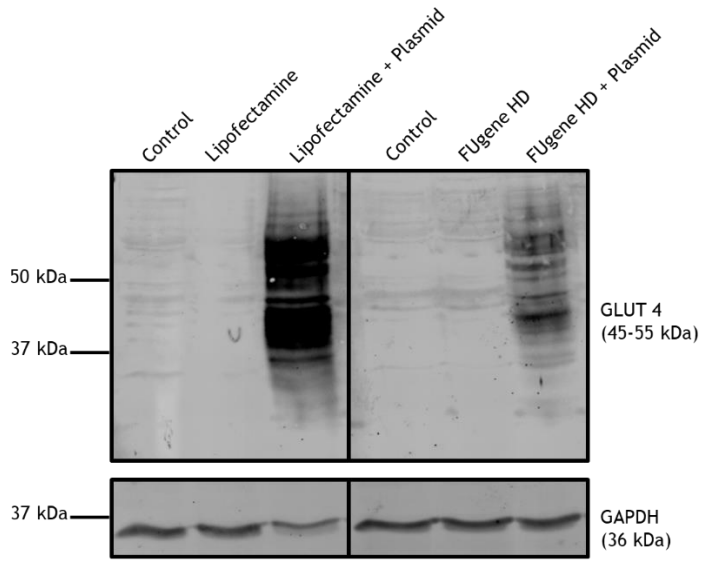

Figure 4-18 Comparison of transfection reagents in HeLa cells
Representative immunoblot of GLUT4 and GAPDH expression in lysates from HeLa cells cultured in maintenance medium supplemented with either Lipofectamine 2000 or FuGENE HD transfection reagents +/- 1250 ng DNA, or completely untreated cells (controls). Cells were maintained on a 12-well plate format. For full transfection protocol details see methods section 2.5.3. Lysates were generated 48 hours post transfection, and 40 µL was loaded for each sample.

Finally, from experience with HeLa cells, it was considered possible that transfection efficiency and/or the ability to detect transfection could be improved by performing the protocol on a larger scale format than a 96-well plate, due to an increased volume of cells and therefore also an increased volume of GLUT4 protein being produced. Therefore, transfection of iPSC-CM was performed on a 12-well plate format. Although extensive optimisation of the original manufacturers protocol was not performed as for on a 96-well plate scale, two independent experiments revealed only a similar 3-fold increase in GLUT4 expression in transfected iPSC-CM (Figure 4-19).

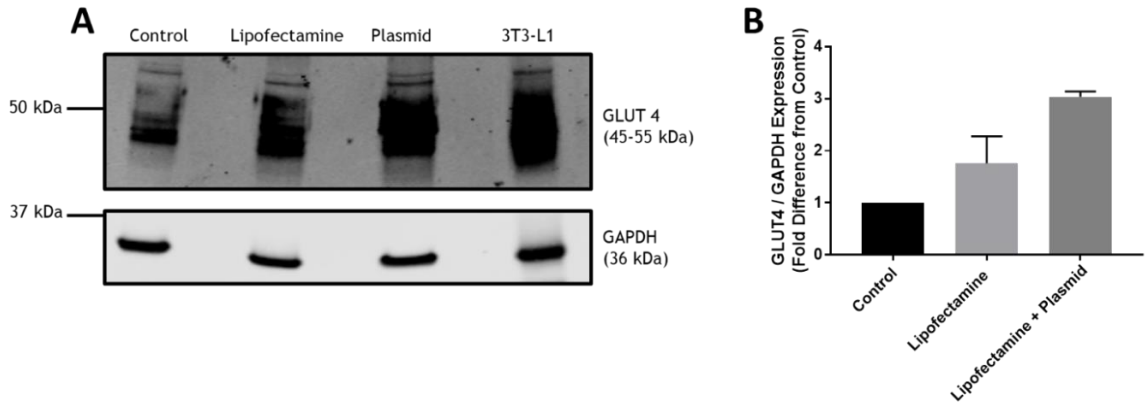

Figure 4-19 iPSC-CM transfection efficiency on a 12-well plate format
A: Representative immunoblot of GLUT4 and GAPDH expression in lysates from iPSC-CM cultured in Cor.4U maintenance medium supplemented with Lipofectamine 2000 +/- 1250 ng DNA, or untreated cells (control). Cells were maintained on a 12-well plate format. For full transfection protocol details see methods section 2.5.3. Lysates were generated 72 hours post transfection, and an appropriate amount of each sample was loaded to achieve loading of approximately equal amounts of total lysate (10-20 µL). 3T3-L1 adipocyte lysate (~10 µL) was also loaded to act as a positive control and reference B: Quantification of 2 independent immunoblots. Values are expressed as mean (+S.D.) fold change in GLUT4 normalised to GAPDH, relative to control.

4.2.5 Generation of novel pCDH-GLUT4 lentiviral vector

Transfection based approaches of the pcDNA3.1(+)-GLUT4 plasmid had yielded a promising increase in GLUT4 protein in iPSC-CM, however it was decided that pursuing a further increase in the level of overexpression towards values recorded from primary cardiomyocytes was the most appropriate next step. Therefore it was decided to move towards development of a lentivirus capable of overexpressing GLUT4. In order to achieve this, the GLUT4 gene sequence from the commercially obtained plasmid would have to be subcloned into a suitable lentiviral vector. Prior to attempting this, it was determined if iPSC-CM are indeed suitable candidates for lentiviral infection. In the lab there were already 2 active lentiviruses in use, one that was produced in-house by Dr. Mohammed Al-Tobi that targeted the overexpression of the t-SNARE Syntaxin 4, and another commercially obtained virus that targeted the overexpression of GLUT4-GFP (based upon the PCDH-CMV-MCS-EF1-HA-GLUT4-GFP plasmid generated by Silke Machauer).

Figure 4-20 depicts Syntaxin 4 expression in the lysates of Sx4 lentiviral infected iPSC-CM, uninfected controls, and 3T3-L1 adipocytes/primary mouse cardiomyocytes (positive controls). No Syntaxin 4 signal was obtained from uninfected cells, but a highly robust signal was obtained from cells infected with fully concentrated virus for 4 and in particular 24 hours. This immunoblot was

replicated in order to confirm findings. Similarly, Figure 4-21 displays confocal images of iPSC-CM infected with the GLUT4-GFP lentivirus and negative controls. The overexpression of this transporter tagged with the fluorescent reporter protein is clear, and is supported by corresponding immunoblots of control iPSC-CM lysates and lysates from cells infected with a range of concentrations of the lentivirus. Whether probing with a GLUT4 or GFP primary antibody, a characteristic smear at approximately 75 kDa was detected in infected samples only. This GLUT4 signal appears higher than the native protein due to being tagged with GFP, which is approximately 27 kDa.

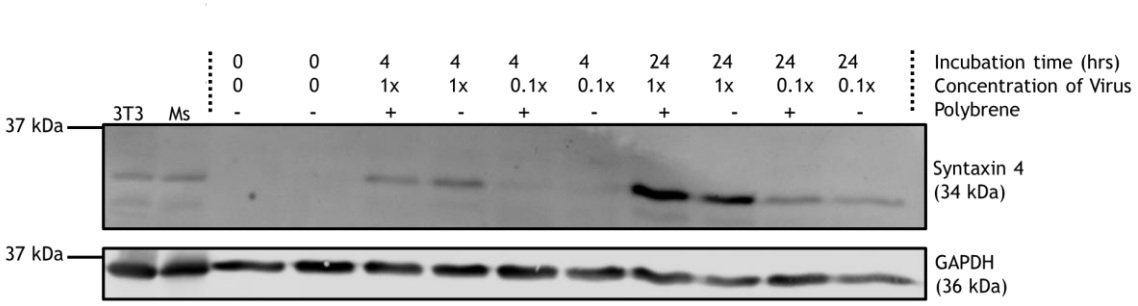

Figure 4-20 Lentivirus mediated overexpression of Syntaxin 4 in iPSC-CM
Representative immunoblot depicting Syntaxin 4 and GAPDH (loading control) expression in lysates from iPSC-CM incubated with concentrated (1x) or 1:10 diluted (0.1x) lentivirus designed to overexpress Syntaxin 4. iPSC-CM were incubated with the virus for 4 or 24 hours with or without 8 µg/mL polybrene as indicated, and lysates were generated 72 hours post infection. For full protocol see methods section 2.5.5. Uninfected iPSC-CM, 3T3-L1 adipoyctes, and primary mouse (Ms) lysates were also probed to act as positive and negative controls. For iPSC-CM samples, an equal amount of lysate was loaded across all samples (20 µL).

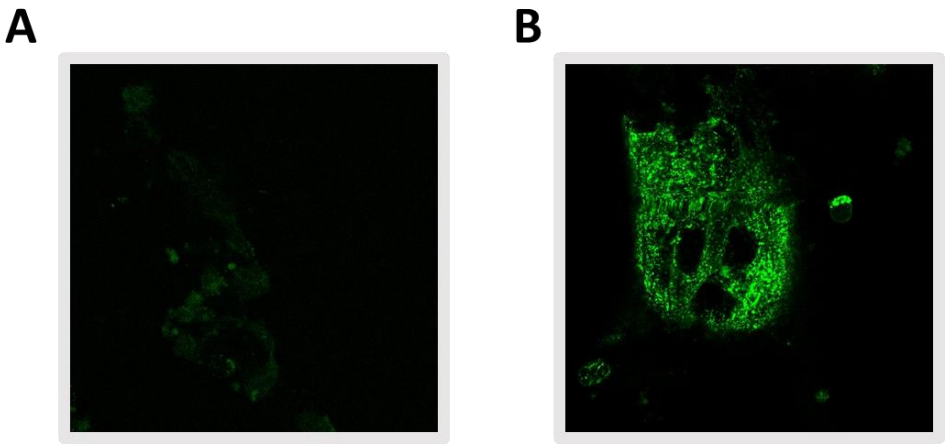

Figure 4-21 Confocal image of lentiviral infected GLUT4-GFP iPSC-CM
Representative confocal images depicting control (A) and lentiviral GLUT4-GFP infected iPSC-CM (B). Infected cells were incubated with lentivirus at an MOI of 105 for 24 hours, and images were recorded a further 72 hours later. Images were obtained with the same excitation intensity settings. For full protocol see methods section 2.5.5.

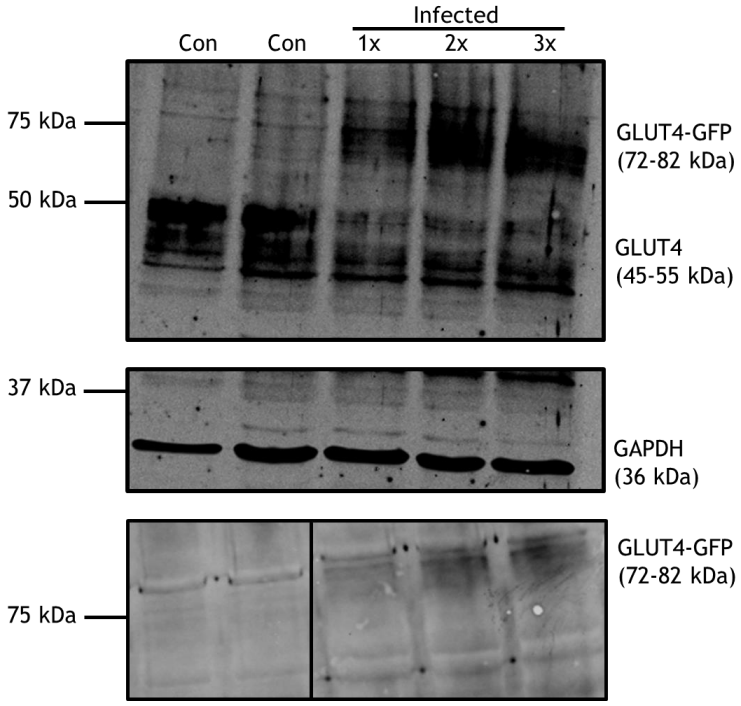

Figure 4-22 Immunoblots of GLUT4-GFP lentiviral infected iPSC-CM
iPSC-CM were incubated with GLUT4-GFP lentivirus for 24 hours, and then 72 hours later lysates were generated and probed via immunoblotting with antibodies for GLUT4 (upper blot), GAPDH (middle blot), or GFP (lower blot). 3 different concentrations of lentivirus were used, where 1x corresponds to an MOI of 35. For full protocol see methods section 2.5.5. Lysates from uninfected control iPSC-CM (con) were also loaded. For all samples an equal amount of lysate was loaded (20 µL).

Initial data confirmed that the expression of exogenous DNA in iPSC-CM is possible using this lentivirus based approach. As mentioned, in order to generate a lentivirus targeting the overexpression of GLUT4, the first step was to sub-clone the GLUT4 gene sequence from the commercially purchased pcDNA3.1(+)-GLUT4 plasmid into a specialised backbone vector suitable for the development of lentivirus, such as pCDH. Therefore, as depicted in Figure 4-23A, after extensive optimisation a protocol was established that facilitated highly efficient double restriction enzyme digest of the pcDNA3.1(+)-GLUT4 and pCDH-CMV-MCS-EF1-HA-GLUT4-GFP plasmids in order to excise the GLUT4 and GLUT4-GFP gene sequences respectively. The GLUT4-GFP fragment should be approximately 2500 bp, whereas the GLUT4 fragment should be approximately 1500 bp. The untagged GLUT4 sequence was then ligated into the open pCDH backbone to generate a novel plasmid - pCDH-CMV-MCS-EF1-GLUT4. In order to confirm that the intended products had indeed been successfully ligated, this newly formed plasmid was digested according to the original protocol (detailed in section 2.5.4.) and the molecular size of the generated fragments were compared to the original plasmids. As displayed in Figure 4-23B, after digestion the backbone of this new

plasmid was identical in size to that of the original pCDH-CMV-MCS-EF1-HA-GLUT4-GFP plasmid and the smaller 'insert' fragment cleaved was identical in size to the fragment from the original pcDNA3.1(+)-GLUT4 plasmid.

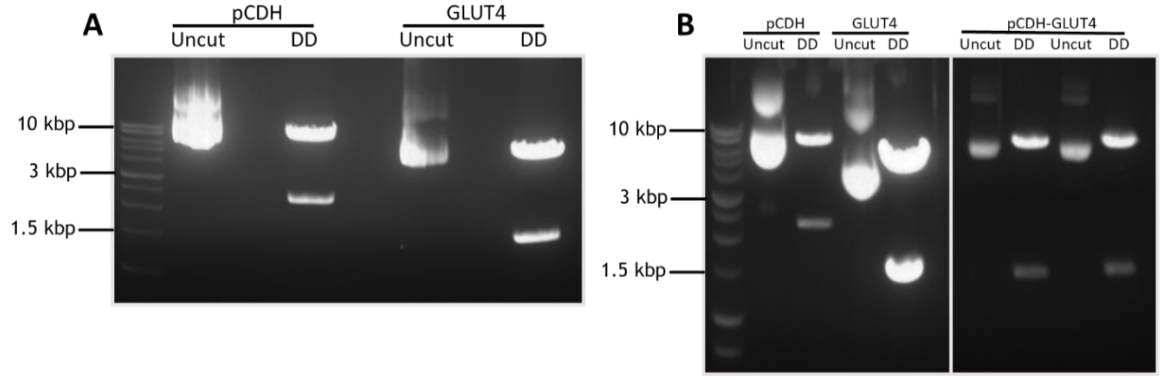

Figure 4-23 Generation of pCDH-CMV-MCS-EF1-GLUT4 DNA plasmid
A: Uncut and double digested (DD) pCDH and GLUT4 plasmids. B: Uncut and DD pCDH, GLUT4, and newly generated pCDH-GLUT4 (2 samples from distinct original colonies) plasmids. This image has been cropped for presentation purposes, but no raw data was altered. For digestion and ligation protocols see section 2.5.4. pCDH = pCDH-CMV-MCS-EF1-HA-GLUT4-GFP. GLUT4 = pcDNA3.1(+)-GLUT4. pCDH-GLUT4 = pCDH-CMV-MCS-EF1-GLUT4.

Finally, in order to complete preparation for future development of the intended lentivirus, it was important to confirm that the newly developed plasmid was still capable of inducing target cells to produce GLUT4 protein. Therefore, the pCDH-CMV-MCS-EF1-GLUT4 plasmid was transformed into NEB 5-alpha competent E.*coli*, amplified in volume, and then prepped in order to isolate a volume of DNA suitable for transfection of mammalian cells in culture. Accordingly, as depicted in Figure 4-24, despite the presence of nonspecific bands within this immunoblot, only lysates from HeLa cells transfected with this plasmid contained clearly detectable levels of GLUT4 protein as indicated by the characteristic smear around 45 kDa, which was not observed in lysates from untransfected control cells.

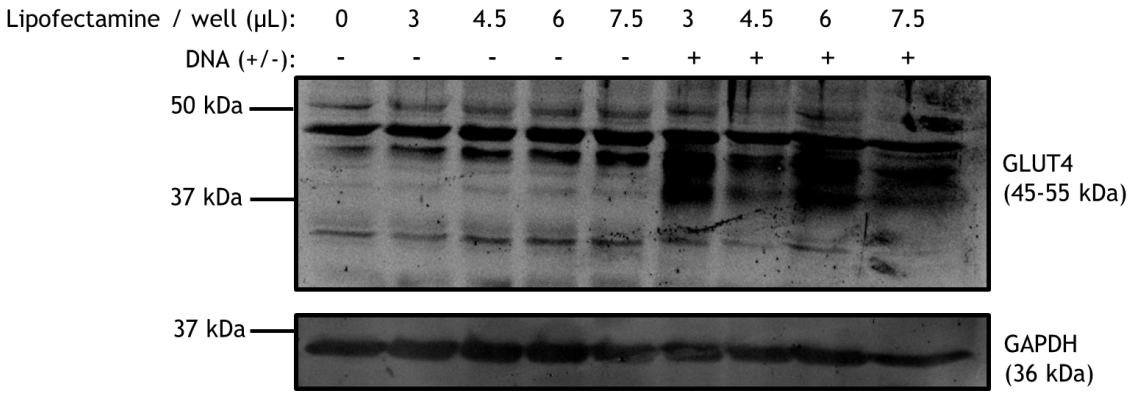

Figure 4-24 Transfection of HeLa cells with pCDH-GLUT4 plasmid
HeLa cells were plated into wells of a 12-well plate and maintained until 90% confluence. Cells were then transfected according to the manufacturer's protocol, as described in methods section 2.5.3. 4 days later lysates were generated and 35 µL of each sample was subjected to SDS-PAGE and immunoblotting in order to assess the expression of GLUT4 and GAPDH (loading control). Final volumes of Lipofectamine 2000 added per well are indicated. In all cases where DNA was also present, it was at a final volume of 1500 ng.

4.3 Discussion

4.3.1 GLUT1 is the predominant glucose transporter in iPSC-CM

The data presented in Figures 4-1 and 4-2 provides a clear depiction of the difference in glucose transporter isoform expression between iPSC-CM and primary insulin sensitive cells. This resolutely consolidates the general conclusions from chapter 3 and provides a target to aim for in terms of increasing iPSC-CM GLUT4 expression. An estimated 3-fold increase would attain levels recorded in insulin sensitive 3T3-L1 adipocytes, whereas an approximate 9-fold increase would attain levels recorded in primary adult mouse cardiomyocytes. Whilst quantification of this nature was not performed, previously published immunoblot data from foetal and neonatal rats shows clearly that cardiac GLUT1 and GLUT4 are very highly/poorly expressed respectively during early development, and that there is a rapid switch in relative expression shortly after birth (Castelló *et al.*, 1994). Therefore it can be concluded that iPSC-CM exhibit glucose transporter isoform expression consistent with foetal physiology.

In Figure 4-1B it can be noted that 3T3-L1 adipocytes express far more GLUT1 than primary mouse cardiomyocytes, despite being generally more sensitive to insulin with regards to glucose uptake (Figures 3-3 and 3-4). This could be partly due to the use of troglitazone during the 8 day differentiation period of these cells, as it has been shown to enhance the pre-adipocyte fibroblast to mature adipocyte transition, but also increases GLUT1 expression (Tafuri, 1996). Additionally, similar to other cell types, primary adipocytes show elements of dedifferentiation after short periods of *in vitro* culture, as their insulin sensitivity is typically decreased and GLUT1 expression is increased (Ruan *et al.*, 2003). Therefore it is perhaps of little surprise that a cell culture model of these cells exhibits relatively high levels of GLUT1. The observation that iPSC-CM were found to exhibit approximately 5-fold higher levels of expression compared to 3T3-L1 adipocytes underlines their physiological immaturity, and that the difference recorded between them and primary cardiomyocytes is not simply a function of being maintained in culture. Quantification of GLUT1 may be of secondary importance compared to GLUT4 in the context of this project, however is still crucial for the interpretation of any intervention. If GLUT4 were to be increased and GLUT1 also increased, then this could be evidence of general glucose transporter upregulation

rather than specific metabolic maturation. In contrast, if GLUT1 levels were unchanged or even decreased then this would support the conclusion that maturation had occurred.

Similar results utilising lysates from CDI iPSC-CM and a primary human sample support the general conclusions from this first section of work, even if it was determined that quantification would have been inappropriate. Ideally human cardiomyocyte lysates would be implemented as the gold standard reference for iPSC-CM in all experiments within this thesis, however this is not possible for 2 reasons. First of all, the access to human myocardial sections is extremely limited. Secondly, the sections that can be obtained are generally from individuals suffering from cardiac disease. In this instance, the donor was undergoing cardiac transplant due to prior MI and subsequent progression to cardiomyopathy and atrial fibrillation. This sample demonstrated the principle that GLUT4 should be readily be detected in cardiomyocytes, however may have actually underrepresented true human primary GLUT4 expression due to known adaptations post-MI.

In this first set of experiments there were 2 technical limitations that must be acknowledged. First of all, quantification of glucose transporter isoforms normalised to GAPDH makes the assumption that GAPDH does indeed adequately represent total protein loaded, and that the relationship between GAPDH and total protein is similar between different cell types. This was tested, as shown in Appendix 1. By comparing ponceau (total protein) and GAPDH signals for 2 different lysates of each relevant cell type it was concluded that it was appropriate to use GAPDH as a loading control for 3T3-L1 adipocytes, Axiogenesis iPSC-CM, and primary mouse cardiomyocytes only. The alternative identified method for quantification was to generate a GLUT signal to copy number standard curve from 3T3-L1 adipocytes and from this work out the number of copies in samples from cardiomyocyte samples and then adjust for the equivalent number of cells loaded. However, this approach would rely upon several assumptions that were essentially impossible to test, such as exact plating density, the percentage of cells harvested during the lysis process, the exact loading volumes of each sample, etc. Therefore whilst not without limitation, it was decided to simply compare signals normalised via GAPDH.

The second issue with this approach is a general point that is relevant for much of this chapter. That is how to perform densitometry when the target proteins appear as smears (due to post-translational modifications) rather than clear and distinct bands. When drawing a box around the target protein using Image Studio Lite there becomes much larger room for human error as determination of where the signal truly starts and ends can be far more subjective. There was no way of totally eradicating this problem, however the fairly good reproducibility of results across technical and biological replicates indicates that quantification was consistent. Additionally, in all cases it supports the initial visual interpretation.

When assessing the estimated glucose transporter isoform expression data in Table 4-1, it would be extremely surprising if GLUT1 was not the predominant functional transporter in iPSC-CM, due to its overwhelmingly dominant expression over GLUT4. However, it was still important to assess this. In order to confirm that the selected assay worked as intended it was first of all performed with 3T3-L1 adipocytes. Although minor, the reduction in insulin stimulated glucose uptake in response to GLUT1 inhibition was unexpected, and suggests that this transporter may have more of a role in insulin stimulated glucose uptake in this cell type than previously thought (Figure 4-4). Whilst it would have been preferable to selectively inhibit GLUT4 alone, the near absence of any [^{3}H]-2DG uptake detected when both GLUT1 and GLUT4 were inhibited confirmed the predominant role that GLUT4 plays in regulating glucose uptake in these cells.

As anticipated, when only GLUT1 was inhibited in iPSC-CM there was a much larger percentage drop in [^{3}H]-2DG uptake (Figure 4-5) compared to 3T3-L1 adipocytes. When the concentration of BAY-876 was increased to also inhibit GLUT4 there appeared to be only a very minor further decrease in recorded uptake and indeed this was not found to be significant. This confirms that the low levels of GLUT4 that are expressed in iPSC-CM are of limited functional relevance. However, intriguingly, inhibition of both of these transporters only inhibited total [^{3}H]-2DG uptake by 40-50% (Figure 4-5). What is accounting for this residual uptake is unclear. Most likely, there may be an additional glucose transporter(s) present in iPSC-CM. Primary candidates would be GLUT3 or GLUT8, which have both been demonstrated to be expressed in myocardium (Grover-McKay *et al.*, 1999; Aerni-Flessner *et al.*, 2012). Attempts were made to assess the expression of these

transporters – in addition to GLUT10 and GLUT12 – via immunoblotting, but unfortunately these were unsuccessful (data not shown).

4.3.2 Maturation medium and T_3 conditioning did not mature iPSC-CM

There is strong evidence from the literature to suggest that altering the primary metabolic substrate that fuels iPSC-CM from glucose to fatty acid can induce maturation. Therefore this approach was implemented, with the primary outcomes being GLUT1 and GLUT4 expression. Consideration of the effect of 4 days MM conditioning upon GLUT4 expression (Figure 4-6B) suggests that maintenance in medium containing no glucose (conditions 1/3/5/7) in general may have matured iPSC-CM GLUT4 content, albeit only 2-fold. However, this conclusion is rapidly dismissed when observing the effect of the same intervention upon GLUT1 expression (Figure 4-7B). This strongly suggests that what actually occurred was a general upregulation of glucose transporters in response to sugar deprivation. It is logical that a much greater fold increase would occur in GLUT1, as we now understand this to be the predominant transporter in these cells.

As has been noted previously, MM conditioning can be toxic to cells, and this proved to be the case once again. In all experiments lysates were generated in an identical manner and an equal volume was probed via immunoblotting. As can be seen in the signals for iPSC-CM maintained in MM for 11 days (Figures 4-6C and 4-7C), there is a general decrease in GAPDH signal relative to untreated cells, which reflects the visually observable decrease in viable cell number prior to the generation of lysates. Given that GAPDH is a metabolic enzyme it could be suggested that this change was reflective of a genuine effect. However, if GAPDH expression was to respond then based upon the GLUT data it would be expected to both be observable after 4 days conditioning and also to increase, not decrease. Interestingly, the cells most affected by the apparent toxicity of MM were those maintained in conditions that most closely replicated the originally recommended formula (MM1 and MM2). Data from CDI iPSC-CM supported the conclusions drawn regarding both the lack of specific maturation and toxic effects of the intervention beyond 4 days of conditioning (Figure 4-8).

Another interesting observation from the data presented is that the effects recorded after 4 days of MM conditioning appear to decrease in size when cells are maintained for a further 7 days. There are several plausible explanations. First of all, it could be that after an initial shock response to the change in conditions, cells adapt (perhaps via upregulation of other relevant proteins) and glucose transporter expression begins to return to normal. Perhaps more likely is that the occurrence of cell death as observed is correlated with the degree of initial response. Therefore the cells that do not respond as strongly are more likely to survive longer in the new medium, and as these lesser or non-responding cells become predominant in the population they more strongly influence the overall results for each condition. Finally, Figure 4-10 indicates that GLUT1 expression may simply increase with time in iPSC-CM. Elevation of control baseline values would reduce the fold impact of any intervention.

It is not explicitly clear why iPSC-CM did not respond more favourably to MM conditioning. Whilst prior studies have reported a degree of toxicity with this approach, it has also been accompanied by maturation of a range of parameters, including metabolic markers such as lactate production and oxygen consumption (Drawnel *et al.*, 2014; Correia *et al.*, 2017). Within the present study, it was demonstrated that iPSC-CM express the mitochondrial electron transport complexes required to complete oxidative metabolism (Figure 4-9). In contrast, there was no detectable expression of the fatty acid transporter CD36 (Figure 4-9). It may well be that other proteins that are essential for fat oxidation are lacking from iPSC-CM, however - similar to the role of GLUT4 for glucose - the first step of fat metabolism must be to transport it into the cell, and therefore this absence of CD36 is an immediate critically limiting factor. In these experiments this alone could account for why medium with no or low glucose was not well tolerated. Why this intervention was successful in previous work remains unexplained. One possible factor could simply be that the differentiation protocol of the cells used was different, and that they had the necessary machinery to effectively metabolise the fat. However, the fact that similar results were obtained with CDI iPSC-CM (Figure 4-8) in this project casts doubt on that explanation. A key challenge when adding fatty acid to medium is the unintentional lowering of the pH value of the solution. However, this was

monitored using indicator strips in order to ensure that pH did not fall below pH 7.

There is a general theme within prior studies indicating that culturing iPSC-CM in environments that better replicate relevant features of the *in vivo* environment can induce maturation. Accordingly, it was considered possible that rather than plating cells on a 96-well plate format, a larger scale environment could facilitate the formation of greater groups of functionally coupled cells capable of transducing increased contractile forces. As introduced, mechanical loading is an important stimulus for the development of the heart (Tulloch *et al.*, 2011), and the rhythmic stretch and contraction of the myocardial wall during every cardiac cycle will greatly exceed the spontaneous contractile forces of iPSC-CM cultured in small groups within a 96-well plate. However, across 2 independent experiments iPSC-CM cultured for 1 week on either a 12 or 24 well format did not show any clear adaptation with regards to GLUT1 or GLUT4 expression (Figure 4-10).

Similarly, there is robust *in vivo* evidence that the hormone T_3 has a critically influencing role in switching the relative expression and contribution of cardiac GLUT1 and GLUT4 during foetal to perinatal development (Castelló *et al.*, 1994). More specific to iPSC-CM, 2 separate papers identified T_3 as capable of inducing several phenotypic adaptations consistent with maturation (Yang *et al.*, 2014; Lin *et al.*, 2017). However, in this project it was found across 3 independent experiments that incubation of iPSC-CM with a range of 4 concentrations of T_3 did not significantly alter GLUT4 expression.

There are a couple of possible explanations as to why T_3 did not have the intended effect. Given that the concentrations selected covered previously implemented and physiologically relevant values, this variable is unlikely to have been the limiting factor. Rather, prior interventions were sustained for 1 week, whereas in this study cells were only incubated for 4 days. This time period was selected in order to harvest cells at the same time point as other measurements within this project, but may have meant cells were exposed for an insufficient period of time. Perhaps of more importance however is that in the prior iPSC-CM based studies mentioned, the authors differentiated the iPSC-CM themselves and then exposed them to T_3 almost immediately. Similarly, *in vivo* manipulation of circulating T_3

levels had a markedly diminished impact on cardiac GLUT4 protein expression in adult compared to foetal or neonatal rats (Castelló *et al.*, 1994). Together this indicates that intervening with T_3 may be most effective during or immediately after the differentiation of iPSC-CM (or any cardiac model), which was not possible to achieve in this project due to obtaining the cells commercially. This approach provides a highly reliable phenotype, but prevents the opportunity to intervene at the earliest stages of their development.

4.3.3 iPSC-CM can efficiently over express functional GLUT4 protein via Lipofectamine 2000 mediated transfection of plasmid DNA

Whilst initial attempts to upregulate iPSC-CM GLUT4 protein expression via interventions that were based upon simulation of natural stimuli that are physiological regulators of this transporter generated interesting insight into these approaches, they were ultimately unsuccessful with regards to the experimental aims. The problem with isolating stimuli in this manner is that it prevents attainment of any cumulative effect of all factors and removes any possible interactions between variables. The majority of physiological mechanisms underlying significant processes such as maturation of any given variable are not simple individual stimulus – response reactions, but rather involve a complicated multifactorial network of factors that may each have different molecular targets, varying levels of importance at different time points, and perhaps are even dependent upon one another. As outlined in the introduction, cardiac development is dependent upon at least an interaction of biomechanical, hormonal, and metabolic factors. To accurately recapitulate all of these stimuli *in vitro* would be extremely challenging. Even if maturation were achieved via manipulation of one variable based upon elicitation of a certain physiological response such as increased GLUT4 expression, it could be argued that it is still not physiologically relevant. If taking this 'physiologically representative' approach, both the intervention and outcome must match the *in vivo* physiology.

After consideration, it was determined that a more forceful and direct molecular approach could be more effective. Rather than prioritising physiologically relevant stimuli, the outcome of enhancing iPSC-CM GLUT4 expression became the sole focus. To achieve this a DNA plasmid containing the GLUT4 gene was purchased

and initially transfected into HeLa cells in order to ensure that it produced detectable levels of protein. There was very clear production of protein in transfected HeLa cell lysates compared to controls (Figure 4-12), however rather than appearing as one distinct smear multiple additional smaller bands were detected. It is common for this protein to run at different molecular weights in different species or cell types, and in fact it runs slightly lower than anticipated in 3T3-L1 adipocytes, as indicated in this immunoblot. Therefore the upper smear in HeLa cell lysates was believed to be fully formed GLUT4 protein. HeLas are highly amenable to the introduction of exogenous DNA and the subsequent overexpression of the relevant protein. As whole cell lysates were generated it is believed that the smaller bands observed were precursors to GLUT4 protein, prior to addition of post-translational modifications.

When adapting this protocol for use in iPSC-CM it was not possible to perform extensive replicates for every possible combination of the identified key variables that could impact transfection efficiency. Therefore, after initial encouragement from following the manufacturer's recommended protocol for a 96-well plate format, several logical adjustments were made in order to maximise the over expression of GLUT4. In particular, between Figures 4-13 and 4-14 it can be appreciated that utilising volumes of Lipofectamine 2000 within the upper recommended range and increasing the time between initial transfection and generation of lysates were particularly effective. It is logical that – up to a certain point – increased volumes of Lipofectamine 2000 will correlate with increased GLUT4 protein expression as there is more reagent available to facilitate the uptake of the plasmid DNA. However, data from Figures 4-15 and 4-19 suggests that Lipofectamine 2000 itself may induce a small increase in GLUT4 content by itself, whereby lysates from cells only treated with this transfection reagent showed levels elevated above untreated control lysates. If this were a genuine effect then there is no obvious physiological mechanism to account for it. It seems highly unlikely that there would be a direct maturation effect. Continual disruption of the cell membrane by DNA-lipid complexes could perhaps initiate a cellular response, but why GLUT4 would be upregulated is unclear. However, this observation was not consistent (e.g. Figure 4-17), and in all cases the increase observed was still well short of the increase in GLUT4 expression recorded from fully transfected iPSC-CM cell lysates.

Final optimisation steps were undertaken to not only ensure that the optimal protocol with Lipofectamine 2000 was being implemented, but that Lipofectamine 2000 was indeed the most suitable transfection reagent to use. Data from Figures 4-(17-19) confirmed that both FuGENE HD and Transit TKO, or Lipofectamine 2000 on a 12-well plate format, were not capable of exceeding the 3-4 fold overexpression of GLUT4 protein achieved in iPSC-CM achieved with Lipofectamine 2000 on a 96-well scale. There are other options that have not been explored that could be used to facilitate transfection of the plasmid such as electroporation, however based on the available evidence it appears a 4-fold increase in GLUT4 protein expression may be the limit that can be expected to be achieved using this general approach.

After optimisation of a protocol that facilitates the overexpression of GLUT4 in iPSC-CM to levels observed approximately in 3T3-L1 adipocytes, it was anticipated that there would be a clear effect on subsequent measurements of [^{3}H]-2DG uptake. This proved to be the case, but ultimately only with regards to basal transport, which as depicted in Figure 4-16 increased approximately 2-fold in transfected cells. The absolute counts in experiment 3 were decreased because a reduced number of cells were plated in each well in an attempt to increase transfection efficiency, and as was established in chapter 3 plating density has a disproportionately strong impact upon [^{3}H]-2DG uptake in iPSC-CM. However, when uptake in transfected cells was expressed as a fold difference from control, the data was very consistent across replicate experiments.

In contrast to the clear impact upon basal transport rates, neither insulin (across all 3 experiments) nor AICAR or Ionomycin (in the experiment shown in Figure 4-16C), could stimulate a significant further increase in [^{3}H]-2DG uptake above basal values. If adequate GLUT4 is present, then insulin should stimulate an increase in uptake via activation of the GLUT4 trafficking pathway detailed in the introduction, whereas AICAR and Ionomycin operate via activation of AMPK and calcium dependent mechanisms respectively. Given the effect on basal uptake, it can be ruled out that the GLUT4 protein being produced is non-functional. One possible explanation is that the protein is not being incorporated into GSVs in preparation for rapid trafficking to the membrane in response to the relevant stimuli applied. Potentially, the new GLUT4 could be being retained permanently

intracellularly and/or being immediately trafficked to the membrane, hence the increase in basal uptake. Finally, it could be that now the factor limiting insulin stimulated GLUT4 trafficking in iPSC-CM has shifted from a lack of GLUT4 protein, to somewhere else in the process. There may be other essential trafficking or signalling molecules that are also absent.

4.3.4 iPSC-CM are amenable to lentiviral mediated infection

The decision to move towards generation of a lentivirus that induces the overexpression of a functional GLUT4 protein was taken because it was concluded that the likely achievable limit of overexpression via transfection had been attained. Typically transfection is most successfully implemented in sub confluent, dividing cells. Given that iPSC-CM are terminally differentiated, and do not tolerate being plated at a low density particularly well, it was considered a success to achieve a 4-fold overexpression of GLUT4 in these cells using this approach.

Initial proof of concept experiments demonstrated that a highly robust overexpression of exogenous genes such as Syntaxin 4 and GLUT4-GFP was possible using a lentivirus approach. A relatively low amount of total protein was loaded in the Syntaxin 4 immunoblot, which may explain why no signal was obtained from control cell lysates (Figure 4-20). However, the key point is that a very strong overexpression was detected in infected cell lysates, which seemed to be associated with higher concentrations of the virus and incubation durations, and also the presence of polybrene, which is designed to improve the absorption of the virus (Davis, *et al.*, 2002). Whilst it was not possible to quantify the fold difference in expression between conditions due to the lack of signal from control cells, a similarly strong overexpression of GLUT4 would likely bring iPSC-CM values towards those recorded from primary cardiomyocytes. In the confocal microscopy images of infected iPSC-CM, the abundance of GLUT4-GFP is striking (Figure 4-21). Unfortunately, when tagged with a reporter GFP protein GLUT4 becomes non-functional, hence why a novel lentivirus must be generated. From the immunoblot presented it appears that with increasing production of exogenous GLUT4 protein, the production of native GLUT4 may have decreased (Figure 4-22). However, given the poor expression of this protein in iPSC-CM, this should not overly impact the efficacy of any intervention.

When developing the novel pCDH-CMV-MCS-EF1-GLUT4 plasmid depicted in Figure 4-23, there were 2 steps that required major optimisation. First of all, the restriction digests were required to be of high efficiency, as any contamination with even small quantities of undigested DNA, or over digested degraded DNA, were unsuitable for subsequent ligation. After extensive manipulation of experimental variables, the key optimal conditions were found to be performing 20 µL total volume reactions for 2 hours. Similarly, successful ligation required several trial and error optimisation steps. The key adjustments were increasing the volume of each fragment within the ligation, and incubating the reaction at 16 degrees overnight. The full protocol for all steps is detailed in methods section 2.5.4. As depicted in Figure 4-24, this novel plasmid was still capable of inducing GLUT4 protein production in HeLa cells, therefore the next step must be to generate a novel lentivirus with the intention of infecting iPSC-CM.

4.3.5 Methodological considerations

Several key methodological issues have already been highlighted and discussed. Additionally, when assessing the impact of MM and T_3 interventions, it would have been useful to validate some of the claimed benefits of these approaches. Despite no clear maturation effect, previous adaptations reported could have been replicated in order to confirm that the protocols had indeed been implemented appropriately. Furthermore, as alluded to, it was not viable to perform extensive or exhaustive optimisation of the transfection process in iPSC-CM. This prevented robust assessment of the effect of all possible combinations of key variables upon transfection efficiency.

4.3.6 Conclusion and outline of further work required

In conclusion, quantification of the expression and functional importance of GLUT1 and GLUT4 in iPSC-CM revealed that with regards to these parameters this cell type exhibits a phenotype highly similar to cardiomyocytes at a foetal stage of development *in vivo*. This also permitted estimation of the magnitude of specific adaptations required to mimic primary cardiac physiology. It was identified that approximately a 10-fold increase in GLUT4 protein expression was required. Initial interventions implementing previously recommended strategies such as MM and T_3 conditioning were deemed unsuccessful. Transfection of a

GLUT4 DNA plasmid achieved a reliable maximum 4-fold overexpression of GLUT4 protein in iPSC-CM, and whilst this increased basal glucose transport it did not enhance the lack of insulin stimulated uptake that is characteristic of these cells. A novel lentiviral vector has been generated that contains the DNA sequence for functional GLUT4 protein. Immediate future aims must be to complete the development of this lentivirus and optimise a protocol to achieve an equally robust overexpression of GLUT4 in iPSC-CM as what was achieved with a lentivirus targeting the overexpression of Syntaxin 4. Longer term aims must focus upon studying the physiological impact of enhancing iPSC-CM GLUT4 content to levels observed in primary adult cardiomyocytes, and how to use this to induce an insulin stimulate glucose uptake response, if this does not happen spontaneously.

5 The regulation of glucose uptake in models of cardiac disease

5.1 Introduction

Previous chapters have reported investigation into the regulation of glucose uptake in iPSC-CM. This is with an ultimate aim of developing a clinically relevant model of DCM. However, when examining the regulation of glucose uptake into the primary adult cardiomyocytes that iPSC-CM are designed to represent, surprisingly little is known. Given both the pathological consequences when this regulation becomes dysfunctional in IR and the need to validate iPSC-CM physiology, this is a limitation that must be addressed.

5.1.1 The importance of SNARE proteins in cardiac physiology

When considering the process of GLUT4 trafficking, as outlined in section 1.2, extensive study of relevant experimental models such as 3T3-L1 adipocytes leads us to understand that there is a significant contribution from dozens of proteins, ranging from insulin signalling intermediates and effector proteins to the glucose transporter itself. Together these facilitate an increase in glucose disposal into insulin sensitive cells in response to insulin stimulation through an increased availability of GLUT4 at the cell surface. However, aside from determining that insulin does increase glucose uptake into cardiomyocytes, many of the key details of the underlying physiological processes have not been conclusively validated in cardiomyocytes. It would seem likely that highly similar mechanisms are present across all insulin sensitive cell types, however this cannot be assumed and even apparently minor intercellular and interspecies differences may be of vital importance when considering disease phenotypes.

Understanding the regulation of the subcellular localisation of the GLUT4 containing GSVs is initially the most obvious immediate aim, however it could be argued that of even greater importance is detailing the final step of GLUT4 trafficking whereby the GSV and plasma membranes fuse. Membrane fusion is a common physiological action in a range of biological contexts that is largely dependent upon the interaction of SNARE proteins. Extensive characterisation of the experimental model 3T3-L1 adipocytes indicates that in the context of GLUT4 trafficking the formation of a stable complex between the GSV associated SNARE protein VAMP2 and the plasma membrane bound SNARE proteins Sx4 and SNAP23 is integral to catalyse the fusion of these membranes (Kawanishi *et al.*, 2000).

Within the context of this project, characterisation of SNARE protein expression in cardiomyocytes is of importance for two reasons. First of all, fatty acid induced IR in the HL-1 mouse atrial cardiac cell line was associated with redistribution of SNAP23 from the cell membrane to developing cytosolic lipid droplets (Boström *et al.*, 2007). Subsequent transfection of SNAP23 reinstated the insulin stimulated glucose uptake response by facilitating an increase in insulin induced GLUT4 plasma membrane expression back to levels recorded prior to the induction of IR. A similar phenotype was observed in human diabetic skeletal muscle samples, whereby SNAP23 was redistributed away from the cell surface relative to healthy control samples (Boström *et al.*, 2010). In these samples the expression of the accessory protein Munc18 that regulates the interaction of SNAP23, Syntaxin 4 and VAMP2 was increased, however the exact action of this protein is still debated (Laidlaw *et al.*, 2017) therefore the importance of this observation is challenging to interpret. This evidence from both a human muscle and cardiac model confirms the powerful potential of SNARE proteins to regulate insulin stimulated glucose uptake. Secondly, functional coupling between SNAP25 and cardiac potassium channels has been uncovered that opens up the possibility of a direct link between SNAREs and ion channel function, which are an integral regulator of cardiac excitability and therefore contractility (Chao *et al.*, 2011). This would give SNARE proteins an influence over both glucose uptake and contractility in the heart, both of which are perturbed in several cardiac diseases, including DCM.

5.1.2 Which SNARE proteins are expressed in the heart?

Where previous literature has investigated SNARE expression in the heart, it is mostly focussed upon the specific expression of one or two isoforms of each category (VAMP, SNAP or Syntaxin), not always within the context of a specific physiological process. For example, generic assessment of SNAP47 distribution in mouse tissues found detectable levels of mRNA in cardiac lysate (Holt *et al.*, 2006). Similarly, VAMP1 and VAMP2 mRNA was detected in rat cardiac samples (Rossetto *et al.*, 1996). Finally, investigation into the machinery that regulates atrial natriuretic hormone release from the heart reported protein expression of SNAP23, Syntaxin 4, and VAMPs 1-3 (but not SNAP25 or Syntaxin 1) in samples of neonatal rat heart (Ferlito *et al.*, 2010). Interestingly, the expression of these proteins varied between atrial and ventricular samples.

On the basis of these highly selectively targeted studies, the expression of the majority of the multiple existing SNARE protein isoforms in cardiomyocytes is ambiguous. However, there is some work that has attempted to detail the expression and interactions of a greater number of SNAREs in cardiac models at one time. First of all, mRNA encoding a wide range of SNAREs was detected in both neonatal and adult rat cardiomyocytes, including all of the known VAMP isoforms except from VAMP 7 (Peters, *et al.*, 2006). A range of Syntaxin isoforms were also identified, however the expression of Syntaxin 16 – which has been previously cited as important in the intracellular sorting of GLUT4 during its trafficking (Proctor *et al.*, 2006) – was not assessed. Nonetheless, immunoprecipitation analysis did identify the presence of 2 complexes, involving VAMP2/SNAP23/Syntaxin4 and VAMP2/Syntaxin1/SNAP25. This does not confirm beyond doubt that this first complex is indeed responsible for mediating GSV-PM membrane fusion in the heart, but does support that theory.

The most insightful prior analysis regarding this topic was performed using the mouse atrial HL-1 cardiomyocyte model. The expression of VAMPs 2-7 (VAMP6 is not recognised and VAMP8 was not detected) was identified and then subsequently each isoform was knocked down and the impact on insulin stimulated GLUT4 delivery to the cell surface and glucose uptake was assessed (Schwenk *et al.*, 2010). This revealed an important role for both VAMP2, but also VAMP5, in insulin stimulated GLUT4 trafficking in this cardiomyocyte model.

In combination, these studies provide considerable evidence that the SNARE complex previously identified as facilitating the GSV-PM interaction in other cell types may also be predominant in the heart. However, there are several important limitations in this previous work. First of all, in several studies only mRNA expression was reported for target SNAREs. It cannot automatically be assumed that this data is also reflective of protein expression, given the possibility of pre and/or post translational regulation. Secondly, where protein expression is reported, it would be more meaningful if the absolute amount of protein detected was reported, rather than a binary system of present or absent. Thirdly, the roles of different SNARE proteins may be interchangeable to at least some degree. Having a narrow focus on a restricted number of SNAREs may prevent full appreciation of the networks and interactions underlying insulin stimulated

glucose uptake. Additionally, within the described literature there was conflicting data. For example, it is not clear whether VAMPs 7 and 8 are expressed in cardiomyocytes, or not. Finally, the work mentioned was performed primarily with atrial cardiomyocytes. *In vivo*, these are outnumbered considerably by ventricular cardiomyocytes, and it is conceivable that the metabolic requirements and regulation of these subpopulations could differ due to their different contractile requirements.

Therefore, a broad characterisation of SNARE protein expression in a more representative cardiac sample would both complement previous literature and act as a guide for future studies. Analysis of changes in expression from diabetic samples could then be undertaken to assess the role of SNAREs in cardiac IR and potentially DCM. Subsequently, more specific factors such as SNARE localisation, interactions (with each other and other proteins), and their roles in various physiological processes could be fully elucidated.

5.1.3 The importance of glycemic control post-MI

When considering cardiac IR in a pathophysiological setting, the majority of individuals presenting with this phenotype will be suffering from diabetes already, or will eventually develop this condition. There are multiple causes and manifestations of diabetes, as outlined in chapter 1. In the context of SNARE protein expression, it would be of significant interest to investigate how this expression may change in a relevant model of diabetes. However, this is not the only context within which glycemic control (or a lack thereof) is of importance. There is an established – although not entirely understood – relationship between IR and MI.

An MI is defined by an occlusion of a coronary artery, which therefore starves the downstream myocardium of oxygen and nutrients. If small and/or transient, individuals confronted with this ischemic event can make a full recovery. However, a prolonged MI that blocks a major vessel supplying a large region of the heart can either cause instant death, or significantly reduce life expectancy. The regeneration capacity of the heart is limited, therefore surviving myocardium must compensate for the loss of pump capacity. This promotes a remodelling process that often leads to progressive heart failure and disruption of the tight

electrical coupling across regions of the heart as the walls of the hearts chambers become thinner, fibrotic, and ultimately less powerful.

There is a body of literature that describes an increased risk/incidence of MI in individuals diagnosed with diabetes (e.g. Laakso *et al.*, 1995). Within a separate diabetic population, an 11 year prospective study found that post-prandial systemic glucose concentration was a significant predictor of MI incidence and all-cause mortality (Hanefeld *et al.*, 1996). This association between glycemic control and risk of MI was further strengthened by the observation in a South Asian population that both fasting and post-prandial blood glucose values were significantly higher relative to appropriate controls in patients admitted to hospital for treatment of an MI, even though they were not diabetic and many of their values were well below the normal thresholds associated with diabetes (Gerstein *et al.*, 1999). This principle established is supported by evidence that uncovered a significant relationship between the presence of systemic IR and incidence of MI in a separate population at less risk of cardiometabolic disease than South Asians (Hedblad *et al.*, 2002).

It could be proposed that this phenomenon is merely observed because of an association of hyperglycemia with other factors more likely to lead to an MI, such as hyperlipidemia or hypertension. This is countered by the fact that in several of the studies mentioned above, these and other relevant variables were accounted for in the statistical analysis employed.

Characterisation of non-diabetic acute MI patients revealed a high proportion of previously undiagnosed diabetes or impaired glucose tolerance (Norhammar *et al.*, 2002). This could be used to just restate the established link between insulin sensitivity and risk of MI, however this relationship has an additional layer of complexity. For example, long term (5 year) survival post-MI is significantly worse in diabetic individuals relative to controls (Koek *et al.*, 2007). In this study it was established that short term (approx. 1 month) survival was not significantly different between groups, indicating that it was unlikely to be simply explained by diabetic individuals being at greater risk of a more severe initial cardiac injury. Rather, it appears that glycemic control may influence the subsequent long term remodelling process post-MI, which is fundamental in determining prognostic outcomes. In accordance with this, intensive insulin therapy improved 1 year post-

MI survival rates in diabetic patients, and was at least in part mediated by improved metabolic regulation as indicated by reduced levels of glycated haemoglobin (Malmberg *et al.*, 1996). However, conflicting research also indicates that regardless of the presence of diagnosed diabetes or not, an MI can induce an elevation of blood glucose concentration (stress hyperglycemia), which significantly increases short term mortality rates post-MI (Capes *et al.*, 2000). An intervention that improved metabolic control immediately post-MI in non-diabetic patients significantly improved functional outcomes, in part linked to reduced inflammation driven remodelling (Marfella *et al.*, 2009).

Overall, it is clear that the ability to regulate blood glucose concentration is important in determining the success of the recovery process post-MI. What is not clear however is whether this is due to alterations in circulating blood glucose levels directly impacting cardiac physiology, or if blood glucose concentration is just an indirect marker that indicates – but does not primarily cause – independent cardiac maladaptation. For example, it could be that systemic elevations in circulating blood glucose concentration correlate with the onset of myocardial IR, and that is what is driving the pathological remodelling process post-MI. Indeed, there is evidence from a rat model that insulin signalling is cardioprotective in ischemic myocardium and reduces cell death (Gao *et al.*, 2002). Changes in substrate availability or utilisation may also be critical under conditions of ischemic stress. It would be impractical (and possibly unethical) to record cardiac glucose uptake post-MI in human patients, however data from an animal model provides a degree of insight. Once again in a rat model, progressive myocardial IR - as indicated by impaired insulin stimulated cardiac fluoro-deoxyglucose uptake and Akt phosphorylation - was detected after only 1 week post-MI (Fu *et al.*, 2015). This myocardial IR was surprisingly not reflected in systemic glycemic control, and treatment or exacerbation of this phenotype lead to improvement or deterioration of cardiac remodelling/function respectively.

This work suggests that cardiac IR may directly influence outcomes post-MI. However, it would be beneficial to replicate these initial findings in a more clinically relevant and translatable model, for example a larger organism. Additionally, this study only recorded myocardial insulin sensitivity up to 2 weeks post-MI. Given that the importance of glycemic control has been implicated in

long term survival, it is necessary to assess if this identified cardiac phenotype extends beyond this initial acute phase. Finally, Fu *et al*. (2015) identified that TNF-α released from the ischemic myocardium and its subsequent inhibition of intracellular insulin signalling may be the mechanism by which cardiac IR occurred post-MI. However, much more work needs to be completed in order to fully detail this mechanism. In the context of this project it would be valuable to assess if cardiac SNARE protein expression changes post-MI, because as outlined before they have a unique link to the regulation of both insulin stimulated glucose uptake and cardiac contractility.

5.1.4 Aims of chapter

Overall, it is clear that there is a severe deficit in knowledge regarding the expression of SNARE proteins in healthy cardiomyocytes, let alone the role they may have in different physiological processes and cardiac disease states. Therefore, in accordance with the previous literature discussed, the following aims will be addressed;

- Identification of SNARE proteins expressed in primary cardiac tissue
- Assessment of changes in cardiac SNARE expression in diabetic models
- Assessment of insulin sensitivity in post-MI primary rabbit model
- Assessment of SNARE protein expression in post-MI rat model

5.2 Results

5.2.1 Quantification of SNARE proteins in primary cardiac tissue

As outlined in section 5.1.2., the expression of many of the known SNARE protein isoforms in cardiac tissue is ambiguous. It is the aim of this project to better characterise this expression in a general way in both health and disease, in order to act as a platform for future more detailed and specific analysis. However, based upon the prior literature there is a specific interest in SNAP23, Syntaxin 4, and VAMP2, based upon their proposed involvement in the fusion of the GSV and plasma membrane during the final step of insulin stimulated GLUT4 trafficking. Therefore, attempts were made to not only confirm the expression of these proteins in primary cardiac samples, but also to attempt quantification of absolute expression in order to allow more powerful interpretation of future work.

In order to quantify the expression of the identified SNAREs in primary cardiac tissue, first of all purified recombinant protein had to be produced in order to generate standards against which signals from known amounts of cell lysate could be compared. This production process is detailed in methods section 2.5.1. At several stages of this process samples were collected in order to assess the efficacy of recombinant protein production and elution. These samples were then subjected to SDS-PAGE and Coomassie staining. Figure 5-1 depicts a typical gel showing the presence of total protein in each of the identified samples. In this case the recombinant protein being produced was Syntaxin 16 (tagged with GST). This protein was produced within this project but not with the intention for use in this section, however it is displayed for presentation purposes because recombinant VAMP2, Syntaxin 4, and SNAP23 were previously produced by Dr. Jessica Sadler. As displayed in Figure 5-1, initial cell lysates contain numerous different proteins as would be expected from complex bacterial cells. However, after purification and elution (E1/E2), only one clear distinct band is visible in the loaded sample, which corresponds to the purified protein at the anticipated molecular weight.

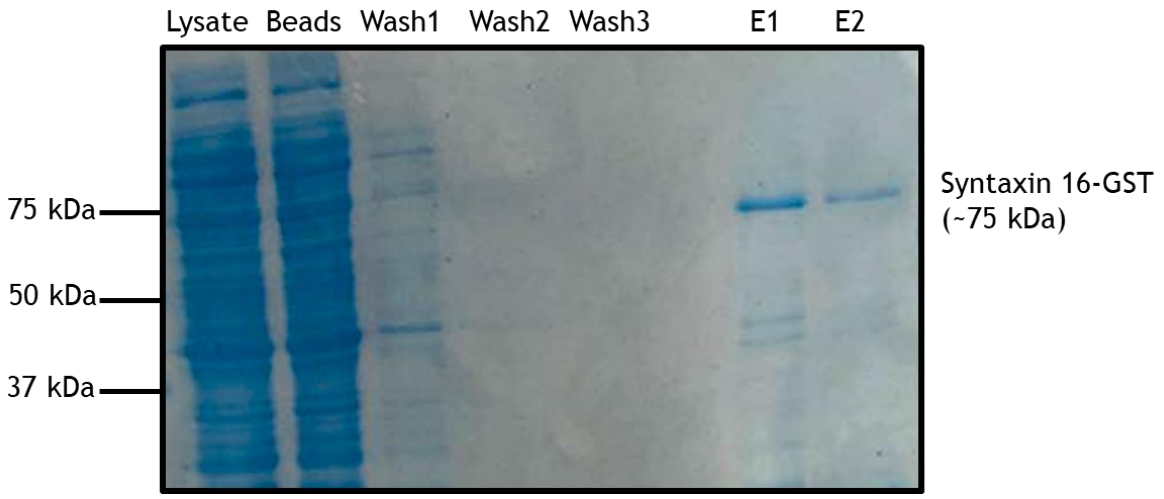

Figure 5-1 Production and purification of recombinant fusion protein
Recombinant fusion protein Syntaxin16-GST was generated according to the method described in section 2.5.1. After each of the following stages a sample was collected and then subsequently subjected to SDS-PAGE and Coomassie staining; lysate generation (Lysate), lysate after incubation with beads (Beads), 3 washes of beads (Wash1-3), 2 rounds of elution of beads (E1-2).

After obtaining recombinant purified protein samples, it was then necessary to quantify their protein concentration. This was achieved by loading several different amounts of each sample against a range of known amounts of BSA. These were once again subjected to SDS-PAGE and Coomassie staining. A representative gel is displayed in Figure 5-2, in this case depicting quantification of Syntaxin 4. Densitometry was performed and a line of best fit was produced from the BSA standard samples, plotting protein concentration against Coomassie signal intensity. The equation of this line was then used to calculate the amount of protein (and therefore concentration) of the unknown samples. Note that prior to use in this study, recombinant proteins had been cleaved of their GST tag.

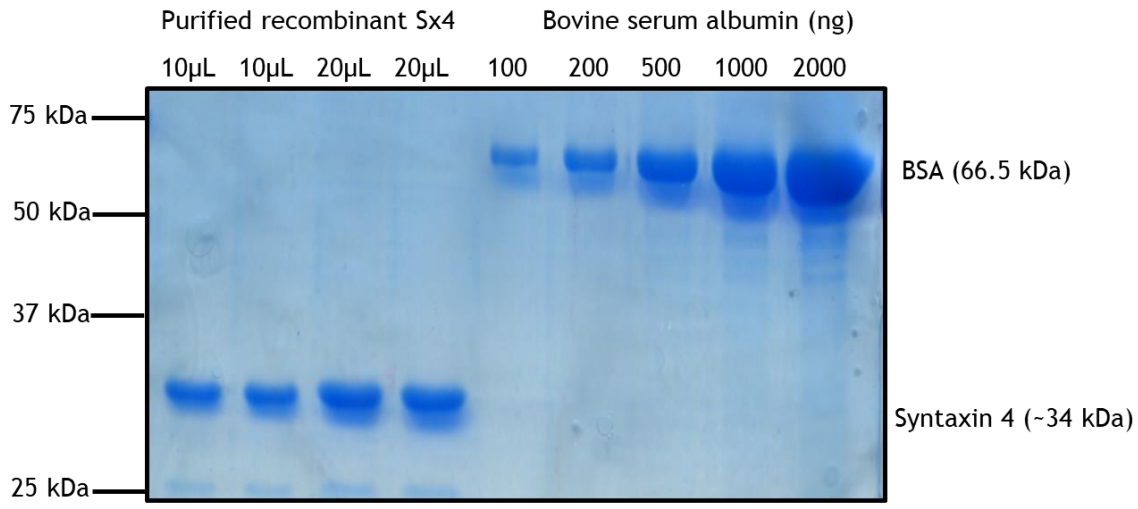

Figure 5-2 Representative quantification of purified protein
Different amounts of purified protein sample of unknown concentration were loaded against a range of known amounts of BSA and subjected to SDS-PAGE and Coomassie staining.

The final preparation step required prior to performing the ultimately intended quantification was to optimise the process of extracting protein from cardiac lysates. When considering this protocol, as described in its full final form in methods section 2.3.3.1, the step where it was most unclear from the literature and personal communications what would provide optimal results was in the process of mechanically homogenising the tissue. This step is required to expose the cardiomyocytes to physical stress in order to fully lyse these cells and liberate the intracellular proteins. Mechanical lysis was used in addition to chemical lysis (cells were also incubated with RIPA buffer) due to the highly fibrous nature of cardiac tissue and the abundance of myofilaments in each myocyte. Therefore, 2 separate homogenisation methods were used to generate 3 lysates from a total of 6 independent mouse hearts. One set of lysates was generated using the manual homogeniser method described in section 2.3.3.1., whereas the other set was generated via 2 x 1 min incubations of cardiac segments in RIPA buffer with stainless steel micro beads within a rapidly shaking plastic vial (25 Hz). All other aspects of the protocols prior and subsequent to this mechanical homogenisation step remained the same. Then protein concentration was estimated via a micro BCA assay and an equal amount of total protein was loaded for each sample. These were then subjected to SDS-PAGE and immunoblotting for different SNARE proteins.

As can be seen in Figure 5-3, there was not a striking difference in the signals obtained between lysates generated via the different methods for either Syntaxin 4 or Syntaxin 8. Both techniques were efficient at extracting protein and facilitating the detection of a clear, clean signal. However, the total amount of protein harvested from the manual homogeniser was much greater than that generated using the micro beads. Therefore, in order to maximise the potential to generate insight into the physiology of cardiomyocytes, this method was selected for future lysate generation and was employed throughout this project.

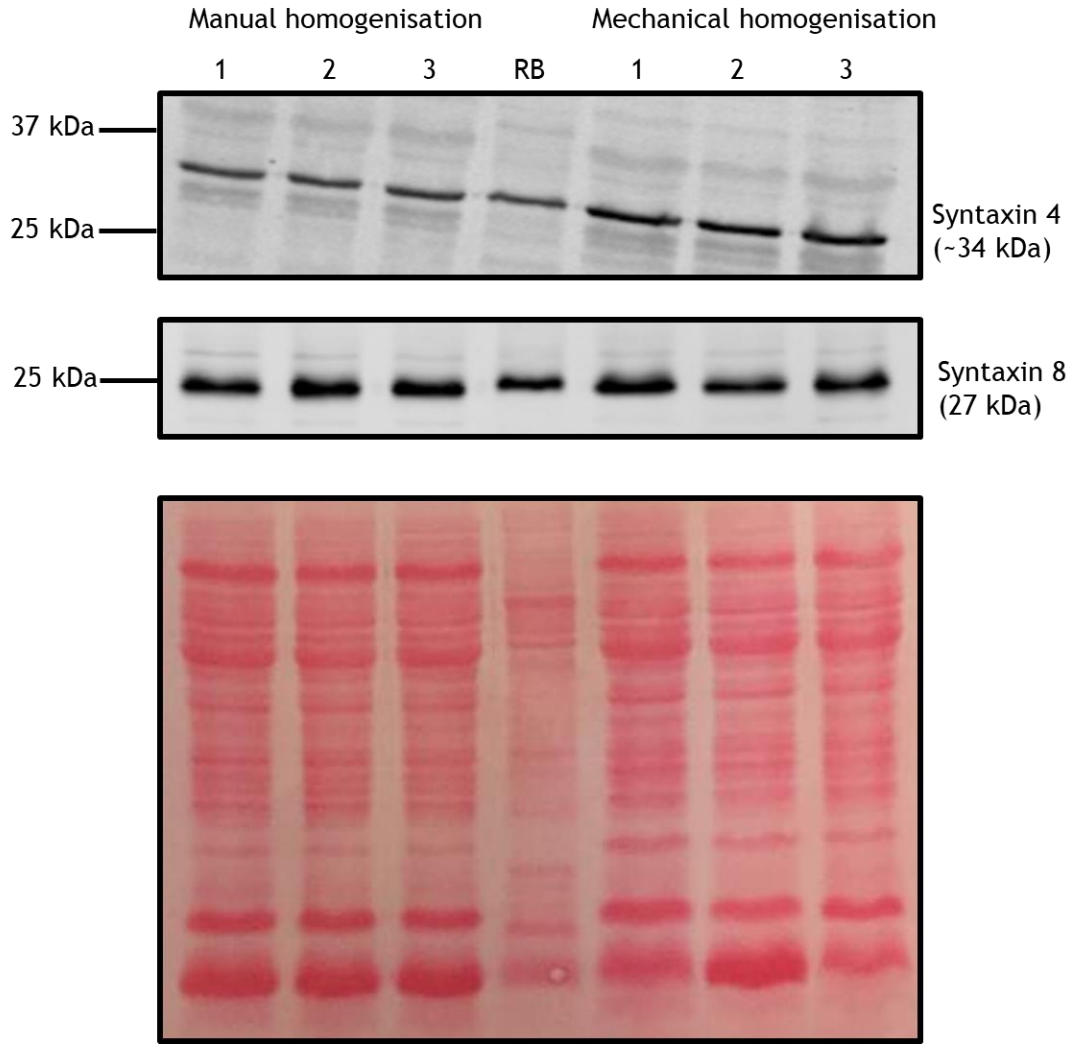

Figure 5-3 Comparison of mechanical homogenisation methods with primary cardiac tissue
6 independent mouse hearts were lysed via 2 separate homogenisation methods and subjected to SDS-PAGE and immunoblotting in order to assess the expression of Syntaxin 4 and Syntaxin 8. Manual homogenisation refers to lysates generated using a manual homogeniser apparatus, whereas mechanical homogenisation refers to lysates generated using beads within a rapidly shaking vial. In all cases, 40 µg of cardiac lysate was loaded. Rat brain lysate (RB) was also loaded in order to act as a positive control. Ponceau stain is displayed in order to indicate relative loading.

In order to quantify the expression of VAMP2, SNAP 23 and Syntaxin 4 in primary rodent cardiomyocytes, known amounts of each lysate were loaded against known amounts of each purified recombinant protein. For primary mouse samples, lysates from 3 independent hearts were analysed individually, whereas the primary rat samples are the product of 3 independent hearts that have been pooled and therefore were analysed together. For the purposes of quantification, immunoblots were subjected to densitometry and then the signal from the purified protein samples was plotted against the amount of protein loaded. A line of best fit was plotted and the equation was used to estimate the amount of the target protein present in each of the cardiac lysates. This number was then converted into number of molecules (copy number) normalised relative to the estimated total amount of protein loaded for each lysate. Where more than one amount of any given lysate was loaded, the average amount of protein detected was calculated. Finally, the average expression for each source of cardiac lysate (mouse/rat) was calculated across all samples on the immunoblot. This procedure was performed several times in an attempt to obtain signals from the cardiac lysates and purified protein within a similar range. This was successfully achieved for SNAP23 and Syntaxin 4. However, for VAMP2 the signals obtained from cardiac samples were slightly out with the range of signals obtained from the standard purified protein.

Figure 5-4 shows a representative immunoblot probing for the expression of Syntaxin 4 in both mouse and rat cardiac lysates, and samples of purified recombinant Syntaxin 4. GAPDH is also displayed in order to indicate relative loading between cardiac samples only. This protein (and any others except from Syntaxin 4) should not be detected in this purified protein sample. Table 5-1 shows the output of quantification of each SNARE protein in both mouse and rat cardiac samples.

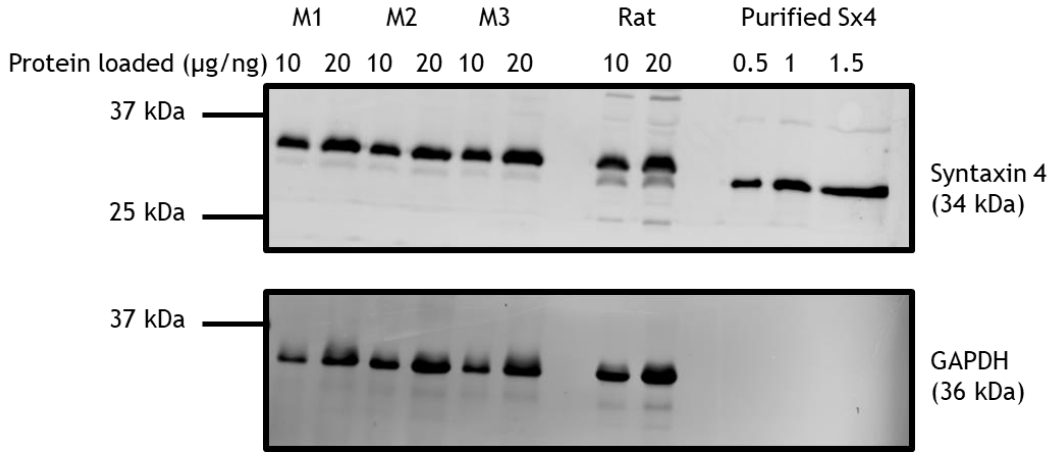

Figure 5-4 Quantification of SNARE proteins in lysates from primary rodent cardiac tissue
Cell lysates were generated from 3 individual primary mouse (M1-3) and 3 pooled rat hearts (Rat), and then subjected to SDS-PAGE and immunoblotting alongside purified recombinant Syntaxin 4 samples, probing for the expression of Syntaxin 4 and GAPDH. 10 and 20 µg of each cardiac sample was loaded, whereas 0.5-1.5 ng of purified Syntaxin 4 was loaded.

Species	SNAP23 Copies / mg	Syntaxin 4 Copies / mg	VAMP2 Copies / mg
Mouse	2.07×10^{12}	7.26×10^{11}	9.72×10^{11}
Rat	1.45×10^{12}	6.82×10^{11}	9.15×10^{11}
3T3-L1 Adipocytes	5.28×10^{12}	1.72×10^{12}	2.28×10^{12}

Table 5-1 Estimated absolute expression of key SNARE proteins in rodent cardiac lysates
Reported values are mean of signals obtained from 3 independent hearts for each species, and are expressed as copy number of each protein per mg of total protein lysate. Values for 3T3-L1 adipocytes were obtained from Hickson *et al.*, (2000).

5.2.2 Cardiac SNARE protein expression in diabetic mouse models

As outlined in section 5.1.1., SNARE proteins are vital in facilitating membrane fusion, which is a common requirement of general intracellular trafficking, including that of GLUT4. Within the context of diabetes, impaired expression of GLUT4 at the cell surface of cardiomyocytes in response to insulin is believed to have a potentially important role in the development of cardiomyopathy. Therefore, considerable work has investigated the role of deficits in insulin signalling within the context of progressive IR. However, there is a lack of research into the expression and possible roles of SNAREs in cardiomyocytes, both in a normal baseline state and within a diabetic phenotype. Therefore, in this project the protein expression of a wide range of SNAREs was probed in cardiac lysates generated from 2 well characterised diabetic mouse models, and relevant controls.

First of all, the *db*/*db* mouse model was investigated. This is a model with a mutation in the leptin receptor gene, which leads to the rapid development of obesity and changes in blood chemistry characteristic of diabetes – including hyperglycemia, hyperlipidemia, and hyperinsulinemia – within the first 6 weeks after birth (Kobayashi *et al.*, 2000). Presently, the multiple physiological changes observed in this model make it the most relevant for studying type 2 diabetes (Burke *et al.*, 2017). Of utmost importance for use within this project is the previous characterisation that hearts from *db*/*db* mice exhibit both impaired contractility and impaired insulin stimulated glucose uptake (Carroll *et al.*, 2005; Panagia *et al.*, 2007). Therefore, cardiac samples from these mice provide an ideal opportunity to study how SNARE protein expression may change in a DCM phenotype.

Figure 5-5 shows a selection of representative images generated from 6 individual *db*/*db* and *db*/*m* (relevant control group) hearts. On each immunoblot a lysate generated from a mouse brain and in some cases where appropriate also a 3T3-L1 adipocyte lysate were loaded in order to act as positive controls. However, for presentation purposes immunoblots have been cropped in order to display expression of the identified SNARE proteins (and GLUT4) only. Borders on the images indicate where cropping has occurred, but no raw data has been altered

between panels. As displayed, the expression of SNAP23 and Syntaxin 4 were clearly detectable, and did not differ between experimental groups. The expression of VAMP2 and VAMP5 appeared to increase/decrease in lysates generated from *db*/*db* hearts respectively, however when attempting to replicate these findings across independent immunoblots with the same samples, they were not reproducible. In contrast, the expression of GLUT4 was significantly ($P<0.05$) decreased in samples from *db*/*db* hearts, and this finding was reproducible. Only 5 *db*/*m* samples were assessed in this immunoblot due to sample availability. The expression of a wide range of additional SNAREs was assessed and is indicated in Table 5-2. Quantification of any potential difference in expression between groups was only undertaken when a clear, reproducible signal was visually observed, and was performed via densitometry. Signals were normalised to Ponceau to account for variations in protein loading, and where appropriate the mean percentage difference in expression is reported in Table 5-2.

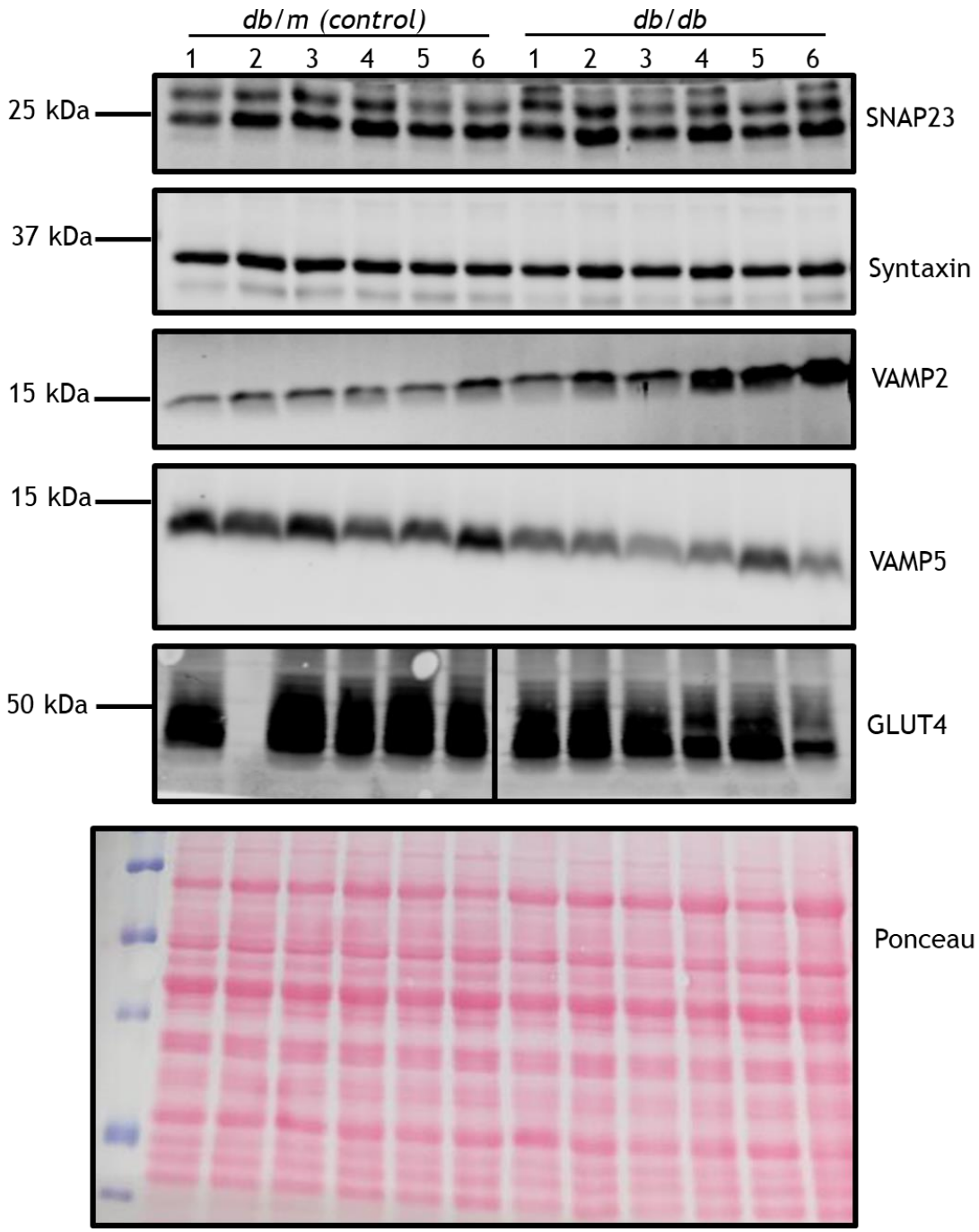

Figure 5-5 SNARE and GLUT4 protein expression in *db/db* and *db/m* cardiac lysates
Lysates were generated from myocardial segments from *db/db* and *db/m* mice and subjected to SDS-PAGE and immunoblotting, assessing the expression of a range of SNARE proteins and GLUT4. In all cases 40 µg of total protein was loaded for each lysate, and variations in loading were assessed by Ponceau staining, as displayed.

Protein	Detected?	Difference?	Protein	Detected?	Difference?
SNAP23	Yes	No	**Syntaxin 16**	Yes	No
SNAP29	Yes	No	**VAMP1**	No	N/A
SNAP47	Yes	No	**VAMP2**	Yes	No
Syntaxin 2	Yes	No	**VAMP3**	Yes	No
Syntaxin 3	Yes	No	**VAMP4**	Yes	No
Syntaxin 4	Yes	No	**VAMP5**	Yes	No
Syntaxin 5	Yes	No	**VAMP7**	No	N/A
Syntaxin 8	Yes	No	**VAMP8**	Yes	No
GLUT4	Yes	Yes, significantly (P<0.05) decreased in *db/db* lysates by 35%			

Table 5-2 SNARE protein expression in cardiac lysates from *db/db* and *db/m* mice
Where appropriate, the mean percentage difference between groups is reported. Statistical analysis was performed with a 2-tailed unpaired t-test on raw data, with the level of significance set at P=0.05.

It is a common approach to use genetically modified animal models in order to induce a desired phenotype and/or investigate the physiological action of target genes/proteins. However, this approach is open to the criticism that the data generated may have limited translational capacity when considering human disease that is primarily induced by environmental factors. In the context of diabetes research, this criticism is partly overcome by the use of high fat feeding (HFD) of rodents in order to induce obesity and a subsequent phenotype characteristic of the early stages of diabetes (Burke *et al.*, 2017). For example, in rats systemic IR was observed after only 3 weeks on a HFD, whereby 60% of total calories were obtained from fat (Kraegen *et al.*, 1991). Similar to *db*/*db* mice, in a rat HFD model impairment of both cardiac insulin signalling and contractile function were observed (Ouwens *et al.*, 2005). Therefore, HFD rodents provide a second, arguably more clinically relevant model, through which SNARE protein expression can be studied in a (pre) diabetic-like cardiac phenotype.

In accordance with this, the expression of a broad range of SNARE proteins was assessed in lysates generated from myocardial segments from HFD mice and appropriate controls (mice on a standard CHOW diet). Data obtained from Dr. Anna White indicated that these HFD mice exhibited significantly greater weight gain relative to controls and also delayed systemic glucose clearance upon challenge via a glucose tolerance test, although this latter difference was not significant between groups (data not shown). As displayed in Figure 5-6 and Table 5-3, once again a range of SNARE proteins were detected from these mouse hearts, regardless of experimental group. CHOW group 2 and HFD group 1 were lysates generated from 3 individual hearts, whereas CHOW group 1 and HFD group 2 were generated from 2 and 4 individual hearts, respectively. Where appropriate, quantification was performed in accordance with the approach detailed above for *db*/*db* mice. In lysates from HFD fed mice VAMP2 (in at least one sample) expression appeared to decrease, whereas VAMP5, SNAP23 (in one sample) and SNAP29 expression appeared to increase. Of these differences, only the increases in SNAP29 and VAMP5 were found to be statistically significant ($P<0.05$). GLUT4 expression was not reduced in this model.

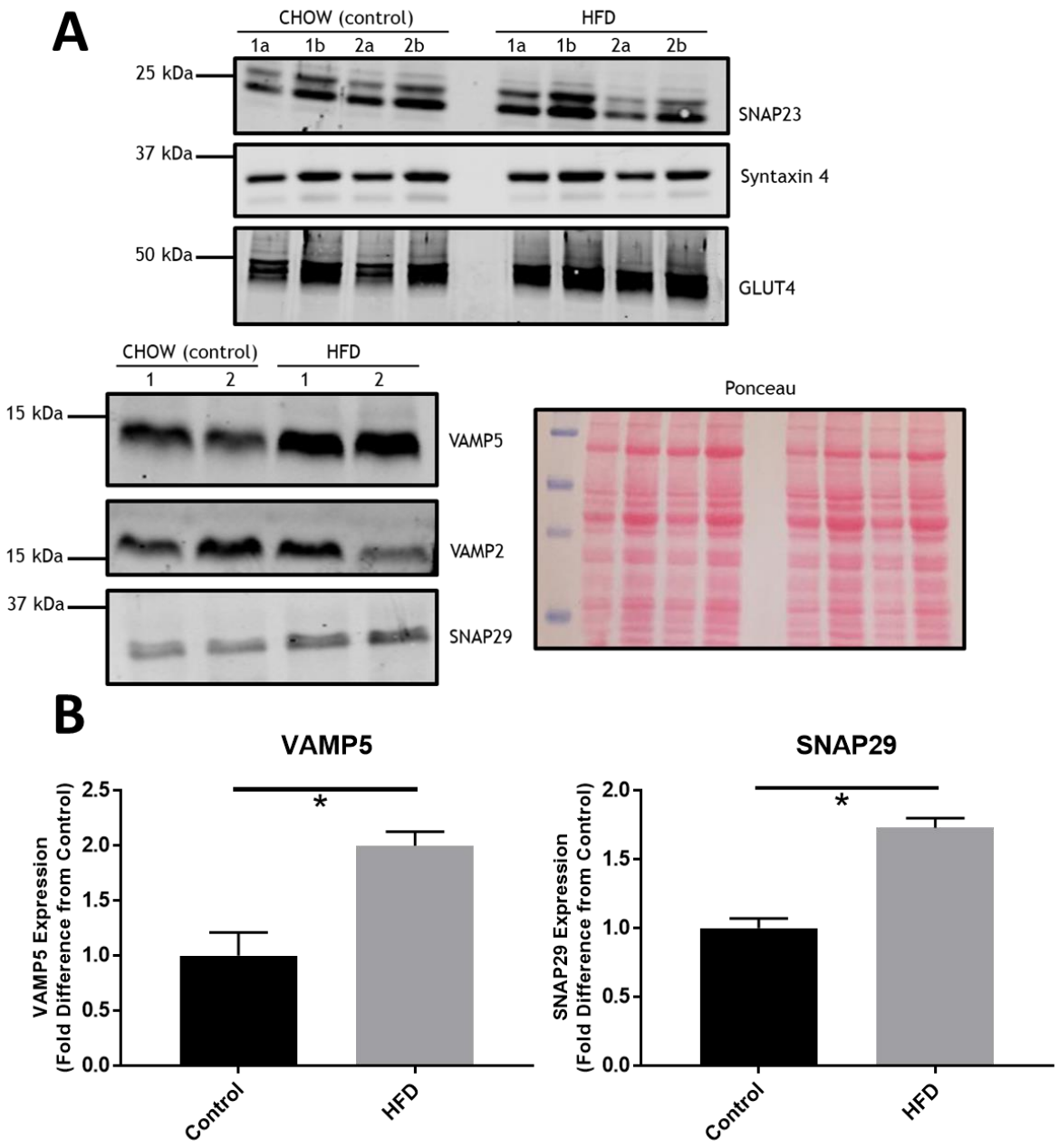

Figure 5-6 SNARE and GLUT4 expression in cardiac lysates from HFD and CHOW mice
A: Lysates were generated from myocardial segments from HFD and CHOW fed mice and subjected to SDS-PAGE and immunoblotting, assessing the expression of a range of SNARE proteins and GLUT4. In all cases 2 distinct samples were loaded for each experimental group, composed of lysates generated from 2-4 individual hearts. For blots displaying SNAP23, Syntaxin 4 and GLUT4, either 20 (a) or 40 (b) µg of total protein was loaded for each lysate. In all other blots only 40 µg of total protein was loaded for each lysate. Variations in loading were assessed by Ponceau staining, and a representative image is displayed.
B: Quantification of the immunoblots displayed for VAMP5 and SNAP29 in panel A. Values are expressed as mean (+S.D.) fold change of each protein normalised to Ponceau staining, relative to control. Statistical analysis was performed with a 2-tailed unpaired t-test on raw data, with the level of significance set at P=0.05. * denotes P<0.05.

Protein	Detected?	Difference?	Protein	Detected?	Difference?
SNAP23	Yes	15% higher expression in HFD lysates, difference was not significant (P>0.05)	**Syntaxin 16**	Yes	No
SNAP29	Yes	Yes, significantly (P<0.05) increased in HFD lysates by 73%	GLUT4	Yes	No
SNAP47	Yes	No	**VAMP1**	No	N/A
Syntaxin 2	Yes	No	**VAMP2**	Yes	23% lower expression in HFD lysates, difference was not significant (P>0.05)
Syntaxin 3	Yes	No	**VAMP3**	Yes	No
Syntaxin 4	Yes	No	**VAMP4**	Yes	No
Syntaxin 5	Yes	No	**VAMP5**	Yes	Yes, significantly (P<0.05) increased in HFD lysates by 100%
Syntaxin 6	Yes	No	**VAMP7**	No	N/A
Syntaxin 7	No	N/A	**VAMP8**	Yes	No
Syntaxin 8	Yes	No			

Table 5-3 SNARE protein expression in cardiac lysates from HFD and CHOW mice
Where appropriate, the mean percentage difference between groups is reported. Where 2 different amounts of the same sample were loaded, signals were averaged to provide 1 value per sample. Statistical analysis was performed with a 2-tailed unpaired t-test on raw data from the corresponding immunoblots displayed in Figure 5-6, with the level of significance set at P=0.05.

5.2.3 Cardiac insulin sensitivity and SNARE expression post-MI

There is strong evidence that glycemic control impacts both the risk of, and recovery from, MI (Laakso *et al.*, 1995; Koek *et al.*, 2007). However, the physiological mechanisms underlying these associations are yet to be fully detailed. A post-MI rat model (Fu *et al.*, 2015) indicated that the development of cardiac IR may be central to pathological outcomes. However, it has not been reproducibly reported in a longer term, more translatable experimental model that cardiac IR actually occurs post-MI, let alone its clinical significance when compared to other variables. Therefore, insulin stimulated glucose uptake and insulin stimulated phosphorylation of Akt was assessed in an 8-12 week post-MI rabbit model.

Prior to assessing the intended outcomes in the experimental and relevant control groups, optimisation of the [^{3}H]-2DG uptake assay that acts as a surrogate for glucose uptake was performed. As reported in chapter 3, extensive optimisation of this technique was performed with iPSC-CM, which facilitated the development of a suitable protocol for measuring uptake on a 96-well plate scale. However, primary cardiomyocytes also have unique challenges. Unlike cells that are maintained in culture prior to the day of the assay, the isolation procedure results in many cells dying or being critically damaged. Whilst there are several washing steps prior to performing the main [^{3}H]-2DG assay, a significant number of dead cells will inevitably be retained throughout the experiment, and may impact the data obtained. Of greatest concern is the potential for these cells to trap residual glucose within the wells or conversely to detach and also remove viable cardiomyocytes. Either of these events would increase the noise of this assay. Therefore, it is desirable to reduce the number of dead cells upon initial plating as much as possible.

Several factors can influence the ratio of living: dead cardiomyocytes upon plating these cells. First of all, the ‘quality’ of the isolation procedure is critical. If incubated with collagenase for too long (over digested) the chances of excessive membrane damage is high, which will greatly increase the number of cells that die. The likelihood of this being a significant problem in this project was minimal, as the isolation was performed by experienced technicians. A second important factor determining the viability of the isolated cells is the time allowed for the

cells to adapt to each level of calcium in the KRP during the stepwise progression from total absence to physiological values, as described in section 2.2.9. Rushing through these steps can lead to calcium induced overload and associated death of cells, but this was accounted for and performed appropriately. Finally, the last factor thought to be critical was which section of the heart the cells were obtained from. Due to the physical dimensions of the heart and associated blood vessels through which collagenase is perfused during the isolation procedure, it is possible that the viability of cells may vary between anatomical regions. Anecdotally, with the protocol employed in the lab, the percentage of living cells obtained seemed to be greater in the septum compared to the left ventricle, and certainly more so than from the atria. Within initial optimisation steps across separate experiments, the variability of glucose uptake between samples from the same heart and associated insulin response of septal cardiomyocytes appeared more robust in comparison to left ventricular cardiomyocytes. Therefore, these fundamental glucose uptake measurements were directly compared between cells from these regions. Atrial cardiomyocytes were never assayed.

Figure 5-7 depicts basal and insulin stimulated glucose uptake in ventricular and septal cardiomyocytes. Importantly, these cells were obtained from the same heart and assayed under identical conditions, therefore facilitating a direct comparison. Statistical analysis revealed that insulin significantly ($P<0.05$) increased [^{3}H]-2DG uptake in both groups, and that there was no significant difference ($P>0.05$) between basal or insulin stimulated values between the conditions. However, the presence of an (assumed) outlier in the left ventricular group was not an uncommon observation across all experiments with these cells (data not shown), and the extremely tight septal basal values meant that for the rest of this project it was decided to use septal cardiomyocytes.

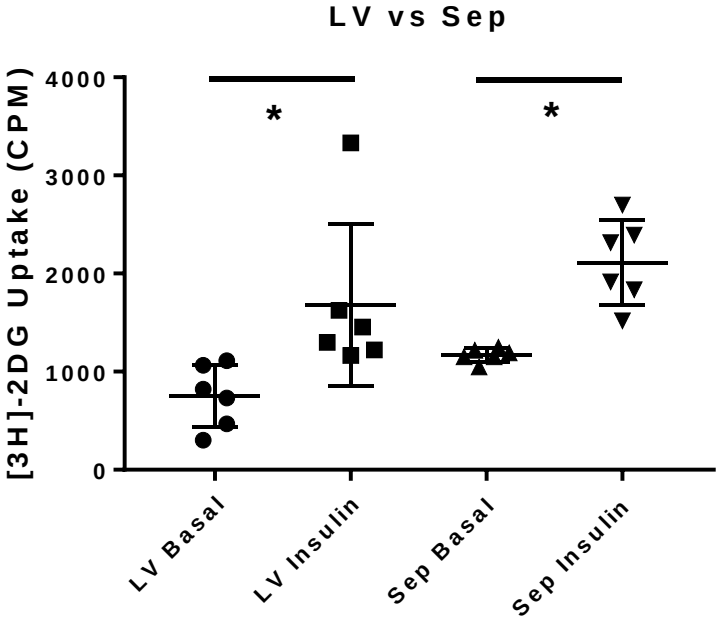

Figure 5-7 Measurement of glucose uptake in LV and septal rabbit cardiomyocytes
Background corrected basal and insulin stimulated [^{3}H]-2DG uptake was assayed in isolated primary rabbit left ventricular (LV) and septal (Sep) cardiomyocytes. Cells were plated at approximately 20,000 viable cells per well, and were incubated with 860 nM insulin for 20 min prior to a 20 min incubation with [^{3}H]-2DG. Each data point represents the value obtained from a single well, in addition to the mean +/- S.D. for each condition. Statistical analysis was performed with a 1 way ANOVA, and the level of significance was set at P=0.05. * denotes P<0.05.

After initial development of an appropriate method for measuring glucose uptake, measurements were obtained from 8-12 week post-MI rabbits and controls. Data was provided by the donors of the tissue that clearly showed that ejection fraction was impaired at 8 weeks post-MI in the experimental group, which indicated successful induction of the intended MI and subsequent heart failure phenotype (data not shown). When performing these [^{3}H]-2DG uptake assays, on each experimental day cells were plated into several wells of a 96-well plate. The number of replicate wells plated varied, but was typically 6 for each condition. This was in order to increase confidence in the responses recorded. However, for the purpose of analysis of the primary intended outcomes, the mean basal and insulin stimulated uptake value for each independent experiment was calculated. Therefore, each independent experiment carried equal weighting in this analysis process. In Figure 5-8, both individual data points (A) and summaries of each condition (B) are presented in order to provide optimal insight into the data generated. Statistical analysis revealed that there was a significant effect of MI upon the recorded uptake values ($P<0.05$). Post-test multiple comparisons found

that the effect of insulin upon uptake values in control cells strongly trended towards significance (P<0.10), however there was no significant effect (P>0.10) in post-MI cells.

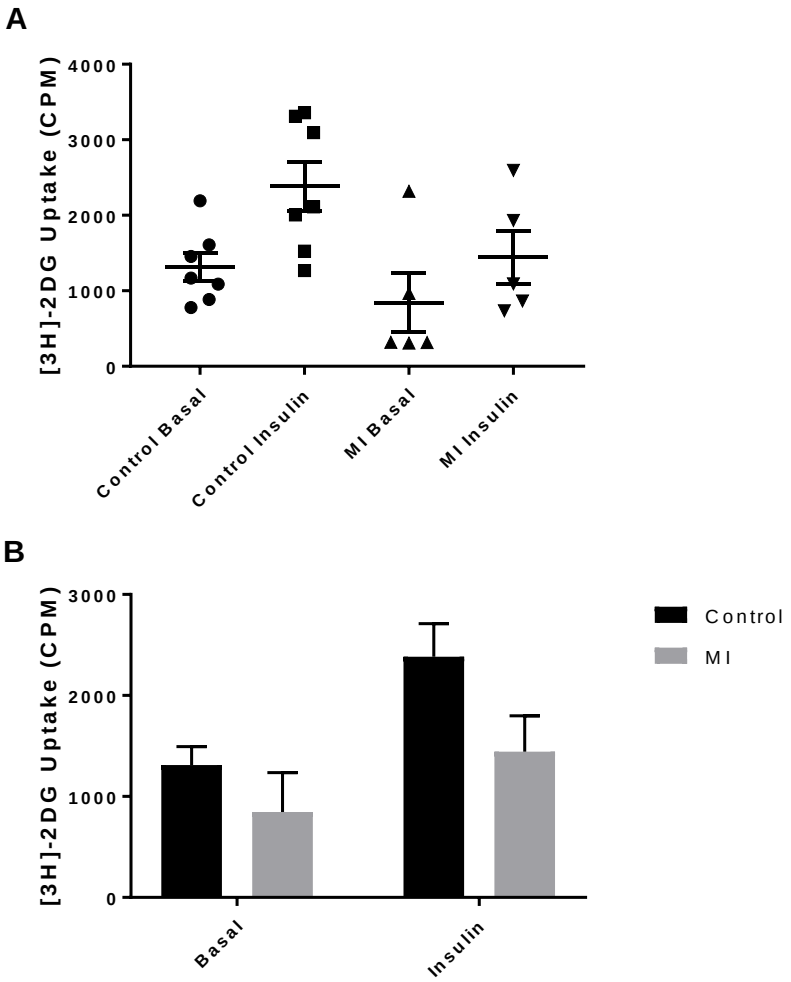

Figure 5-8 Basal and insulin stimulated [^{3}H]-2DG uptake in post-MI rabbit cardiomyocytes
Background corrected basal and insulin stimulated [^{3}H]-2DG uptake was assayed in isolated primary rabbit septal cardiomyocytes. Cells were plated at approximately 15,000 viable cells per well, and were incubated with 860 nM insulin for 20-30 min prior to a 20 min incubation with [^{3}H]-2DG. Data is presented as both individual data points and mean +/- S.E.M. for each condition (A) or only as summaries of each condition presented as mean + S.E.M. (B). Each data point represents the value obtained from a single animal. Statistical analysis was performed with a 2 way ANOVA, where the identified factors were insulin stimulation and MI. The level of significance was set at P=0.05.

In addition to assessing the impact of MI upon insulin stimulated glucose uptake, the effect upon a primary intracellular signalling target of insulin was also investigated. In total, replicate samples from a minimum of 4 independent hearts from each experimental group was assessed for phosphorylation of Akt in a basal and insulin stimulated state. As displayed in the representative images in Figure 5-9, both groups displayed a strong activation of Akt in response to insulin.

Quantification was not performed because of technical difficulties in attempts to assess the expression of total Akt, and therefore in some cases (as displayed) GAPDH was used as a loading control instead. It would not be appropriate to compare phosphorylation values obtained from normalisation against different loading controls.

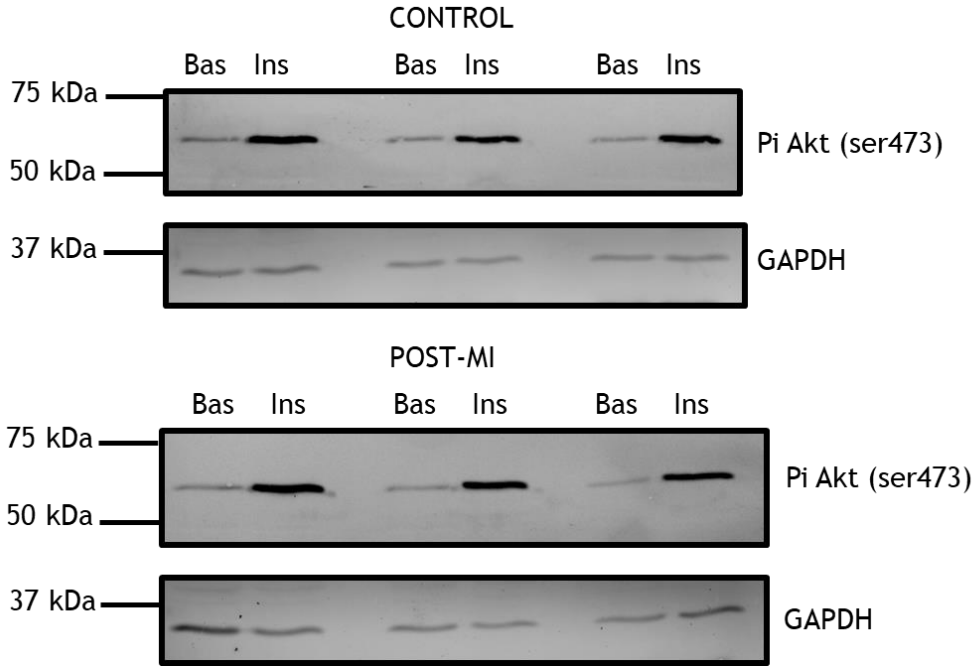

Figure 5-9 Insulin stimulated Akt phosphorylation in post-MI rabbit cardiomyocytes
Representative images depicting the expression of phosphorylated Akt (ser473) and GAPDH in lysates generated from post-MI and control isolated primary rabbit cardiomyocytes that were stimulated with 0 (Basal -Bas) or 860 (Ins) nM insulin for 20-30 min, and then subjected to SDS-PAGE and immunoblotting. These are representative immunoblots showing 3 replicate samples for each condition within one experimental day, and in total a minimum of 4 independent experiments were performed with samples obtained from separate animals. In all cases, an equal amount of total protein was loaded across samples contained within each immunoblot.

After assessing parameters related to insulin sensitivity, the impact of MI upon GLUT4 expression was assessed. For each experimental group, enough material was available to provide insight from 5 biologically independent samples. Some of these lysates were generated after plating, whereas others were generated directly after isolation, hence why there is variability in the amount of protein loaded for each sample as indicated by GAPDH. However, as depicted in Figure 5-10, there was considerable variation in the levels of expression recorded. Whilst in several post-MI samples it appeared as though expression was reduced, statistical analysis revealed no significant ($P>0.05$) difference between groups overall.

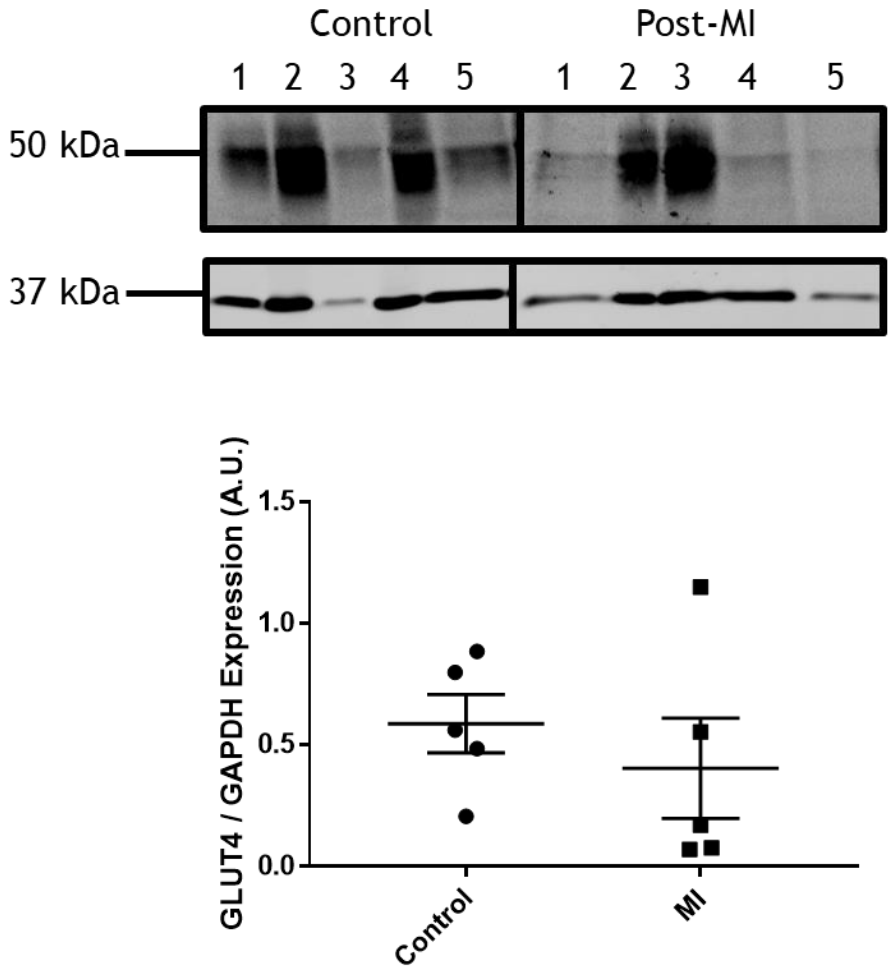

Figure 5-10 GLUT4 protein expression in post-MI rabbit cardiomyocytes
Lysates were generated from post-MI and control rabbit cardiomyocytes and subjected to SDS-PAGE and immunoblotting, in order to assess the expression of GLUT4 and GAPDH. Quantification of GLUT4 normalised to GAPDH is presented, displaying both individual data points and the mean +/- S.E.M. for each group. Statistical analysis was performed with an unpaired t-test, and the level of significance was set at P=0.05.

Finally, it was a key experimental aim to also assess the impact of MI upon SNARE protein expression. However, sample availability meant that this could not be achieved with the rabbit cells used to generate the data presented in Figures 5-7 to 5-10. Alternatively, access was provided to myocardial samples from post-MI and control Wistar rats. The induction of MI was performed according to a highly similar protocol to that of the rabbit model. Analysis of lysates generated from these rat samples was focussed upon SNARE proteins cited as being relevant to GLUT4 trafficking. As displayed in Figure 5-11, all of the target proteins were identified. However, across replicate immunoblots no clear or consistent differences were noted between groups, therefore quantification is not presented.

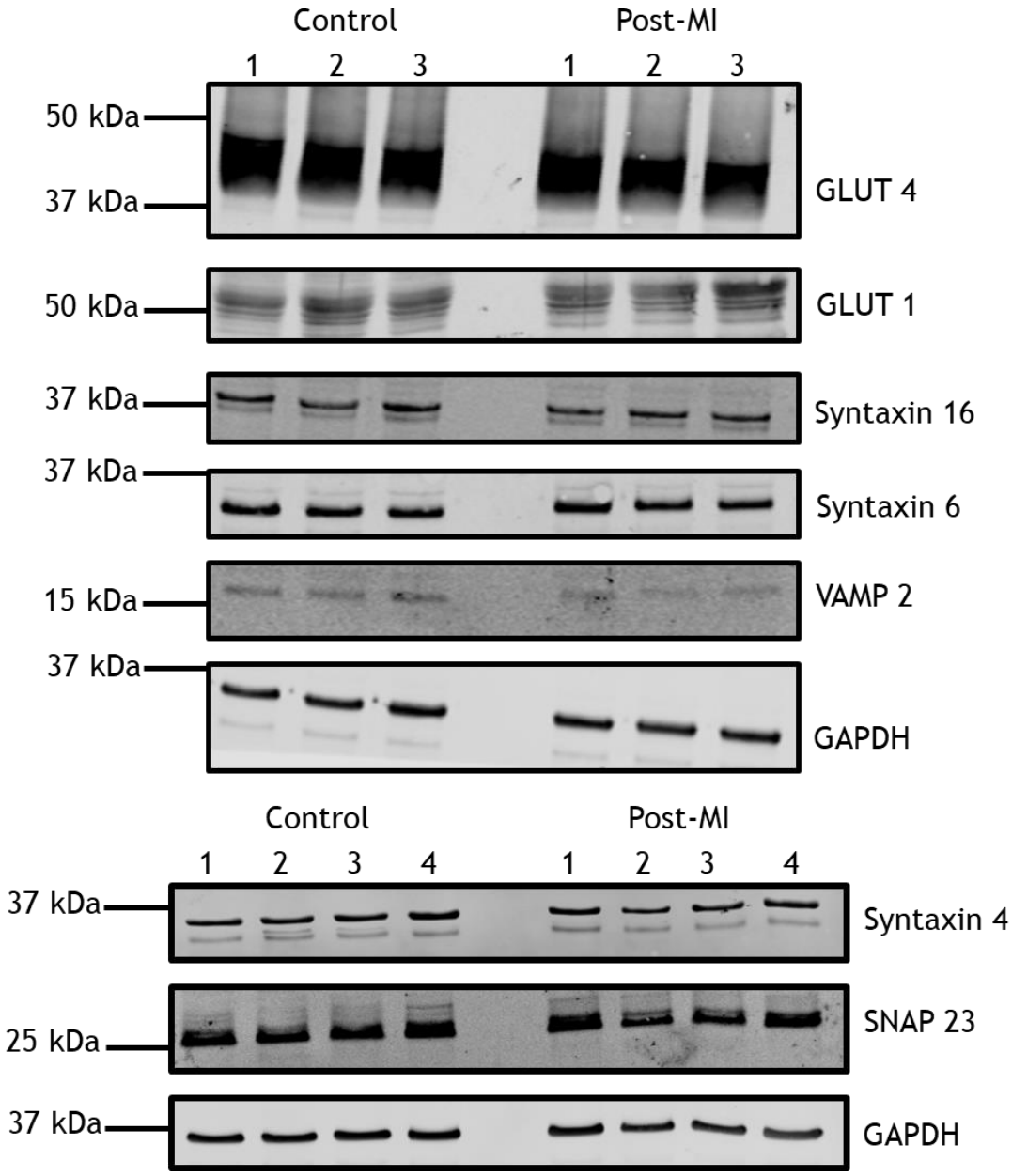

Figure 5-11 SNARE and GLUT1/4 protein expression in post-MI and control rat cardiomyocytes
Lysates were generated from post-MI and control rat cardiac segments and subjected to SDS-PAGE and immunoblotting, in order to assess the expression of a range of proteins involved in GLUT4 trafficking. GAPDH expression was also assessed to act as a loading control. Each sample number refers to lysate generated from an independent heart.

5.3 Discussion

5.3.1 Syntaxin 4, SNAP 23 and VAMP 2 are expressed to varying degrees in primary cardiac tissue

When considering the expression of the SNARE proteins Syntaxin 4, SNAP23 and VAMP2 in cardiac tissue, it would be highly valuable to not only confirm that they are present, but also to estimate their relative and absolute abundance in order to aid the interpretation of future work. As displayed in Figures 5-1 – 5-4 this was attempted in this project via the use of immunoblotting to compare signals from known amounts of purified protein against known amounts of cardiac lysate. Before consideration of the generated results, several assumptions inherent to this approach must be acknowledged. This quantification protocol involved a two-step process whereby first BSA was used as a protein standard to estimate the concentration of the generated purified protein samples, and then these samples were in turn used as standards for the cardiac lysates. Both of these processes rely on the assumption that antibody/coomassie binding and the corresponding detected signal was linear across the ranges loaded, and that the reported amount of all samples loaded was accurate. Additionally, there was an assumption that each of the 3 proteins targeted were extracted via the cell lysis procedure with high efficiency, as expression was normalised against total protein loaded. For the membrane bound SNAP23 and Syntaxin 4, this is a reasonable assumption. However, the smaller GSV bound VAMP2 is notoriously difficult to extract and detect, therefore there is a risk of underestimation of the expression of this protein.

After consideration of the noted potential limitations, there are several findings of interest. First of all, quantification of this nature has been performed previously using 3T3-L1 adipocytes (Hickson *et al.*, 2000), as displayed in Table 5-1. In these insulin sensitive cells there was similar expression levels of VAMP2 and Syntaxin 4, and 2-3 times more SNAP23. As reported in Table 5-1, the relative expression of these proteins was highly similar in primary cardiac lysates. There was very close agreement in the generated numbers between the mouse and rat samples for Syntaxin 4 and VAMP2, with a more substantial discrepancy for SNAP23. It is not clear why this was the case, however expression still exceeded that of the other 2 SNARE proteins in both species. There are several possible reasons why

SNAP23 is expressed to a considerably greater extent than Syntaxin 4 and VAMP2. For example, it may be involved in other trafficking events in addition to that of GLUT4. This would mimic the multiple roles of Syntaxin 6, which is known to interact with many other SNARE proteins (not restricted to one SNAP isoform and one VAMP isoform) and therefore contributes to the regulation of several different cellular trafficking events, in a cell type specific manner (Wendler and Tooze, 2001).

The quantification values displayed in Table 5-1 also compare favourably to the estimated quantification of GLUT4 in primary cardiomyocytes. Conversion of the value reported in Table 4-1 produced an estimated expression of 8.76×10^{11} copies of GLUT4 per mg of total protein lysate. This corresponds almost exactly to the number obtained for Syntaxin 4 and VAMP2, which is to be expected if we assume that their joint physiological role in GLUT4 trafficking in other cell types also applies to cardiomyocytes. Hickson *et al.*, (2000) reported that the total levels of GLUT4 per 3T3-L1 adipocyte were approximately 50-100% below that of these proteins. When considering the ratio of expression of each of these 3 SNARE proteins to GLUT4 transporters, it can be appreciated that this relationship will be more in favour of the SNARE proteins in 3T3-L1 adipocytes in comparison to primary cardiomyocytes. Additionally, the absolute expression of SNARE proteins was higher in 3T3-L1 adipocytes (Table 5-1). This suggests that there would be more fusion machinery available to complete the final step of GLUT4 trafficking in these cells. This could offer a potential explanation as to why 3T3-L1 adipocytes exhibit such a greater fold insulin stimulated glucose uptake response than primary cardiomyocytes (Figures 3-3 and 3-4), despite expressing less GLUT4.

5.3.2 Alterations in SNARE and GLUT4 protein expression may contribute towards diabetic myocardial IR

In order to assess the possible role of SNAREs in the insulin resistant heart, cardiac lysates from 2 different diabetic mouse models were probed for a wide range of SNARE proteins. It must be acknowledged that whilst the literature and provided supporting evidence strongly suggests that these samples are most likely to have been obtained from animals exhibiting cardiac IR induced by genetic or dietary interventions, this was not measured directly. Additionally, if we (reasonably) assume that these hearts were insulin resistant, any limitation in contractile

function and the presence of corresponding vascular disease was not assessed. Therefore, care must be taken when stating the physiological context of any findings. It is highly likely that the samples from the 2 models exhibited IR, but it cannot be stated with confidence that they exhibited a complete DCM phenotype, although it also cannot be totally discounted.

Before considering any difference between groups, it is important to first of all consider the wide range of SNARE proteins detected in these primary mouse cardiac lysates, which has been detailed in this general manner for the first time. Previous literature had reported the expression of selective SNAREs in cardiac tissue, often in non-primary models. However, as reported in Tables 5-2 and 5-3, there is in fact a wide range of SNARE machinery present in these cells. Both sets of lysates produced identical results regarding the expression of each target protein, with only Syntaxin 7, VAMP1 and VAMP7 being identified as absent in the lysates. The next logical step in a general sense must be to identify interactions between these proteins *in vivo*, before then identifying the physiological role of each complex.

As has been inferred, evidence of the expression of SNARE proteins in cardiomyocytes previously cited as important in GLUT4 trafficking – both in the internal sorting processes and GSV-PM fusion – cannot be taken as evidence that they are also exclusively responsible for regulating this process in cardiomyocytes. However, it is of particular interest that of the broad range of 19 relevant proteins assessed, the only ones that appeared to differ between diabetic samples and controls are those that were previously identified as relevant to GLUT4 trafficking (in addition to SNAP29).

When designing experiments with HFD and CHOW samples it was initially thought that pooling samples from independent hearts would be necessary in order to generate enough lysate to obtain strong signals from the target proteins. However, this was in fact unnecessary and unfortunately only served to reduce the statistical power of quantitative analysis. Whilst subjectively it appeared as though VAMP2 and SNAP23 expression may have been altered, these differences were not found to be statistically significant. In contrast, VAMP5 and SNAP29 expression were found to significantly increase in lysates from HFD mice. This is of interest as these proteins have not been previously cited (SNAP29) or conclusively demonstrated

(VAMP5) to be of significant relevance to GLUT4 trafficking. SNAP29 has been described as displaying fairly indiscriminate binding to Syntaxin isoforms and is yet to be associated predominantly with any one physiological process (Hohenstein and Roche, 2001), therefore the interpretation of these findings is dependent upon future investigation.

In cardiac lysates from *db*/*db* and *db*/*m* mice, no reproducible differences in expression of any SNARE protein was noted between experimental groups. However, a significant decrease in GLUT4 protein expression was detected in *db*/*db* lysates. This is of significance for the regulation of glucose uptake, and could largely account for the deficit in cardiac insulin stimulated glucose uptake reported in the literature from these mice (Carroll *et al.*, 2005). The observation that there was no notable difference in GLUT4 between HFD and CHOW fed mice also supports a previously introduced theory. It has been stated that HFD mice represent an early diabetic phenotype, whereas *db*/*db* mice are more similar in many aspects to a more established manifestation of this condition (Burke *et al.*, 2017). Accordingly, relatively subtle alterations in insulin signalling networks – and therefore perhaps also in SNARE expression/interaction/localisation – are likely to drive initial development of IR, whereas a reduction in GLUT4 protein content is a more permanent change that indicates progression to a more severe state of diabetes. Therefore, the changes in cardiac GLUT4 content observed within this study are consistent with the initial theory regarding the characterisation of the two employed models. Often when identified disease phenotypes are discussed and characterised we look for one explanation and mechanism, but the probability is that the different factors underlying an overall pathophysiological outcome will likely vary at different stages of disease progression.

5.3.3 Glucose transport is impaired in a post-MI rabbit model

The link between glycemic control and MI is multifaceted and complex. Of particular interest within this project is whether or not previously non-diabetic rabbits show signs of cardiac IR 8-12 weeks post-MI. This model has several benefits that make it an attractive alternative to a previously employed short term rat model. Most importantly, the size of the animal (and associated characterised cardiac physiology) and increased duration post-MI prior to obtaining measurements increase the clinical relevance.

After initial optimisation (Figure 5-7), analysis of recorded [^{3}H]-2DG uptake under identical conditions revealed a significant effect of MI upon the recorded signal. Therefore it can be concluded that MI induces a reduction in cardiac glucose uptake. An immediate concern could be that this simply reflects measurements obtained from less cells. MI would without question induce a considerable degree of cell death. However, as a reminder, these cells were plated based upon number of viable cells per well, not total number of cells. In fact based upon this it could be predicted that an increase in recorded signal may be recorded from post-MI cells due to there likely being a greater number of dead cells per well that could trap residual glucose during the course of the assay. A second concern is that cardiomyocyte isolation is itself a stressful procedure for the cells. Post-MI cells may already be in a heightened state of vulnerability, therefore subsequent exposure to this isolation procedure, in addition to radioactivity, could induce a stress response. What appears to be a reduction in glucose uptake post-MI could actually just be an enhanced stress response post-isolation. However, this is also countered by the observation that in a state of stress (e.g. ischemia) glucose uptake often increases, not decreases (Russell *et al.*, 2004). Therefore, after consideration, it can be concluded that the reduction in glucose uptake post-MI is likely a reflection of a genuine physiological adaptation.

This observation and possible explanation becomes much clearer when considering statistical post-test multiple comparisons. Although subjectively there appears to be a difference between both basal and insulin stimulated glucose uptake when comparing control and post-MI cells, these differences were not found to be significant. This may be partly linked to the variation and lower number of replicates performed in the post-MI condition, on account of sample availability. Additionally, insulin increased the recorded glucose uptake signal by a mean of 597 CPM in post-MI cells from 845 to 1443 CPM, which was not found to be a significant increase (P=0.64). In contrast, insulin increased the recorded glucose uptake by a mean of 1073 CPM in control cells from 1311 to 2383 CPM. Although this was not found to be significant (P=0.06), it can be taken as evidence that there was a considerably stronger insulin response in control cells compared to post-MI cells. Therefore it is reasonable to conclude that the overall significant effect of MI upon recorded uptake values is largely attributable to a reduction in

absolute insulin response, indicative of reduced cardiac insulin sensitivity induced by MI.

An important point to consider is that the process of recording glucose uptake from isolated cells of rabbits 8-12 weeks post-MI could create a 2-step unintended selection process that may bias results. First of all, it has been demonstrated that glycemic control in the immediate period post-MI is important for survival outcomes (Capes *et al.*, 2000). Therefore, the animals that survive to 8-12 weeks post-MI (<100%) may be less likely to have suffered from the onset of cardiac IR. However, it must be acknowledged that the predominant reason for survival or otherwise is likely to be the severity of the initial cardiac injury.

Secondly, the process of cardiomyocyte isolation is physiologically stressful, and a large number of cells will always die. It is logical that the cells that survive may be in a superior physiological condition to those that do not. Additionally, even if a heart is characterised as insulin resistant, significant heterogeneity in phenotype will still exist on the cellular level. It is entirely possible that cells that are not fully representative of the overall phenotype of the heart from which they were derived will predominate the population of isolated cells. Therefore, combined there is an overall risk of selecting the 'healthiest' cells from 'healthiest' hearts within the post-MI rabbit population, whereby in this instance 'healthiest' refers to least insulin resistant. In order to counter this risk, it would be beneficial to record whole heart basal and insulin stimulated glucose uptake in both populations at several points before and after the induction of MI.

With these limitations in mind, it can still be argued that reduced insulin sensitivity was observed in post-MI cardiomyocytes. Therefore, the underlying mechanism must be considered. The data presented in Figure 5-9 strongly suggests that an impairment of insulin stimulated Akt phosphorylation is not the issue. In isolated cardiomyocytes from both control and post-MI rabbits, a weak phospho-Akt signal was obtained in unstimulated cells. However, insulin stimulation strongly and reproducibly increased this signal several fold, in samples from all hearts assessed. It is a possibility that insulin signalling downstream of Akt may be impaired, but more often in insulin resistant myocytes deficits originate at or proximal to Akt and therefore would be expected to also impact the activation of this protein. Similarly, overall there was no statistically significant reduction in

GLUT4 protein content post-MI. Therefore this cannot be used as a general explanation for the reduced insulin stimulated glucose uptake in this group. However, when looking at individual data points, it is reasonable to suggest that this may have been a strong influencing factor in some cases.

Finally, immunoblot analysis revealed no difference in expression of the SNARE proteins primarily associated with GLUT4 trafficking in cardiac lysates obtained from post-MI and control rats. These samples were kindly donated from long term storage, as opposed to freshly isolated tissue, therefore it was not possible to assay glucose uptake and assess if they were insulin resistant or not. Based upon prior literature employing a similar protocol, it was anticipated that they would be. This analysis is particularly valuable because it confirms the data obtained from mice regarding the expression of this range of proteins in primary cardiac tissue in a second species. However, at this point the mechanism underlying IR in the heart post-MI remains unclear.

5.3.4 Methodological considerations

There are 2 additional issues to consider regarding the work discussed in this chapter. First of all, as alluded to throughout section 5.3, many assumptions had to be made regarding the phenotype of the animal models studied. Whilst prior literature and data was used to guide the interpretation of results generated within this study, it would have been preferable to confirm disease phenotypes directly through independent measurements. However, given the number of disease models (HFD mice, *db*/*db* mice, post-MI rabbit, post-MI rat) access was generously provided to, this would have required resources out with the scope of this project. Secondly, the use of Ponceau staining to solely account for normalisation of protein loading is unique to this section of the thesis. In chapters 3 and 4, when reporting data from iPSC-CM, Ponceau staining was always used during the immunoblotting procedure in order to act as a guide and ensure successful transfer. However, in almost all cases a housekeeping protein such as GAPDH was also probed for via immunoblotting in order to provide a well-recognised quantifiable loading control. The reason only Ponceau staining was used during the work described within this chapter is that at the time of study, guidelines from reputable journals were indicating that this was preferable to the use of GAPDH. However, through experience it was determined that this approach

also has many limitations. Primarily, it is challenging to image with the same quality and resolution as an immunoblot for a housekeeping gene, and staining across lanes can become uneven when washing to reduce background.

5.3.5 Conclusion and outline of further work required

In conclusion, this body of work has demonstrated that the key SNARE proteins involved in various steps in GLUT4 trafficking are present in several primary rodent cardiac models. The members of the complex believed to initiate GSV-PM fusion – SNAP23, Syntaxin 4, and VAMP2 – were found to be expressed in absolute terms at a similar ratio as previously identified in 3T3-L1 adipocytes. However, a range of additional SNAREs were also shown to be present in cardiomyocytes, therefore future work must fully elucidate the functional interactions and roles of each of these. Work using *db*/*db* and HFD mice demonstrated that cardiac GLUT4 content may be reduced only once a more severe diabetic phenotype has been attained. Alterations in SNARE protein expression do not seem to play an important role in the development of cardiac IR, however the functions of SNAP29 and VAMP5 require further study. Finally, cardiac insulin stimulated glucose uptake appears to be reduced in a clinically relevant post-MI model. Initial investigation did not indicate that any of the most obvious physiological adaptations (reduction in GLUT4 content, impaired insulin signalling) were present in these post-MI cells. Therefore, further characterisation of this model is required in order to generate novel hypotheses and molecular targets for future interventions.

6 Discussion

6.1 Key findings from this study

iPSC-CM have previously been demonstrated to exhibit cardiomyocyte like features with regards to the expression of critical genes and proteins, and also their function. However, from the various perspectives from which they have been studied, there is a strong general consensus that these cells represent cardiomyocyte physiology at a foetal or at best neonatal stage of development. This is particularly true when considering their spontaneous contractile activity on account of an unstable membrane potential, and disordered arrangement of myofilaments.

The primary aim of this thesis was to examine the potential of these cells to form the basis of a novel cellular model of DCM. In order to be suitable candidates they must meet several criteria, but of critical importance is that they exhibit an insulin stimulated glucose uptake response. Despite extensive investigation and several attempts to intervene, no robust or reproducible response was detected at any point. Several parts of the GLUT4 trafficking machinery required to elicit this response were present and activated by insulin (to at least some degree), however the critically limiting factor appeared to be a fundamental lack of GLUT4 expression. Whilst there are detectable levels of this protein in iPSC-CM lysate, it is approximately 10-fold less than what was recorded from the primary mature cardiomyocytes they are designed to mimic. Functional studies inhibiting the action of glucose transporters confirmed that the GLUT4 that is present in iPSC-CM is of limited importance to overall glucose uptake, and instead GLUT1 is predominant. GLUT1 is primarily responsible for regulating glucose uptake in foetal cardiomyocytes, therefore this data is consistent with the general characterisation of the developmental stage of iPSC-CM in the field. Of the interventions applied in this study in an attempt to increase GLUT4 content, only Lipofectamine 2000 mediated transfection was successful (3-4 fold), and yet this still did not induce an insulin response.

Through undertaking research in order to detail the *in vivo* human cardiac standard against which iPSC-CM must be compared, it became evident that there is a large deficit in the current literature regarding the understanding of the regulation of cardiac glucose uptake under baseline conditions. Within the context of DCM research, this is a serious issue. In order to counteract cardiac IR, the

mechanisms underpinning the action of insulin – in this case translocation of GLUT4 to the PM – must be fully understood. Even if a DCM model was generated via iPSC-CM, if the underlying physiology was not understood then it would not be efficient or effective to simply apply different compounds and observe their effect in the hope of increasing insulin sensitivity. Rather, it is necessary to design interventions based upon identified pathophysiological alterations, in order to enhance both the chances of success and safety of the applied intervention.

Within this project, for the first time, a wide range of SNARE proteins were demonstrated to be present in cardiac lysates generated from several rodent models. In addition to those previously cited as important in GLUT4 trafficking, several other VAMP, Syntaxin, and SNAP isoforms were identified. This is the first step of a full characterisation that is required in order to better detail intracellular trafficking within cardiomyocytes, in particular that of GLUT4. Additionally, insulin sensitivity was found to be reduced in cardiomyocytes isolated from a post-MI rabbit model. Therefore, this provides a clinically relevant model through which the complex relationship between glycemic control and MI physiology can be studied in an experimental setting. The expression of key SNARE proteins did not vary between either post-MI or diabetic (*db*/*db* and HFD) animal cardiomyocyte models and controls, however GLUT4 protein expression was reduced in the most severe (*db*/*db*) diabetic model.

6.2 Implications for previous literature

With regards to previous literature, the work most relevant to the data presented in this project was performed by Drawnel *et al.*, (2014). They claimed to not only have successfully matured iPSC-CM physiology through culturing the cells in medium depleted of glucose and instead supplemented with fatty acids, but also to have induced a DCM phenotype through subsequent addition of 'pro-diabetic' factors to the culture conditions. When diagnosing any disease, or in this case assessing whether an experimental model matches a disease phenotype, there are usually several criteria that have to be met. This is also true for diabetes, however there is one factor that is crucial and non-negotiably essential. Without the presence of IR, it is not possible to state that a diabetic phenotype is present. As discovered within this project, iPSC-CM do not increase glucose uptake in response to insulin stimulation. Therefore, it cannot be concluded from the study

introduced that a true DCM phenotype was indeed induced in iPSC-CM. If the range of other adaptations reported in response to diabetic conditioning (cellular hypertrophy, impaired intracellular calcium cycling, arrhythmic contraction) were accompanied by IR, then this model would be of utmost importance and value.

The work reported in this thesis serves to build upon extensive prior characterisation of iPSC-CM, and improve our understanding of the metabolic profile of these cells. Whilst previous study of iPSC-CM metabolism is limited, the findings from this study are complimentary. For example, iPSC-CM primarily rely upon glycolytic metabolism of glucose to generate ATP (Rana *et al.*, 2012), which is a far less productive and sustainable mechanism than the aerobic metabolism of fatty acids that predominates in the mitochondria of primary cardiomyocytes. This aspect of the iPSC-CM phenotype closely mimics foetal physiology (Werner *et al.*, 1983). The only situation in which primary cardiomyocytes would typically depend upon glucose is in a state of acute or chronic stress, such as ischemia or cardiomyopathy (Montessuit *et al.*, 1998; Dávila-Román *et al.*, 2002). Therefore, findings within this study that iPSC-CM express very high levels of the glucose transporter isoform GLUT1 and low levels of expression of GLUT4 and the fatty acid transporter CD36 are consistent with the dependence of iPSC-CM upon glucose as the primary metabolic substrate.

In general, there are two possible approaches that can be employed when developing disease models with iPSC-CM. First of all, if iPSC-CM are generated in a healthy baseline condition, then an external stimulus (or stimuli) of an appropriate nature can be applied in order to induce the desired phenotype. This is the approach employed by Drawnel *et al.*, (2014) when attempting to induce a DCM phenotype. At present, with the metabolic characteristics of iPSC-CM as described, any model of this type is of questionable relevance, regardless of the condition attempting to be replicated. Even if the primary physiological characteristic of a cardiac disease is not related to metabolism, when considering the vital role of metabolism in general cellular physiology, let alone in the adaptive process in response to disease (e.g. post-MI), if the metabolic profile of iPSC-CM is at an immature stage of development then the interpretation of data generated from any disease model with these cells becomes highly complicated. There are already several issues to address when inducing phenotypes in a cell

type over the course of a few days or weeks and claiming that they are representative of conditions that develop over a series of months or years, as is normally the case in cell culture disease models. However, if that cell type is also well characterised to be of foetal physiology, then that limitation must be overcome before any models are developed.

In contrast, disease phenotypes have also (more commonly) been studied with iPSC-CM generated from patients already suffering from certain conditions. In this instance, cells can spontaneously display a physiological deficit corresponding to the appropriate disease. For example, hypertrophy and prolonged action potential durations were recorded in iPSC-CM from individuals suffering from LEOPARD and long QT syndrome respectively, relative to controls (Carvajal-Vergara *et al.*, 2010b; Itzhaki, Maizels, *et al.*, 2011). Where the phenotype in question is believed to have a defined genetic origin and relatively non-complex physiological mechanism, the strict correspondence of all aspects of iPSC-CM to an adult phenotype is less critical. In this case, what is of more importance is that results regarding the efficacy and safety of any applied interventions translate accurately to an *in vivo* human setting. Currently, iPSC-CM are widely used to assess the cardiotoxic potential of novel drugs in development, however the reverse case of whether drugs identified as potentially effective via iPSC-CM research exhibit a high degree of off-target effects also requires assessment. Overall, the findings reported in this study enhance the interpretation of data generated via this approach, but does not necessarily impact its translational capacity.

With regards to the reported data generated with primary cardiomyocytes (chapter 5), the biggest implication regarding previous literature is to clear up ambiguities regarding the expression of certain SNARE proteins and provide a platform of characterisation that can inform a range of future research questions. Of particular note is the finding that VAMP7 protein was not detected, whereas VAMP8 was indeed found to be expressed (Table 5-2 and Table 5-3). Prior work with mouse cell lines had produced contradictory findings (Peters *et al.,* 2006; Schwenk *et al.*, 2010). Similarly, the detection of reduced cardiac insulin stimulated glucose uptake in 8-12 weeks post-MI rabbits confirms that the previously identified cardiac IR detected in rats 2 weeks post-MI (Fu *et al.*, 2015)

extends to this more clinically relevant model, and provides a suitable model upon which further theories can be tested.

6.3 What next for iPSC-CM?

Overall, the biggest contribution of this body of work for the field of iPSC-CM research has been to provide novel characterisation of the regulation of glucose uptake in these cells, and indicate initial steps towards developing techniques that may increase cellular GLUT4 content and thereby possibly also induce an insulin response. Based upon this and an abundance of prior data considering other aspects of iPSC-CM physiology, the most pressing requirement for the future of research with these cells is the development of effective maturation strategies.

The term maturation can be interpreted in many different ways. The physiological maturity of a cell is not defined by any single parameter, but rather by the combination of all aspects of its gene/protein expression, structure, and function. An argument could be made that maturation of the metabolic phenotype is of primary importance, due to the critical role metabolism plays in numerous processes in every cell. Specifically, enhancing GLUT4 protein content could have knock on effects for iPSC-CM substrate utilisation and ATP generation, which in turn could enhance calcium cycling and contractility and therefore generate an increased demand for improved efficiency of myofilament organisation and electrical activation. However, due to the current unmet clinical need for treatments targeting cardiac disease and therefore the demand for development of superior testing platforms and disease models, ultimately maturation of iPSC-CM via any successful method is desirable.

An important principle was established during the course of this project, which was the importance of quantification of both the current iPSC-CM and the intended adult cardiomyocyte phenotype. As displayed in Figure 4-1 and Figure 4-2, the levels of GLUT1 and GLUT4 were estimated in both iPSC-CM and primary mouse cardiomyocytes. This permitted estimation of the absolute change in transporter expression required to achieve parity between phenotypes. This principle must be applied to other areas of iPSC-CM biology, and a range of standard principles agreed upon. This would turn the maturation of iPSC-CM into a quantifiable process, whereby values for the crucial identified parameters must

fall within the agreed standard range. Of course across a population of hearts, or even within a population of cardiomyocytes from the same heart, there is significant heterogeneity in phenotype between individual cells. However, through robust study of the gold standard human primary cardiomyocyte model, an appropriate range of acceptable standards can be generated. As introduced in chapter 5, the understanding of the regulation of glucose transport is not fully elucidated in the human heart, and this is undoubtedly true for other areas of study. Therefore further work is required to both clearly define these standards, and then properly move iPSC-CM towards the identified phenotype.

The big question that requires answering is how iPSC-CM maturation will ultimately be achieved. Arguably the most promising advances with iPSC-CM have come from development of the capacity to insert these cells into the hearts of various animal models *in vivo,* as they integrate effectively to form contractile grafts that have a meaningful effect on cardiac function (Shiba *et al.*, 2012). Logically, given that culture conditions designed to induce iPSC-CM maturation mimic this *in vivo* environment, it may be the case that this insertion protocol is also optimal to produce maturation of these cells. However, we cannot insert cells into a human (or any other species) heart, and then re-extract the cells at an appropriate time simply for the purpose of maturation. The number of cells that could be harvested from this approach would render this approach both highly inefficient and unethical. Therefore, advances must originate from within cell culture based approaches.

The most up to date research using approaches introduced and/or utilised within this project are still showing progress. For example, culturing iPSC-CM in the presence of thyroid and glucocorticoid hormones during the initial differentiation period and subsequent transfer to a specially designed extracellular matrix induced the development of T-tubules, a critical feature normally lacking in these cells (Parikh *et al.*, 2017). T-tubules are invaginations of the cell membrane that are critical for enabling uniform excitation across the whole cell. Accordingly, the timing of intracellular calcium release between different areas of the same cell became more synchronous in response to this intervention, unlike in control cells where areas closer to the myocyte membrane reached peak calcium concentration more rapidly. Interestingly, T_3 was applied at a concentration of 100 nM, which is

almost 10x greater than what was utilised during work reported in this thesis. This suggests that previously recommended concentrations may have been suboptimal for the purposes of iPSC-CM differentiation. The authors also highlighted the potential importance of not only utilising appropriate stimuli, but also applying them in a specific order and only at appropriate times during the differentiation process.

Despite this reported success, it was conceded that T-tubule density and orientation was still not fully representative of mature adult cardiomyocytes, and instead corresponded to that of early post-natal cells. Therefore, additional progress is still required, which may necessitate further innovation and development of novel techniques. Certainly, from the literature and evidence generated within this thesis, it seems unlikely that simply maintaining iPSC-CM within a 2D culture environment and exposing them to relevant stimuli thought to regulate cardiac development *in vivo* will be sufficient to induce the desired phenotype. The observation that primary cells tend to dedifferentiate *in vitro* perhaps gives insight into the importance of the immediate structural and biomechanical environment for cellular physiology, particularly in an organ such as the heart where functional capacity is so dependent upon organ level structure. These issues are partly addressed in the principles underlying 3D cell culture, however this idea needs to be extended and developed further. For example, perhaps a micro scaffold of suitable material could be devised within which iPSC-CM could be inserted, whilst still permitting the regulation of the hormonal and metabolic environment. Critically, if excitation and rhythmic stretching of the simulated chambers could be induced then this would generate a highly representative artificial environment. Once a successful model was generated, the underlying principles could be adapted to enable a high throughput system amenable to generation of the substantial numbers of cells required to power significant amounts of research.

Accordingly, the most successful recent iPSC-CM maturation based research published utilised a similar approach to that just described, within the realms of current technological limits. Ronaldson-Bouchard *et al.*, (2018) generated a protocol whereby as soon as spontaneous contraction was detected in iPSC-CM they were used to form a section of cardiac tissue in combination with fibroblasts

within a hydrogel, which could be subjected to both external stretch and excitation. Importantly, the frequency of contraction of iPSC-CM can be easily regulated, but the corresponding force cannot be. The authors reported that initiating pacing at the earliest possible point, and inducing progressively higher workloads (from 2-6 Hz over 3 weeks), successfully induced structural and metabolic maturation. Critically, they provided quantification that detailed iPSC-CM sarcomere length had elongated to 2.2 μM and mitochondrial density had increased to 30% of total cell area, distinct values associated with adult cardiomyocytes. Further evidence such as increased oxygen consumption was provided to display that metabolism had shifted to a more predominantly oxidative form, however no information was provided regarding GLUT4 or insulin sensitivity. Critically, whilst several parameters of excitation contraction coupling indicated maturation had occurred – including a decrease in resting membrane potential and the overall shape of the subsequently generated action potential – the improvement in contractile force generated was still far below values recorded from primary tissue in absolute terms. Therefore whilst this technique achieved significant progress, it still requires further optimisation.

The alternative to physiological stimulus based iPSC-CM maturation is to use biomolecular tools to artificially manipulate the phenotype of iPSC-CM. In accordance with this, significant steps were taken towards the development of a lentivirus capable of increasing iPSC-CM GLUT4 protein expression, as reported in section 4.2.5. This is on the premise that a fundamental lack of GLUT4 protein expression is primarily limiting progression to a more mature metabolic status in these cells. Other physiological adaptations are also required, however increasing GLUT4 protein expression in appropriate tissues is a cornerstone of postnatal development, and may act as a trigger to induce these other changes within this experimental context.

There are several benefits to utilising this approach. Most importantly, there is preliminary evidence to suggest that it can be successful in inducing GLUT4 protein expression to the levels recorded in primary adult cardiomyocytes. As displayed in Figure 4-20, iPSC-CM are susceptible to the strong overexpression of proteins via this technique (in this case Syntaxin 4). Additionally, the GLUT4 gene sequence at the core of the novel pCDH-GLUT4 plasmid (Figure 4-23) has already been

demonstrated within this project to effectively produce this protein within iPSC-CM. With packaging into a more effective delivery method (lentivirus) it is anticipated that this will facilitate the approximate 10-fold overexpression of GLUT4 protein that is required. This approach is also efficient from a practical experimental point of view. After inevitable initial optimisation, sufficient overexpression of GLUT4 protein in iPSC-CM via lentivirus will be achievable within 1 week post-plating via a protocol primarily dependent upon 1 variable (the continued efficacy of the lentivirus). This provides a relatively fast and simple technique to provide reproducible and robust outcomes, in contrast to a prolonged complex (and probably more expensive) protocol involving multiple factors e.g. different hormones and culture conditions.

The main limitation of this approach is that it is highly targeted, rather than activating multiple intracellular signalling pathways in a manner analogous to certain relevant hormones. However, as alluded to, enhancing the metabolic phenotype of iPSC-CM may have positive follow on consequences for other areas of their physiology. Additionally, in all other major physiological processes within cardiomyocytes, either no single protein is primarily responsible for regulating that process, or where there is indeed one single protein responsible, it is present in iPSC-CM. In contrast, when considering insulin stimulated glucose uptake, cellular GLUT4 protein content is by far the most important factor. Therefore if any protein is to be selectively targeted in this manner, GLUT4 is an ideal candidate. Even if this approach does not result in global maturation, at minimum it would significantly advance our knowledge of the role of GLUT4 in cardiac biology. Alternatively, if an insulin stimulated glucose uptake response were induced by this approach it would transform our capacity to study the causes and mechanisms of cardiac IR.

6.4 What next for the study of DCM?

When considering the future of DCM research, the issue remains regarding a lack of a suitable experimental model. The maturation of the metabolic profile of iPSC-CM is of utmost importance for this area of study, as they are by far the best candidate for the basis of any novel cellular model. More generally, in order to identify the areas relevant to this topic demanding immediate attention, the ultimate end goal must be considered, and then strategies can be devised to

bridge the gap from our current position. Clearly the overall aim of this research area must be to generate novel treatments that improve cardiac function in individuals suffering from DCM, in order to improve prognostic outcomes associated with the diagnosis of diabetes. When considering novel treatments, often the assumption is that this refers to novel pharmacological interventions targeting specific molecular mechanisms identified through prior research. This is a valid approach, however in this instance there may be an alternative strategy.

DCM is a limitation of metabolic flexibility and contractile capacity in the heart. Arguably, the most potent stimulus to activate (acutely) and adapt (chronically) these factors in skeletal and cardiac muscle is exercise. This observation is the basic principle underlying the training of endurance athletes in a range of sports, where the objective is to develop the capacity to compete at high intensities for prolonged periods of time. In a clinical setting, exercise training has been shown to enhance whole body aerobic capacity and quality of life in patients after coronary artery bypass surgery (Moholdt *et al.*, 2009). Similarly, several animal models have demonstrated the capacity of exercise to enhance/preserve cardiac function post-MI (de Waard *et al.*, 2007; Wan *et al.*, 2007). Of specific interest to this field of research is that exercise training protocols have also been found to restore cardiac/cardiomyocyte contractile function in the *db*/*db* mouse model (Stølen *et al.*, 2009; Wang *et al.*, 2015). These studies cited changes in the activation of PGC-1α, Akt, CamKII and PKA as contributing towards the normalisation of intracellular calcium handling and reduced cardiac fibrosis, however interestingly did not report any accompanying changes in whole body glucose homeostasis.

This preliminary rodent data strongly suggests that targeted exercise programmes could be a valuable treatment option in patients with DCM. However, this work still raises several questions. First of all, it is notable that neither of the papers mentioned reported improvements in metabolic markers. This is surprising, given that in humans exercise training has previously been shown to increase skeletal muscle GLUT4 protein content and whole body insulin sensitivity (O'Gorman *et al.*, 2006). A major challenge when attempting to interpret the significance of exercise based interventions in rodents for the application to human disease settings is that often the intensity and/or duration of stimulus applied is

unrealistic to attain in humans, particularly those that are poorly conditioned. For example, Stølen *et al.*, (2009) designed an intervention whereby mice ran 4 minute intervals at 90% of VO_{2max} with 2 minutes recovery for 80 minutes per day, 5 days per week. In humans this intensity would almost certainly be above the lactate threshold, therefore even well trained individuals would struggle to complete one of these sessions, let alone repeatedly over 5 consecutive days for 13 weeks.

One of the foundational principles of exercise training is specificity, whereby any stimulus applied elicits a specific response. The evidence introduced thus far indicates that exercise training has the capacity to improve contractile and metabolic outcomes in muscle, in individuals suffering from disease. Immediate future aims must be to perform clinical research in order to examine which protocols (duration/intensity/modality) are optimal to alleviate the symptoms of DCM. In order to achieve this, the mechanisms by which exercise can induce adaptation must be fully elucidated. Significant progress has already been made in this area. For example, increased calcium cycling during exercise activates CamKII, which has several downstream targets in order to enhance myocyte contractility, for example the SERCA inhibitor phospholamban (Rose *et al.*, 2006). In addition to regulating the acute response to exercise, inhibition of CamKII was also found to nullify exercise training induced improvements in cardiomyocyte contractility in a mouse model (Kemi *et al.*, 2007). However, there are several more theories and mechanisms that require investigation.

Of greatest interest to the themes discussed within this thesis is evidence that SNARE proteins and ion channels may in some cell types be functionally coupled. For example, preliminary data indicates that complex formation involving SNAP25 and Syntaxin 1 may directly regulate the activation of the voltage gated potassium channel (Kv2.1), which ultimately is critical to the release of insulin from pancreatic beta cells (Wolf-Goldberg *et al.*, 2006). Interestingly, extensive work by Chao *et al.*, (2011) indicates that a similar mechanism may be active in cardiomyocytes. They propose that SNAREs directly regulate the expression and excitability of Kv channels at the myocyte membrane, therefore having the potential to impact the overall membrane potential. Significant questions arise, for example if there is a similar regulation by SNAREs of membrane bound calcium

channels, given the critical role of calcium influx to excitation contraction coupling. Logically it would be efficient to have a mechanism of coupling an increase in glucose uptake with increased metabolic demands associated with contraction (and therefore increased excitation). The action of SNARE proteins in mediating GLUT4 trafficking and membrane excitability would achieve this aim, and would also have profound implications for the relevance of SNARE proteins in cardiac function both in health and disease.

6.5 Conclusion

Overall, this thesis has detailed several novel findings regarding the regulation of glucose uptake in iPSC-CM, and the efficacy of several interventions designed to achieve increased GLUT4 protein content and metabolic maturation. The progression of these interventions will be critical in attaining the ultimate experimental goal of developing a novel cellular model of DCM. The future of iPSC-CM research in general relies upon novel maturation strategies, in order to increase the clinical relevance of work performed with these cells. However, significant progress has been achieved since their initial development, and interest in these cells is constantly expanding due to their potential. Similarly, novel mechanisms that regulate metabolism and contractility in the heart are still being uncovered, and will continue to inform future strategies contributing to the development of novel therapeutic interventions for the treatment of DCM.

7 Appendices

7.1 Assessment of GAPDH as a loading control for immunoblotting of cardiac lysates

In order to determine the validity of using GAPDH expression as a representative marker of total protein loading in lysates generated from 3T3-L1 adipocytes, iPSC-CM, and primary mouse and human cardiomyocytes, two amounts of each lysate were probed for total protein expression and this was compared to generated GAPDH signals. It was determined that GAPDH expression should reflect relative differences between both different amounts of the same lysate, and also between lysates from different cell types. Qualitative analysis concluded that GAPDH was a robust representative of total protein for 3T3-L1 adipocytes and primary mouse cardiomyocytes. It was also considered acceptable for use with iPSC-CM, however it may slightly overestimate the total protein loaded. In contrast, there was a great disparity between the GAPDH signal obtained and total protein signals for primary human cardiomyocyte lysates.

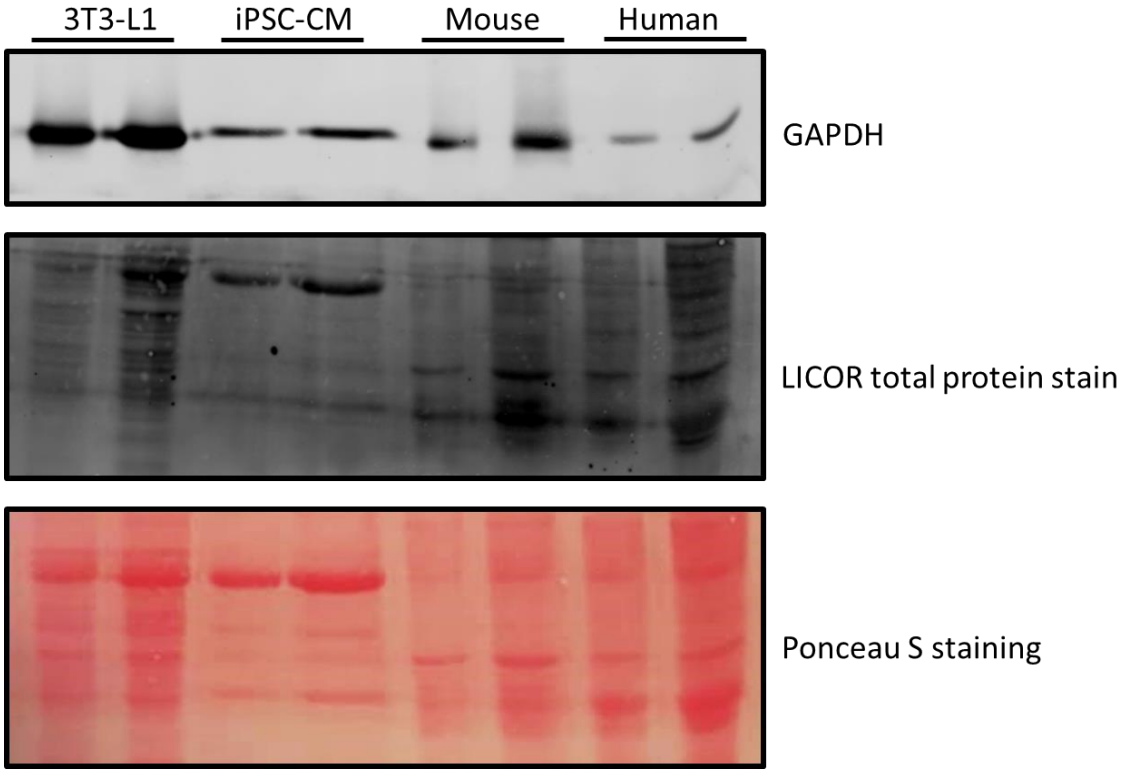

Figure 7-1 Assessment of GAPDH expression as a surrogate marker of total protein loading
Lysates from 3T3-L1 adipocytes, iPSC-CM, primary mouse cardiomyocytes, and primary human cardiomyocytes were subjected to SDS-PAGE and transferred to a nitrocellulose membrane. Ponceau S stain was applied, prior to immunoblotting for GAPDH. Subsequently the blot was stripped and reprobed with a specialised LICOR total protein stain and imaged via the LICOR imaging system. For all samples, 2 amounts of lysate were loaded (1x, 2x), corresponding to the range loaded during quantification of GLUT1 and GLUT4 in these cell types as reported in section 4.2.1.

7.2 Basal and insulin stimulated glucose uptake in 3T3-L1 adipocytes in the presence of GLUT1 and GLUT4 inhibition

Condition 1	Value 1	Condition 2	Value 2	95% CI of difference	Significant?	P value
Control Basal	3201	**Control Insulin**	9887	-7279 to -6093	Yes	<0.0001
20 nM Basal	2479	**20 nM Insulin**	6418	-4532 to -3346	Yes	<0.0001
2 µM Basal	38	**2 µM Insulin**	451	-1006 to 179	No	0.3229
Control Basal	3201	**20 nM Basal**	2479	129 to 1315	Yes	0.0086
Control Basal	3201	**2 µM Basal**	38	2570 to 3756	Yes	<0.0001
20 nM Basal	2479	**2 µM Basal**	38	1848 to 3034	Yes	<0.0001
Control Insulin	9887	**20 nM Insulin**	6418	2876 to 4062	Yes	<0.0001
Control Insulin	9887	**2 µM Insulin**	451	8843 to 10028	Yes	<0.0001
20 nM Insulin	6418	**2 µM Insulin**	451	5373 to 6559	Yes	<0.0001

Table 7-1 Summary of key statistical outcomes from [^{3}H]-2DG uptake assays in 3T3-L1 adipocytes in the presence of BAY-876
Data displayed is output of post-test multiple comparisons following a 2-way ANOVA, where the identified factors were experimental day and drug treatment. Values expressed are mean of all replicates for each condition across 3 independent experiments, recorded in CPM.

List of References

Abel, E. D. *et al.* (1999) 'Cardiac hypertrophy with preserved contractile function after selective deletion of GLUT4 from the heart', *Journal of Clinical Investigation*, 104(12), pp. 1703–1714. doi: 10.1172/JCI7605.

Adams, J. M. *et al.* (2004) 'Ceramide content is increased in skeletal muscle from obese insulin-resistant humans.', *Diabetes*, 53(1), pp. 25–31.

Aerni-Flessner, L. *et al.* (2012) 'GLUT4, GLUT1, and GLUT8 are the dominant GLUT transcripts expressed in the murine left ventricle.', *Cardiovascular Diabetology*. BioMed Central, 11, p. 63. doi: 10.1186/1475-2840-11-63.

Ahmed, Z. and Pillay, T. S. (2003) 'Adapter protein with a pleckstrin homology (PH) and an Src homology 2 (SH2) domain (APS) and SH2-B enhance insulin-receptor autophosphorylation, extracellular-signal-regulated kinase and phosphoinositide 3-kinase-dependent signalling.', *The Biochemical Journal*, 371(Pt 2), pp. 405–12. doi: 10.1042/BJ20021589.

del Álamo, J. C. *et al.* (2016) 'High throughput physiological screening of iPSC-derived cardiomyocytes for drug development', *Biochimica et Biophysica Acta (BBA) - Molecular Cell Research*. Elsevier, 1863(7), pp. 1717–1727. doi: 10.1016/J.BBAMCR.2016.03.003.

Aledo, J. C. *et al.* (1997) 'Identification and characterization of two distinct intracellular GLUT4 pools in rat skeletal muscle: evidence for an endosomal and an insulin-sensitive GLUT4 compartment.', *The Biochemical Journal*, 325 (Pt 3, pp. 727–32.

An, D. and Rodrigues, B. (2006) 'Role of changes in cardiac metabolism in development of diabetic cardiomyopathy', *American Journal of Physiology-Heart and Circulatory Physiology*. American Physiological Society, 291(4), pp. H1489–H1506. doi: 10.1152/ajpheart.00278.2006.

Andersen, N. H. *et al.* (2003) 'Decreased left ventricular longitudinal contraction in normotensive and normoalbuminuric patients with Type II diabetes mellitus: a

Doppler tissue tracking and strain rate echocardiography study', *Clinical Science*, 105(1), pp. 59–66. doi: 10.1042/CS20020303.

Anderson, M. E., Brown, J. H. and Bers, D. M. (2011) 'CaMKII in myocardial hypertrophy and heart failure', *Journal of Molecular and Cellular Cardiology*. Academic Press, 51(4), pp. 468–473. doi: 10.1016/J.YJMCC.2011.01.012.

Arai, M., Matsui, H. and Periasamy, M. (1994) 'Sarcoplasmic reticulum gene expression in cardiac hypertrophy and heart failure.', *Circulation Research*, 74(4), pp. 555–564. doi: 10.1161/01.RES.74.4.555.

Bajaj, M. *et al.* (2004) 'Sustained Reduction in Plasma Free Fatty Acid Concentration Improves Insulin Action without Altering Plasma Adipocytokine Levels in Subjects with Strong Family History of Type 2 Diabetes', *The Journal of Clinical Endocrinology & Metabolism*, 89(9), pp. 4649–4655. doi: 10.1210/jc.2004-0224.

Ban, J. *et al.* (2006) 'Embryonic Stem Cell-Derived Neurons Form Functional Networks In Vitro', *STEM CELLS*, 25(3), pp. 738–749. doi: 10.1634/stemcells.2006-0246.

Bassani, J. W., Yuan, W. and Bers, D. M. (1995) 'Fractional SR Ca release is regulated by trigger Ca and SR Ca content in cardiac myocytes.', *The American journal of physiology*, 268(5 Pt 1), pp. C1313-9. doi: 10.1152/ajpcell.1995.268.5.C1313.

Batalov, I. and Feinberg, A. W. (2015) 'Differentiation of Cardiomyocytes from Human Pluripotent Stem Cells Using Monolayer Culture.', *Biomarker insights*. SAGE Publications, 10(Suppl 1), pp. 71–6. doi: 10.4137/BMI.S20050.

Belke, D. D. *et al.* (2000) 'Altered metabolism causes cardiac dysfunction in perfused hearts from diabetic (*db* / *db*) mice', *American Journal of Physiology-Endocrinology and Metabolism*, 279(5), pp. E1104–E1113. doi: 10.1152/ajpendo.2000.279.5.E1104.

Belke, D. D. and Dillmann, W. H. (2004) 'Altered cardiac calcium handling in

diabetes.', *Current hypertension reports*, 6(6), pp. 424–9.

Belke, D. D., Swanson, E. A. and Dillmann, W. H. (2004) 'Decreased sarcoplasmic reticulum activity and contractility in diabetic db/db mouse heart.', *Diabetes*, 53(12), pp. 3201–8.

Bernardo, B. C. *et al.* (2010) 'Molecular distinction between physiological and pathological cardiac hypertrophy: Experimental findings and therapeutic strategies', *Pharmacology & Therapeutics*. Pergamon, 128(1), pp. 191–227. doi: 10.1016/J.PHARMTHERA.2010.04.005.

Bers, D. M. (2002) 'Cardiac excitation–contraction coupling', *Nature*, 415(6868), pp. 198–205. doi: 10.1038/415198a.

Björnholm, M. *et al.* (1997) 'Insulin Receptor Substrate-1 Phosphorylation and Phosphatidylinositol 3-Kinase Activity in Skeletal Muscle From NIDDM Subjects After In Vivo Insulin Stimulation', *Diabetes*. American Diabetes Association, 46(3), pp. 524–527. doi: 10.2337/DIAB.46.3.524.

Bloch, R. (1973) 'Inhibition of glucose transport in the human erythrocyte by cytochalasin B', *Biochemistry*. American Chemical Society, 12(23), pp. 4799–4801. doi: 10.1021/bi00747a036.

Blüher, M. *et al.* (2006) 'Circulating Adiponectin and Expression of Adiponectin Receptors in Human Skeletal Muscle: Associations with Metabolic Parameters and Insulin Resistance and Regulation by Physical Training', *The Journal of Clinical Endocrinology & Metabolism*. Oxford University Press, 91(6), pp. 2310–2316. doi: 10.1210/jc.2005-2556.

Bogan, J. S. and Kandror, K. V (2010) 'Biogenesis and regulation of insulin-responsive vesicles containing GLUT4', *Current Opinion in Cell Biology*, 22(4), pp. 506–512. doi: 10.1016/j.ceb.2010.03.012.

Boheler, K. R. *et al.* (2002) 'Differentiation of pluripotent embryonic stem cells into cardiomyocytes.', *Circulation research*, 91(3), pp. 189–201.

Bose, A. *et al*. (2002) 'Glucose transporter recycling in response to insulin is facilitated by myosin Myo1c', *Nature*, 420(6917), pp. 821–824. doi: 10.1038/nature01246.

Boström, P. *et al*. (2007) 'SNARE proteins mediate fusion between cytosolic lipid droplets and are implicated in insulin sensitivity'. *Nature cell biology*. 9(11), pp.1286. doi: 10.1038/ncb1648.

Boström, P. *et al*. (2010) 'The SNARE protein SNAP23 and the SNARE-interacting protein Munc18c in human skeletal muscle are implicated in insulin resistance/type 2 diabetes.', *Diabetes*. American Diabetes Association, 59(8), pp. 1870–8. doi: 10.2337/db09-1503.

Boucher, J., Kleinridders, A. and Kahn, C. R. (2014) 'Insulin receptor signaling in normal and insulin-resistant states.', *Cold Spring Harbor perspectives in biology*. Cold Spring Harbor Laboratory Press, 6(1). doi: 10.1101/cshperspect.a009191.

Boucher, J., Tseng, Y.-H. and Kahn, C. R. (2010) 'Insulin and insulin-like growth factor-1 receptors act as ligand-specific amplitude modulators of a common pathway regulating gene transcription.', *The Journal of biological chemistry*. American Society for Biochemistry and Molecular Biology, 285(22), pp. 17235–45. doi: 10.1074/jbc.M110.118620.

Boudina, S. *et al*. (2009) 'Contribution of Impaired Myocardial Insulin Signaling to Mitochondrial Dysfunction and Oxidative Stress in the Heart', *Circulation*, 119(9), pp. 1272–1283. doi: 10.1161/CIRCULATIONAHA.108.792101.

Boudina, S. and Abel, E. D. (2010) 'Diabetic cardiomyopathy, causes and effects.', *Reviews in endocrine & metabolic disorders*. NIH Public Access, 11(1), pp. 31–9. doi: 10.1007/s11154-010-9131-7.

Bouzakri, K. *et al*. (2003) 'Reduced activation of phosphatidylinositol-3 kinase and increased serine 636 phosphorylation of insulin receptor substrate-1 in primary culture of skeletal muscle cells from patients with type 2 diabetes.', *Diabetes*, 52(6), pp. 1319–25.

Boyer, J. K. *et al.* (2004) ‘Prevalence of ventricular diastolic dysfunction in asymptomatic, normotensive patients with diabetes mellitus’, *The American Journal of Cardiology*. Excerpta Medica, 93(7), pp. 870–875. doi: 10.1016/J.AMJCARD.2003.12.026.

Bruce, C. R. *et al.* (2009) ‘Overexpression of carnitine palmitoyltransferase-1 in skeletal muscle is sufficient to enhance fatty acid oxidation and improve high-fat diet-induced insulin resistance.’, *Diabetes*. American Diabetes Association, 58(3), pp. 550–8. doi: 10.2337/db08-1078.

Bryant, N. J. and Gould, G. W. (2011) ‘SNARE Proteins Underpin Insulin-Regulated GLUT4 Traffic’, *Traffic*, 12(6), pp. 657–664. doi: 10.1111/j.1600-0854.2011.01163.x.

Buchanan, J. *et al.* (2005) ‘Reduced Cardiac Efficiency and Altered Substrate Metabolism Precedes the Onset of Hyperglycemia and Contractile Dysfunction in Two Mouse Models of Insulin Resistance and Obesity’, *Endocrinology*, 146(12), pp. 5341–5349. doi: 10.1210/en.2005-0938.

Bugger, H. and Abel, E. D. (2014) ‘Molecular mechanisms of diabetic cardiomyopathy’, *Diabetologia*. Springer Berlin Heidelberg, 57(4), pp. 660–671. doi: 10.1007/s00125-014-3171-6.

Burke, S. J. *et al.* (2017) ‘db/db Mice Exhibit Features of Human Type 2 Diabetes That Are Not Present in Weight-Matched C57BL/6J Mice Fed a Western Diet.’, *Journal of diabetes research*. Hindawi Limited, 2017, p. 8503754. doi: 10.1155/2017/8503754.

Cade, W. T. (2008) ‘Diabetes-related microvascular and macrovascular diseases in the physical therapy setting.’, *Physical therapy*. Oxford University Press, 88(11), pp. 1322–35. doi: 10.2522/ptj.20080008.

Calderhead, D. M. *et al.* (1990) ‘Insulin regulation of the two glucose transporters in 3T3-L1 adipocytes.’, *The Journal of biological chemistry*, 265(23), pp. 13801–8.

Capes, S. E. *et al.* (2000) 'Stress hyperglycaemia and increased risk of death after myocardial infarction in patients with and without diabetes: a systematic overview', *The Lancet*. Elsevier, 355(9206), pp. 773–778. doi: 10.1016/S0140-6736(99)08415-9.

Carroll, R. *et al.* (2005) 'Metabolic effects of insulin on cardiomyocytes from control and diabetic *db/db* mouse hearts', *American Journal of Physiology-Endocrinology and Metabolism*, 288(5), pp. E900–E906. doi: 10.1152/ajpendo.00491.2004.

Carvajal-Vergara, X. *et al.* (2010a) 'Patient-specific induced pluripotent stem-cell-derived models of LEOPARD syndrome', *Nature*. Nature Publishing Group, 465(7299), pp. 808–812. doi: 10.1038/nature09005.

Carvajal-Vergara, X. *et al.* (2010b) 'Patient-specific induced pluripotent stem-cell-derived models of LEOPARD syndrome', *Nature*. Nature Publishing Group, 465(7299), pp. 808–812. doi: 10.1038/nature09005.

Cassidy, S. *et al.* (2016) 'High intensity intermittent exercise improves cardiac structure and function and reduces liver fat in patients with type 2 diabetes: a randomised controlled trial', *Diabetologia*. Springer Berlin Heidelberg, 59(1), pp. 56–66. doi: 10.1007/s00125-015-3741-2.

Castelló, A. *et al.* (1994) 'Perinatal hypothyroidism impairs the normal transition of GLUT4 and GLUT1 glucose transporters from fetal to neonatal levels in heart and brown adipose tissue. Evidence for tissue-specific regulation of GLUT4 expression by thyroid hormone.', *The Journal of biological chemistry*, 269(8), pp. 5905–12.

Chakraborty, A. *et al.* (2010) 'Inositol Pyrophosphates Inhibit Akt Signaling, Thereby Regulating Insulin Sensitivity and Weight Gain', *Cell*. Cell Press, 143(6), pp. 897–910. doi: 10.1016/J.CELL.2010.11.032.

Chang, L., Chiang, S.-H. and Saltiel, A. R. (2007) 'TC10α Is Required for Insulin-Stimulated Glucose Uptake in Adipocytes', *Endocrinology*, 148(1), pp. 27–33. doi: 10.1210/en.2006-1167.

Chao, C. C. T. *et al.* (2011) 'SNARE protein regulation of cardiac potassium channels and atrial natriuretic factor secretion', *Journal of Molecular and Cellular Cardiology*, 50(3), pp. 401–407. doi: 10.1016/j.yjmcc.2010.11.018.

Cheatham, B. *et al.* (1996) 'Insulin-stimulated translocation of GLUT4 glucose transporters requires SNARE-complex proteins.', *Proceedings of the National Academy of Sciences of the United States of America*. National Academy of Sciences, 93(26), pp. 15169–73. doi: 10.1073/PNAS.93.26.15169.

Chen, X.-W. *et al.* (2007) 'Activation of RalA Is Required for Insulin-Stimulated Glut4 Trafficking to the Plasma Membrane via the Exocyst and the Motor Protein Myo1c', *Developmental Cell*. Cell Press, 13(3), pp. 391–404. doi: 10.1016/J.DEVCEL.2007.07.007.

Chen, X.-W. *et al.* (2011) 'A Ral GAP complex links PI 3-kinase/Akt signaling to RalA activation in insulin action.', *Molecular biology of the cell*, 22(1), pp. 141–52. doi: 10.1091/mbc.E10-08-0665.

Cho, H. *et al.* (2001) 'Insulin resistance and a diabetes mellitus-like syndrome in mice lacking the protein kinase Akt2 (PKB beta).', *Science (New York, N.Y.)*. American Association for the Advancement of Science, 292(5522), pp. 1728–31. doi: 10.1126/science.292.5522.1728.

Chong, J. J. H. *et al.* (2014) 'Human embryonic-stem-cell-derived cardiomyocytes regenerate non-human primate hearts', *Nature*. Nature Publishing Group, 510(7504), pp. 273–277. doi: 10.1038/nature13233.

Chun, Y. W. *et al.* (2015) 'Combinatorial polymer matrices enhance in vitro maturation of human induced pluripotent stem cell-derived cardiomyocytes', *Biomaterials*. Elsevier, 67, pp. 52–64. doi: 10.1016/J.BIOMATERIALS.2015.07.004.

Ciaraldi, T. P. *et al.* (2005) 'Skeletal Muscle GLUT1 Transporter Protein Expression and Basal Leg Glucose Uptake Are Reduced in Type 2 Diabetes', *The Journal of Clinical Endocrinology & Metabolism*, 90(1), pp. 352–358. doi: 10.1210/jc.2004-0516.

Clarke, J. F. *et al.* (1994) 'Inhibition of the translocation of GLUT1 and GLUT4 in 3T3-L1 cells by the phosphatidylinositol 3-kinase inhibitor, wortmannin.', *The Biochemical journal*, 300 (Pt 3), pp. 631–5.

Coderre, L. *et al.* (1992) 'Alteration in the expression of GLUT-1 and GLUT-4 protein and messenger RNA levels in denervated rat muscles.', *Endocrinology*, 131(4), pp. 1821–1825. doi: 10.1210/endo.131.4.1396328.

Correia, C. *et al.* (2017) 'Distinct carbon sources affect structural and functional maturation of cardiomyocytes derived from human pluripotent stem cells', *Scientific Reports*. Nature Publishing Group, 7(1), p. 8590. doi: 10.1038/s41598-017-08713-4.

Czech, M. P. and Buxton, J. M. (1993) 'Insulin action on the internalization of the GLUT4 glucose transporter in isolated rat adipocytes.', *The Journal of biological chemistry*, 268(13), pp. 9187–90.

Dávila-Román, V. G. *et al.* (2002) 'Altered myocardial fatty acid and glucose metabolism in idiopathic dilated cardiomyopathy', *Journal of the American College of Cardiology*. Elsevier, 40(2), pp. 271–277. doi: 10.1016/S0735-1097(02)01967-8.

Davis, H. E., Morgan, J. R. and Yarmush, M. L. (2002) 'Polybrene increases retrovirus gene transfer efficiency by enhancing receptor-independent virus adsorption on target cell membranes.', *Biophysical chemistry*, 97(2–3), pp. 159–72.

Deng, J.-Y. *et al.* (2007) 'Impairment of cardiac insulin signaling and myocardial contractile performance in high-cholesterol/fructose-fed rats', *American Journal of Physiology-Heart and Circulatory Physiology*, 293(2), pp. H978–H987. doi: 10.1152/ajpheart.01002.2006.

Desrois, M. *et al.* (2004) 'Initial steps of insulin signaling and glucose transport are defective in the type 2 diabetic rat heart.', *Cardiovascular research*, 61(2), pp. 288–96.

Dixon, J. B. *et al.* (2008) 'Adjustable Gastric Banding and Conventional Therapy for Type 2 Diabetes', *JAMA*. American Medical Association, 299(3), pp. 316–323. doi: 10.1001/jama.299.3.316.

Dorweiler, B. *et al.* (2007) 'Ischemia-Reperfusion Injury', *European Journal of Trauma and Emergency Surgery*. Urban & Vogel, 33(6), pp. 600–612. doi: 10.1007/s00068-007-7152-z.

Drawnel, F. M. *et al.* (2014) 'Disease Modeling and Phenotypic Drug Screening for Diabetic Cardiomyopathy using Human Induced Pluripotent Stem Cells', *Cell Reports*, 9(3), pp. 810–820. doi: 10.1016/j.celrep.2014.09.055.

Dresner, A. *et al.* (1999) 'Effects of free fatty acids on glucose transport and IRS-1–associated phosphatidylinositol 3-kinase activity', *Journal of Clinical Investigation*, 103(2), pp. 253–259. doi: 10.1172/JCI5001.

Drosatos, K. and Schulze, P. C. (2013) 'Cardiac Lipotoxicity: Molecular Pathways and Therapeutic Implications', *Current Heart Failure Reports*. Current Science Inc., 10(2), pp. 109–121. doi: 10.1007/s11897-013-0133-0.

Du, D. T. M. *et al.* (2015) 'Action potential morphology of human induced pluripotent stem cell-derived cardiomyocytes does not predict cardiac chamber specificity and is dependent on cell density.', *Biophysical journal*. The Biophysical Society, 108(1), pp. 1–4. doi: 10.1016/j.bpj.2014.11.008.

Du, X. L. *et al.* (2001) 'Hyperglycemia inhibits endothelial nitric oxide synthase activity by posttranslational modification at the Akt site.', *The Journal of clinical investigation*. American Society for Clinical Investigation, 108(9), pp. 1341–8. doi: 10.1172/JCI11235.

Dupuis, J. *et al.* (2010) 'New genetic loci implicated in fasting glucose homeostasis and their impact on type 2 diabetes risk', *Nature Genetics*. Nature Publishing Group, 42(2), pp. 105–116. doi: 10.1038/ng.520.

Dutka, D. P. *et al.* (2006) 'Myocardial Glucose Transport and Utilization in Patients With Type 2 Diabetes Mellitus, Left Ventricular Dysfunction, and

Coronary Artery Disease', *Journal of the American College of Cardiology*, 48(11), pp. 2225–2231. doi: 10.1016/j.jacc.2006.06.078.

Dutta, K. *et al.* (2001) 'Cardiomyocyte dysfunction in sucrose-fed rats is associated with insulin resistance.', *Diabetes*, 50(5), pp. 1186–92.

Erickson, J. R. *et al.* (2013) 'Diabetic hyperglycaemia activates CaMKII and arrhythmias by O-linked glycosylation', *Nature*. Nature Publishing Group, 502(7471), pp. 372–376. doi: 10.1038/nature12537.

Erion, D. M. and Shulman, G. I. (2010) 'Diacylglycerol-mediated insulin resistance.', *Nature medicine*. NIH Public Access, 16(4), pp. 400–2. doi: 10.1038/nm0410-400.

Esteves, J. V., Enguita, F. J. and Machado, U. F. (2017) 'MicroRNAs-Mediated Regulation of Skeletal Muscle GLUT4 Expression and Translocation in Insulin Resistance', *Journal of Diabetes Research*. Hindawi, 2017, pp. 1–11. doi: 10.1155/2017/7267910.

Ewart, M.-A. *et al.* (2005) 'Evidence for a Role of the Exocyst in Insulin-stimulated Glut4 Trafficking in 3T3-L1 Adipocytes', *Journal of Biological Chemistry*, 280(5), pp. 3812–3816. doi: 10.1074/jbc.M409928200.

Fabiato, A. (1983) 'Calcium-induced release of calcium from the cardiac sarcoplasmic reticulum.', *The American journal of physiology*, 245(1), pp. C1-14. doi: 10.1152/ajpcell.1983.245.1.C1.

Farman, G. P. *et al.* (2008) 'Blebbistatin: use as inhibitor of muscle contraction', *Pflügers Archiv - European Journal of Physiology*. Springer-Verlag, 455(6), pp. 995–1005. doi: 10.1007/s00424-007-0375-3.

Fasshauer, D. (2003) 'Structural insights into the SNARE mechanism.', *Biochimica et biophysica acta*, 1641(2–3), pp. 87–97.

Ferlito, M. *et al.* (2010) 'VAMP-1, VAMP-2, and syntaxin-4 regulate ANP release from cardiac myocytes', *Journal of Molecular and Cellular Cardiology*. Academic

Press, 49(5), pp. 791–800. doi: 10.1016/J.YJMCC.2010.08.020.

Fischer, Y. *et al.* (1996) ‘Contraction-independent effects of catecholamines on glucose transport in isolated rat cardiomyocytes’, *American Journal of Physiology-Cell Physiology*, 270(4), pp. C1204–C1210. doi: 10.1152/ajpcell.1996.270.4.C1204.

Fischer, Y. *et al.* (1997) ‘Insulin-induced recruitment of glucose transporter 4 (GLUT4) and GLUT1 in isolated rat cardiac myocytes. Evidence of the existence of different intracellular GLUT4 vesicle populations.’, *The Journal of biological chemistry*, 272(11), pp. 7085–92.

Fong, A. H. *et al.* (2016) ‘Three-Dimensional Adult Cardiac Extracellular Matrix Promotes Maturation of Human Induced Pluripotent Stem Cell-Derived Cardiomyocytes’, *Tissue Engineering Part A*. Mary Ann Liebert, Inc., 22(15–16), pp. 1016–1025. doi: 10.1089/ten.tea.2016.0027.

Fowler, M. J. (2008) 'Microvascular and Macrovascular Complications of Diabetes', *Clinical Diabetes*. 26(2), pp.77-82.

Francis Stuart, S. D. *et al.* (2016) ‘The crossroads of inflammation, fibrosis, and arrhythmia following myocardial infarction’, *Journal of Molecular and Cellular Cardiology*. Academic Press, 91, pp. 114–122. doi: 10.1016/J.YJMCC.2015.12.024.

Frangogiannis, N. G. (2014) ‘The inflammatory response in myocardial injury, repair, and remodelling.’, *Nature reviews. Cardiology*. NIH Public Access, 11(5), pp. 255–65. doi: 10.1038/nrcardio.2014.28.

Franz, M. J. *et al.* (2015) ‘Lifestyle Weight-Loss Intervention Outcomes in Overweight and Obese Adults with Type 2 Diabetes: A Systematic Review and Meta-Analysis of Randomized Clinical Trials’, *Journal of the Academy of Nutrition and Dietetics*, 115, pp. 1447–1463. doi: 10.1016/j.jand.2015.02.031.

Fu, F. *et al.* (2015) ‘Direct Evidence that Myocardial Insulin Resistance following Myocardial Ischemia Contributes to Post-Ischemic Heart Failure.’, *Scientific*

reports. Nature Publishing Group, 5, p. 17927. doi: 10.1038/srep17927.

Gao, F. *et al.* (2002) 'Nitric oxide mediates the antiapoptotic effect of insulin in myocardial ischemia-reperfusion: the roles of PI3-kinase, Akt, and endothelial nitric oxide synthase phosphorylation.', *Circulation*, 105(12), pp. 1497–502.

Garvey, W. T. *et al.* (1992a) 'Gene expression of GLUT4 in skeletal muscle from insulin-resistant patients with obesity, IGT, GDM, and NIDDM.', *Diabetes*. American Diabetes Association, 41(4), pp. 465–75. doi: 10.2337/DIAB.41.4.465.

Garvey, W. T. *et al.* (1992b) 'Gene expression of GLUT4 in skeletal muscle from insulin-resistant patients with obesity, IGT, GDM, and NIDDM.', *Diabetes*, 41(4), pp. 465–75.

Gastaldelli, A., Gaggini, M. and DeFronzo, R. A. (2017) 'Role of Adipose Tissue Insulin Resistance in the Natural History of Type 2 Diabetes: Results From the San Antonio Metabolism Study.', *Diabetes*. American Diabetes Association, 66(4), pp. 815–822. doi: 10.2337/db16-1167.

Gerstein, H. C. *et al.* (1999) 'Relationship of glucose and insulin levels to the risk of myocardial infarction: a case-control study', *Journal of the American College of Cardiology*. 33(3), pp. 612–619. doi: 10.1016/S0735-1097(98)00637-8.

Goldsmith, S. R. (2006) 'The role of vasopressin in congestive heart failure.', *Cleveland Clinic journal of medicine*, 73 Suppl 3, pp. S19-23.

Goodpaster, B. H. *et al.* (2001) 'Skeletal Muscle Lipid Content and Insulin Resistance: Evidence for a Paradox in Endurance-Trained Athletes', *The Journal of Clinical Endocrinology & Metabolism*. Oxford University Press, 86(12), pp. 5755–5761. doi: 10.1210/jcem.86.12.8075.

Graham, E. L. *et al.* (2013) 'Isolation, culture, and functional characterization of adult mouse cardiomyoctyes.', *Journal of visualized experiments : JoVE*. MyJoVE Corporation, (79), p. e50289. doi: 10.3791/50289.

Grant, B. D. and Donaldson, J. G. (2009) 'Pathways and mechanisms of endocytic

recycling', *Nature reviews. Molecular cell biology*. NIH Public Access, 10(9), p. 597. doi: 10.1038/NRM2755.

Graveleau, C. *et al.* (2005) 'Mouse and human resistins impair glucose transport in primary mouse cardiomyocytes, and oligomerization is required for this biological action.', *The Journal of biological chemistry*. American Society for Biochemistry and Molecular Biology, 280(36), pp. 31679–85. doi: 10.1074/jbc.M504008200.

Griffin, M. E. *et al.* (1999) 'Free fatty acid-induced insulin resistance is associated with activation of protein kinase C theta and alterations in the insulin signaling cascade.', *Diabetes*. American Diabetes Association, 48(6), pp. 1270–4. doi: 10.2337/DIABETES.48.6.1270.

Grover-McKay, M., Walsh, S. A. and Thompson, S. A. (1999) 'Glucose transporter 3 (GLUT3) protein is present in human myocardium.', *Biochimica et biophysica acta*, 1416(1–2), pp. 145–54.

Guilherme, A. *et al.* (2008) 'Adipocyte dysfunctions linking obesity to insulin resistance and type 2 diabetes.', *Nature reviews. Molecular cell biology*. NIH Public Access, 9(5), pp. 367–77. doi: 10.1038/nrm2391.

Guo, L. *et al.* (2017) 'Maturation of Human iPSC-cardiomyocytes in Long-term Culture for Cardiotoxicity Testing', *Journal of Pharmacological and Toxicological Methods*. Elsevier, 88, pp. 237–238. doi: 10.1016/J.VASCN.2017.09.227.

Gurley, J. M., Griesel, B. A. and Olson, A. L. (2016) 'Increased Skeletal Muscle GLUT4 Expression in Obese Mice After Voluntary Wheel Running Exercise Is Posttranscriptional.', *Diabetes*. American Diabetes Association, 65(10), pp. 2911–9. doi: 10.2337/db16-0305.

Hanefeld, M. *et al.* (1996) 'Risk factors for myocardial infarction and death in newly detected NIDDM: the Diabetes Intervention Study, 11-year follow-up', *Diabetologia*. Springer-Verlag, 39(12), pp. 1577–1583. doi: 10.1007/s001250050617.

Hedblad, B. *et al.* (2002) 'Insulin resistance in non-diabetic subjects is associated with increased incidence of myocardial infarction and death', *Diabetic Medicine*. Wiley/Blackwell (10.1111), 19(6), pp. 470–475. doi: 10.1046/j.1464-5491.2002.00719.x.

Hickson, G. R. X. *et al.* (2000) 'Quantification of SNARE Protein Levels in 3T3-L1 Adipocytes: Implications for Insulin-Stimulated Glucose Transport'. *Biochemical and biophysical research communications*. 270(3), pp. 841-845. doi: 10.1006/bbrc.2000.2525.

Hohenstein, A. C. and Roche, P. A. (2001) 'SNAP-29 Is a Promiscuous Syntaxin-Binding SNARE', *Biochemical and Biophysical Research Communications*. Academic Press, 285(2), pp. 167–171. doi: 10.1006/BBRC.2001.5141.

Holt, M. *et al.* (2006) 'Identification of SNAP-47, a novel Qbc-SNARE with ubiquitous expression.', *The Journal of biological chemistry*. American Society for Biochemistry and Molecular Biology, 281(25), pp. 17076–83. doi: 10.1074/jbc.M513838200.

Hong, W. (2005) 'SNAREs and traffic', *Biochimica et Biophysica Acta (BBA) - Molecular Cell Research*, 1744(2), pp. 120–144. doi: 10.1016/j.bbamcr.2005.03.014.

Hotamisligil, G. S. *et al.* (1995) 'Increased adipose tissue expression of tumor necrosis factor-alpha in human obesity and insulin resistance.', *Journal of Clinical Investigation*, 95(5), pp. 2409–2415. doi: 10.1172/JCI117936.

Huang, S. and Czech, M. P. (2007) 'The GLUT4 Glucose Transporter', *Cell Metabolism*, 5(4), pp. 237–252. doi: 10.1016/j.cmet.2007.03.006.

Hussey, S. E. *et al.* (2011) 'Exercise training increases adipose tissue GLUT4 expression in patients with type 2 diabetes', *Diabetes, Obesity and Metabolism*. Wiley/Blackwell (10.1111), 13(10), pp. 959–962. doi: 10.1111/j.1463-1326.2011.01426.x.

Huynh, K. *et al.* (2010) 'Cardiac-specific IGF-1 receptor transgenic expression

protects against cardiac fibrosis and diastolic dysfunction in a mouse model of diabetic cardiomyopathy.', *Diabetes*. American Diabetes Association, 59(6), pp. 1512–20. doi: 10.2337/db09-1456.

Hwang, H. S. *et al.* (2015) 'Comparable calcium handling of human iPSC-derived cardiomyocytes generated by multiple laboratories', *Journal of Molecular and Cellular Cardiology*. Academic Press, 85, pp. 79–88. doi: 10.1016/J.YJMCC.2015.05.003.

Ibrahim, M. *et al.* (2011) 'The structure and function of cardiac t-tubules in health and disease.', *Proceedings. Biological sciences*. The Royal Society, 278(1719), pp. 2714–23. doi: 10.1098/rspb.2011.0624.

Inoue, M. *et al.* (2003) 'The exocyst complex is required for targeting of Glut4 to the plasma membrane by insulin', *Nature*. Nature Publishing Group, 422(6932), pp. 629–633. doi: 10.1038/nature01533.

Inoue, M. *et al.* (2006) 'Compartmentalization of the exocyst complex in lipid rafts controls Glut4 vesicle tethering.', *Molecular biology of the cell*. American Society for Cell Biology, 17(5), pp. 2303–11. doi: 10.1091/mbc.e06-01-0030.

Iozzo, P. *et al.* (2001) 'Physiological hyperinsulinemia impairs insulin-stimulated glycogen synthase activity and glycogen synthesis', *American Journal of Physiology-Endocrinology and Metabolism*, 280(5), pp. E712–E719. doi: 10.1152/ajpendo.2001.280.5.E712.

Iozzo, P. *et al.* (2002) 'Independent association of type 2 diabetes and coronary artery disease with myocardial insulin resistance.', *Diabetes*, 51(10), pp. 3020–4.

Itani, S. I. *et al.* (2002) 'Lipid-induced insulin resistance in human muscle is associated with changes in diacylglycerol, protein kinase C, and IkappaB-alpha.', *Diabetes*. American Diabetes Association, 51(7), pp. 2005–11. doi: 10.2337/DIABETES.51.7.2005.

Itzhaki, I., Rapoport, S., *et al.* (2011) 'Calcium handling in human induced pluripotent stem cell derived cardiomyocytes.', *PloS one*. Public Library of

Science, 6(4), p. e18037. doi: 10.1371/journal.pone.0018037.

Itzhaki, I., Maizels, L., *et al.* (2011) 'Modelling the long QT syndrome with induced pluripotent stem cells', *Nature*. Nature Publishing Group, 471(7337), pp. 225–229. doi: 10.1038/nature09747.

Jedrychowski, M. P. *et al.* (2010) 'Proteomic analysis of GLUT4 storage vesicles reveals LRP1 to be an important vesicle component and target of insulin signaling.', *The Journal of biological chemistry*. American Society for Biochemistry and Molecular Biology, 285(1), pp. 104–14. doi: 10.1074/jbc.M109.040428.

Jordens, I. *et al.* (2010) 'Insulin-regulated Aminopeptidase Is a Key Regulator of GLUT4 Trafficking by Controlling the Sorting of GLUT4 from Endosomes to Specialized Insulin-regulated Vesicles', *Molecular Biology of the Cell*. 21(12), pp. 2034–2044. doi: 10.1091/mbc.e10-02-0158.

Kamakura, T. *et al.* (2013) 'Ultrastructural Maturation of Human-Induced Pluripotent Stem Cell-Derived Cardiomyocytes in a Long-Term Culture', *Circulation Journal*. The Japanese Circulation Society, 77(5), pp. 1307–1314. doi: 10.1253/circj.CJ-12-0987.

Kampmann, U. *et al.* (2011) 'GLUT4 and UBC9 Protein Expression Is Reduced in Muscle from Type 2 Diabetic Patients with Severe Insulin Resistance', *PLoS ONE*. Public Library of Science, 6(11), p. e27854. doi: 10.1371/journal.pone.0027854.

Kannel, W. B., Hjortland, M. and Castelli, W. P. (1974) 'Role of diabetes in congestive heart failure: the Framingham study.', *The American journal of cardiology*. Elsevier, 34(1), pp. 29–34. doi: 10.1016/0002-9149(74)90089-7.

Kannel, W. B. and McGee, D. L. (1979) 'Diabetes and glucose tolerance as risk factors for cardiovascular disease: the Framingham study.', *Diabetes care*. American Diabetes Association, 2(2), pp. 120–6. doi: 10.2337/DIACARE.2.2.120.

Karakikes, I. *et al.* (2015) 'Human induced pluripotent stem cell-derived cardiomyocytes: insights into molecular, cellular, and functional phenotypes.',

Circulation research. American Heart Association, Inc., 117(1), pp. 80–8. doi: 10.1161/CIRCRESAHA.117.305365.

Kawanishi, M. *et al.* (2000) 'Role of SNAP23 in insulin-induced translocation of GLUT4 in 3T3-L1 adipocytes. Mediation of complex formation between syntaxin4 and VAMP2.', *The Journal of biological chemistry*. American Society for Biochemistry and Molecular Biology, 275(11), pp. 8240–7. doi: 10.1074/JBC.275.11.8240.

Kemi, O. J. *et al.* (2007) 'Aerobic interval training enhances cardiomyocyte contractility and Ca2+ cycling by phosphorylation of CaMKII and Thr-17 of phospholamban', *Journal of Molecular and Cellular Cardiology*. Academic Press, 43(3), pp. 354–361. doi: 10.1016/J.YJMCC.2007.06.013.

Kemp, C. D. and Conte, J. V. (2012) 'The pathophysiology of heart failure', *Cardiovascular Pathology*. Elsevier, 21(5), pp. 365–371. doi: 10.1016/J.CARPATH.2011.11.007.

Kido, Y. *et al.* (2000) 'Tissue-specific insulin resistance in mice with mutations in the insulin receptor, IRS-1, and IRS-2.', *The Journal of clinical investigation*. American Society for Clinical Investigation, 105(2), pp. 199–205. doi: 10.1172/JCI7917.

Kim, F. *et al.* (2017) 'Brain natriuretic peptide and insulin resistance in older adults', *Diabetic Medicine*, 34(2), pp. 235–238. doi: 10.1111/dme.13139.

Kim, J. K. *et al.* (2004) 'PKC-theta knockout mice are protected from fat-induced insulin resistance.', *The Journal of clinical investigation*. American Society for Clinical Investigation, 114(6), pp. 823–7. doi: 10.1172/JCI22230.

Kim, Y.-B. *et al.* (1999) 'Normal insulin-dependent activation of Akt/protein kinase B, with diminished activation of phosphoinositide 3-kinase, in muscle in type 2 diabetes', *The Journal of Clinical Investigation*. American Society for Clinical Investigation, 104(6), pp. 733–741. doi: 10.1172/JCI6928.

Kim, Y.-B. *et al.* (2005) 'Muscle-specific deletion of the Glut4 glucose

transporter alters multiple regulatory steps in glycogen metabolism.', *Molecular and cellular biology*. American Society for Microbiology, 25(21), pp. 9713–23. doi: 10.1128/MCB.25.21.9713-9723.2005.

Kioumourtzoglou, D., Gould, G. W. and Bryant, N. J. (2014) 'Insulin stimulates syntaxin4 SNARE complex assembly via a novel regulatory mechanism.', *Molecular and cellular biology*. American Society for Microbiology (ASM), 34(7), pp. 1271–9. doi: 10.1128/MCB.01203-13.

Knip, M. *et al.* (2005) 'Environmental Triggers and Determinants of Type 1 Diabetes', *Diabetes*. American Diabetes Association, 54(suppl 2), pp. S125–S136. doi: 10.2337/DIABETES.54.SUPPL_2.S125.

Kobayashi, K. *et al.* (2000) 'The db/db mouse, a model for diabetic dyslipidemia: molecular characterization and effects of Western diet feeding.', *Metabolism: clinical and experimental*, 49(1), pp. 22–31.

Koek, H. L. *et al.* (2007) 'Short- and long-term mortality after acute myocardial infarction: comparison of patients with and without diabetes mellitus.', *European journal of epidemiology*. Springer, 22(12), pp. 883–8. doi: 10.1007/s10654-007-9191-5.

Kohn, A. D. *et al.* (1996) 'Expression of a constitutively active Akt Ser/Thr kinase in 3T3-L1 adipocytes stimulates glucose uptake and glucose transporter 4 translocation.', *The Journal of biological chemistry*. American Society for Biochemistry and Molecular Biology, 271(49), pp. 31372–8. doi: 10.1074/JBC.271.49.31372.

Kolanowski, T. J., Antos, C. L. and Guan, K. (2017) 'Making human cardiomyocytes up to date: Derivation, maturation state and perspectives', *International Journal of Cardiology*. Elsevier, 241, pp. 379–386. doi: 10.1016/J.IJCARD.2017.03.099.

Koves, T. R. *et al.* (2008) 'Mitochondrial Overload and Incomplete Fatty Acid Oxidation Contribute to Skeletal Muscle Insulin Resistance', *Cell Metabolism*, 7(1), pp. 45–56. doi: 10.1016/j.cmet.2007.10.013.

Kowalski, G. M. *et al.* (2015) 'In vivo cardiac glucose metabolism in the high-fat fed mouse: Comparison of euglycemic–hyperinsulinemic clamp derived measures of glucose uptake with a dynamic metabolomic flux profiling approach', *Biochemical and Biophysical Research Communications*. Academic Press, 463(4), pp. 818–824. doi: 10.1016/J.BBRC.2015.06.019.

Kraegen, E. W. *et al.* (1991) 'Development of muscle insulin resistance after liver insulin resistance in high-fat-fed rats.', *Diabetes*. American Diabetes Association, 40(11), pp. 1397–403. doi: 10.2337/DIAB.40.11.1397.

Kraegen, E. W. *et al.* (1993) 'Glucose transporters and in vivo glucose uptake in skeletal and cardiac muscle: fasting, insulin stimulation and immunoisolation studies of GLUT1 and GLUT4.', *The Biochemical journal*, 295 (Pt 1), pp. 287–93.

Kramer, H. F. *et al.* (2006) 'AS160 regulates insulin- and contraction-stimulated glucose uptake in mouse skeletal muscle.', *The Journal of biological chemistry*. American Society for Biochemistry and Molecular Biology, 281(42), pp. 31478–85. doi: 10.1074/jbc.M605461200.

Kraniou, G. N., Cameron-Smith, D. and Hargreaves, M. (2006) 'Acute exercise and GLUT4 expression in human skeletal muscle: influence of exercise intensity', *Journal of Applied Physiology*, 101(3), pp. 934–937. doi: 10.1152/japplphysiol.01489.2005.

Krssak, M. *et al.* (1999) 'Intramyocellular lipid concentrations are correlated with insulin sensitivity in humans: a 1 H NMR spectroscopy study', *Diabetologia*, 42(1), pp. 113–116. doi: 10.1007/s001250051123.

Laakso, M. *et al.* (1995) 'Does NIDDM increase the risk for coronary heart disease similarly in both low- and high-risk populations?', *Diabetologia*, 38(4), pp. 487–93.

Laflamme, M. A. *et al.* (2007) 'Cardiomyocytes derived from human embryonic stem cells in pro-survival factors enhance function of infarcted rat hearts', *Nature Biotechnology*. Nature Publishing Group, 25(9), pp. 1015–1024. doi: 10.1038/nbt1327.

Laidlaw, K. M. E. *et al.* (2017) 'SNARE phosphorylation: a control mechanism for insulin-stimulated glucose transport and other regulated exocytic events.', *Biochemical Society transactions*. Portland Press Limited, 45(6), pp. 1271–1277. doi: 10.1042/BST20170202.

Larance, M. *et al.* (2005) 'Characterization of the Role of the Rab GTPase-activating Protein AS160 in Insulin-regulated GLUT4 Trafficking', *Journal of Biological Chemistry*, 280(45), pp. 37803–37813. doi: 10.1074/jbc.M503897200.

Lazo, M. *et al.* (2013) 'NH $_2$ -Terminal Pro–Brain Natriuretic Peptide and Risk of Diabetes', *Diabetes*, 62(9), pp. 3189–3193. doi: 10.2337/db13-0478.

Lee, J. and Pilch, P. F. (1994) 'The insulin receptor: structure, function, and signaling', *American Journal of Physiology-Cell Physiology*, 266(2), pp. C319–C334. doi: 10.1152/ajpcell.1994.266.2.C319.

Lee, Y.-K. *et al.* (2011) 'Calcium homeostasis in human induced pluripotent stem cell-derived cardiomyocytes.', *Stem cell reviews*. Springer, 7(4), pp. 976–86. doi: 10.1007/s12015-011-9273-3.

Leto, D. and Saltiel, A. R. (2012) 'Regulation of glucose transport by insulin: traffic control of GLUT4', *Nature Reviews Molecular Cell Biology*, 13(6), pp. 383–396. doi: 10.1038/nrm3351.

Li, H. and Forstermann, U. (2000) 'Nitric oxide in the pathogenesis of vascular disease', *The Journal of Pathology*. Wiley-Blackwell, 190(3), pp. 244–254. doi: 10.1002/(SICI)1096-9896(200002)190:3<244::AID-PATH575>3.0.CO;2-8.

Liang, P. *et al.* (2013) 'Drug screening using a library of human induced pluripotent stem cell-derived cardiomyocytes reveals disease-specific patterns of cardiotoxicity.', *Circulation*. NIH Public Access, 127(16), pp. 1677–91. doi: 10.1161/CIRCULATIONAHA.113.001883.

Lieu, D. K. *et al.* (2009) 'Absence of Transverse Tubules Contributes to Non-Uniform Ca $^{2+}$ Wavefronts in Mouse and Human Embryonic Stem Cell–Derived Cardiomyocytes', *Stem Cells and Development*, 18(10), pp. 1493–1500. doi:

10.1089/scd.2009.0052.

Lihn, A. S., Pedersen, S. B. and Richelsen, B. (2005) 'Adiponectin: action, regulation and association to insulin sensitivity', *Obesity Reviews*, 6(1), pp. 13–21. doi: 10.1111/j.1467-789X.2005.00159.x.

Lin, B. *et al.* (2017) 'Culture in Glucose-Depleted Medium Supplemented with Fatty Acid and 3,3',5-Triiodo-l-Thyronine Facilitates Purification and Maturation of Human Pluripotent Stem Cell-Derived Cardiomyocytes.', *Frontiers in endocrinology*. Frontiers Media SA, 8, p. 253. doi: 10.3389/fendo.2017.00253.

Liu, J. *et al.* (2002) 'APS facilitates c-Cbl tyrosine phosphorylation and GLUT4 translocation in response to insulin in 3T3-L1 adipocytes.', *Molecular and cellular biology*, 22(11), pp. 3599–609.

Livingstone, C. *et al.* (1996) 'Compartment ablation analysis of the insulin-responsive glucose transporter (GLUT4) in 3T3-L1 adipocytes.', *The Biochemical journal*. Portland Press Ltd, 315 (Pt 2), pp. 487–95.

Lo, C. W. (2000) 'Role of Gap Junctions in Cardiac Conduction and Development', *Circulation Research*, 87(5), pp. 346–348. doi: 10.1161/01.RES.87.5.346.

Lombardi, V., Piazzesi, G. and Linari, M. (1992) 'Rapid regeneration of the actin-myosin power stroke in contracting muscle', *Nature*. Nature Publishing Group, 355(6361), pp. 638–641. doi: 10.1038/355638a0.

Louch, W. E., Sheehan, K. A. and Wolska, B. M. (2011) 'Methods in cardiomyocyte isolation, culture, and gene transfer.', *Journal of molecular and cellular cardiology*. NIH Public Access, 51(3), pp. 288–98. doi: 10.1016/j.yjmcc.2011.06.012.

Lyon, A. R. *et al.* (2009) 'Loss of T-tubules and other changes to surface topography in ventricular myocytes from failing human and rat heart.', *Proceedings of the National Academy of Sciences of the United States of America*. National Academy of Sciences, 106(16), pp. 6854–9. doi:

10.1073/pnas.0809777106.

Ma, J. *et al.* (2011) 'High purity human-induced pluripotent stem cell-derived cardiomyocytes: electrophysiological properties of action potentials and ionic currents.', *American journal of physiology. Heart and circulatory physiology*. American Physiological Society, 301(5), pp. H2006-17. doi: 10.1152/ajpheart.00694.2011.

Malmberg, K. *et al.* (1996) 'Effects of insulin treatment on cause-specific one-year mortality and morbidity in diabetic patients with acute myocardial infarction', *European Heart Journal*. Oxford University Press, 17(9), pp. 1337–1344. doi: 10.1093/oxfordjournals.eurheartj.a015067.

Marfella, R. *et al.* (2009) 'Tight Glycemic Control Reduces Heart Inflammation and Remodeling During Acute Myocardial Infarction in Hyperglycemic Patients', *Journal of the American College of Cardiology*. Journal of the American College of Cardiology, 53(16), pp. 1425–1436. doi: 10.1016/j.jacc.2009.01.041.

Martin, S. *et al.* (1996) 'The glucose transporter (GLUT-4) and vesicle-associated membrane protein-2 (VAMP-2) are segregated from recycling endosomes in insulin-sensitive cells.', *The Journal of cell biology*, 134(3), pp. 625–35.

Maruthur, N. M. *et al.* (2016) 'Diabetes Medications as Monotherapy or Metformin-Based Combination Therapy for Type 2 Diabetes', *Annals of Internal Medicine*. American College of Physicians, 164(11), p. 740. doi: 10.7326/M15-2650.

Mazumder, P. K. *et al.* (2004) 'Impaired cardiac efficiency and increased fatty acid oxidation in insulin-resistant ob/ob mouse hearts.', *Diabetes*, 53(9), pp. 2366–74.

McCarroll, C. S. *et al.* (2018) 'Runx1 Deficiency Protects Against Adverse Cardiac Remodeling After Myocardial Infarction', *Circulation*, 137(1), pp. 57–70. doi: 10.1161/CIRCULATIONAHA.117.028911.

McCully, J. D. *et al.* (2004) 'Differential contribution of necrosis and apoptosis in

myocardial ischemia-reperfusion injury', *American Journal of Physiology-Heart and Circulatory Physiology*, 286(5), pp. H1923–H1935. doi: 10.1152/ajpheart.00935.2003.

McGee, S. L. *et al.* (2006) 'Exercise increases MEF2- and GEF DNA-binding activity in human skeletal muscle', *The FASEB Journal*. Federation of American Societies for Experimental Biology, 20(2), pp. 348–349. doi: 10.1096/fj.05-4671fje.

McGee, S. L. and Hargreaves, M. (2004) 'Exercise and myocyte enhancer factor 2 regulation in human skeletal muscle.', *Diabetes*. American Diabetes Association, 53(5), pp. 1208–14. doi: 10.2337/DIABETES.53.5.1208.

McNew, J. A. *et al.* (2000) 'Compartmental specificity of cellular membrane fusion encoded in SNARE proteins', *Nature*, 407(6801), pp. 153–159. doi: 10.1038/35025000.

Michael, L. F. *et al.* (2001) 'Restoration of insulin-sensitive glucose transporter (GLUT4) gene expression in muscle cells by the transcriptional coactivator PGC-1.', *Proceedings of the National Academy of Sciences of the United States of America*. National Academy of Sciences, 98(7), pp. 3820–5. doi: 10.1073/pnas.061035098.

Miki, T. *et al.* (2013) 'Diabetic cardiomyopathy: pathophysiology and clinical features', *Heart Failure Reviews*. Springer, 18(2), pp. 149–166. doi: 10.1007/s10741-012-9313-3.

Mingrone, G. *et al.* (2012) 'Bariatric Surgery versus Conventional Medical Therapy for Type 2 Diabetes', *New England Journal of Medicine*. Massachusetts Medical Society, 366(17), pp. 1577–1585. doi: 10.1056/NEJMoa1200111.

Minokoshi, Y., Kahn, C. R. and Kahn, B. B. (2003) 'Tissue-specific ablation of the GLUT4 glucose transporter or the insulin receptor challenges assumptions about insulin action and glucose homeostasis.', *The Journal of biological chemistry*. American Society for Biochemistry and Molecular Biology, 278(36), pp. 33609–12. doi: 10.1074/jbc.R300019200.

Mitcheson, J. S., Hancox, J. C. and Levi, A. J. (1998) 'Cultured adult cardiac myocytes: future applications, culture methods, morphological and electrophysiological properties.', *Cardiovascular research*, 39(2), pp. 280–300.

Moholdt, T. T. *et al.* (2009) 'Aerobic interval training versus continuous moderate exercise after coronary artery bypass surgery: A randomized study of cardiovascular effects and quality of life', *American Heart Journal*. Mosby, 158(6), pp. 1031–1037. doi: 10.1016/J.AHJ.2009.10.003.

Montessuit, C. *et al.* (1998) 'Post-ischemic Stimulation of 2-deoxyglucose Uptake in Rat Myocardium: Role of Translocation of Glut-4', *Journal of Molecular and Cellular Cardiology*. Academic Press, 30(2), pp. 393–403. doi: 10.1006/JMCC.1997.0602.

Montessuit, C. *et al.* (2004) 'Regulation of glucose transporter expression in cardiac myocytes: P38 MAPK is a strong inducer of GLUT4', *Cardiovascular Research*, 64(1), pp. 94–104. doi: 10.1016/j.cardiores.2004.06.005.

Mora, A. *et al.* (2005) 'Role of the PDK1-PKB-GSK3 pathway in regulating glycogen synthase and glucose uptake in the heart', *FEBS Letters*, 579(17), pp. 3632–3638. doi: 10.1016/j.febslet.2005.05.040.

Mueckler, M. and Thorens, B. (2013) 'The SLC2 (GLUT) family of membrane transporters.', *Molecular aspects of medicine*. NIH Public Access, 34(2–3), pp. 121–38. doi: 10.1016/j.mam.2012.07.001.

Muretta, J. M., Romenskaia, I. and Mastick, C. C. (2008) 'Insulin Releases Glut4 from Static Storage Compartments into Cycling Endosomes and Increases the Rate Constant for Glut4 Exocytosis', *Journal of Biological Chemistry*, 283(1), pp. 311–323. doi: 10.1074/jbc.M705756200.

Myerburg, R. J., Kessler, K. M. and Castellanos, A. (1992) 'Sudden cardiac death. Structure, function, and time-dependence of risk.', *Circulation*, 85(1 Suppl), pp. I2-10.

Nagueh, S. F. *et al.* (1997) 'Doppler Tissue Imaging: A Noninvasive Technique for

Evaluation of Left Ventricular Relaxation and Estimation of Filling Pressures', *Journal of the American College of Cardiology*. 30(6), pp. 1527–1533. doi: 10.1016/S0735-1097(97)00344-6.

Neubauer, S. *et al.* (1997) 'Myocardial Phosphocreatine-to-ATP Ratio Is a Predictor of Mortality in Patients With Dilated Cardiomyopathy', *Circulation*, 96(7), pp. 2190–2196. doi: 10.1161/01.CIR.96.7.2190.

Ng, Y. *et al.* (2008) 'Rapid Activation of Akt2 Is Sufficient to Stimulate GLUT4 Translocation in 3T3-L1 Adipocytes', *Cell Metabolism*, 7(4), pp. 348–356. doi: 10.1016/j.cmet.2008.02.008.

Nishigaki, K. *et al.* (1996) 'Marked expression of plasma brain natriuretic peptide is a special feature of hypertrophic obstructive cardiomyopathy', *Journal of the American College of Cardiology*, 28(5), pp. 1234–1242. doi: 10.1016/S0735-1097(96)00277-X.

Norhammar, A. *et al.* (2002) 'Glucose metabolism in patients with acute myocardial infarction and no previous diagnosis of diabetes mellitus: a prospective study', *The Lancet*. Elsevier, 359(9324), pp. 2140–2144. doi: 10.1016/S0140-6736(02)09089-X.

O'Gorman, D. J. *et al.* (2006) 'Exercise training increases insulin-stimulated glucose disposal and GLUT4 (SLC2A4) protein content in patients with type 2 diabetes', *Diabetologia*. 49(12), pp. 2983–2992. doi: 10.1007/s00125-006-0457-3.

Ogasawara, T. *et al.* (2017) 'Impact of extracellular matrix on engraftment and maturation of pluripotent stem cell-derived cardiomyocytes in a rat myocardial infarct model', *Scientific Reports*. Nature Publishing Group, 7(1), p. 8630. doi: 10.1038/s41598-017-09217-x.

Ogurtsova, K. *et al.* (2017) 'IDF Diabetes Atlas: Global estimates for the prevalence of diabetes for 2015 and 2040', *Diabetes Research and Clinical Practice*. Elsevier, 128, pp. 40–50. doi: 10.1016/J.DIABRES.2017.03.024.

Oh, E. *et al.* (2005) 'Munc18c Heterozygous Knockout Mice Display Increased

Susceptibility for Severe Glucose Intolerance', *Diabetes*. American Diabetes Association, 54(3), pp. 638–647. doi: 10.2337/DIABETES.54.3.638.

Ohtake, T. *et al.* (1995) 'Myocardial glucose metabolism in noninsulin-dependent diabetes mellitus patients evaluated by FDG-PET.', *Journal of nuclear medicine*. 36(3), pp. 456–63.

Olson, A. L., Knight, J. B. and Pessin, J. E. (1997) 'Syntaxin 4, VAMP2, and/or VAMP3/cellubrevin are functional target membrane and vesicle SNAP receptors for insulin-stimulated GLUT4 translocation in adipocytes.', *Molecular and cellular biology*. American Society for Microbiology Journals, 17(5), pp. 2425–35. doi: 10.1128/MCB.17.5.2425.

Olson, A. L., Trumbly, A. R. and Gibson, G. V. (2001) 'Insulin-mediated GLUT4 Translocation Is Dependent on the Microtubule Network', *Journal of Biological Chemistry*, 276(14), pp. 10706–10714. doi: 10.1074/jbc.M007610200.

Ouwens, D. M. *et al.* (2005) 'Cardiac dysfunction induced by high-fat diet is associated with altered myocardial insulin signalling in rats', *Diabetologia*. Springer-Verlag, 48(6), pp. 1229–1237. doi: 10.1007/s00125-005-1755-x.

Panagia, M. *et al.* (2007) 'Abnormal function and glucose metabolism in the type-2 diabetic db/db mouse heart.' *Canadian Journal of Physiology and Pharmacology*, 85(3–4), pp. 289–294. doi: 10.1139/Y07-028.

Parikh, S. S. *et al.* (2017) 'Thyroid and Glucocorticoid Hormones Promote Functional T-Tubule Development in Human-Induced Pluripotent Stem Cell–Derived Cardiomyocytes', *Circulation Research*, 121(12), pp. 1323–1330. doi: 10.1161/CIRCRESAHA.117.311920.

Park, S.-Y. *et al.* (2005) 'Unraveling the temporal pattern of diet-induced insulin resistance in individual organs and cardiac dysfunction in C57BL/6 mice.', *Diabetes*, 54(12), pp. 3530–40.

Park, S.-Y. *et al.* (2014) 'Cardiac, skeletal, and smooth muscle mitochondrial respiration: are all mitochondria created equal?', *American journal of*

physiology. Heart and circulatory physiology. American Physiological Society, 307(3), pp. H346-52. doi: 10.1152/ajpheart.00227.2014.

Pelliccia, A. *et al.* (1991) 'The Upper Limit of Physiologic Cardiac Hypertrophy in Highly Trained Elite Athletes', *New England Journal of Medicine*. Massachusetts Medical Society , 324(5), pp. 295–301. doi: 10.1056/NEJM199101313240504.

Pendsey, S. P. (2010) 'Understanding diabetic foot.', *International journal of diabetes in developing countries*. Springer, 30(2), pp. 75–9. doi: 10.4103/0973-3930.62596.

Perera, H. K. I. *et al.* (2003) 'Syntaxin 6 regulates Glut4 trafficking in 3T3-L1 adipocytes.', *Molecular biology of the cell*. American Society for Cell Biology, 14(7), pp. 2946–58. doi: 10.1091/mbc.e02-11-0722.

Periasamy, M. and Kalyanasundaram, A. (2007) 'SERCA pump isoforms: Their role in calcium transport and disease', *Muscle & Nerve*. Wiley-Blackwell, 35(4), pp. 430–442. doi: 10.1002/mus.20745.

Perreault, L. *et al.* (2018) 'Intracellular localization of diacylglycerols and sphingolipids influences insulin sensitivity and mitochondrial function in human skeletal muscle', *JCI Insight*, 3(3). doi: 10.1172/jci.insight.96805.

Perseghin, G. *et al.* (1997) 'Metabolic defects in lean nondiabetic offspring of NIDDM parents: a cross-sectional study.', *Diabetes*, 46(6), pp. 1001–9.

Peters, C. G., Miller, D. F. and Giovannucci, D. R. (2006) 'Identification, localization and interaction of SNARE proteins in atrial cardiac myocytes', *Journal of Molecular and Cellular Cardiology*. Academic Press, 40(3), pp. 361–374. doi: 10.1016/J.YJMCC.2005.12.007.

Peterson, L. R. *et al.* (2004) 'Effect of Obesity and Insulin Resistance on Myocardial Substrate Metabolism and Efficiency in Young Women', *Circulation*, 109(18), pp. 2191–2196. doi: 10.1161/01.CIR.0000127959.28627.F8.

Picht, E. *et al.* (2007) 'CaMKII inhibition targeted to the sarcoplasmic reticulum

inhibits frequency-dependent acceleration of relaxation and Ca2+ current facilitation', *Journal of Molecular and Cellular Cardiology*, 42(1), pp. 196–205. doi: 10.1016/j.yjmcc.2006.09.007.

Pioner, J. M. *et al.* (2016) 'Isolation and Mechanical Measurements of Myofibrils from Human Induced Pluripotent Stem Cell-Derived Cardiomyocytes', *Stem Cell Reports*. Cell Press, 6(6), pp. 885–896. doi: 10.1016/J.STEMCR.2016.04.006.

Plomgaard, P. *et al.* (2005) 'Tumor necrosis factor-alpha induces skeletal muscle insulin resistance in healthy human subjects via inhibition of Akt substrate 160 phosphorylation.', *Diabetes*. American Diabetes Association, 54(10), pp. 2939–45. doi: 10.2337/DIABETES.54.10.2939.

Poulsen, M. K. *et al.* (2010) 'Left Ventricular Diastolic Function in Type 2 Diabetes Mellitus Prevalence and Association With Myocardial and Vascular Disease'. *Circulation Cardiovascular Imaging*. 3(1) pp.24-31. doi: 10.1161/CIRCIMAGING.109.855510.

Proctor, K. M. *et al.* (2006) 'Syntaxin 16 controls the intracellular sequestration of GLUT4 in 3T3-L1 adipocytes', *Biochemical and Biophysical Research Communications*. Academic Press, 347(2), pp. 433–438. doi: 10.1016/J.BBRC.2006.06.135.

Puigserver, P. *et al.* (2003) 'Insulin-regulated hepatic gluconeogenesis through FOXO1–PGC-1α interaction', *Nature*. Nature Publishing Group, 423(6939), pp. 550–555. doi: 10.1038/nature01667.

Quon, M. J. *et al.* (1994) 'Insulin receptor substrate 1 mediates the stimulatory effect of insulin on GLUT4 translocation in transfected rat adipose cells.', *The Journal of biological chemistry*, 269(45), pp. 27920–4.

Rajkhowa, M. *et al.* (2009) 'Insulin resistance in polycystic ovary syndrome is associated with defective regulation of ERK1/2 by insulin in skeletal muscle in vivo', *Biochem. J*, 418, pp. 665–671. doi: 10.1042/BJ20082176.

Rana, P. *et al.* (2012) 'Characterization of Human-Induced Pluripotent Stem

Cell–Derived Cardiomyocytes: Bioenergetics and Utilization in Safety Screening', *Toxicological Sciences*. Oxford University Press, 130(1), pp. 117–131. doi: 10.1093/toxsci/kfs233.

Rens, J.-M. *et al.* (1994) 'Exercise Induces Rapid Increases in GLUT4 Expression, Glucose Transport Capacity, and Insulin-stimulated Glycogen Storage in Muscle.' *The Journal of Biological Chemistry*. 269(20), pp. 14396–14401.

Resnick, H. E. *et al.* (2000) 'Relation of weight gain and weight loss on subsequent diabetes risk in overweight adults.', *Journal of epidemiology and community health*. BMJ Publishing Group, 54(8), pp. 596–602. doi: 10.1136/JECH.54.8.596.

Rijzewijk, L. J. *et al.* (2008) 'Myocardial Steatosis Is an Independent Predictor of Diastolic Dysfunction in Type 2 Diabetes Mellitus', *Journal of the American College of Cardiology*. 52(22), pp. 1793–1799. doi: 10.1016/j.jacc.2008.07.062.

Rijzewijk, L. J. *et al.* (2009) 'Altered Myocardial Substrate Metabolism and Decreased Diastolic Function in Nonischemic Human Diabetic Cardiomyopathy', *Journal of the American College of Cardiology*, 54(16), pp. 1524–1532. doi: 10.1016/j.jacc.2009.04.074.

Rippon, H. J. and Bishop, A. E. (2004) 'Embryonic stem cells', *Cell Proliferation*. Wiley/Blackwell (10.1111), 37(1), pp. 23–34. doi: 10.1111/j.1365-2184.2004.00298.x.

Ronaldson-Bouchard, K. *et al.* (2018) 'Advanced maturation of human cardiac tissue grown from pluripotent stem cells', *Nature*. Nature Publishing Group, 556(7700), pp. 239–243. doi: 10.1038/s41586-018-0016-3.

Rose, A. J., Kiens, B. and Richter, E. A. (2006) 'Ca $^{2+}$ -calmodulin-dependent protein kinase expression and signalling in skeletal muscle during exercise', *The Journal of Physiology*. Wiley/Blackwell (10.1111), 574(3), pp. 889–903. doi: 10.1113/jphysiol.2006.111757.

Rossetto, O. *et al.* (1996) 'VAMP/synaptobrevin isoforms 1 and 2 are widely and

differentially expressed in nonneuronal tissues.', *The Journal of cell biology*. Rockefeller University Press, 132(1–2), pp. 167–79. doi: 10.1083/JCB.132.1.167.

Ruan, H. *et al.* (2003) 'Standard isolation of primary adipose cells from mouse epididymal fat pads induces inflammatory mediators and down-regulates adipocyte genes.', *The Journal of biological chemistry*. American Society for Biochemistry and Molecular Biology, 278(48), pp. 47585–93. doi: 10.1074/jbc.M305257200.

Russell, R. R. *et al.* (2004) 'AMP-activated protein kinase mediates ischemic glucose uptake and prevents postischemic cardiac dysfunction, apoptosis, and injury', *The Journal of Clinical Investigation*. American Society for Clinical Investigation, 114(4), pp. 495–503. doi: 10.1172/JCI19297.

Sadler, J. B. A., Bryant, N. J. and Gould, G. W. (2015) 'Characterization of VAMP isoforms in 3T3-L1 adipocytes: implications for GLUT4 trafficking', *Molecular Biology of the Cell*. 26(3), pp. 530–536. doi: 10.1091/mbc.E14-09-1368.

Sano, H. *et al.* (2007) 'Rab10, a Target of the AS160 Rab GAP, Is Required for Insulin-Stimulated Translocation of GLUT4 to the Adipocyte Plasma Membrane', *Cell Metabolism*, 5(4), pp. 293–303. doi: 10.1016/j.cmet.2007.03.001.

Santalucía, T. *et al.* (2001) 'A novel functional co-operation between MyoD, MEF2 and TRalpha1 is sufficient for the induction of GLUT4 gene transcription.', *Journal of molecular biology*, 314(2), pp. 195–204. doi: 10.1006/jmbi.2001.5091.

Schannwell, C. M. *et al.* (2002) 'Left Ventricular Diastolic Dysfunction as an Early Manifestation of Diabetic Cardiomyopathy'. *Cardiology*, 98(1–2), pp. 33–39. doi: 10.1159/000064682.

Scheuermann-Freestone, M. *et al.* (2003) 'Abnormal Cardiac and Skeletal Muscle Energy Metabolism in Patients With Type 2 Diabetes', *Circulation*, 107(24), pp. 3040–3046. doi: 10.1161/01.CIR.0000072789.89096.10.

Schwenk, R. W. *et al.* (2010) 'Requirement for distinct vesicle-associated membrane proteins in insulin- and AMP-activated protein kinase (AMPK)-induced

translocation of GLUT4 and CD36 in cultured cardiomyocytes', *Diabetologia*. Springer-Verlag, 53(10), pp. 2209–2219. doi: 10.1007/s00125-010-1832-7.

Semeniuk, L. M., Kryski, A. J. and Severson, D. L. (2002) 'Echocardiographic assessment of cardiac function in diabetic *db*/*db* and transgenic *db*/*db* -hGLUT4 mice', *American Journal of Physiology-Heart and Circulatory Physiology*. 283(3), pp. H976–H982. doi: 10.1152/ajpheart.00088.2002.

Shang, Y. *et al*. (2016) 'Assessment of Left Ventricular Structural Remodelling in Patients with Diabetic Cardiomyopathy by Cardiovascular Magnetic Resonance', *Journal of Diabetes Research*. pp. 1–8. doi: 10.1155/2016/4786925.

Shewan, A. M. *et al*. (2000) 'The cytosolic C-terminus of the glucose transporter GLUT4 contains an acidic cluster endosomal targeting motif distal to the dileucine signal.', *The Biochemical journal*. Portland Press Ltd, 350(1), pp. 99–107.

Shewan, A. M. *et al*. (2003) 'GLUT4 recycles via a trans-Golgi network (TGN) subdomain enriched in Syntaxins 6 and 16 but not TGN38: involvement of an acidic targeting motif.', *Molecular biology of the cell*. American Society for Cell Biology, 14(3), pp. 973–86. doi: 10.1091/mbc.e02-06-0315.

Shi, J. and Kandror, K. V. (2005) 'Sortilin Is Essential and Sufficient for the Formation of Glut4 Storage Vesicles in 3T3-L1 Adipocytes', *Developmental Cell*. Cell Press, 9(1), pp. 99–108. doi: 10.1016/J.DEVCEL.2005.04.004.

Shiba, Y. *et al*. (2012) 'Human ES-cell-derived cardiomyocytes electrically couple and suppress arrhythmias in injured hearts', *Nature*. Nature Publishing Group, 489(7415), pp. 322–325. doi: 10.1038/nature11317.

Shiba, Y. *et al*. (2016) 'Allogeneic transplantation of iPS cell-derived cardiomyocytes regenerates primate hearts', *Nature*. Nature Publishing Group, 538(7625), pp. 388–391. doi: 10.1038/nature19815.

Siebeneicher, H. *et al*. (2016) 'Identification and Optimization of the First Highly Selective GLUT1 Inhibitor BAY-876', *ChemMedChem*, 11(20), pp. 2261–2271. doi:

10.1002/cmdc.201600276.

Skovbro, M. *et al.* (2008) 'Human skeletal muscle ceramide content is not a major factor in muscle insulin sensitivity', *Diabetologia*, 51(7), pp. 1253–1260. doi: 10.1007/s00125-008-1014-z.

Sowers, J. R., Epstein, M. and Frohlich, E. D. (2001) 'Diabetes, Hypertension, and Cardiovascular Disease', *Hypertension*, 37(4), pp. 1053–1059. doi: 10.1161/01.HYP.37.4.1053.

Stenbit, A. E. *et al.* (1997) 'GLUT4 heterozygous knockout mice develop muscle insulin resistance and diabetes', *Nature Medicine*. Nature Publishing Group, 3(10), pp. 1096–1101. doi: 10.1038/nm1097-1096.

Stenmark, H. (2009) 'Rab GTPases as coordinators of vesicle traffic', *Nature Reviews Molecular Cell Biology*. Nature Publishing Group, 10(8), pp. 513–525. doi: 10.1038/nrm2728.

Stitt, T. N. *et al.* (2004) 'The IGF-1/PI3K/Akt Pathway Prevents Expression of Muscle Atrophy-Induced Ubiquitin Ligases by Inhibiting FOXO Transcription Factors', *Molecular Cell*. Cell Press, 14(3), pp. 395–403. doi: 10.1016/S1097-2765(04)00211-4.

Stølen, T. O. *et al.* (2009) 'Interval Training Normalizes Cardiomyocyte Function, Diastolic Ca $^{2+}$ Control, and SR Ca $^{2+}$ Release Synchronicity in a Mouse Model of Diabetic Cardiomyopathy'. *Circulation Research*, 105(6), pp. 527–536. doi: 10.1161/CIRCRESAHA.109.199810.

Sun, Y. *et al.* (2010) 'Rab8A and Rab13 are activated by insulin and regulate GLUT4 translocation in muscle cells', *Proceedings of the National Academy of Sciences*, 107(46), pp. 19909–19914. doi: 10.1073/pnas.1009523107.

Tafuri, S. R. (1996) 'Troglitazone Enhances Differentiation, Basal Glucose Uptake, and Glut1 Protein Levels in 3T3-L1 Adipocytes.' *Endocrinology,* 137(11), pp. 4706-4712.

Takahashi, K. *et al.* (2007) 'Induction of Pluripotent Stem Cells from Adult Human Fibroblasts by Defined Factors', *Cell*. Cell Press, 131(5), pp. 861–872. doi: 10.1016/J.CELL.2007.11.019.

Takahashi, K. and Yamanaka, S. (2006) 'Induction of Pluripotent Stem Cells from Mouse Embryonic and Adult Fibroblast Cultures by Defined Factors', *Cell*, 126(4), pp. 663–676. doi: 10.1016/j.cell.2006.07.024.

Takahashi, M. *et al.* (2008) 'Chemerin enhances insulin signaling and potentiates insulin-stimulated glucose uptake in 3T3-L1 adipocytes', *FEBS Letters*. Wiley-Blackwell, 582(5), pp. 573–578. doi: 10.1016/j.febslet.2008.01.023.

Tamemoto, H. *et al.* (1994) 'Insulin resistance and growth retardation in mice lacking insulin receptor substrate-1', *Nature*, 372(6502), pp. 182–186. doi: 10.1038/372182a0.

Thai, M. V *et al.* (1998) 'Myocyte enhancer factor 2 (MEF2)-binding site is required for GLUT4 gene expression in transgenic mice. Regulation of MEF2 DNA binding activity in insulin-deficient diabetes.', *The Journal of biological chemistry*. American Society for Biochemistry and Molecular Biology, 273(23), pp. 14285–92. doi: 10.1074/JBC.273.23.14285.

Thurmond, D. C. *et al.* (1998) 'Regulation of insulin-stimulated GLUT4 translocation by Munc18c in 3T3L1 adipocytes.', *The Journal of biological chemistry*, 273(50), pp. 33876–83.

Todd, J. A. *et al.* (2007) 'Robust associations of four new chromosome regions from genome-wide analyses of type 1 diabetes', *Nature Genetics*. Nature Publishing Group, 39(7), pp. 857–864. doi: 10.1038/ng2068.

Tong, P. *et al.* (2001) 'Insulin-induced cortical actin remodeling promotes GLUT4 insertion at muscle cell membrane ruffles', *Journal of Clinical Investigation*, 108(3), pp. 371–381. doi: 10.1172/JCI12348.

Torrance, C. J. *et al.* (1997) 'Effects of Thyroid Hormone on GLUT4 Glucose Transporter Gene Expression and NIDDM in Rats', *Endocrinology*. Oxford

University Press, 138(3), pp. 1204–1214. doi: 10.1210/endo.138.3.4981.

Tulloch, N. L. *et al.* (2011) 'Growth of Engineered Human Myocardium With Mechanical Loading and Vascular Coculture', *Circulation Research*, 109(1), pp. 47–59. doi: 10.1161/CIRCRESAHA.110.237206.

Utriainen, T. *et al.* (1998) 'Insulin resistance characterizes glucose uptake in skeletal muscle but not in the heart in NIDDM', *Diabetologia*, 41(5), pp. 555–559. doi: 10.1007/s001250050946.

Voipio-Pulkki, L. M. *et al.* (1993) 'Heart and skeletal muscle glucose disposal in type 2 diabetic patients as determined by positron emission tomography.', *Journal of nuclear medicine*, 34(12), pp. 2064–7.

de Waard, M. C. *et al.* (2007) 'Early Exercise Training Normalizes Myofilament Function and Attenuates Left Ventricular Pump Dysfunction in Mice With a Large Myocardial Infarction', *Circulation Research*, 100(7), pp. 1079–1088. doi: 10.1161/01.RES.0000262655.16373.37.

Walker, A. M. *et al.* (2016) 'Diabetes mellitus is associated with adverse structural and functional cardiac remodelling in chronic heart failure with reduced ejection fraction', *Diabetes and Vascular Disease Research*, 13(5), pp. 331–340. doi: 10.1177/1479164116653342.

Wan, W. *et al.* (2007) 'Effect of Post–Myocardial Infarction Exercise Training on the Renin-Angiotensin-Aldosterone System and Cardiac Function', *The American Journal of the Medical Sciences*. Elsevier, 334(4), pp. 265–273. doi: 10.1097/MAJ.0B013E318068B5ED.

Wang, H. *et al.* (2015) 'Exercise Prevents Cardiac Injury and Improves Mitochondrial Biogenesis in Advanced Diabetic Cardiomyopathy with PGC-1α and Akt Activation.', *Cellular physiology and biochemistry : international journal of experimental cellular physiology, biochemistry, and pharmacology*. Karger Publishers, 35(6), pp. 2159–68. doi: 10.1159/000374021.

Weinstein, S. P., O'Boyle, E. and Haber, R. S. (1994) 'Thyroid hormone increases

basal and insulin-stimulated glucose transport in skeletal muscle. The role of GLUT4 glucose transporter expression.', *Diabetes*. American Diabetes Association, 43(10), pp. 1185–9. doi: 10.2337/DIAB.43.10.1185.

Weiss, A. and Leinwand, L. A. (1996) 'THE MAMMALIAN MYOSIN HEAVY CHAIN GENE FAMILY', *Annual Review of Cell and Developmental Biology*, 12(1), pp. 417–439. doi: 10.1146/annurev.cellbio.12.1.417.

Wendler, F. and Tooze, S. (2001) 'Syntaxin 6: The Promiscuous Behaviour of a SNARE Protein', *Traffic*. Wiley/Blackwell (10.1111), 2(9), pp. 606–611. doi: 10.1034/j.1600-0854.2001.20903.x.

Werner, J. C. *et al.* (1983) 'Fatty acid and glucose utilization in isolated, working newborn pig hearts.', *The American journal of physiology*. 244(1), pp. E19-23. doi: 10.1152/ajpendo.1983.244.1.E19.

Wisløff, U. *et al.* (2001) 'Increased contractility and calcium sensitivity in cardiac myocytes isolated from endurance trained rats', *Cardiovascular Research*. Oxford University Press, 50(3), pp. 495–508. doi: 10.1016/S0008-6363(01)00210-3.

Wolf-Goldberg, T. *et al.* (2006) 'Target soluble N-ethylmaleimide-sensitive factor attachment protein receptors (t-SNAREs) differently regulate activation and inactivation gating of Kv2.2 and Kv2.1: Implications on pancreatic islet cell Kv channels.', *Molecular pharmacology*. American Society for Pharmacology and Experimental Therapeutics, 70(3), pp. 818–28. doi: 10.1124/mol.105.021717.

Xu, H. *et al.* (2003) 'Chronic inflammation in fat plays a crucial role in the development of obesity-related insulin resistance.', *The Journal of clinical investigation*. American Society for Clinical Investigation, 112(12), pp. 1821–30. doi: 10.1172/JCI19451.

Yamauchi, T. *et al.* (2001) 'The fat-derived hormone adiponectin reverses insulin resistance associated with both lipoatrophy and obesity', *Nature Medicine*. Nature Publishing Group, 7(8), pp. 941–946. doi: 10.1038/90984.

Yang, X. *et al.* (2014) 'Tri-iodo-l-thyronine promotes the maturation of human cardiomyocytes-derived from induced pluripotent stem cells', *Journal of Molecular and Cellular Cardiology*. Academic Press, 72, pp. 296–304. doi: 10.1016/J.YJMCC.2014.04.005.

Yang, X., Pabon, L. and Murry, C. E. (2014) 'Engineering Adolescence: Maturation of Human Pluripotent Stem Cell-Derived Cardiomyocytes', *Circulation Research*, 114(3), pp. 511–523. doi: 10.1161/CIRCRESAHA.114.300558.

Yeh, T.-Y. J. *et al.* (2007) 'Insulin-stimulated exocytosis of GLUT4 is enhanced by IRAP and its partner tankyrase.', *The Biochemical journal*. Portland Press Limited, 402(2), pp. 279–90. doi: 10.1042/BJ20060793.

Yip, M. F. *et al.* (2008) 'CaMKII-Mediated Phosphorylation of the Myosin Motor Myo1c Is Required for Insulin-Stimulated GLUT4 Translocation in Adipocytes', *Cell Metabolism*. Cell Press, 8(5), pp. 384–398. doi: 10.1016/J.CMET.2008.09.011.

Zahiti, B. F. *et al.* (2013) 'Left ventricular diastolic dysfunction in asymptomatic type 2 diabetic patients: detection and evaluation by tissue Doppler imaging.', *Acta informatica medica*. 21(2), pp. 120–3. doi: 10.5455/aim.2013.21.120-123.

Zhang, L. *et al.* (2011) 'Cardiac diacylglycerol accumulation in high fat-fed mice is associated with impaired insulin-stimulated glucose oxidation', *Cardiovascular Research*, 89(1), pp. 148–156. doi: 10.1093/cvr/cvq266.

Zorzano, A., Palacin, M. and Guma, A. (2005) 'Mechanisms regulating GLUT4 glucose transporter expression and glucose transport in skeletal muscle', *Acta Physiologica Scandinavica*. Wiley/Blackwell (10.1111), 183(1), pp. 43–58. doi: 10.1111/j.1365-201X.2004.01380.x.